AD_____

Award Number: DAMD17-99-1-9061

TITLE: Angiogenesis and Cancer Prevention by Selenium

PRINCIPAL INVESTIGATOR: Junxuan Lu, Ph.D.

CONTRACTING ORGANIZATION: AMC Cancer Research Center
Denver, Colorado 80214

REPORT DATE: June 2002

TYPE OF REPORT: Final

PREPARED FOR: U.S. Army Medical Research and Materiel Command
Fort Detrick, Maryland 21702-5012

DISTRIBUTION STATEMENT: Approved for Public Release;
Distribution Unlimited

The views, opinions and/or findings contained in this report are
those of the author(s) and should not be construed as an official
Department of the Army position, policy or decision unless so
designated by other documentation.

# REPORT DOCUMENTATION PAGE

Public reporting burden for this collection of information is estimated to average 1 hour per response, including the time for reviewing instructions, searching existing data sources, gathering and maintaining the data needed, and completing and reviewing this collection of information. Send comments regarding this burden estimate or any other aspect of this collection of information, including suggestions for reducing this burden to Washington Headquarters Services, Directorate for Information Operations and Reports, 1215 Jefferson Davis Highway, Suite 1204, Arlington, VA 22202-4302, and to the Office of Management and Budget, Paperwork Reduction Project (0704-0188), Washington, DC 20503

| 1. AGENCY USE ONLY (Leave blank) | 2. REPORT DATE<br>June 2002 | 3. REPORT TYPE AND DATES COVERED<br>Final (15 May 99 – 14 May 02) | |
|---|---|---|---|

**4. TITLE AND SUBTITLE**
Angiogenesis and Cancer Prevention by Selenium

**5. FUNDING NUMBERS**
DAMD17-99-1-9061

**6. AUTHOR(S):**
Junxuan Lu, Ph.D.

**7. PERFORMING ORGANIZATION NAME(S) AND ADDRESS(ES)**

AMC Cancer Research Center
Denver, Colorado  80214

**E-MAIL:**
Jlu@hi.umn.edu

**8. PERFORMING ORGANIZATION REPORT NUMBER**

**9. SPONSORING / MONITORING AGENCY NAME(S) AND ADDRESS(ES)**

U.S. Army Medical Research and Materiel Command
Fort Detrick, Maryland 21702-5012

**10. SPONSORING / MONITORING AGENCY REPORT NUMBER**

**11. SUPPLEMENTARY NOTES**

**12a. DISTRIBUTION / AVAILABILITY STATEMENT**
Approved for Public Release; Distribution Unlimited

**12b. DISTRIBUTION CODE**

**13. ABSTRACT (Maximum 200 Words)**
Our overall aim is to understand the role of inhibition of angiogenesis by selenium (Se) in breast cancer chemoprevention. We first established the anti-angiogenesis phenomenon of chemopreventive intake of Se with data supporting an association of reduced microvessel density and decreased vascular endothelial growth factor expression with mammary cancer prevention by Se (Mol. Carcinog. 1999). We discovered a specific inhibitory effect of methylselenium on vascular endothelial expression of matrix metalloproteinase-2 and vascular endothelial growth factor by breast and prostate cancer epithelial cells (Mol. Carcinog. 2000). Since endothelial proliferation is a critical component of the angiogenic responses, we have investigated a potent inhibitory effect of methylselenium on mitogenesis of vascular endothelial cells and established phosphatidylinositol 3-kinase as a potential target pathway for signaling G1 arrest (Cancer Res 2001, Mol Carcinog. 2002). We also developed methods for evaluating anti-angiogenic attributes (pro-angiogenic factors, mitogenesis, apoptosis, capillary differentiation etc) of Se and validated with other agents. In summary, our results support the methylselenol metabolite pool with desirable anti-angiogenic attributes in addition to inhibitory actions on cell proliferation (G1 arrest) and survival (caspase-mediated apoptosis). In total, ten publications and 3 grants (total direct $1,400,000) have resulted from this support.

**14. SUBJECT TERMS**
Selenium, angiogenesis, breast cancer

**15. NUMBER OF PAGES**
84

**16. PRICE CODE**

| 17. SECURITY CLASSIFICATION OF REPORT<br>Unclassified | 18. SECURITY CLASSIFICATION OF THIS PAGE<br>Unclassified | 19. SECURITY CLASSIFICATION OF ABSTRACT<br>Unclassified | 20. LIMITATION OF ABSTRACT<br>Unlimited |
|---|---|---|---|

# FOREWORD

Opinions, interpretations, conclusions and recommendations are those of the author and are not necessarily endorsed by the U.S. Army.

✓ Where copyrighted material is quoted, permission has been obtained to use such material.

___ Where material from documents designated for limited distribution is quoted, permission has been obtained to use the material.

___ Citations of commercial organizations and trade names in this report do not constitute an official Department of Army endorsement or approval of the products or services of these organizations.
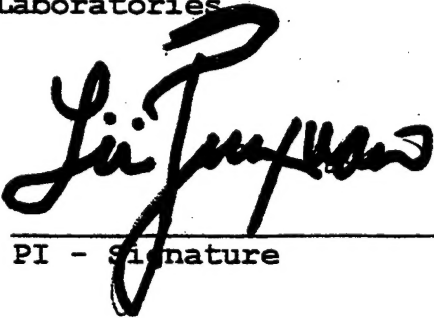
X In conducting research using animals, the investigator(s) adhered to the "Guide for the Care and Use of Laboratory Animals," prepared by the Committee on Care and use of Laboratory Animals of the Institute of Laboratory Resources, national Research Council (NIH Publication No. 86-23, Revised 1985).

___ For the protection of human subjects, the investigator(s) adhered to policies of applicable Federal Law 45 CFR 46.

___ In conducting research utilizing recombinant DNA technology, the investigator(s) adhered to current guidelines promulgated by the National Institutes of Health.

___ In the conduct of research utilizing recombinant DNA, the investigator(s) adhered to the NIH Guidelines for Research Involving Recombinant DNA Molecules.

___ In the conduct of research involving hazardous organisms, the investigator(s) adhered to the CDC-NIH Guide for Biosafety in Microbiological and Biomedical Laboratories.

_____ _____
PI - Signature                           Date

3

# Table of Contents

(7 reprints)

# 1. Introduction

The overall aim of this project is to understand the role of inhibition of angiogenesis by selenium (Se) in breast cancer prevention. We first established the anti-angiogenesis phenomenon of chemopreventive intake of Se in mammary cancer prevention (Jiang, et al, Mol. Carcinog. 1999) with data supporting an association of reduced microvessel density and decreased vascular endothelial growth factor expression with mammary cancer prevention by Se. We discovered a specific inhibitory effect of methylselenium on vascular endothelial expression of matrix metalloproteinase-2 (MMP-2) and vascular endothelial growth factor (VEGF) by breast and prostate cancer epithelial cells (Jiang et al, Mol. Carcinog. 2000). Since endothelial proliferation is a critical component of the angiogenic responses, we have investigated a potent inhibitory effect of methylselenium and methylselenol itself on mitogenesis of human umbilical vein endothelial cells (HUVEC) through G1 arrest and established PI3K as a potential target pathway for signaling G1 arrest (Wang et al, Cancer Res 2001; Wang et al, Mol Carcinog. 2002). In addition, we have also developed methodologies for evaluating anti-angiogenic attributes (pro-angiogenic factors, mitogenesis, apoptosis, capillary differentiation etc) of Se and validated with other agents (Jiang et al, BBRC, 2000, Jiang et al, Cancer Res 2001). In total, ten publications have resulted from this support. Our data suggest that the methylselenol metabolite pool possesses desirable anti-angiogenic attributes in addition to inhibitory actions on cancer epithelial proliferation and survival.

The key purpose of the DOD IDEA awards is to stimulate high-risk and high pay-off research. Data generated during these activities enabled us to successfully compete for grant supports from Komen Foundation ($200,000 direct, started October 2000) and DOD prostate cancer program ($375,000 direct, started Jan 2002) and from NCI ($825,000 direct, to be initiated in Jan 2003). Thanks for the faith and support, DOD!

# 2. Key research accomplishments.

- As reported in the December issue of *Molecular Carcinogenesis*, 1999, we have documented an association of reduction of tumor microvessel density with chemoprevention of mammary cancer in a chemically induced rat mammary carcinogenesis model. We have made the novel observation that such changes were associated with a decreased in vivo expression of VEGF, an important in vivo angiogenic cytokine molecule. Furthermore, we have documented a potent apoptogenic activity of methyl-selenium on endothelial cells and discovered a specific inhibitory effect of this Se pool, the putative chemopreventive Se metabolite (1-3), on the expression of MMP-2 by vascular endothelial cells (see Appendix 1). This article was featured as a cover story.

- As reported in the December issue of *Molecular Carcinogenesis*, 2000, we have discovered a methylselenium specific inhibitory effects on the expression of VEGF, by breast and prostate cancer epithelial cells in vitro, in addition to methyl selenium specific inhibitory effect on the expression of MMP-2 by vascular endothelial cells (see Appendix 2). In HUVEC, zymographic analyses showed that short-term exposure to methylseleninic acid (MSeA) and methylselenocyanate (MSeCN), both immediate methylselenol precursors, decreased the MMP-2 gelatinolytic activity in a concentration-dependent manner. In contrast, Se forms that enter the hydrogen selenide pool lacked any inhibitory effect. The methyl Se inhibitory effect on MMP-2 was cell-dependent as direct incubation with Se compounds in the test tube did not result in its inactivation. Immunoblot and ELISA analyses showed that a decrease of the MMP-2 protein level largely accounted for the methyl Se-induced reduction of gelatinolytic activity. The effect of MSeA on MMP-2 expression occurred within 0.5 h of

exposure and preceded MSeA-induced reduction of the phosphorylation level of mitogen-activated protein kinases (MAPK)1/2 (~3 h) and endothelial apoptosis (~25 h). In addition to these biochemical effects in monolayer culture, MSeA and MSeCN exposure decreased HUVEC viability and cell retraction in a 3-dimensional context of capillary tubes formed on Matrigel, whereas comparable or higher concentrations of selenite failed to exert such effects. In human prostate cancer (DU145) and breast cancer (MCF-7 and MDA-MB-468) cell lines, exposure to MSeA, but not selenite, led to a rapid and sustained decrease of cellular (lysate) and secreted (conditioned medium) VEGF protein levels irrespective of the serum level (serum free vs. 10% fetal bovine serum) in which Se treatments were carried out. The concentration of MSeA required for suppressing VEGF expression was much lower than that needed for apoptosis induction. Taken together, the data support the hypothesis that the monomethyl Se pool is a proximal Se for inhibiting the expression of MMP-2 and VEGF and angiogenesis. The data further indicate that the methyl Se-specific inhibitory effects on these proteins are rapid and primary actions, preceding and/or independent of inhibitory effects on mitogenic signaling at the level of MAPK1/2 and on cell growth and survival. These findings provide mechanistic insights into the cellular and biochemical processes that are potentially targeted by Se to regulate the angiogenic switch during mammary carcinogenesis. This article was featured as a cover story.

- As reported in April, 2001 in *Cancer Research*, we have invested in developing the expertise to study apoptosis execution and signaling, using the DU-145 prostate cancer cells as our model (Appendix 3). Our earlier work has indicated that distinct cell death pathways are likely involved in apoptosis induced by the methylselenol and the hydrogen selenide pools of Se metabolites. To explore the role of caspases in cancer cell apoptosis induced by Se, we examined the involvement of these molecules in the death of the DU-145 cells induced by MSeA, a novel penultimate precursor of the putative critical anticancer metabolite methylselenol. Sodium selenite, a representative of the genotoxic Se pool, was used as a reference for comparison. The results show that MSeA-induced apoptosis was accompanied by the activation of multiple caspases (caspase-3, -7, -8 and -9), mitochondrial release of cytochrome c (CC), poly(ADP-ribose) polymerase (PARP) cleavage and DNA fragmentation. In contrast, selenite-induced apoptotic DNA fragmentation was observed in the absence of these changes, but was associated with the phosphorylation of JNK1/2 and p38MAPK/SAPK2. A general caspase inhibitor, zVADfmk, blocked MSeA-induced cleavages of procaspases and PARP, CC release and DNA nucleosomal fragmentation, but did not prevent cell detachment. Furthermore, PARP cleavage and caspase activation were confined exclusively to detached cells, indicating that MSeA-induction of cell detachment was a prerequisite for caspase activation and apoptosis execution. This process therefore resembled "anoikis", a special mode of apoptosis induction when adherent cells lost contact with the extracellular matrix. Additional experiments with irreversible caspase inhibitors show that MSeA-induced anoikis involved caspase-3- and caspase-7-mediated PARP cleavage that was initiated by caspase-8 and probably amplified through CC-caspase-9 activation and a feedback activation loop from caspase-3. Taken together, the data support a methyl selenium-specific induction of DU-145 cell apoptosis that involved cell detachment as a prerequisite (anoikis) and was executed principally through caspase-8 activation and its cross-talk with multiple caspases. These results supported our success in obtaining DOD prostate cancer fund (idea development award, $375,000 direct). We extended our investigation into vascular endothelial cells (see next paragraph).

- As reported in October 2001 issue of *Cancer Res* (Appendix 4), we have investigated the effect of methylselenium on the mitogenic response of vascular endothelial cells. Using

human umbilical vein endothelial cells (HUVEC), we examined the effects of MSeA on selected protein kinase signaling transduction pathways in order to characterize their role in methylselenium induction of HUVEC cell cycle arrest and apoptosis. Exposure of asynchronous HUVEC for 30 h to 3-5 µM MSeA led to a profound $G_1$ arrest and exposure to higher levels of MSeA not only led to $G_1$ arrest, but also to DNA fragmentation and caspase-mediated cleavage of poly(ADP-ribose)polymerase, both being biochemical hallmarks of apoptosis. Immunoblot analyses indicated that $G_1$ arrest induced by the sub-lethal doses of MSeA was associated with dose-dependent reductions of the levels of phospho-AKT/PKB, phospho-ERK1/2, and phospho-JNK1/2 in the absence of any change in p38MAPK phosphorylation. Apoptosis induced by MSeA was associated with an increased phosphorylation of p38MAPK in addition to the dephosphorylation of the above kinases. In HUVEC deprived of endothelial cell growth supplement (ECGS) for 48 h, resumption of ECGS stimulation resulted in ~ 10-fold increase in mitogenic response as indicated by $^3$H-thymidine incorporation into DNA. The ECGS-stimulated mitogenic response was dose-dependently inhibited by MSeA exposure with $IC_{50\%}$ ~ 1 µM and a complete blockage at 3 µM. Wortmannin, an inhibitor of PI3K upstream of AKT, potently inhibited the ECGS-stimulated DNA synthesis ($IC_{50\%}$ ~ 40 nM). Combining MSeA with wortmannin showed an additive anti-mitogenic effect. An inhibitor of MEK1, PD98059, also inhibited ECGS-stimulated DNA synthesis ($IC_{50\%}$ ~55 µM), but combining PD98059 with MSeA had a similar effect as when PD98059 was used alone. A time course experiment indicated that PI3K (AKT, S6K) activation occurred between 6 and 12 h of ECGS stimulation and 3 µM MSeA exposure decreased AKT phosphorylation after 12 h of exposure whereas no inhibitory effect was observed for ERK1/2 phosphorylation throughout the 30-h exposure duration. Additional experiments indicated that MSeA, wortmannin or a more specific PI3K inhibitor LY294002 appeared to target, in the mid- to late $G_1$ phase, a common mechanism(s) controlling $G_1$ progression to S, while having no inhibitory effect on DNA synthesis once S phase had initiated. Taken together, the results support a potent inhibitory activity at achievable serum levels of MSeA on ECGS-stimulated mitogenesis in the mid- to late $G_1$ phase, and the target(s) of this inhibitory activity appears to be PI3K or components of this signal pathway. At pharmacologic levels of exposure, modulation of ERK1/2 and other protein kinases may be relevant for the pro-apoptotic action of MSeA.

- As reported in *Mol Carcinogenesis* (2002), we tested the hypothesis that methylselenol itself was responsible for exerting these G1 arrest and caspase-mediated apoptosis (Appendix 5). We generated methylselenol enzymatically using seleno-L-methionine as a substrate for L-methionine-α-deamino-γ-mercaptomethane lyase (EC4.4.1.11, also known as methioninase). Exposure of DU145 cells to methylselenol so generated in the sub-micromolar range led to caspase-mediated cleavage of poly(ADP-ribose)polymerase, nucleosomal DNA fragmentation and morphological apoptosis and resulted in a similar profile of biochemical effects as exemplified by the inhibition of phosphorylation of protein kinase B/AKT and extracellularly-regulated kinases 1/2 when compared to methylseleninic acid (MSeA) exposure. In HUVEC, methylselenol exposure recapitulated the $G_1$ arrest action of MSeA on mitogen-stimulated $G_1$ progression during mid- to late-$G_1$. This stage-specificity was mimicked by inhibitors of the phosphatidylinositol 3-kinase. Taken together, the results support methylselenol as an active selenium metabolite for inducing caspase-mediated apoptosis and cell cycle $G_1$ arrest. This cell-free methylselenol generation system is expected to have a significant utility for studying the biochemical and molecular targeting mechanisms of this critical metabolite and may constitute the basis of a novel therapeutic approach for cancer.

- As reported in October, 2000 in *Biochemical and Biophysical Research Communications*, we have developed various assays for angiogenic attributes by extending investigations into silymarin which is an antioxidant polyphenolic compound extracted from milk thistle (Appendix 6). The results indicate that this compound possesses anti-angiogenic attributes in terms of inhibiting VEGF and MMP-2 expression and inhibiting in vitro capillary differentiation. They also showed mechanistic similarities and differences between this class of agents from methyl Se, as expected of the structural differences. These results supported our success in securing a grant ($200,000 direct) from the Komen Foundation to study the anti-cancer and anti-angiogenic activity of silymarin in October, 2000.

- We have published 2 book chapters and 2 invited reviews on the subject of selenium in apoptosis and angiogenesis (See list below).

## 3. Reportable outcomes:

### 3.1 Publications/Manuscripts

1. Jiang, C., W Jiang, C Ip, H. Ganther and <u>JX, Lu</u>. Selenium-induced inhibition of angiogenesis in mammary cancer at chemopreventive levels of intake. *Mol. Carcinogenesis.* 26:213-225, 1999. (**cover story**)

2. Jiang, C. Ganther H and <u>Lu, JX.</u> Monomethyl selenium-specific inhibition of MMP-2 and VEGF expression: Implications for angiogenic switch regulation. *Mol Carcinogenesis.* 29: 236-250, 2000. (**cover story**)

3. Jiang C. Wang, Z. Ganther, H and <u>Lu, JX</u>. Caspases as key executors of methyl selenium induced apoptosis (anoikis) of DU-145 human prostate cancer cells. *Cancer Res.* 61: 3062-3070, 2001.

4. Wang, Z. Jiang, C. Ganther, H. and <u>Lu JX</u>. Antimitogenic and proapoptotic activities of methylseleninic acid in vascular endothelial cells and associated effects on PI3K-AKT, ERK, JNK and p38MAPK signaling. *Cancer Res.* 61: 7171-7178, 2001.

5. Wang, Z. Jiang, C. and <u>Lu JX</u>. Induction of caspase-mediated apoptosis and cell cycle $G_1$ arrest by selenium metabolite methylselenol. *Mol Carcinogenesis*, 34: 113-120, 2002.

6. Jiang C. Agarwal, R and <u>Lu. JX</u>. Anti-angiogenic potential of a cancer chemopreventive flavonoid antioxidant, silymarin: inhibition of key attributes of vascular endothelial cells and angiogenic cytokine secretion by cancer epithelial cells. *Biochem Biophys Res Comm.* 276, 371-378, 2000.

7. <u>Lu, JX</u> Apoptosis and angiogenesis in cancer prevention by selenium. Book chapter 11. *Nutrition and Cancer Prevention*, Pp131-145. Kluwer/ Plenum Publishers, New York, NY. 2000.
8. <u>Lu, JX</u> and Jiang, C. Anti-angiogenic activity of selenium in cancer chemoprevention: Metabolite-specific effects. *Nutrition and Cancer* 40: 64-73, 2001. Invited review.

9. Raich, P., <u>Lu, JX</u>., Thompson, H. and Combs, Jr, G.F. Selenium in cancer prevention: Clinical issues and implications. *Cancer Investigation.* 19:540-553, 2001. Invited review.

10. Combs, GF Jr. and Lu, JX. Selenium as a cancer preventive agent. Chapter 17. In *Selenium: its molecular biology and role in human health.* D.L. Hatfield (editor). Kluwer Academic Publishers, Hingham, MA, 2001.

## 3.2 Abstracts presented at national meetings

J Lu, C. Jiang, Z. Wang, and H. Ganther. Selenium and cancer angioprevention: metabolite-specific anti-angiogenic attributes. Era of Hope 2002 DoD Breast Cancer Research Program Meeting September 25-28, 2002, at the Orange County Convention Center, Orlando, Florida. (Poster presentation).

C. Jiang, Z. Wang and J. Lu. Selenium metabolite methylselenol inhibits $G_1$ to S progression of vascular endothelial cells by targeting phosphatidylinositol 3-kinase (PI3K) pathway during mid- to late-$G_1$ phase. American Association for Cancer Research 93rd Annual meeting. San Francisco, 2002. (Poster presentation).

J Lu, C Jiang and H. Ganther  Methylselenium specific inhibition of cancer epithelial expression of vascular endothelial growth factor. American Association for Cancer Research 92st Annual meeting, New Orleans, 2001 (Poster presentation).

C. Jiang, Z. Wang, H.Ganther and J. Lu. Methylselenol-induced cancer cell anoikis is executed through a caspase-dependent mechanism. American Association for Cancer Research 92st Annual meeting, New Orleans, 2001 (Poster presentation).

Lu, J., Jiang, C., Wang, Z. and Ganther, H. Methylselenol as a proximal inhibitory selenium metabolite for matrix metalloproteinases and angiogenesis (poster presentation) American Association for Cancer Research 91st Annual meeting, San Francisco, April 1-5, 2000.

Jiang, C., Agarwal, R. and Lu, J. Silymarin, a flavonoid phytochemical, inhibits key angiogenic attributes of vascular endothelial cells. American Association for Cancer Research 91st Annual meeting, San Francisco, April 1-5, 2000 (poster presentation).

Lu, J,X. Jiang, W., Jiang, C., Agarwal, C., Wang, Z. and Ip, C. Anti-angiogenic Effects Associated with Mammary Cancer Chemoprevention by Selenium. 90th annual meeting of the American Association for Cancer Research, 1999. Philadelphia (Mini-symposium presentation).

Jiang C., Ganther, H and J. Lu. Methylseleninic acid induces apoptosis and inhibts matrix metalloproteinases of vascular endothelial cells. (Abstract) American Institute for Cancer Research Annual Research Conference. Washington, DC. Sept 2&3, 1999.

## 3.3 Symposium and seminar presentations concerning selenium and angiogenesis by PI

| | |
|---|---|
| March, 2002. | University of Oklahoma School of Medicine, Oklahoma City, OK |
| Feb, 2002. | University of Missouri, Columbia, Mo. |
| Feb, 2002. | University of Louisville, KY. |
| Jan, 2002. | North Carolina State University School of Veterinary Medicine, Raleigh, NC |
| Dec. 2001. | American Health Foundation, Valhalla, NY. |
| Nov. 2001. | University of Kansas Medical Center, Kansas City, KS. |
| Nov. 2001. | University of Illinois School of Medicine at Rockford. |
| Nov. 2001. | Henry Ford Health Systems, Department of Urology, Detroit, MI. |
| Oct. 2001. | Univ of Colorado Health Sciences Center, Medical Oncology. Denver, CO. |

June, 2001.    AMC Cancer Research Center Research Seminar.
May, 2001.    Anti-Cancer, Inc., San Diego, CA.
May, 2001    Department of Pathology, University of Tennessee, Knoxville, TN.
May, 2001    Department of Nutrition. Oklahoma State University, Stillwater, OK.
April, 2001    Eppley Institute for Cancer Research, University of Nebraska, Omaha, NE.
April, 2001    Department of Animal Science, University of Connecticut. Storrs, CT.
March, 2001    Hormel Institute, University of Minnesota, Austin, MN.
Oct, 2000.    US Expert Delegation to Jiangsu Provincial Conference on Agri/Biotechnology. Nanjing, China.
Oct , 2000.    Nanjing University of Chinese Medicine and Pharmacy. Nanjing, China
Oct, 2000.    Nanjing Agriculture University, Nanjing, China.
Nov. 2000.    Chinese Academy of Agricultural Sciences, Beijing.
Oct, 1999.    Cornell University, Ithaca, NY. Div of Nutritional Sciences.
Nov, 1999.    Univ of Colorado Health Sciences Center, Cancer Center Cell Biology Program.
Sept, 1999.    AMC Cancer Research Center,
Sept, 1999.    Symposium speaker. "apoptosis and angiogenesis in cancer chemoprevention by selenium". American Institute for Cancer Research 1999 Annual Research Conference. Washington, DC.

## 3.4. Grants awarded based on data generated during funding period

**Source:**    National Cancer Institute
Title:    Methyl selenium regulation of angiogenic switch mechanisms
Principal investigator:    Lu, Junxuan
Total direct requested:    $825,000 (4 years)

The goal of this grant is to investigate the mechanisms of methylselenium inhibition of mitogenesis, survival and the expression of angiogenic molecule MMP-2 in vascular endothelial cells. This grant will start January 2003.

**Source:**    Department of Defense-Prostate Cancer Program
Title:    Methylselenium and prostate cancer apoptosis
Principal investigator:    Lu, Junxuan
Dates of entire period:    Jan. 7, 2002-Dec 2004
Total direct:    $375,000

**Source:**    Komen Foundation
Title:    Silymarin as a novel breast cancer preventive agent with anti-angiogenic action
Principal investigator:    Lu, Junxuan
Dates of entire period:    10/01/2000-09/30/2002
Total direct for entire period:    $200,000

## 4. Discussion of original specific aims:

Our efforts to develop and refine a Matrigel plug in vivo angiogenesis model of Passaniti et al (4) yielded mixed results. We focused our initial effort on using VEGF as the angiogenic factor. Exogenous VEGF proved to be a very poor stimulant for Matrigel plug assay. After consulting with Dr. Passaniti, we experimented with basic fibroblast growth factor (bFGF) and were able to demonstrate much-enhanced angiogenesis. However, the large inter-animal and

intra-plug variability of vessel responses has limited our application of this assay to test the anti-angiogenic effect of selenium in this model. A significant complication appears to be the immune response mounted by the Sprague-Dawley rats and C57B mice to the injected bFGF-Matrigel solution. After discussions of the variability issue with a number of researchers familiar with this assay, a consensus that emerged out of this interchange of information was that the angiogenic responses and reproducibility could be improved in syngenic or immunodeficient mice.

Because of our discovery of metabolite-specific effects of selenium on MMP-2, VEGF expression and caspase-mediated apoptosis, we pursued these leads that resulted in a greater understanding of the potential targets and mechanisms involved by specific selenium metabolites to account for anti-angiogenic action. These findings extended our original aim of studying structure-activity relationships in the in vivo model. We have been granted funding by NCI to further pursue the investigation concerning angiogenic switch mechanisms.

## 5. Conclusions

The specific inhibitory effects of methylselenium on vascular endothelial cell expression of MMP-2 and on cancer epithelial expression of VEGF and the potent anti-mitogenic and apoptosis activities (through caspases) support and extend the anti-angiogenic activity of selenium in chemoprevention which we first reported in 1999. These observations provide plausible mechanistic explanations of the in vivo finding by Ip and co-workers (1-3) that methylselenol pool appears to be the active cancer chemopreventive Se metabolite. Selenium agents that selectively increase this metabolite pool may be of greater breast cancer preventive benefit in women. Much work remains ahead to test this hypothesis in prevention/clinical trials.

## 6. References cited:

1. Ip C, Ganther HE. Activity of methylated forms of selenium in cancer prevention. Cancer Res. 1990 Feb 15;50(4):1206-11.

2. Ip C, Hayes C, Budnick RM, Ganther HE Chemical form of selenium, critical metabolites, and cancer prevention. Cancer Res. 1991 Jan 15;51(2):595-600.

3. Ip, C. Lessons from basic research in selenium and cancer prevention. J Nutr. 1998. Nov;128(11):1845-54. Review.

4. Passaniti A, Taylor RM, Pili R, Guo Y, Long PV, Haney JA, Pauly RR, Grant DS, Martin GR. A simple, quantitative method for assessing angiogenesis and antiangiogenic agents using reconstituted basement membrane, heparin, and fibroblast growth factor. Lab Invest. 1992 Oct;67(4):519-28.

## 7. List of Appendices

1. Jiang, C., W Jiang, C Ip, H. Ganther and JX. Lu. Selenium-induced inhibition of angiogenesis in mammary cancer at chemopreventive levels of intake. *Mol. Carcinogenesis*. 26:213-225, 1999. (**cover story**)

2. Jiang, C. Ganther H and Lu, JX. Monomethyl selenium-specific inhibition of MMP-2 and VEGF expression: Implications for angiogenic switch regulation. *Mol Carcinogenesis*. 29: 236-250, 2000. (**cover story**)

3. Jiang C. Wang, Z. Ganther, H and Lu, JX. Caspases as key executors of methyl selenium induced apoptosis (anoikis) of DU-145 human prostate cancer cells. *Cancer Res*. 61: 3062-3070, 2001.

4. Wang, Z. Jiang, C. Ganther, H. and Lu JX. Antimitogenic and proapoptotic activities of methylseleninic acid in vascular endothelial cells and associated effects on PI3K-AKT, ERK, JNK and p38MAPK signaling. *Cancer Res*. 61: 7171-7178, 2001.

5. Wang, Z. Jiang, C. and Lu JX. Induction of caspase-mediated apoptosis and cell cycle $G_1$ arrest by selenium metabolite methylselenol. *Molecular Carcinogenesis* 34: 113-120, 2002.

6. Jiang C. Agarwal, R and Lu. JX. Anti-angiogenic potential of a cancer chemopreventive flavonoid antioxidant, silymarin: inhibition of key attributes of vascular endothelial cells and angiogenic cytokine secretion by cancer epithelial cells. *Biochem Biophys Res Comm*. 276, 371-378, 2000.

7. Lu, JX and Jiang, C. Anti-angiogenic activity of selenium in cancer chemoprevention: Metabolite-specific effects. *Nutrition and Cancer* 40: 64-73, 2001. Invited review.

# PI: Lu, Junxuan

# Final report

# Appendices (7 reprints)

# ■ BRIEF COMMUNICATION ■

# Selenium-Induced Inhibition of Angiogenesis in Mammary Cancer at Chemopreventive Levels of Intake

Cheng Jiang,[1] Weiqin Jiang,[1] Clement Ip,[2] Howard Ganther,[3] and Junxuan Lu[1]*

[1]Center for Cancer Causation and Prevention, AMC Cancer Research Center, Denver, Colorado
[2]Roswell Park Cancer Institute, Buffalo, New York
[3]University of Wisconsin-Madison, Madison, Wisconsin

The trace element nutrient selenium (Se) has been shown to possess cancer-preventive activity in both animal models and humans, but the mechanisms by which this occurs remain to be elucidated. Because angiogenesis is obligatory for the genesis and growth of solid cancers, we investigated, in the study presented here, the hypothesis that Se may exert its cancer-preventive activity, at least in part, by inhibiting cancer-associated angiogenesis. The effects of chemopreventive levels of Se on the intra-tumoral microvessel density and the expression of vascular endothelial growth factor in 1-methyl-1-nitrosourea–induced rat mammary carcinomas and on the proliferation and survival and matrix metalloproteinase activity of human umbilical vein endothelial cells in vitro were examined. Increased Se intake as Se-enriched garlic, sodium selenite, or Se-methylselenocysteine led to a significant reduction of intra-tumoral microvessel density in mammary carcinomas, irrespective of the manner by which Se was provided: continuous exposure (7-wk feeding) with a chemoprevention protocol or acute bolus exposure (3 d) after carcinomas had established. Compared with the untreated controls, significantly lower levels of vascular endothelial growth factor expression were observed in a sizeable proportion of the Se-treated carcinomas. In contrast to the mammary carcinomas, the microvessel density of the uninvolved mammary glands was not altered by Se treatment. In cell culture, direct exposure of human umbilical vein endothelial cells to Se induced cell death predominantly through apoptosis, decreased the gelatinolytic activities of matrix metalloproteinase-2, or both. These results indicate a potential for Se metabolites to inhibit key attributes (proliferation, survival, and matrix degradation) of endothelial cells critical for angiogenic sprouting. Therefore, inhibition of angiogenesis associated with cancer may be a novel mechanism for the anticancer activity of Se in vivo, and multiple mechanisms are probably involved in mediating the anti-angiogenic activity. *Mol. Carcinog. 26:213–225, 1999.* © 1999 Wiley-Liss, Inc.

Key words: intratumoral microvessel density; vascular epithelial growth factor; matrix metalloproteinase; apoptosis; 1-methyl-1-nitrosourea

## INTRODUCTION

The published results of a prospective, double-blinded, randomized, placebo-controlled trial by Clark and coworkers demonstrate for the first time that selenized yeast, when used as a supra-nutritional supplement, may be a very effective preventive agent for several major human epithelial cancers [1]. This human trial corroborates the findings from studies of animal models that have shown a potent anti-cancer activity of selenium (Se) in many organ sites with differing biochemical, hormonal, and metabolic profiles [reviewed in 2,3]. The studies using animal model systems have provided significant insight into the possible mechanisms of action of Se in this role. Ip and coworkers have shown that a monomethyl Se metabolite such as methylselenol (CH₃SeH) may be the active Se in vivo against chemically induced mammary carcinogenesis and that the chemopreventive efficacy of a given Se compound may depend on the rate of its metabolic conversion to

that active form [2,4,5]. Mechanistic studies using cell-culture models have so far focused almost exclusively on the cancerous epithelial cells as the targets of the anti-cancer activity of Se and have shown differential cellular, biochemical, and gene expression responses to different forms of Se [2,3,6–8]. To our knowledge, no published report has examined the nonepithelial components as potential targets through which Se might exert a cancer-

preventive effect. Because angiogenesis, that is, the formation of microvessels, is an obligatory component of the carcinogenesis process for supporting clonal expansion, lesion progression, and growth of solid tumors [9–13], we hypothesize that Se may exert its cancer-preventive activity, at least in part, by inhibiting neo-angiogenesis. In this report, we describe animal experiments showing that high levels of Se intake, given either chronically (7-wk feeding) in a chemoprevention setting or acutely (3-d feedings) in bolus doses after mammary carcinomas had reached a certain size, were able to decrease the density of microvessels in chemically induced rat mammary carcinomas. In the chemoprevention experiments, Se-enriched garlic (Se-garlic) and sodium selenite were used. In the acute treatment experiment, selenite and Se-methylselenocysteine (MSeC) were used, the latter being a predominant form of Se identified in Se-garlic [14] and a metabolic methylselenol precursor [4,5]. All three Se forms have been demonstrated to possess potent cancer chemopreventive activity in vivo [2].

Angiogenesis is regulated by the balance between angiogenic factors and inhibitors [10–13]. A primary angiogenic factor is vascular endothelial growth factor (VEGF)/vascular permeability factor [15,16]. The VEGF gene is organized into eight exons and, as a result of alternative splicing, at least four transcripts have been detected that encode mature monomeric VEGFs of 121, 165, 189, and 206 amino acid residues in humans [17]. $VEGF_{121}$ and $VEGF_{165}$ are diffusible forms capable of activating angiogenesis in a paracrine/endocrine manner [17]. The role of $VEGF_{189}$ and $VEGF_{206}$ is less well defined, as they are synthesized but apparently not secreted [17]. VEGF forms symmetric homodimers through intermolecular disulfide bonds, and the dimeric forms are biologically active [18]. VEGF is essential for normal vasculogenesis as well as angiogenesis. A loss of even one VEGF allele has been shown to lead to embryonic lethality, and homozygous mutant embryonic stem cells are incapable of forming tumor [19,20]. Hypoxia, a condition that the cancer cells create and are subjected to in their deregulated growth, is a potent inducer of VEGF expression [21]. In addition, many pro-angiogenic factors such as insulin-like growth factor, tumor necrosis factor-α, fibroblast growth factor, and cytokines [22–25] as well as oncogenic mutations [26–30] stimulate the production of VEGF, supporting its primary role as an angiogenic mediator. In this paper, we present data documenting an inhibitory effect of Se on the in vivo expression of VEGF as one possible mechanism for Se's regulation of the angiogenic switch in a sizeable proportion of the chemically induced mammary carcinomas.

The angiogenesis process itself involves a complex sequence of events [9–13]. When the vascular endothelial cells in existing vessels are stimulated to grow, they secrete proteases such as matrix metalloproteinases (MMPs) [31], which digest the basement membrane surrounding the vessels. The junctions between endothelial cells are altered, cell projections pass through the space created, and the newly formed sprout grows toward the source of the angiogenic stimulus. Continued capillary sprouting angiogenesis depends on the following conditions or processes: the angiogenic stimulus (angiogenic factors, hypoxia, etc.) must be maintained, the endothelial cells must secrete MMPs required to break down the adjacent tissue matrix, the cells themselves must be capable of movement and migration, and endothelial cells must proliferate to provide the necessary number of cells for the growing vessels. The crucial role of specific MMPs such as MMP-2 in angiogenesis has been documented by using knockout as well as other approaches [32–34]. To provide insights into Se action in some of these key processes, we examined the effects of direct Se exposure in cell culture on the proliferation, survival, and gelatinolytic activities of human umbilical vein endothelial cells (HUVEC). The results indicate potential inhibitory effects of Se on endothelial proliferation/survival and the matrix degradation activity critical for sprouting angiogenesis.
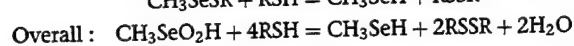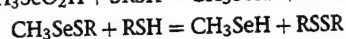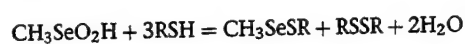
## MATERIALS AND METHODS

### Chemicals and Reagents

Sodium selenite pentahydrate was purchased from J. T. Baker, Inc. (Phillipsburg, NJ). Se-garlic was cultivated and prepared as described previously [35,36]. d,l-MSeC was synthesized by H. Ganther as described elsewhere [4,5]. Rabbit anti–factor VIII and rabbit anti-mouse antibodies were purchased from DAKO Corporation (Carpenteria, CA). Monoclonal mouse anti-VEGF was purchased from Santa Cruz Biotechnology, Inc. (Santa Cruz, CA). Biotinylated donkey anti-rabbit Fab'2 secondary antibody was purchased from Jackson ImmunoResearch Laboratories, Inc. (West Grove, PA). Conjugated alkaline phosphatase–streptavidin was purchased from Biogenex (San Ramon, CA). Protein size markers and enhanced chemoluminescence reagents were purchased from Amersham Life Science (Arlington Heights, IL).

Methylseleninic acid (MSeA; $CH_3SeO_2H$) was recently synthesized by H. Ganther as a proximal precursor of methylselenol, a putative active chemopreventive Se metabolite [2–5]. Briefly, dimethyldiselenide (Aldrich Chemical Co., Milwaukee, WI) was oxidized with hydrogen peroxide (3%) at 65°C until the yellow color of the diselenide had disappeared. The solution was adjusted to pH 7 with KOH and then applied to a column of Dowex 1 (chloride). After washing with water until a negative starch/iodide test was obtained, the MSeA was eluted with 0.01 N HCl. The main starch/iodide-

positive fractions were pooled, adjusted to pH 7 with KOH, and analyzed for total Se by fluorometric analysis. Thin-layer chromatography on cellulose in butanol:acetic acid:water (5:2:3 vol/vol/vol) showed a single starch/iodide-positive spot of $RF = 0.42$. Reduction with excess borohydride gave a single ultraviolet peak (252 nm; mM extinction coefficient, 6.35), corresponding in wavelength and intensity to that of aliphatic selenolates.

Upon reaction with thiols or other reducing agents, MSeA is expected to undergo a four-electron reduction to methylselenol by way of an intermediate selenenylsulfide:

$$CH_3SeO_2H + 3RSH = CH_3SeSR + RSSR + 2H_2O$$
$$CH_3SeSR + RSH = CH_3SeH + RSSR$$
$$Overall: \quad CH_3SeO_2H + 4RSH = CH_3SeH + 2RSSR + 2H_2O$$

Under cellular conditions, it is expected that MSeA initially will react with glutathione to give the glutathioninyl methylselenenylsulfide. This intermediate will undergo further reduction to methylselenol (which ionizes to methyl selenolate at neutral pH) through nonenzymic reduction by excess thiol or by enzymatic reduction through NADPH-linked reductases such as glutathione reductase.

### Design of Animal Experiments

The effects of Se provided in different chemical forms on selected angiogenic parameters were assessed in both a conventional chemoprevention setting in which Se was provided continuously after carcinogen treatment and in an acute-exposure setting after palpable mammary carcinomas had established. Female Sprague-Dawley rats were purchased from Taconic Farms (Germantown, NY) at 21 d of age. The rats were fed a modified AIN-76–based purified diet with corn oil (5%) substituted for soybean oil as the fat source and glucose substituted for sucrose. The animals were housed three per cage in an environment-controlled animal room maintained at $22 \pm 1°C$ with 50% relative humidity and a 12-h light/12-hour dark cycle.

### Continuous Se Exposure Protocol

Two independent animal experiments identical in design were performed on different occasions. Weanling rats were fed the control diet (containing 0.1 ppm Se) until 50 d of age, at which time each rat was given an intraperitoneal injection of 50 mg/kg 1-methyl-1-nitrosourea (MNU) to induce mammary carcinogenesis [37]. Seven days after the MNU injection, one group remained on the control diet, and the other group was fed a diet supplemented with 3 ppm Se as either Se-garlic (Experiment 1) or sodium selenite (Experiment 2). At 8 wk after the MNU injection (i.e., 7 wk of Se intervention, in contrast to a typical 6-mo protocol for most carcinogenesis experiments), the rats were killed by inhalation of gaseous carbon dioxide and cervical dislocation. Mammary tumors were dissected, and those greater than 0.1 g were frozen in liquid nitrogen. Uninvolved mammary tissue was also obtained from the Se-garlic experiment, fixed in formalin, and processed for microvessel staining. As shown in Table 1, consumption of either Se-garlic or selenite at a chemopreventive level led to decreased tumor multiplicity, decreased tumor burden, or both.

### Acute Se Exposure Protocol

In experiment 3, female rats were given an intraperitoneal injection of 50 mg MNU/kg body weight at 21 d of age to induce mammary carcinogenesis [38]. Starting 4 wk after the carcinogen was administered all rats were palpated daily for the detection of mammary tumors. Tumor dimensions were measured using a caliper. When mammary tumors reached or exceeded approximately 1 cm on the longest dimension, the tumor-bearing rats were randomly assigned to one of three groups: (i) gavage control (ii) once-daily gavage of 2 mg Se/kg body weight as MSeC, or (iii) once-daily gavage of 2 mg

Table 1. Effects of Dietary Supplementation with Se-garlic (Experiment 1) or Selenite (Experiment 2) on MNU-Induced Mammary Carcinogenesis*

| Supplemental selenium | Supplement level | Number of rats | Number of carcinomas[†] | Total Tumor burden[‡] |
|---|---|---|---|---|
| Experiment 1 | | | | |
| None | 0 | 9 | 9 | 5.3 g |
| Se-garlic | 3 ppm | 9 | 6 | 2.7 g |
| Experiment 2 | | | | |
| None | 0 | 15 | 25 | ND |
| Selenite | 3 ppm | 15 | 7 | ND |

*Mammary tumors were collected from Sprague-Dawley rats at the end of the 7-wk feeding intervention.
[†]In the Se-garlic experiment (Experiment 1), only lesions greater than 0.1 g were collected. In the selenite experiment (Experiment 2), all lesions visible under 7 × magnification were collected, but the tumor weight was not recorded.
[‡]Tumor burden is the sum of tumor weight for tumor bearing animals for each group. ND, not determined.

Se/kg body weight as sodium selenite. The Se gavage was repeated two more days for a total exposure of 6 mg of Se/kg body weight over 3 d. At 24 h after the last Se dose, the rats were killed, and the mammary tumors were dissected. A portion of each tumor was fixed in formalin for histological analysis and immunohistochemical (IHC) staining, and the rest was frozen in liquid nitrogen for later biochemical analyses.

## Microvessel Evaluation

Microvessels were detected by staining for vascular endothelial cells by using an antibody specific for factor VIII/von Willebrand's factor–related antigen, a marker for vascular endothelial cells [39,40]. Formalin-fixed, paraffin-embedded carcinomas were cut into 5-µm sections and placed on 3-amino propyltriethaoxysilane treated slides (X-tra Surgipath, Richmond, IL). The sections were immobilized at 60°C for 20 min and deparaffinized with three changes of xylene for 5 min each. After rehydration in a series of graded ethanols and, finally, distilled water, the sections were treated with 0.4% pepsin (0.4 g+100 mL $H_2O$+500 µL of 2 N HCl) at 37°C for 15 min to retrieve the antigen. Normal donkey serum (diluted 1:5 in phosphate-buffered saline (PBS)) was added to block nonspecific binding for 20 min at room temperature after the sections had been rinsed with three changes of distilled water and PBS each. Excess serum was drained and primary rabbit anti–factor VIII antibody (diluted 1:800) was applied for 30 min. After three rinses with PBS for 5 min each, biotinylated donkey anti–rabbit Fab'2 secondary antibody (diluted 1:1000) was applied for 30 min, and the sections were rinsed. Conjugated alkaline phosphatase–streptavidin (diluted 1:80) was applied for 30 min. The slides were rinsed with three changes of PBS for 5 min each, incubated with one tablet of fast red chromogen (Biogenex, San Ramon, CA) plus 5 mL of naphthol buffer for 10 min, and counterstained with Harris hematoxylin (diluted 1:10) for 2 min.

The intratumoral microvessels were counted separately for the stromal areas and within the tumor epithelium–rich lobules (intra-lobular), each on 10 hot-spot fields [40] representing a total area of 0.5 mm². To facilitate counting, each hot-spot field was projected onto a computer screen (CAS-200; Becton-Dickinson/Cellular Analysis Systems, San Jose, CA), and the contrast was adjusted to highlight the vessels. All vessels within a preset rectangle (equivalent to 0.05 mm²) were counted. To determine whether Se might exert a differential effect on microvessels of different sizes, we classified the microvessels into three categories: "large," a cross-section diameter of 10 or more cells; "medium," five to nine cells; and "small," one to four cells. For the uninvolved mammary glands, which were composed of mostly adipocytes and a very small fraction of mammary epithelial structures (ducts, lobules), microvessels in 10 random fields were counted according to these three size categories.

## VEGF Expression

The pattern of VEGF expression in MNU-induced rat mammary carcinomas was determined by IHC staining on formalin-fixed sections after microwave antigen retrieval in 10 mM sodium citrate buffer, pH 6. Mouse anti-VEGF primary antibody was incubated at room temperature. Conjugated horseradish peroxidase–streptavidin (Dako P397; DAKO corporation) diluted 1:1000 was used for binding to biotinylated rabbit anti-mouse secondary antibody (diluted 1:100; PAKO corporation). After rinsing in PBS, the slides were incubated with diaminobenzidine chromogenic substrates (Sigma #D5637; Sigma Chemical Co., St. Louis, MO, at 3 mg of diaminobenzidine in 5 mL of PBS+20 µL of $H_2O_2$) for 10 min. The expression level of VEGF protein isoforms was assessed by immunoblot analyses of carcinoma extracts. Histologically classified adenocarcinomas (frozen) were homogenized in nine volumes of RIPA buffer (50 mM Tris-HCl, pH 7.4; 150 mM NaCl; 2 mM EDTA; 50 mM NaF; 1% Triton X-100; 1% Sodium deoxycholate; 0.1% sodium dodecyl sulfate (SDS); 1 mM dithiotratol; 5 mM sodium orthovanadate; and 1 mM phenylmethylsulfonyl fluoride and 38 µg/mL aprotinin were added fresh). After centrifugation (14 000 × $g$ for 20 min) the supernatants were recovered, and the protein content was quantified by the Bradford dye-binding assay (Bio-Rad Laboratories, Richmond, CA). Forty microgram of total protein was size-separated by electrophoresis on 15% SDS-polyacrylamide gels under non-reducing conditions. Equal loading was confirmed by Coomassie staining of replicate gels and by reprobing blots for β-actin expression. Protein size markers were loaded on each gel to estimate the sizes of the proteins being detected. The proteins were electroblotted onto nitrocellulose membranes, and the VEGF proteins were detected by probing with the same antibody used for IHC staining. Lung tissue was used as a positive-control source of in vivo VEGF. The relative protein level was determined by enhanced chemiluminescence and x-ray film detection. The exposure time was adjusted so that the signal intensity remained in the quantifiable range. The x-ray films were digitized with a transmission scanner, and the signal intensity was quantitated with the UN-SCAN-IT gel-scanner software (Silk Scientific, Inc., Orem, UT). The signals (pixels) were normalized to those of the corresponding β-actin. The normalized expression data were used for statistical evaluations.

## Cell Culture

HUVEC were obtained from the American Type Culture Collection (Manassas, VA). They were

propagated in F12K medium containing 10% fetal bovine serum, 2 mM L-glutamine, 100 μg/mL heparin (Sigma Chemical Co.), and 30 μg/mL bovine endothelial cell growth supplement (ECGS; Sigma Chemical Co.). Experiments were conducted within 15 passages of receipt from the American Type Culture Collection. For growth and survival experiments, HUVEC were seeded into 6-well plates for 24–48 h to reach a confluence of about 50%. Fresh medium was replaced, and Se as either sodium selenite or MSeA was added from 100 × stock solutions prepared in PBS. Morphological responses were monitored over time, the cells remaining adherent were fixed in 1% glutaraldehyde and stained with methylene blue, and the cell number was then counted on three high-power (200 ×) fields. Detached cells (in 500 μL of medium) were centrifuged onto slides, fixed in 1% glutaraldehyde, and stained in hematoxylin and eosin.

## Zymogram Analysis

HUVEC were seeded into 6-well plates in complete medium for 24–48 h to reach 70–80% confluence. The cells were washed two times with PBS to remove spent medium and refed serum-free medium supplemented with 100 μg/mL ECGS and treated with selenite or MSeA for 6 h (a time frame that did not result in visible cell death or detachment). Conditioned medium and cell lysates (prepared in 1% Triton X-100; 0.5 M Tris-HCl, pH 7.6; and 200 mM NaCl) were analyzed for gelatinolytic activities on substrate gels [41]. Type I gelatin (Sigma Chemical Co.) was added to the standard acrylamide mixture in the resolving gels at a final concentration of 0.3%. Samples were mixed with 5 × loading buffer (10% SDS; 50% glycerol; 0.4 M Tris-HCl, pH 6.7; and 0.1% bromophenol blue) and loaded onto 5% stacking/10% resolving gels. The gels were run at room temperature with cooling (85 V, 4–5 h). After running, the gels were soaked in 2.5% Triton X-100 with gentle shaking for 20 min. The washing was repeated two more times to remove the SDS. The gels were then washed in water once for 20 min and incubated at 37°C for 24–48 h in substrate buffer (50 mM Tris-HCl, pH 8.0, and 5 mM CaCl$_2$). After incubation, the gels were stained for 1 h in Brilliant Blue R250 and destained until clear bands appeared on a blue background. The gels were digitized with a transmission scanner and band intensity (on inverted images) was quantified by using the UN-SCAN-IT gel-scanner software (Silk Scientific, Inc.).

## Statistical Analyses

The microvessel counts among groups were compared by student's t-test or analysis of variance, as appropriate. For VEGF expression, for which the variance was not normally distributed, the rank-order test was used.

## RESULTS

### Effect of Se on Microvessel Density and VEGF Expression in a Chemoprevention Context

In MNU-induced mammary carcinomas, the microvessels were concentrated in the fibro-connective stromal areas and spread along stromal ridges on the periphery of epithelial-rich tumor lobules. Microvessels were occasionally observed within such tumor lobules; these vessels are referred to in this report as intra-lobular microvessels. Table 2 presents the vessel counts in carcinomas obtained from rats consuming either the control diet or Se-supplemented diets for 7 wk. In the Se-garlic experiment (Experiment 1), the total microvessel densities (counts/0.5 mm$^2$) in the stromal and intra-lobular areas from Se-fed rats were 34% and 61% lower, respectively, than in those of rats fed the control diet. When categorized by the size of the microvessels, small microvessels (with a crosssection diameter of one to four cells) accounted for most of the microvessels in the intra-lobular and stromal areas (Table 2). The observed reduction in intra-tumoral microvessel density (IMVD) in the Se-garlic–fed group occurred almost exclusively in these small microvessels in both the stromal and intra-lobular areas (Table 2). The microvessel density of the uninvolved mammary glands was not decreased by Se-garlic treatment (Table 2); the vessel size distribution in the normal glands was less in favor of the small vessels in comparison with that seen in carcinomas. In the selenite experiment (Experiment 2), 3 ppm selenite exerted a similar degree of reduction of microvessel density in the stromal area of the mammary carcinomas, and the inhibitory effect was again observed predominantly in the small microvessels (Table 2).

Because large carcinomas were likely to contain larger and more vessels than were their small counterparts, it would be expected that the observed lower IMVD in the Se-treated animals might have been biased by the size of the carcinomas examined. To investigate this issue, we analysed the IMVD data against the sizes of the carcinomas in the Se-garlic experiment (Experiment 1), in which the approximate weight of each individual carcinoma was available (Figure 1). The stromal microvessel density in both the control and Se-garlic groups showed a modest linear regression trend over the size (Figure 1A). However, the regression trend line for the Se-garlic group was downshifted in parallel to that of the control group, indicating a reduction of vessel density across the tumor-size ranges evaluated (Figure 1A). The intra-lobular microvessels displayed a greater degree of difference between the control and Se-treated groups as the tumor size increased (Figure 1B). Albeit limited by the small sample size analyzed, these data indicated that the

Table 2. Effects of Dietary Supplementation with Se-garlic (Experiment 1) or Selenite (Experiment 2) on Microvessel Density (counts/0.5 mm$^2$) of MNU-Induced Rat Mammary Carcinomas and Non-involved Mammary Glands*

| Dietary group | Number of rats | Total microvessels | Large ($\geq$ 10 cells) | Medium (5–9 cells) | Small (1–4 cells) |
|---|---|---|---|---|---|
| Experiment 1 | | | | | |
| Stromal areas: | | | | | |
| Control | 9 | 69.4 ± 6.0$^a$ | 4.8 ± 0.8 | 9.9 ± 1.2 | 54.8 ± 5.7$^a$ |
| Se-garlic, 3 ppm | 6 | 45.8 ± 6.4$^b$ | 3.0 ± 1.1 | 7.7 ± 2.0 | 35.2 ± 5.7$^b$ |
| Intra-lobular areas: | | | | | |
| Control | 9 | 16.0 ± 2.2$^a$ | 0 ± 0 | 0.4 ± 0.2 | 15.6 ± 2.3$^a$ |
| Se-garlic, 3 ppm | 6 | 6.2 ± 1.2$^b$ | 0.2 ± 0.2 | 0.3 ± 0.3 | 5.7 ± 1.2$^b$ |
| Uninvolved mammary tissue: | | | | | |
| Control | 6 | 8.7 ± 0.7 | 1.8 ± 0.5 | 2.7 ± 0.4 | 4.2 ± 0.8 |
| Se-garlic, 3 ppm | 6 | 7.2 ± 0.9 | 1.3 ± 0.4 | 2.0 ± 0.7 | 3.8 ± 0.6 |
| Experiment 2 | | | | | |
| Stromal areas: | | | | | |
| Control | 8 | 80.0 ± 4.4$^a$ | 0.9 ± 0.4 | 4.4 ± 1.7 | 74.8 ± 5.3$^a$ |
| Selenite, 3 ppm | 4 | 61.0 ± 3.0$^b$ | 0.3 ± 0.3 | 3.8 ± 2.8 | 57.0 ± 2.1$^b$ |

*Values are presented as means ± standard errors of the mean. The values within a column bearing dissimilar superscripts ($^a$ and $^b$) are significantly different ($P < 0.05$).

observed reduction of IMVD as a result of chronic exposure to a chemopreventive level of Se could not be entirely accounted for by tumor-size differences.

IHC staining for VEGF proteins in the MNU-induced mammary carcinomas was confined to the cytosol and was mostly localized in the cancerous epithelial cells, with light staining in some stromal cells. Such a staining pattern indicated that the cancerous epithelial cells were the major source of the in vivo expression of this angiogenic factor in this chemically induced model of mammary cancer. Figure 2 shows representative western immunoblot analyses of VEGF expression in selected carcinomas (i.e., those that were large enough for the biochemical assessment). The rat lung tissue (positive control for VEGF) expressed VEGF proteins with apparent dimeric sizes of about 32 and 36 kDa, presumably corresponding to the VEGF$_{164}$ protein (the rat proteins are one amino acid shorter than their human homologs) of varying glycosylation states [14] or VEGF$_{164}$/VEGF$_{188}$. The 32 and 36 kDa VEGF proteins were the most predominantly expressed bands in the mammary carcinomas; other smaller bands suggestive of VEGF$_{120}$ were also expressed. Based on the limited number of samples analyzed, two of five carcinomas in the Se-garlic group (Figure 2A) and two of four carcinomas in the selenite group (Figure 2B) showed a marked reduction in VEGF expression to almost undetectable levels. Overall, carcinomas from Se-garlic– or selenite-fed rats displayed 45% and 75% reductions of VEGF expression, respectively, in comparison with the levels from the control rats.

Acute Effects of Se on Microvessel Density and VEGF Expression in Established Carcinomas

As shown in Table 3, acute treatment of established mammary carcinomas with either MSeC or selenite decreased the IMVD by 28–32% in the

**A. Stromal microvessel density**
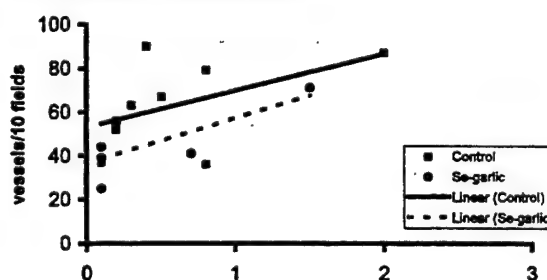


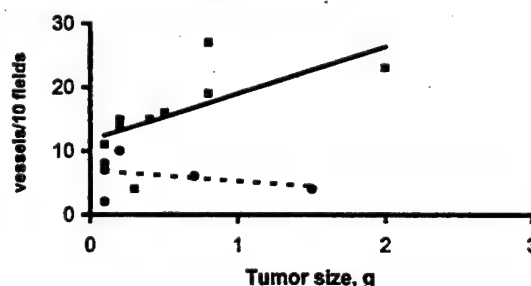**B. Intralobular microvessel density**



Figure 1. Correlation plots of stromal (A) and intra-lobular (B) microvessel densities against the approximate sizes of the MNU-induced mammary carcinomas examined. The linear regression trend line for each group is shown.
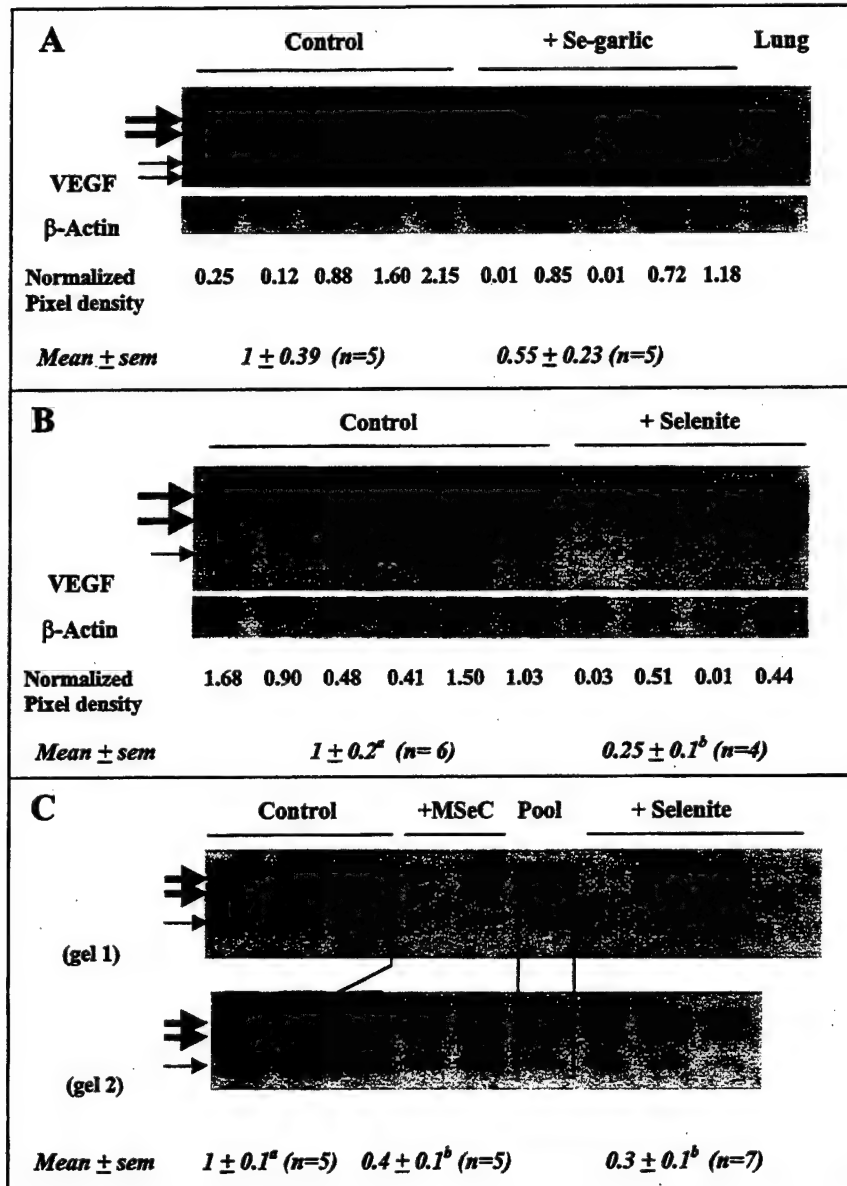
Figure 2. Western blot analyses (nonreducing gel) of the expression level of VEGF proteins in MNU-induced rat mammary adenocarcinomas. Two bands with apparent dimer masses of 32 and 36 kDa (marked by heavy arrows) were presumably $VEGF_{164}$ of varying glycosylation states [14] or $VEGF_{164}$ and $VEGF_{188}$. The additional smaller bands (marked by light arrows) were most likely $VEGF_{120}$. Forty micrograms (by the Bradford dye assay) of carcinoma protein extract was loaded from each sample. After probing for VEGF, the membrane was stripped and reprobed for β-actin expression to correct for loading differences. Rat lung was used as a positive control for VEGF expression. The normalized expression level (pixel intensity) for individual samples is shown below each lane. The group means and number of samples analyzed are shown for each experiment, and those means within the same experiment bearing different superscripts were statistically different. (A) Se-garlic chemoprevention experiment (Experiment 1). (B) Selenite chemoprevention experiment (Experiment 2). (C) Acute Se treatment experiment (Experiment 3). Two separate gels were used in this experiment to accommodate all the samples. Pool = a pooled sampled of the carcinoma extracts from the various groups.

stromal areas; the effect was most profound with the small and medium-size microvessels. Both Se treatments led to a 60–70% reduction in VEGF proteins (Figure 2C). As in the chemoprevention experiments only a sizeable proportion of the mammary carcinomas showed marked reduction of VEGF expression in response to acute Se treatments; the remainder were not altered (Figure 2C).

### Effects of Se on Growth/Survival of HUVEC

Treatment of HUVEC with MSeA led to cell retraction (Figure 3A vs. B) and detachment from the flask (Figure 3C). Such changes began to appear 10–12 h after treatment was initiated. Morphologically, most affected cells displayed apoptotic features, as indicated by nuclear condensation and

Table 3. Effects of Acute Se Treatment on Microvessel Density (Counts/0.5 mm$^2$) in the Stromal Areas of Established Mammary Carcinomas (Experiment 3)*

| Treatment group | Number of carcinomas | Total microvessels | Large ($\geq$ 10 cells) | Medium (5–9 cells) | Small (1–4 cells) |
|---|---|---|---|---|---|
| Control | 5 | 93.6 ± 4.7[a] | 2.2 ± 0.6 | 11.0 ± 0.8[a] | 80.4 ± 4.5[a] |
| MSeC | 7 | 67.3 ± 5.9[b] | 4.7 ± 0.9 | 8.1 ± 0.7[b] | 54.4 ± 6.3[b] |
| Selenite | 6 | 63.8 ± 3.0[b] | 3.8 ± 1.0 | 7.8 ± 1.6[b] | 52.2 ± 3.4[b] |

*Values are presented as means ± standard errors of the mean. The values within a column bearing dissimilar superscripts ([a] and [b]) are significantly different ($P < 0.05$).

formation of apoptotic bodies. Replating these detached cells in fresh medium did not result in any cell attachment or growth. After 48 h of MSeA treatment, the adherent cell number was reduced by as much as 80% at 2 µM, and virtually no cell remained attached at 6 µM (Figure 3F). Treatment with selenite at 4 µM or lower for 48 h did not decrease the number of adherent cells and resulted in a concentration-dependent decrease beyond this level (Figure 3F). Morphologically, selenite treatment resulted in both apoptosis and detachment of cells, some of which did not show cell retraction and nuclear condensation (Figure 3D and E).

### Effects of Se on Gelatinolytic (MMP) Activities

A brief treatment (6 h, before overt morphological changes) with MSeA led in both the conditioned medium and the cell lysates to a Se concentration–dependent reduction in gelatinolytic activities of a 72 kDa species, corresponding to the latent form of gelatinase A/MMP-2 (Figure 4, lanes 2–5 and 9–12) [31,41]. The gelatinolytic activity of a 53-kDa species [41], which was less abundant than MMP-2, showed a similar pattern of inhibition by MSeA in the medium (Figure 4, lanes 2–5). Incubating the conditioned medium from the untreated cells for 6 h at 37°C with 10 µM MSeA in a test tube did not inhibit the gelatinolytic activities (Figure 4, lane 7 vs. lane 6). This comparison indicated that the inhibitory effect did not result from direct reaction of MSeA with the secreted gelatinases/MMPs and was therefore dependent on cell metabolism to generate the active Se, presumably methylselenol or its derivatives. In contrast to treatment with MSeA, treatment with 10 µM selenite for 6 h did not significantly affect the gelatinolytic activities in either the conditioned medium or the cell lysates (Figure 4, lane 8 vs. lane 2 and lane 13 vs. lane 9).

### DISCUSSION

To our knowledge, this communication is the first to report a reduction of the density of microvessels, especially of capillaries with a crosssection diameter of four of fewer cells, in MNU-induced mammary carcinomas by the consumption of chemopreventive levels of Se. This effect was observed with different forms of Se (i.e., Se-garlic, selenite, and MSeC) and with different Se exposure protocols. In the conventional chemoprevention setting, feeding Se for 7 wk (chronic exposure) led to decreased tumor multiplicity, decreased tumor burden, or both (Table 1) and a significant reduction in IMVD in both the fibro-connective stromal areas and the epithelial-rich intra-lobular areas (Table 2). Furthermore, the observed reduction in IMVD could not be entirely accounted for by the tumor-size differences between the groups (Figure 1); this was especially apparent for the intra-lobular microvessels. Because the microvessel density of the uninvolved mammary glands was not decreased by Se-garlic (Table 2), the effect of chemopreventive levels of Se on IMVD reduction appeared to be neoplasia specific. In both stromal areas and intra-lobular areas, the small microvessels with crosssection diameters of one to four cells were most responsive to the Se effect.

However, it is noteworthy that in a chemoprevention setting, carcinomas that emerge in the presence of the selective pressure exerted by an intervening agent would be considered relatively refractory or resistant to the action of that agent. Therefore, the observed reduction in IMVD in carcinomas from the groups chronically fed Se may in fact indicate an underestimation of the true extent of an anti-angiogenic response in the "sensitive" lesions, which would take a longer time to reach a detectable size or would never have reached a detectable size. To seek more direct evidence of anti-angiogenic activity, we examined the effects of acute Se treatment on IMVD in the established mammary carcinomas (Table 3). We observed a one-third reduction in IMVD after 3 d of Se gavage. As in the chemoprevention setting, decreases in the number of the small microvessels accounted for this observed effect on IMVD.

Because growing or newly sprouted vessels are likely to be smaller, the observation of exclusive reduction of small microvessels suggests that chemopreventive intake levels of Se may target regulatory mechanisms governing genesis, survival, or both of the growing microvessels in the tumor environment. In the work reported here, we investigated the impact of Se on the in vivo expression of
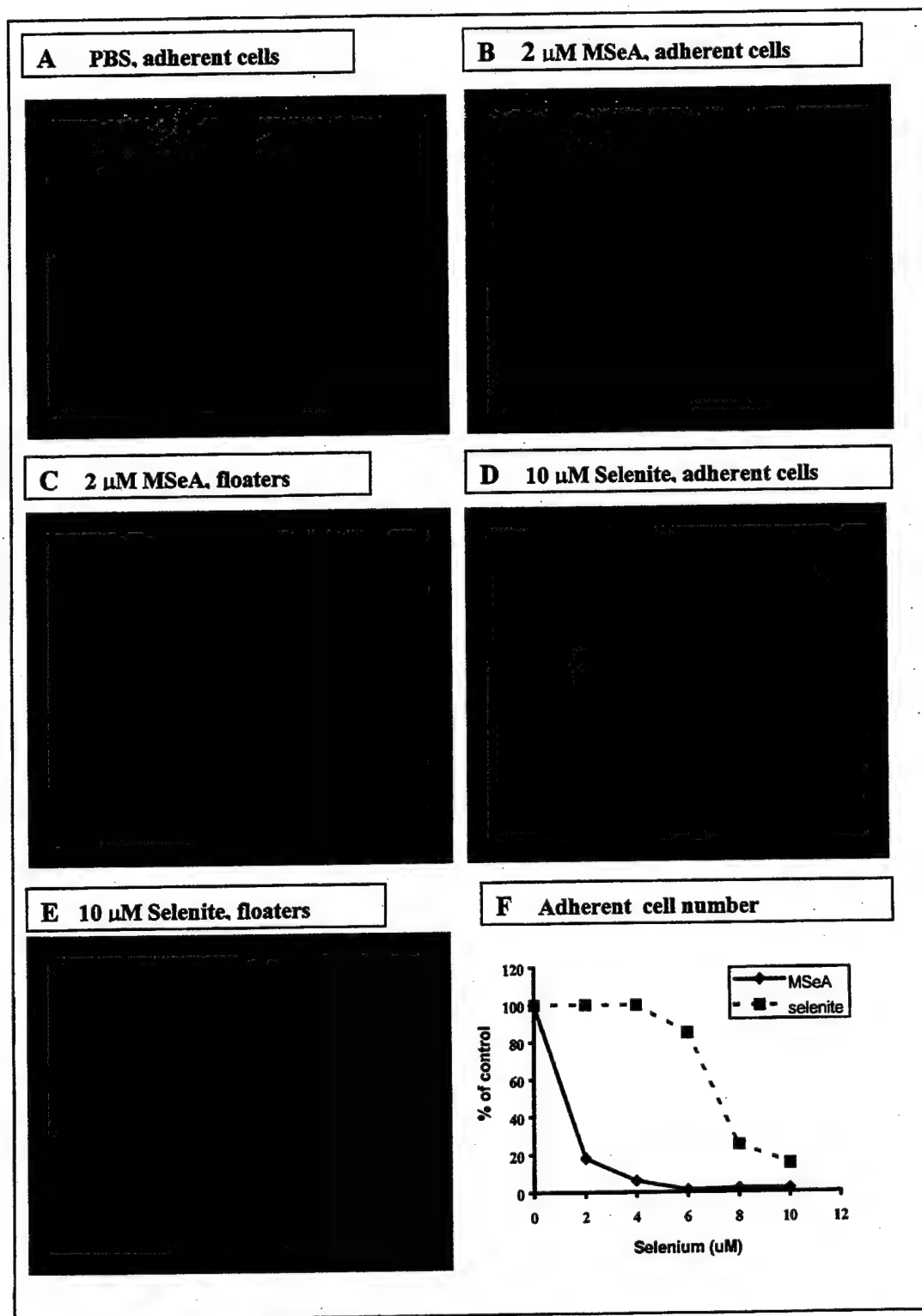
Figure 3. Effects of selenium treatment on the growth and survival of HUVEC. (A) HUVEC treated with PBS (vehicle) for 48 h as controls. (B) Adherent cells after 48 h of treatment with 2 µM MSeA. (C) Detached cells as a result of treatment with 2 µM MSeA for 48 h. Note the extensive nuclear condensation and fragmentation. (D) Adherent cells after 48 h of treatment with 10 µM selenite. (E) Detached cells as a result of treatment with 10 µM selenite for 48 h. Note the extensive nuclear condensation in some but not other cells. (F) Adherent cell number as a function of the Se concentration after 48 h of treatment.

**A  Conditioned Medium**  **B  Cell Lysate**

| | | MSeA | | | MSeA | | Sel | | | MSeA | | Sel | |
|---|---|---|---|---|---|---|---|---|---|---|---|---|---|---|
| | 0 | 2 | 5 | 10 | 0+0 | 0+10 | 10 | 0 | 2 | 5 | 10 | 10 | µM |

72 kD
53kD

Lane # 1 2 3 4 5 6 7 8 9 10 11 12 13

72 kD
53 kD

**Pixel Density**

%  100 54 34 27    94 100 48 33 14 83

%, test tube incubation   100 99

Figure 4. Representative zymographic analyses of the effects of selenium treatment of HUVECs on their secreted (A) and cell-associated (B) gelatinolytic activities. HUVECs were treated with either MSeA or Sel in a 6-well plate for 6 h in serum-free medium supplemented with 100 µg/mL ECGS. The gelatinase activities of the conditioned media (panel A, lanes 2–5 and 8) and cell lysates (panel B) were analyzed on gelatin I–impregnated substrate gels. Conditioned medium from untreated cells was also incubated with 10 µM MSeA (lane 7) or PBS (lane 6) for 6 h and analyzed zymographically to determine whether MMP inactivation was caused by direct reaction between the enzyme proteins with MSeA per se. The inverted images of the zymograms (lower panels) were used for densitometric quantitation. The relative pixel density for the 72-kDa gelatinase A/MMP-2 is shown below each lane. The arrowheads on the left mark the positions of molecular mass standards corresponding to (from top) 97, 66, and 47 kDa. Lane 1 contains serum-free medium as a blank control.

VEGF, a primary angiogenic molecule crucial for the genesis and survival of capillary vessels. IHC staining showed that the cancerous epithelial cells were the major source of VEGF in the mammary carcinomas induced by MNU. This expression pattern agrees with that reported for mammary carcinomas induced by a different mammary chemical carcinogen, 7,12-dimethylbenz[a]anthracene [42]. In both the chemopreventive and acute-treatment exposure settings, the VEGF expression level in a sizeable proportion, but not all, of the Se-treated carcinomas was significantly lower than in untreated controls (Figure 2), regardless of the form of Se used. The role of VEGF in initiating and especially in maintaining neo-angiogenic processes and in supporting endothelial survival has been extensively documented. Whereas overexpression of VEGF is linked to increased angiogenesis and more aggressive tumor behavior [43,44], anti-angiogenic interventions, especially those based on VEGF antibodies or interference with signal transduction through its receptors [45–49], have been shown to result in the inhibition of tumor growth and induction of endothelial apoptosis. More profoundly, germline knockout experiments have shown that loss of even one VEGF allele leads to embryonic lethality in heterozygotes and that

homozygous mutant embryonic stem cells are incapable of forming tumors [19,20], suggesting a critical threshold effect of VEGF level to mediate and maintain normal vasculogenesis and neo-angiogenesis. In light of the crucial role of VEGF in endothelial proliferation and survival [45–49], it is therefore possible for Se-induced reduction of VEGF production in those affected tumors to lead to reduced endothelial proliferation and survival and consequently a reduction in the density of small microvessels.

In addition to or independent of VEGF inhibition, the direct apoptogenic effect of Se exposure on vascular endothelial cells, the inhibition of the endothelial cells' ability to degrade tissue matrix, or both may also contribute to the anti-angiogenic activity. The consequence of endothelial apoptosis could be collapse of microvessels and reduction in microvessel density. Vascular endothelial cells, by their very nature of lining the blood vessels, are exposed to Se before the delivery of serum Se to the cancerous mammary epithelial cells. The cell-culture data presented in Figure 3 indicate that serum-achievable levels (2 µM or less) of Se as MSeA, a proximal Se precursor of the putative active anti-cancer Se metabolite methylselenol [2–5], induced apoptosis of HUVEC by direct exposure. Selenite

also exerted cytocidal effects on HUVEC but a higher exposure level (fourfold) was needed to achieve the same extent of cell death. Furthermore, a brief treatment (6 h) of HUVEC with MSeA resulted in concentration-dependent inhibition of secreted and/or cell-associated gelatinolytic activities (Figure 4). The inhibitory effect of MSeA on MMPs was dependent on cell/metabolism-activation to yield the putative active Se metabolite methylselenol, because direct incubation of the conditioned medium with MSeA in a test tube did not affect the gelatinase activities (Figure 4). In support of a MSeA/methylselenol-specific inhibitory effect on MMPs, selenite at a level (10 μM) that induced apoptotic and cytolytic effects on HUVEC did not significantly inhibit MMP activity. The crucial role of MMP-2 in capillary angiogenesis was recently established in germline knockout as well as other model systems [32–34]. The MMP inhibitory activity observed here extends the active Se metabolite hypothesis of cancer chemoprevention [2–5] to include a specific action of methylselenol or its derivatives on a key process crucial for angiogenesis, that is, the matrilytic activity of the stimulated endothelial cells to invade the fibro-connective support structures during sprouting. This may offer an explanation for the greater in vivo chemopreventive efficacy of methylselenol precursor compounds (MSeC, Se-garlic, and methylselenocyanate) over selenite and conventional selenoamino acids [2]. That both methylselenol precursors and selenite were observed in this study to reduce VEGF expression and IMVD in the mammary carcinomas in the animal model may reflect the ability of in vivo Se metabolism to generate the active Se metabolites with endothelial apoptogenic and MMP inhibitory activities. This metabolic conversion activity is probably relatively inefficient, if not absent, in cell culture. Future work will determine the significance of and mechanisms involved in Se-induced endothelial apoptosis and MMP inhibition in cancer chemoprevention.

As a matter of speculation on the mechanisms of Se regulation of VEGF expression, MMP activity, and apoptosis, a common thread may rest in redox regulation of the activity of transcriptional factors or redox modification of functional state/activity of redox-sensitive proteins. In the case of VEGF, hypoxia is a potent inducer of VEGF expression [21], and this effect is principally mediated by the hypoxia-inducible factor-1 and activator protein-1 (AP-1) [50–53]. The activity of many nuclear factors such as hypoxia-inducible factor-1 and AP-1 is redox regulated [53,54]. Because hypoxia is commonly experienced by cancerous epithelial cells as the expanding clones strive to grow in size [55], it is possible that Se may inhibit hypoxia induction of VEGF expression by modulating the activity of these transcriptional factors. Thioredoxin has been considered a critical redox mediator for these nuclear

factors [53], and its redox state may be controlled by Se through thioredoxin reductase, a newly recognized selenoprotein [56–59]. Indeed, severe Se deficiency has been reported to differentially modulate the DNA binding activity of liver nuclear extract to AP-1 and NF-kB sequences [60]. It is conceivable that the transcriptional activity of these factors, and consequently VEGF expression, may be redox-regulated by thioredoxin reductase in the nutritional range of Se supplementation. On the other hand, AP-1 and NF-kB activities have been shown to be potently inhibited by high levels of Se exposure in cell culture [61,62]. Such an inhibitory effect, which is probably more relevant to chemopreventive levels of Se exposure, may result from the modulation of cysteine residues by Se through formation of Se-S mixed disulfides or selenotrisulfides in these factors and other intracellular proteins. This topic was recently reviewed [63]. As far as MMPs are concerned, the inhibitory effect was not caused by MSeA per se, but most likely through the intracellular generation of methyselenol or its derivatives as described earlier. It remains to be determined whether the inhibitory effect is at the mRNA level or the protein level or whether it results from a direct modification of the MMP enzymatic activity. Relevant to the latter, MMP-2 expression in fibroblasts has been shown to be regulated by thiol antioxidants [64] and oxidation of MMP-2 in the test tube has been found to lead to its inactivation [65]. Because apoptosis initiation and execution in many models involve cysteine proteases (caspases), an additional hypothesis to be tested is that Se somehow exerts apoptogenic effects through modulation of the cysteine in such caspases [63].

Taken together, the in vivo and in vitro data presented are consistent with a potential anti-angiogenic effect of Se at chemopreventive intake levels. If proven true, the anti-angiogenesis effect may warrant a paradigm shift concerning cancer prevention research with Se. The carcinogenesis targets, i.e., the epithelial cells, do not exist in isolation in vivo but instead interact with the extracellular matrix and nonepithelial cells (e.g., fibroblasts, lymphocytes, and blood vessels) that reside in the stroma. By inhibiting neoplasia-driven angiogenesis and inducing growth arrest and apoptosis of cancer epithelial cells, Se may inhibit the conversion of avascular lesions to a vascular phenotype, thereby suppressing the progression and growth of the epithelial lesions. Further work is needed to establish the significance of an anti-angiogenic activity as a mechanism of the cancer-preventive activity of Se, especially when used as a nutritional supplement.

## REFERENCES

1. Clark LC, Combs GF Jr, Turnbull BW, et al. Effects of selenium supplementation for cancer prevention in patients with carcinoma of the skin. A randomized controlled trial. Nutritional Prevention of Cancer Study Group. JAMA 1996;276:1957–1963.
2. Ip C. Lessons from basic research in selenium and cancer prevention. J Nutr 1998;128:1845–1854.
3. Combs GF Jr, Gray WP. Chemopreventive agents: Selenium. Pharmacol Ther 1998;79:179–192.
4. Ip C, Ganther HE. Activity of methylated forms of selenium in cancer prevention. Cancer Res 1990;50:1206–1211.
5. Ip C, Hayes C, Budnick RM, Ganther HE. Chemical form of selenium, critical metabolites, and cancer prevention. Cancer Res 1991;51:595–600.
6. Lu J, Jiang C, Kaeck M, Ganther H, Vadhanavikit S, Ip C, Thompson H. Dissociation of the genotoxic and growth inhibitory effects of selenium. Biochem Pharmacol 1995;50: 213–219.
7. Lu J, Pei H, Ip C, Lisk D, Ganther H, Thompson HJ. Effect of an aqueous extract of selenium enriched garlic on in vitro markers and in vivo efficacy in cancer prevention. Carcinogenesis 1996;17:1903–1907.
8. Kaeck M, Lu J, Strange R, Ip C, Ganther HE, Thompson HJ. Differential induction of growth arrest inducible genes by selenium compounds. Biochem Pharmacol 1997;53: 921–926.
9. Folkman J. Tumor angiogenesis: Therapeutic implications. N Engl J Med 1971;285:1182–1186.
10. Folkman J. New perspectives in clinical oncology from angiogenesis research. Eur J Cancer. 1996;32A:2534–2539.
11. Hanahan D, Folkman J. Patterns and emerging mechanisms of the angiogenic switch during tumorigenesis. Cell 1996;86:353–364.
12. Bouck N, Stellmach V, Hsu SC. How tumors become angiogenic. Adv Cancer Res 1996;69:135–174.
13. Zetter BR. Angiogenesis and tumor metastasis. Annu Rev Med 1998;49:407–424.
14. Cai XJ, Block E, Unden PC, Zhang X, Quimby BD, Sullivan JJ. Allium chemistry: Identification of selenoamino acids in ordinary and selenium-enriched garlic, onion and broccoli using gas chromatography with atomic emission detection. J Agric Food Chem 1995;43:1754–1757.
15. Leung DW, Cachianes G, Kuang WJ, Goeddel DV, Ferrara N. Vascular endothelial growth factor is a secreted angiogenic mitogen. Science 1989;246:1306–1309.
16. Keck PJ, Hauser SD, Krivi G, et al. Vascular permeability factor, an endothelial cell mitogen related to PDGF. Science 1989;246:1309–1312.
17. Houck KA, Ferrara N, Winer J, Cachianes G, Li B, Leung DW. The vascular endothelial growth factor family: Identification of a fourth molecular species and characterization of alternative splicing of RNA. Mol Endocrinol 1991;5: 1806–1814.
18. Claffey KP, Senger DR, Spiegelman BM. Structural requirements for dimerization, glycosylation, secretion, and biological function of VPF/VEGF. Biochim Biophys Acta 1995;1246:1–9.
19. Ferrara N, Carver-Moore K, Chen H, et al. Heterozygous embryonic lethality induced by targeted inactivation of the VEGF gene. Nature 1996;380:439–442.
20. Carmeliet P, Ferreira V, Breier G, et al. Abnormal blood vessel development and lethality in embryos lacking a single VEGF allele. Nature 1996;380:435–439.
21. Levy AP, Levy NS, Wegner S, Goldberg MA. Transcriptional regulation of the rat vascular endothelial growth factor gene by hypoxia. J Biol Chem 1995;270:13333–13340.
22. Akagi Y, Liu W, Zebrowski B, Xie K, Ellis LM. Regulation of vascular endothelial growth factor expression in human colon cancer by insulin-like growth factor-I. Cancer Res 1998;58:4008–4014.
23. Yoshida S, Ono M, Shono T, et al. Involvement of interleukin-8, vascular endothelial growth factor, and basis fibroblast growth factor in tumor necrosis factor alpha-dependent angiogenesis. Mol Cell Biol 1997;17:4015–4023.
24. Ryuto M, Ono M, Izumi H, et al. Induction of vascular endothelial growth factor by tumor necrosis factor alpha in human glioma cells. Possible roles of SP-1. J Biol Chem 1996;271:28220–28228.
25. Deroanne CF, Hajitou A, Calberg-Bacq CM, Nusgens BV, Lapiere CM. Angiogenesis by fibroblast growth factor 4 is mediated through an autocrine up-regulation of vascular endothelial growth factor expression. Cancer Res 1997;57: 5590–5597.
26. Rak J, Mitsuhashi Y, Bayko L, et al. Mutant ras oncogenes upregulate VEGF/VPF expression: Implications for induction and inhibition of tumor angiogenesis. Cancer Res 1995;55: 4575–4580.
27. Grugel S, Finkenzeller G, Weindel K, Barleon B, Marme D. Both v-Ha-Ras and v-Raf stimulate expression of the vascular endothelial growth factor in NIH 3T3 cells. J Biol Chem 1995;270:25915–25919.
28. Mazure NM, Chen EY, Yeh P, Laderoute KR, Giaccia AJ. Oncogenic transformation and hypoxia synergistically act to modulate vascular endothelial growth factor expression. Cancer Res 1996;56:3436–3440.
29. Arbiser JL, Moses MA, Fernandez CA, et al. Oncogenic H-ras stimulates tumor angiogenesis by two distinct pathways. Proc Natl Acad Sci USA 1997;94:861–866.
30. Rak J, Filmus J, Finkenzeller G, Grugel S, Marme D, Kerbel RS. Oncogenes as inducers of tumor angiogenesis. Cancer Metastasis Rev 1995;14:263–277.
31. Coussens LM, Werb Z. Matrix metalloproteinases and the development of cancer. Chem Biol 1996;3:895–904.
32. Itoh T, Tanioka M, Yoshida H, Yoshioka T, Nishimoto H, Itohara S. Reduced angiogenesis and tumor progression in gelatinase A-deficient mice. Cancer Res 1998;58:1048–1051.
33. Deryugina EI, Bourdon MA, Reisfeld RA, Strongin A. Remodeling of collagen matrix by human tumor cells requires activation and cell surface association of matrix metalloproteinase-2. Cancer Res 1998;58:3743–3750.
34. Hiraoka N, Allen E, Apel IJ, Gyetko MR, Weiss SJ. Matrix metalloproteinases regulate neovascularization by acting as pericellular fibrinolysins. Cell 1998;95:365–377.
35. Ip C, Lisk DJ. Enrichment of selenium in allium vegetables for cancer prevention. Carcinogenesis 1994;15:1881–1885.
36. Ip C, Lisk DJ. Efficacy of cancer prevention by high-selenium garlic is primarily dependent on the action of selenium. Carcinogenesis 1995;16:2649–2652.
37. Thompson HJ, Adlakha H. Dose-responsive induction of mammary gland carcinomas by the intraperitoneal injection of 1-methyl-1 nitrosourea. Cancer Res 1991;51:3411–3415.
38. Thompson HJ, McGinley JN, Rothhammer K, Singh M. Rapid induction of mammary intraductal proliferations, ductal carcinoma in situ and carcinomas by the injection of sexually immature female rats with 1-methyl-1-nitrosourea. Carcinogenesis 1995;16:2407–2411.
39. Tonnesen MG, Jenkins D Jr, Siegal SL, Lee LA, Huff JC, Clark RA. Expression of fibronectin, laminin, and factor VIII-

related antigen during development of the human cutaneous microvasculature. J Invest Dermatol 1985;85: 564–568.

40. Weidner N, Semple JP, Welch WR, Folkman J. Tumor angiogenesis and metastasis–correlation in invasive breast carcinoma. N Engl J Med 1991;324:1–8.

41. Thaloor D, Singh AK, Sidhu GS, Prasad PV, Kleinman HK, Maheshwari RK. Inhibition of angiogenic differentiation of human umbilical vein endothelial cells by curcumin. Cell growth Differ 1998;9:305–312.

42. Nakamura J, Savinov A, Lu Q, Brodie A. Estrogen regulates vascular endothelial growth/permeability factor expression in 7,12-dimethylbenz(a)anthracene-induced rat mammary tumors. Endocrinology 1996;137:5589–5596.

43. Zhang HT, Craft P, Scott PA, et al. Enhancement of tumor growth and vascular density for transfection of vascular endothelial cell growth factor into MCF-7 human breast carcinoma cells. J Natl Cancer Inst 1995;87: 213–219.

44. McLeskey SW, Tobias CA, Vezza PR, Filie AC, Kern FG, Hanfelt J. Tumor growth of FGF or VEGF transfected MCF-7 breast carcinoma cells correlates with density of specific microvessels independent of the transfected angiogenic factor. Am J Pathol 1998;153:1993–2006.

45. Borgstrom P, Hillan KJ, Sriramarao P, Ferrara N. Complete inhibition of angiogenesis and growth of microtumors by anti-vascular endothelial growth factor neutralizing antibody: Novel concepts of angiostatic therapy from intravital videomicroscopy. Cancer Res 1996;56:4032–4039.

46. Borgstrom P, Bourdon MA, Hillan KJ, Sriramarao P, Ferrara N. Neutralizing anti-vascular endothelial growth factor antibody completely inhibits angiogenesis and growth of human prostate carcinoma micro tumors in vivo. Prostate 1998;35:1–10.

47. Meeson AP, Argilla M, Ko K, Witte L, Lang RA. VEGF deprivation-induced apoptosis is a component of programmed capillary regression. Development 1999;126: 1407–1415.

48. Benjamin LE, Golijanin D, Itin A, Pode D, Keshet E. Selective ablation of immature blood vessels in established human tumors follows vascular endothelial growth factor withdrawal. J Clin Invest 1999;103:159–165.

49. Benjamin LE, Keshet E. Conditional switching of vascular endothelial growth factor (VEGF) expression in tumors: Induction of endothelial cell shedding and regression of hemangioblastoma-like vessels by VEGF withdrawal. Proc Natl Acad Sci USA 1997;94:8761–8766.

50. Forsythe JA, Jiang BH, Iyer NV, et al. Activation of vascular endothelial growth factor gene transcription by hypoxiainducible factor 1. Mol Cell Biol 1996;16:4604–4613.

51. Wang GL, Semenza GL. General involvement of hypoxiainducible factor 1 in transcriptional response to hypoxia. Proc Natl Acad Sci USA 1993;90:4304–4308.

52. Damert A, Ikeda E, Risau W. Activator-protein-1 binding potentiates the hypoxia-inducible factor-1-mediated hypoxia-induced transcriptional activation of vascularendothelial growth factor expression in C6 glioma cells. Biochem J 1997;327(Pt 2):419–423.

53. Hirota K, Matsui M, Iwata S, Nishiyama A, Mori K, Yodoi J, AP-1 transcriptional activity is regulated by a direct association between thioredoxin and Ref-1. Proc Natl Acad Sci USA 1997;94:3633–3638.

54. Huang LE, Arany Z, Livingston DM, Bunn HF. Activation of hypoxia-inducible transcription factor depends primarily upon redox-sensitive stabilization of its alpha subunit. J Biol Chem 1996;271:32253–32259.

55. Brown JM, Giaccia AJ. The unique physiology of solid tumors: Opportunities (and problems) for cancer therapy. Cancer Res 1998;58:1408–1416.

56. Tamura T, Stadtman TC. A new selenoprotein from human lung adenocarcinoma cells: Purification, properties, and thioredoxin reductase activity. Proc Natl Acad Sci USA 1996;93:1006–1011.

57. Gladyshev VN, Jeang KT, Stadtman TC. Selenocysteine, identified as the penultimate C-terminal residue in human T-cell thioredoxin reductase, corresponds to TGA in the human placental gene. Proc Natl Acad Sci USA 1996;93: 6146–6151.

58. Gallegos A, Berggren M, Gasdaska JR, Powis G. Mechanisms of the regulation of thioredoxin reductase activity in cancer cells by the chemopreventive agent selenium. Cancer Res. 1997;57:4965–4970.

59. Berggren M, Gallegos A, Gasdaska J, Powis G. Cellular thioredoxin reductase activity is regulated by selenium. Anticancer Res 1997;17:3377–3380.

60. Christensen MJ, Pusey NW. Binding of nuclear proteins to transcription regulatory elements in selenium deficiency. Biochim Biophys Acta 1994;1225:338–341.

61. Spyrou G, Bjornstedt M, Kumar S, Holmgren A. AP-1 DNAbinding activity is inhibited by selenite and selenodiglutathione. FEBS Lett 1995;368:59–63.

62. Kim IY, Stadtman TC. Inhibition of NF-kappaB DNA binding and nitric oxide induction in human T cells and lung adenocarcinoma cells by selenite treatment. Proc Natl Acad Sci USA 1997;94:12904–12907.

63. Ganther, HE. Selenium metabolism, selenoproteins, and mechanisms of cancer prevention: Complexities with thioredoxin reductase. Carcinogenesis, in press.

64. Tyagi SC, Kumar S, Borders S. Reduction-oxidation (redox) state regulation of extracellular matrix metalloproteinases and tissue inhibitors in cardiac normal and transformed fibroblast cells. J Cell Biochem 1996;61: 139–151.

65. Mattana J, Margiloff L, Sharma P, Singhal PC. Oxidation of the mesangial matrix metalloproteinase-2 impairs gelatinolytic activity. Inflammation 1998;22:269–276.
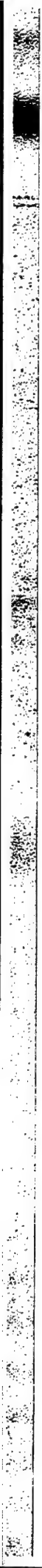
# Monomethyl Selenium–Specific Inhibition of MMP-2 and VEGF Expression: Implications for Angiogenic Switch Regulation

Cheng Jiang,[1] Howard Ganther,[2] and Junxuan Lu[1]*

[1]AMC Cancer Research Center, Denver, Colorado
[2]University of Wisconsin, Madison, Wisconsin

Previous work suggested that antiangiogenic activity may be a novel mechanism contributing to the cancer chemopreventive activity of selenium (Se). Because methylselenol has been implicated as an in vivo active chemopreventive Se metabolite, experiments were conducted to test the hypothesis that this metabolite pool might inhibit the expression of matrix metalloproteinase-2 (MMP-2) by vascular endothelial cells and of vascular endothelial growth factor (VEGF) by cancer epithelial cells, two proteins critical for angiogenesis and its regulation. In human umbilical vein endothelial cells (HUVECs), zymographic analyses showed that short-term exposure to methylseleninic acid (MSeA) and methylselenocyanate (MSeCN), both immediate methylselenol precursors, decreased the MMP-2 gelatinolytic activity in a concentration-dependent manner. In contrast, Se forms that enter the hydrogen selenide pool lacked any inhibitory effect. The methyl Se inhibitory effect on MMP-2 was cell dependent because direct incubation with Se compounds in the test tube did not result in its inactivation. Immunoblot and enzyme-linked immunosorbent assay analyses showed that a decrease of the MMP-2 protein level largely accounted for the methyl Se–induced reduction of gelatinolytic activity. The effect of MSeA on MMP-2 expression occurred within 0.5 h of exposure and preceded MSeA-induced reduction of the phosphorylation level of mitogen-activated protein kinases (MAPKs) 1 and 2 (~3 h) and endothelial apoptosis (~25 h). In addition to these biochemical effects in monolayer culture, MSeA and MSeCN exposure decreased HUVEC viability and cell retraction in a three-dimensional context of capillary tubes formed on Matrigel, whereas comparable or higher concentrations of selenite failed to exert such effects. In human prostate cancer (DU145) and breast cancer (MCF-7 and MDA-MB-468) cell lines, exposure to MSeA but not to selenite led to a rapid and sustained decrease of cellular (lysate) and secreted (conditioned medium) VEGF protein levels irrespective of the serum level (serum-free medium vs. 10% fetal bovine serum) in which Se treatments were carried out. The concentration of MSeA required for suppressing VEGF expression was much lower than that needed for apoptosis induction. Taken together, the data support the hypothesis that the monomethyl Se pool is a proximal Se for inhibiting the expression of MMP-2 and VEGF and of angiogenesis. The data also indicate that the methyl Se–specific inhibitory effects on these proteins are rapid and primary actions, preceding or independent of inhibitory effects on mitogenic signaling at the level of MAPK1/2 and on cell growth and survival. *Mol. Carcinog.* 29:236–250, 2000.   © 2000 Wiley-Liss, Inc.

Key words: selenium; methylselenol; matrix metalloproteinase-2; vascular endothelial growth factor; mitogen-activated protein kinase; angiogenesis

## INTRODUCTION

The results of recent human prevention trials using selenium (Se) alone [1,2] or in combination with other agents [3] have demonstrated potential cancer chemopreventive utility for multiple organ sites. Such efficacy has supported by the potent chemopreventive activity of Se in most animal carcinogenesis models when its intake exceeds that required for meeting the nutritional requirement for normal physiologic functions [4,5]. Although several hypotheses have been advanced to account for the anticarcinogenic effects of Se [4,5], the underlying mechanisms remain to be elucidated. We recently reported data that were consistent with an inhibitory effect of Se at chemopreventive intake levels on tumor angiogenesis [6]. Because angiogenesis is obligatory for early lesion growth and

progression [7–9] as well as metastasis [10], an antiangiogenic activity may be a novel mechanism contributing to the cancer chemopreventive activity of Se. Because methylselenol has been implicated as a critical Se metabolite pool for cancer chemopreventive activity [4,11,12], the present study was designed to test the hypothesis that this Se pool might exert specific inhibitory activities on angiogenic switch mechanisms.

Angiogenic switch in epithelial lesions is controlled through at least two principal cell compartments, i.e., the transformed epithelial cells that serve as a main source of angiogenic factors and the vascular endothelial cells that constitute the targets for the angiogenic signals [8,9]. With angiogenic stimulation, the vascular endothelial cells increase their expression and secretion of matrix metalloproteinases (MMPs) to break down the extracellular and tissue matrix, increase cell motility, and undergo cell division to provide the necessary number of cells for the growing vessels. The essential role of MMP-2 in angiogenesis has been well documented [13–16]. Consistent with a methyl Se–specific hypothesis for Se regulation of angiogenesis, we previously reported a potent inhibitory activity of methylseleninic acid (MSeA), a novel penultimate methylselenol precursor, on MMP-2 gelatinolytic activity (zymographic analyses) in human umbilical vein endothelial cells (HUVECs) that was absent for selenite at an exposure level that produced equivalent inhibitory effect on HUVEC growth and survival [6]. In the present study we extended that work by delineating the Se metabolite specificity for MMP-2 inhibition by comparing Se compounds known to enter the hydrogen selenide pool (sodium selenide and selenite) or methylselenol pool (MSeA and methylselenocyanate (MSeCN)). We characterized the temporal relation of methyl Se inhibition of MMP-2 expression with its effects on HUVEC mitogenic signaling and endothelial growth and survival. In addition, we contrasted the effects of methyl Se versus selenite on HUVEC cell viability and retraction in the three-dimensional context of capillary tubes formed on Matrigel, an extracellular matrix extract of EHS sarcoma.

A key for initiating and sustaining angiogenic responses is increased production of angiogenic stimulators [8,9]. A positive, primary angiogenic factor is vascular endothelial growth factor (VEGF) or vascular permeability factor [17,18]. Transformed epithelial cells are the major source of VEGF expression in many types of solid cancers [19–23]; however, recent data have suggested that stromal cells and even vascular endothelial cells may also express VEGF in the angiogenic microenvironment of tumors [24]. Previously, we documented a decrease of VEGF protein level in a sizable proportion of the chemically induced mammary carcino-

mas treated with Se in vivo [6], suggesting inhibition of VEGF expression as one possible mechanism for Se to regulate the angiogenic switch. In the present study, we investigated the Se metabolite specificity for this effect and report a rapid and sustained methyl Se–specific inhibitory effect on VEGF expression in prostate and breast cancer epithelial cells. We extended our work to a prostate cancer cell line for comparison with breast cancer cell lines because of the results of the trial by Clark et al. [1] in which the prostate appeared to be the most responsive organ site for Se cancer-preventive activity. In addition, a recent study has linked higher Se intake as indicated by the Se content in toe-nail clippings to lower prostate cancer risk in U.S. men [25].

Cell growth, function, and survival are regulated through multiple signaling pathways. Receptor tyrosine kinases as well as mitogen-activated protein kinase (MAPK) or extracellular regulated kinase pathways transduce signals initiated extracellularly by way of cascades of protein kinases to the nucleus [26,27]. The phosphorylated MAPK1 and 2 (phospho-MAPK1/2) are the active forms that translocate to the nucleus, where they phosphorylate protein substrates, leading to cell-type–specific responses including in many cells the activation of the cell-cycle machinery for mitogenesis. MAPK1/2 (44 and 42 kDa, respectively) and p38$^{MAPK}$ have been shown to regulate the expression of some MMPs [28,29] and mediate VEGF-induced endothelial responses such as hyperpermeability and cell motility and proliferation [30–33], although little is known about their involvement in MMP-2 expression in vascular endothelial cells. Similarly, the MAPK cascade has been implicated in VEGF expression regulation by proangiogenic factors such as basic fibroblast growth factor [34], and nothing is known about its role, if any, in methyl Se inhibition of VEGF expression in cancer epithelial cells. Therefore, the phosphorylation state of MAPK1/2 was characterized in relation to the methyl Se–specific inhibitory effects on MMP-2 and VEGF expression in vascular endothelial and cancer epithelial cells, respectively.

## MATERIALS AND METHODS

### Chemicals and Reagents

Sodium selenite pentahydrate was purchased from J. T. Baker, Inc. (Phillipsburg, NJ). Sodium selenide was purchased from Alfa Products (Danvers, MA). MSeA (CH$_3$SeO$_2$H) and MSeCN (CH$_3$SeCN) were synthesized as described elsewhere [6,35]. Intracellularly, MSeCN and MSeA most likely react with reduced glutathione to generate methylselenol. A VEGF enzyme-linked immunosorbent assay (ELISA) kit was purchased from R&D Systems (Minneapolis, MN). Human recombinant proMMP-

2 protein and MMP-2 ELISA kits were purchased from Oncogene Research Products (Cambridge, MA). Antibodies to MMP-2 for immunoblots were purchased from Lab Vision Corp. (Fremont, CA). Antibodies to MAPK1/2 and phospho-MAPK1/2 were purchased from New England Biolaboratories (Beverely, MA). Matrigel, a reconstituted extracellular matrix preparation of the EHS sarcoma, was purchased from Becton-Dickinson Labware (Bedford, MA).

## Cell Lines

HUVECs were obtained from American Type Culture Collection (ATCC; Manassas, VA) and were propagated in F12K medium containing 10% fetal bovine serum (FBS), 2 mM L-glutamine, 100 µg/mL heparin (Sigma Chemical Co., St. Louis, MO), and 30 µg/mL bovine endothelial cell growth supplement (ECGS; Sigma Chemical Co.) as described previously [6]. DU145 prostate cancer cells and MDA-MB-468 breast cancer cells were kindly provided by Dr. Rajesh Agarwal, who originally obtained these cells from ATCC. MCF-7 breast cancer cells were obtained from ATCC. DU145 cells were cultured in RPMI-1640 medium supplemented with 10% FBS and 2 mM L-glutamine. MCF-7 and MDA-MB-468 breast cancer cells were cultured in Dulbecco's minimum essential medium supplemented with 10% FBS and 2 mM L-glutamine.

## Zymogram Analysis for HUVEC MMP-2

Unless otherwise specified, HUVECs were seeded into six-well plates in complete medium (10% FBS, 2 mM L-glutatmine, 100 µg/mL heparin, and 30 µg/mL ECGS) for 24–48 h to reach near confluence. The cells were washed three times with phosphate-buffered saline (PBS) to remove spent medium, refed serum-free medium supplemented with 100 µg ECGS/mL, and treated with the various forms of Se for 6 h (a time frame that did not result in visible cellular changes). For time-course experiments, aliquots were taken from the medium at different durations of exposure to MSeA. To evaluate the reversibility of MMP-2 inhibition, HUVECs were treated for 3 h with MSeA or PBS as described above, and the conditioned media were harvested. The cells were washed three times with PBS and were refed serum-free fresh medium supplemented with 100 µg ECGS/mL. Aliquots were taken from conditioned media at 1, 3, 6, and 12 h after MSeA withdrawal. Gelatinolytic activities were analyzed on substrate gels as described previously [6]. Each experiment was replicated at least once.

## Western and ELISA Analyses for MMP-2 Protein Quantitation

HUVECs were seeded in T75 flasks in complete medium and grown until near confluence. After spent medium was removed and cells were washed three times with PBS, the cells were treated with MSeA for different durations in serum-free medium supplemented with 100 µg ECGS/mL. Conditioned media were collected, aliquots were saved for zymographic analyses, and the remainder portion was concentrated with Centricon spin filters (30-kDa cutoff; Millipore Corp., Bedford, MA) for ~50-fold. The concentrated samples were used for MMP-2 quantitation by western blotting [6]. Recombinant human proMMP-2 (72 kDa) was loaded on the gels as a positive standard. In a separate experiment, conditioned media were concentrated (approximately fivefold) by evaporation in a Speedvac Concentrator and used for ELISA according to the manufacturer's instructions (Oncogene Research Products).

## Capillary Tube Formation on Matrigel
## (In Vitro Angiogenesis)

Kubota et al. [36] showed that, when seeded on Matrigel, an extracellular matrix extract from the EHS sarcoma, vascular endothelial cells undergo rapid differentiation into capillarylike structures. This affords a simple assay for assessing the impact of agents such as Se compounds on capillary differentiation in vitro and cell viability and function in a simulated histogenic three-dimensional context. HUVECs were harvested by trypsinization, and ~40 000 cells per well were seeded onto 24-well plates coated with 300 µL of Matrigel (solidified at 37°C for 1 h before the addition of Se stock solutions). Before cell seeding, 0.5 mL of medium was added to each well, and Se stock solution was added at two times the desired concentration. HUVECs were added in 0.5 mL of medium per well. Tube formation was observed periodically over time under a phase-contrast microscope and photographed with a Polaroid camera. At 72 h after seeding, 3-(4,5-dimethylthiazol-2-yl)-2,5-diphenyl tetrazolium bromide (MTT) [37] was added to test the metabolic viability of Se-exposed HUVECs.

## ELISA Analyses of VEGF Expression in
## Cancer Epithelial Cells

In short-term dose-response experiments, DU145 prostate cancer cells and MCF-7 (estrogen dependent) and MDA-MB-468 (estrogen independent) breast cancer cells were seeded in T25 flasks in complete medium until near confluence. The spent medium was removed, and flasks (cells) were washed three times with PBS. Cells were treated in either serum-rich complete medium (10% FBS) or serum-free medium with increasing concentrations of MSeA or selenite for up to 6 h. VEGF content in conditioned media and cell lysates (prepared with calibrator diluent buffer RD5K provided with the ELISA kit) was analyzed with the use of an ELISA kit according to the manufacturer's instructions (R&D

Systems). In time-course experiments, near-confluent DU145 cells were treated with PBS, selenite, or MseA, and aliquots of the culture media were taken at hourly intervals for VEGF ELISA. Samples were measured in duplicate or triplicate, and experiments were replicated at least once.

In long-term experiments to examine whether the methyl Se–inhibitory effect on VEGF expression was transient, MSeA doses that led to growth arrest without significant induction of apoptosis were applied daily to DU145 prostate cells, starting in log-phase growing (~40–50% confluence) cells, in fresh complete medium. DNA content in cell lysate was measured by Hoechst dye binding to approximate cell number. VEGF content in cell lysate was measured by ELISA and normalized to DNA content to estimate VEGF expression on a per-cell basis.

## Cell Growth and Apoptosis Evaluation

Cells were seeded in six-well plates until 50% confluence and were treated in fresh serum-rich (10% FBS) medium with increasing concentrations of MSeA or selenite for 48 h or as specified. Adherent cells were fixed in 1% glutaldehyde and stained with crystal violet for cell enumeration as described previously [6]. To verify that DU145 cells underwent apoptotic cell death with Se treatment, cells were treated in T75 flasks with MSeA or selenite for 24 h, and DNA from both adherent and detached cells was extracted and analyzed as previously described [38]. To standardize Se exposure across different cell culture vessels, 0.2 mL of medium per square centimeter of vessel surface (e.g., 15 mL for a T75 flask, 5 mL for a T25 flask, and 2 mL for each well of a six-well plate) was used.

## Immunoblot Analyses of Phospho-MAPK1/2 and MAPK1/2

To determine whether the MAPK signaling cascade was associated with the inhibition of MMP-2 and VEGF expression by methyl Se exposure, cell lysates were prepared in RIPA buffer (50 mM Tris-HCl, pH 7.4, 150 mM NaCl, 2 mM ethylenediaminetetraacetic acid, 50 mM sodium fluoride, 1% Triton X-100, 1% sodium deoxycholate, 0.1% sodium dodecyl sulfate, 1 mM dithiothreitol, 5 mM sodium orthovanadate; 1 mM phenylmethylsulfonyl fluoride, and 38 $\mu$g/mL aprotinin were added fresh). Supernatants were recovered after centrifugation (14 000$g$ for 20 min, 4°C), and the protein content was quantified by the Bradford dye-binding assay (Bio-Rad Laboratories, Richmond, CA). Forty micrograms of total protein was size separated by electrophoresis on 15% sodium dodecyl sulfate–polyacrylamide gels. The proteins were electro-blotted onto nitrocellulose membranes and probed for phospho-MAPK1/2 (pp44/pp42) and MAPK1/2 (p44/p42).

## RESULTS

### Part I: HUVEC MMP-2 Expression and In Vitro Capillary Tube Formation

*Exposure to methylselenol precursors led to decreased endothelial MMP-2 expression*

Treatment of HUVECs for 6 h with MSeA led to a concentration-dependent reduction of the secreted 72-kDa MMP-2 gelatinolytic activity in the conditioned medium (Figure 1A) and in cell lysate, as previously reported [6]. The inhibitory efficacy was remarkable, with an IC$_{50}$ of ~2 $\mu$M, which is within the upper range of plasma Se concentration in most U.S. residents [1]. Similarly, treatment with MSeCN resulted in a concentration-dependent decrease of MMP-2, and the inhibitory efficacy was comparable to that of MSeA (Figure 1A). In contrast, treatment with hydrogen selenide precursors (up to 20 $\mu$M sodium selenite or 50 $\mu$M sodium selenide) did not significantly decrease MMP-2 in the conditioned medium (Figure 1A).

Incubation of HUVEC-conditioned medium (containing secreted MMP-2) with all four Se forms in the test tube for 6 h at 37°C did not decrease the gelatinolytic activity (Figure 1B), indicating that MSeA or MSeCN per se did not react directly with MMP-2 protein to inactivate its activity. The inhibitory action of these methylselenol precursor compounds was therefore dependent on cellular metabolism.

*Reduction of MMP-2 protein level largely accounted for methyl Se inhibition of MMP-2*

Western blot analyses of the MMP-2 protein level in conditioned medium of HUVECs treated with MSeA indicated that a reduction in the MMP-2 protein level closely paralleled the observed loss of MMP-2 gelatinolytic activity (Figure 1C), whereas selenite treatment had minimal effect on both the gelatinolytic activity and MMP-2 protein level (Figure 1C). Consistent with the immunoblot results, ELISA quantitation of MMP-2 in the conditioned medium in a separate experiment indicated that 5 $\mu$M MSeA treatment for 8 h decreased the MMP-2 level from 1.81 $\pm$ 0.24 ng/mL to 0.38 $\pm$ 0.02 ng/mL, a reduction of 79%.

*Methyl Se inhibition of MMP-2 expression was rapid and sustained*

In time-course experiments, the inhibitory effect of MSeA on MMP-2 showed a lag time of 10 min, and by 30 min, ~50% reduction was detected (Figures 2A and 3C). In exposure-and-withdrawal experiments (Figure 2B), the MMP-2 inhibitory action of a 3-h MSeA exposure persisted for at least 12 h because the linear slope of the MMP-2 versus the time plot of the MSeA-exposed cells indicated no exponential recovery once MSeA was withdrawn.
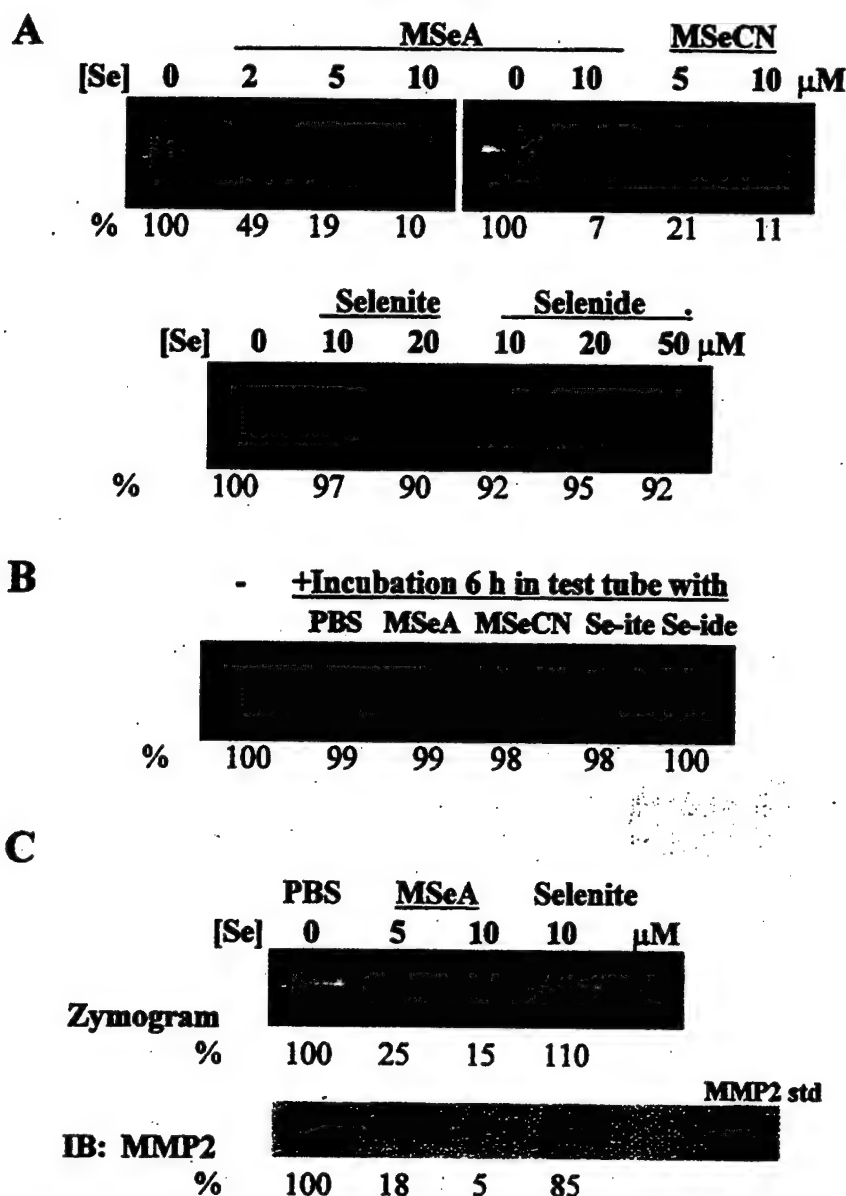
**A**



|  | | MSeA | | | | MSeCN | |
|---|---|---|---|---|---|---|---|
| [Se] | 0 | 2 | 5 | 10 | 0 | 10 | 5 | 10 μM |

% 100  49  19  10    100  7  21  11

|  | | Selenite | | Selenide | |
|---|---|---|---|---|---|---|
| [Se] | 0 | 10 | 20 | 10 | 20 | 50 μM |

% 100  97  90  92  95  92

**B**

- **+Incubation 6 h in test tube with**
**PBS  MSeA  MSeCN  Se-ite  Se-ide**



% 100  99  99  98  98  100

**C**

|  | PBS | MSeA | | Selenite | |
|---|---|---|---|---|---|
| [Se] | 0 | 5 | 10 | 10 | μM |

**Zymogram**

% 100  25  15  110

**MMP2 std**

**IB: MMP2**

% 100  18  5  85

Figure 1. (A) The inhibitory specificity of Se forms on HUVEC MMP-2. Representative zymographic analyses of MMP-2 in conditioned medium of HUVECs treated for 6 h (in separate experiments) with methylseleninic acid (MSeA), methylselenocyanate (MSeCN), sodium selenite, or sodium selenide in serum-free medium supplemented with 100 μg/mL ECGS. Relative pixel density as a percentage of control cells is presented below each lane. (B) Lack of MMP-2 inactivation by direct incubation of HUVEC conditioned medium with Se compounds in test tubes at 37°C for 6 h. Each Se was added to 10 μM. Se-ite and Se-ide denote sodium selenite and sodium selenide, respectively. (C) Immunoblot analyses of MMP-2 protein in conditioned medium. HUVECs (in T75 flasks) were treated with MSeA or selenite for 3 h in the presence of 100 μg/mL ECGS. Aliquots of the condition medium were analyzed by zymography for gelatinolytic activity. The bulk of the conditioned media was concentrated ~50-fold using Centricon spin filters (Millipore Corp.) and analyzed by western blotting, with recombinant 72-kD proMMP-2 protein (10 ng) as the standard.

In similar exposure-and-withdrawal experiments, MSeA treatment for 12 h or shorter duration did not decrease the number of HUVECs surviving to 52 h, in contrast to the fast action of MSeA on MMP-2 (Figure 2C). It took 25 h or longer of continued exposure to MSeA to result in cell number reduction (Figure 2C), predominantly through induction of apoptosis, as previously reported [6].

*Methyl Se inhibition of MMP-2 occurred irrespective of ECGS stimulation and preceded phospho-MAPK1/2 reduction*

Two known responses of vascular endothelial cells with angiogenic stimulation are increased expression of MMP-2 and increased mitogenic signaling leading to cell proliferation. As expected, ECGS supplementation for 6 h to ECGS-starved (~48 h)

**A**

| Time | 10' | | 30' | | 1 h | | 3 h | | 6 h | |
|------|-----|---|-----|---|-----|---|-----|---|-----|---|
| MSeA(10 μM) | - | + | - | + | - | + | - | + | - | + |

%Inhibited      0      44      49      73      80

**B**

⇓ MSeA withdrawn from medium

| Time | 3 h | | 1 h | | 3 h | | 6 h | | 12 h | |
|------|-----|---|-----|---|-----|---|-----|---|------|---|
| MSeA | - | + | - | +/- | - | +/- | - | +/- | - | +/- |



**Hour after MSeA withdrawn**

**C**    **Cell number at 52 hours**



**Duration of MSeA treatment before withdrawal**
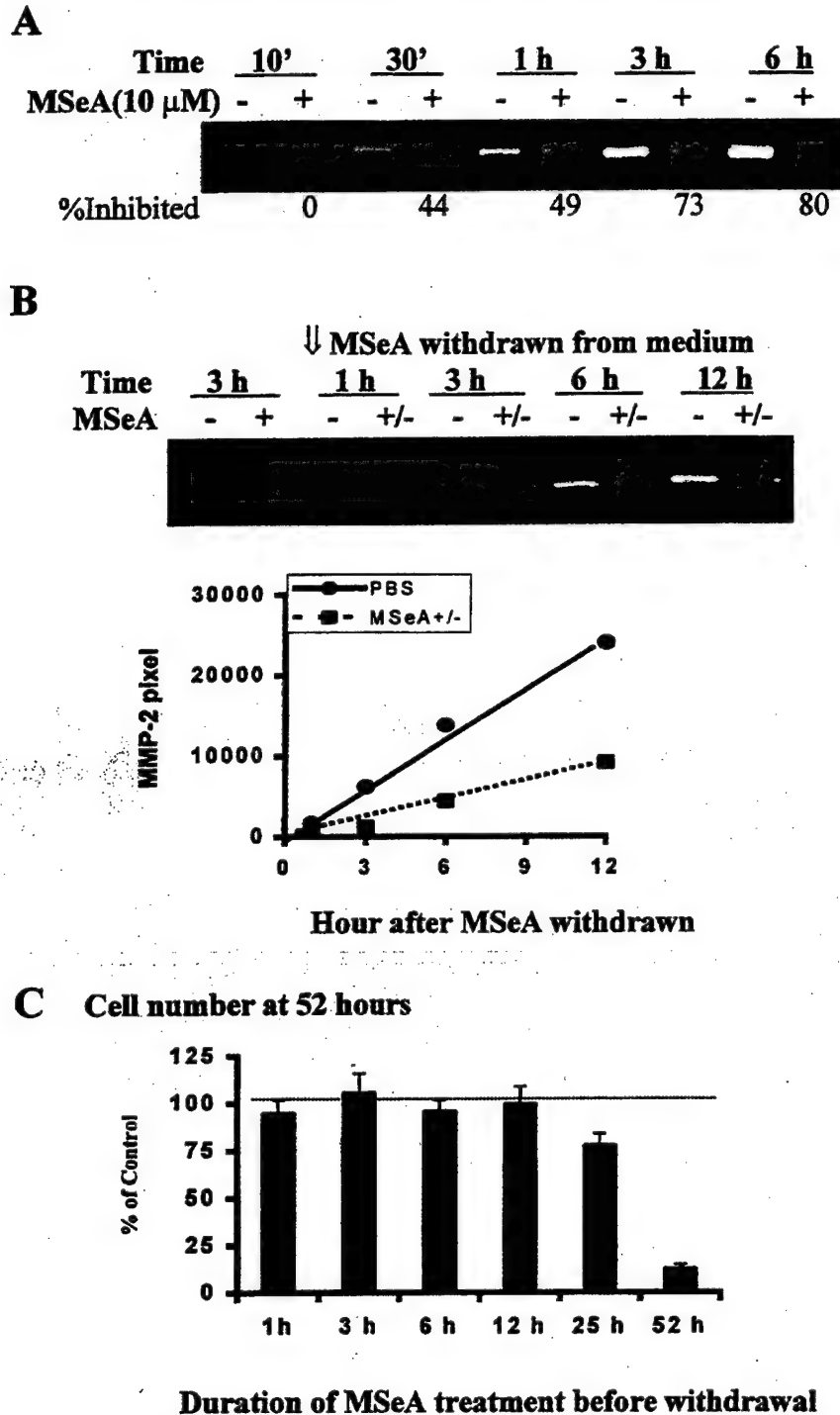
Figure 2. (A) Time course of MMP-2 inhibition by MSeA (10 μM) exposure of HUVECs. Aliquots of medium taken at the different time points were analyzed by zymography. Percentages of inhibition relative to the PBS-treated control at each time point are presented below the treated lanes. (B) Reversibility of MSeA-induced MMP-2 inhibition. HUVECs were treated for 3 h with PBS or MSeA (10 μM), and the cells were washed three times with PBS and re-fed serum-free medium supplemented with 100 μg/mL ECGS. Aliquots of medium taken at the different time points were analyzed by zymography. The MMP-2 pixel density was plotted against time to evaluate the kinetics of MMP-2 recovery in cells exposed once to MSeA. A linear slope of the curve indicated a lasting inhibitory effect after MSeA withdrawal. (C) Effect of duration of MSeA (5 μM) exposure on number of HUVECs surviving in MSeA-free medium to 52 h. HUVECs were treated with either PBS or MSeA for the time indicated, the medium was removed, cells were washed three times with PBS, and fresh medium was fed until cells were fixed at 52 h. The bar graph represents the number of MSeA-treated cells as a percentage of the respective PBS treated-controls. Error bars indicate SEM of six random fields counted.

**A**



**B**



**C**
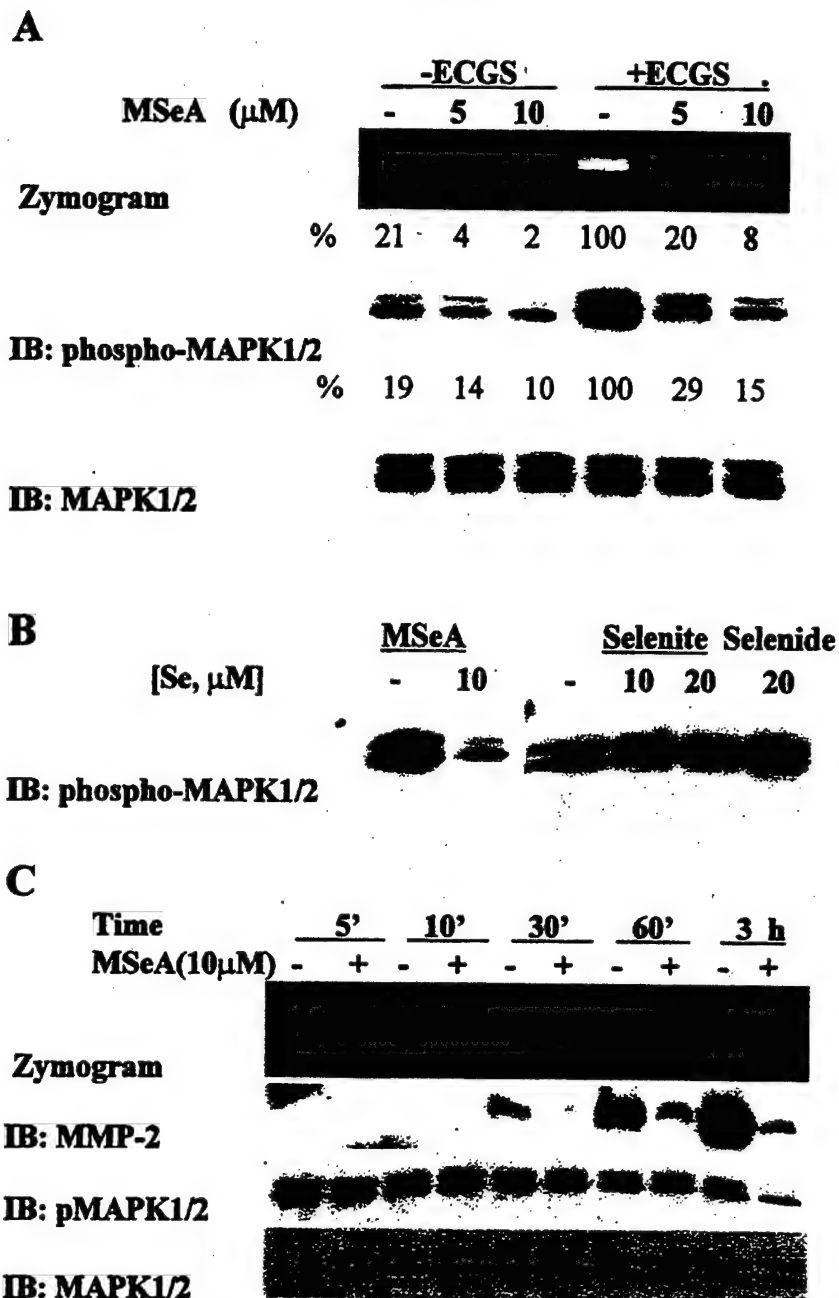


Figure 3. (A) Effects of MSeA exposure (6 h) on MMP-2 expression and MAPK1/2 phosphorylation status in synchronized HUVECs. HUVECs (T75 flasks) were deprived (synchronized) of ECGS for ~48 h and, after PBS washing, were treated with MSeA for 6 h in the presence or absence of 100 µg/mL ECGS. Conditioned medium was used for zymography. Forty micrograms of cell lysate was immunoblotted for phospho-MAPK1/2 and total MAPK1/2. (B) Lack of inhibitory effect of selenite and selenide exposure for 6 h on HUVEC phospho-MAPK1/2 level. (C) Temporal relation between MseA inhibition of MMP-2 expression (zymogram and immunoblot) and phospho-MAPK1/2 inactivation in synchronized HUVECs (T75 flasks) treated in the presence of 100 µg/mL ECGS.

HUVECs increased secreted MMP-2 by 4.8-fold (Figure 3A). Western blot analyses of HUVEC lysates showed that a 5.3-fold increase of MAPK1/2 phosphorylation was associated with the ECGS-stimulated MMP-2 expression. Exposure to MSeA decreased MMP-2 in a concentration-dependent manner, not only in ECGS-stimulated cells but also in ECGS-starved cells (basal expression). Further,

exposure to MSeA led to a reduction of phospho-MAPK1/2 level in a concentration-dependent manner, and this inhibition closely paralleled that for MMP-2, especially in the ECGS-stimulated cells. The expression level of total MAPK1/2 was not affected by treatment with either ECGS or MSeA. In contrast to MSeA, exposure to selenite and selenide, which lacked inhibitory effect on MMP-2 expression, did

not decrease the level of MAPK1/2 phosphorylation (Figure 3B).

Given the close parallel changes observed between MMP-2 expression and phospho-MAPK1/2 levels, a time-course experiment examined the temporal relation between these MSeA-induced events in ECGS-stimulated HUVECs that had been deprived of ECGS for ~48 h (Figure 3C). Whereas MMP-2 expression was significantly lowered at 30 min, a significant reduction of phospho-MAPK1/2 levels occurred at 3 h. These results indicated that the effect of methyl Se on MMP-2 expression took place before its inhibition of phospho-MAPK1/2.

## Methylselenol precursors inhibited HUVEC capillary retraction and survival on Matrigel

When seeded on Matrigel, HUVECs underwent rapid reorganization (visible within 1–2 h) and subsequently formed capillarylike structures (in vitro differentiation). When added simultaneously with cell seeding, none of the Se compounds at the concentration ranges tested negatively affected the initial tube formation, i.e., differentiation, program within the first 28 h (Figure 4A–D). As time progressed, the capillary structures in the PBS control wells started to retract into spheroids (Figure 4E and I) that were metabolically viable at 72 h as measured by their ability to metabolize MTT (Figure 4M). Exposure to 5 µM MSeA (Figure 4F and J) or MSeCN (Figure 4G and K) resulted in a blockage of the capillary tubes from retracting into such spheroids. By 72 h of exposure to either MSeA or MSeCN, only a minor proportion of the cells in the protracted capillaries were still metabolically viable, as judged by their ability to metabolize MTT (Figure 4N and O). Most cells displayed morphologic apoptotic characteristics. In contrast to these methylselenol precursors, selenite at concentrations as high as 10 µM did not inhibit tube retraction or cell viability (Figure 4H, L, and P). These results indicated that methyl Se was more effective than selenite in a three-dimensional capillary histogenic context at inhibiting HUVEC cell viability and retraction.

## Part II: VEGF Expression in Cancer Epithelial Cells

## MSeA rapidly decreased VEGF expression in cancer epithelial cells

In short-term experiments, exposure of near-confluent DU145 prostate cancer cells to increasing concentrations of MSeA or selenite in serum-rich medium (10% FBS) for 6 h led to very distinct effects on VEGF expression, as shown in Figure 5A and B. MSeA treatment decreased both cellular (cellular lysate, Figure 5A) and secreted (conditioned medium, Figure 5B) VEGF levels in an Se concentration-dependent manner, with $IC_{50\%}$ ~2 µM. The inhibitory effect of MSeA on VEGF expression was also observed in serum-free medium with almost identical patterns (data not shown). In contrast, exposure to selenite in the same dose range did not decrease VEGF expression; in fact, a slight increase (5–10%) in VEGF expression was often observed in selenite-treated cells. The methyl Se inhibitory action was exerted very rapidly in that exposure to 5 µM MSeA in serum-rich medium decreased the secreted VEGF level by ~50% within 2 h (Figure 5C).

## Lower MSeA concentration was required for inhibiting VEGF expression than for inducing apoptosis

Exposure of DU145 prostate cancer cells to either sodium selenite or MSeA above some threshold levels for longer durations led to apoptosis, as indicated by DNA nucleosomal fragmentation (Figure 5D), and decreased the number of cells remaining adherent after 48 h (Figure 5E). MSeA was more efficacious than selenite at inhibiting cell growth and survival. The inhibitory effect of MSeA on VEGF expression was observed at a concentration (2 µM) that was twofold lower than that needed to induce significant apoptosis (4 µM and above). Although selenite exposure at 5 µM achieved a similar extent of DNA fragmentation and cell number reduction as MSeA at 5 µM, the difference in the potency of the respective Se to inhibit VEGF expression within a few hours of exposure was self-evident. These results indicated that the inhibitory action of MSeA was not a consequence of cell "poisoning".

## Sustained inhibition of VEGF expression required continued presence of MSeA

The possibility that the observed decrease of VEGF expression by MSeA was a transient effect was assessed through daily exposure of DU145 cells (starting when cells were in log-phase growth, ~40–50% confluent) to a low dose (3 µM) that predominantly led to growth arrest (Figure 6). Consistent with the results in confluent cells shown above, greater than 50% decrease of VEGF expression was observed at 6 h of exposure and the effect was sustained throughout the exposure period of 72 h (Figure 6A). The daily exposure to MSeA led to detectable growth inhibition by 48 h as assessed through DNA measurement (Figure 6B). When expressed on a per-cell basis, i.e., normalized to DNA content, this level of MSeA exposure led to a sustained ~50% decrease of VEGF expression level throughout the exposure duration (Figure 6C). Selenite at the same dose level did not affect cell growth (Figure 6B) or VEGF expression (Figure 6A and C). In a separate experiment, withdrawal of MSeA (3 µM) after 96 h of exposure led to the rebound of VEGF expression (Figure 6D). These results indicate that the mechanism(s) suppressing VEGF expression was reversible and that continued presence of MSeA was necessary to inhibit VEGF expression.
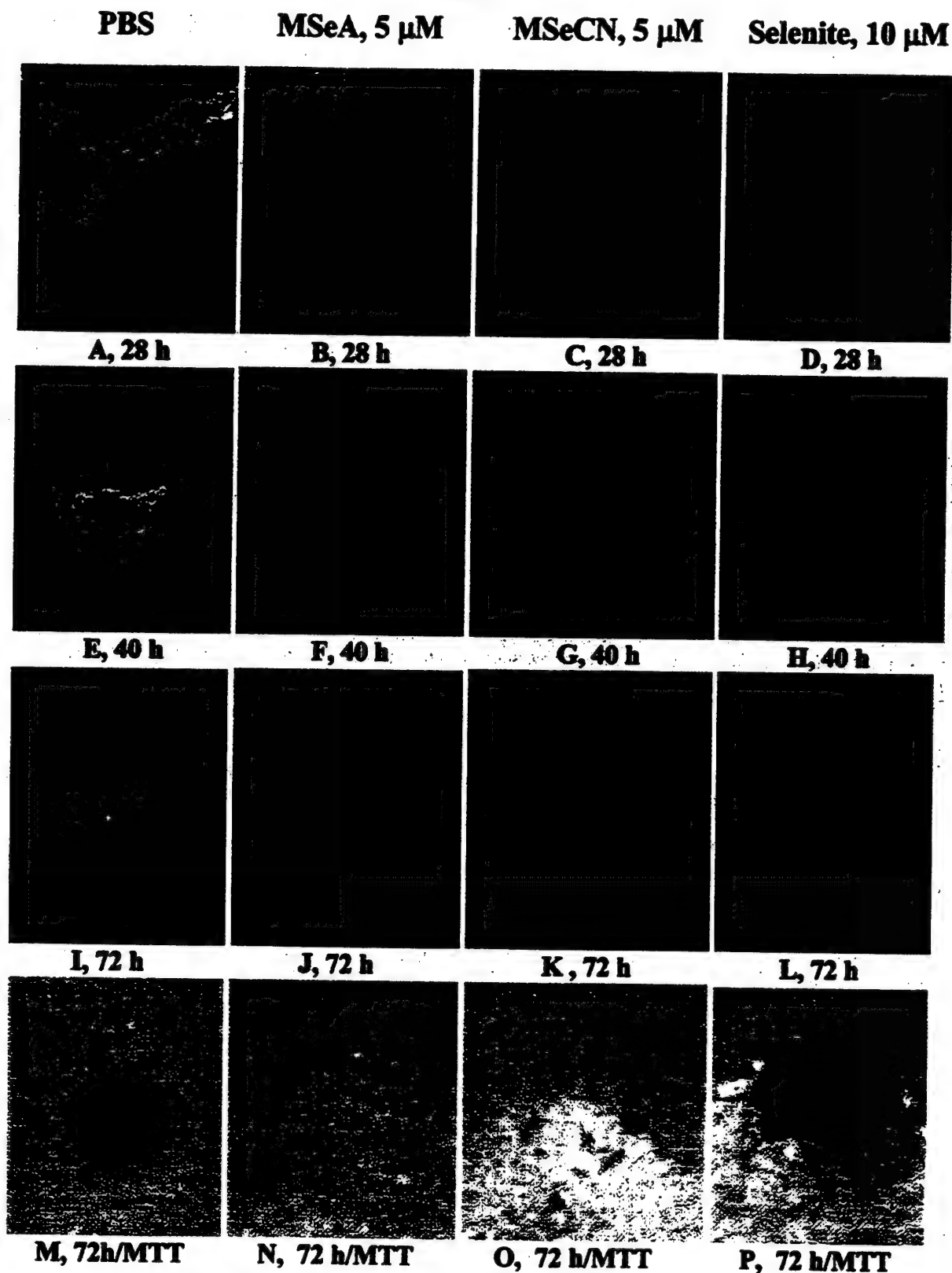
| PBS | MSeA, 5 μM | MSeCN, 5 μM | Selenite, 10 μM |
|-----|-----------|-------------|------------------|



| A, 28 h | B, 28 h | C, 28 h | D, 28 h |
| E, 40 h | F, 40 h | G, 40 h | H, 40 h |
| I, 72 h | J, 72 h | K, 72 h | L, 72 h |
| M, 72h/MTT | N, 72 h/MTT | O, 72 h/MTT | P, 72 h/MTT |

Figure 4. Effects of Se forms on HUVEC retraction and viability in an in vitro capillary differentiation assay. HUVECs (~40 000/well) were seeded into Matrigel-coated, 24-well plates that had been provided with 2 × concentrations of the indicated Se forms, and phase-contrast photomicrographs (magnification, 100 ×) were taken at 28 h (A–D), 40 h (E–H), and 72 h (I–L) of treatment. At 72 h (M–P), MTT was added to each well and incubated for an additional 5 h, and brightfield photomicrographs were taken (magnification, 200 ×). Black products indicate mitochondrial conversion of MTT by metabolically viable cells.

## A. Lysate VEGF, 6 h

## B. Secreted VEGF, 6 h

## C. Time course, secreted



## D. DNA apoptotic fragmentation at 24 h

## E. Adherent cell number at 48 h
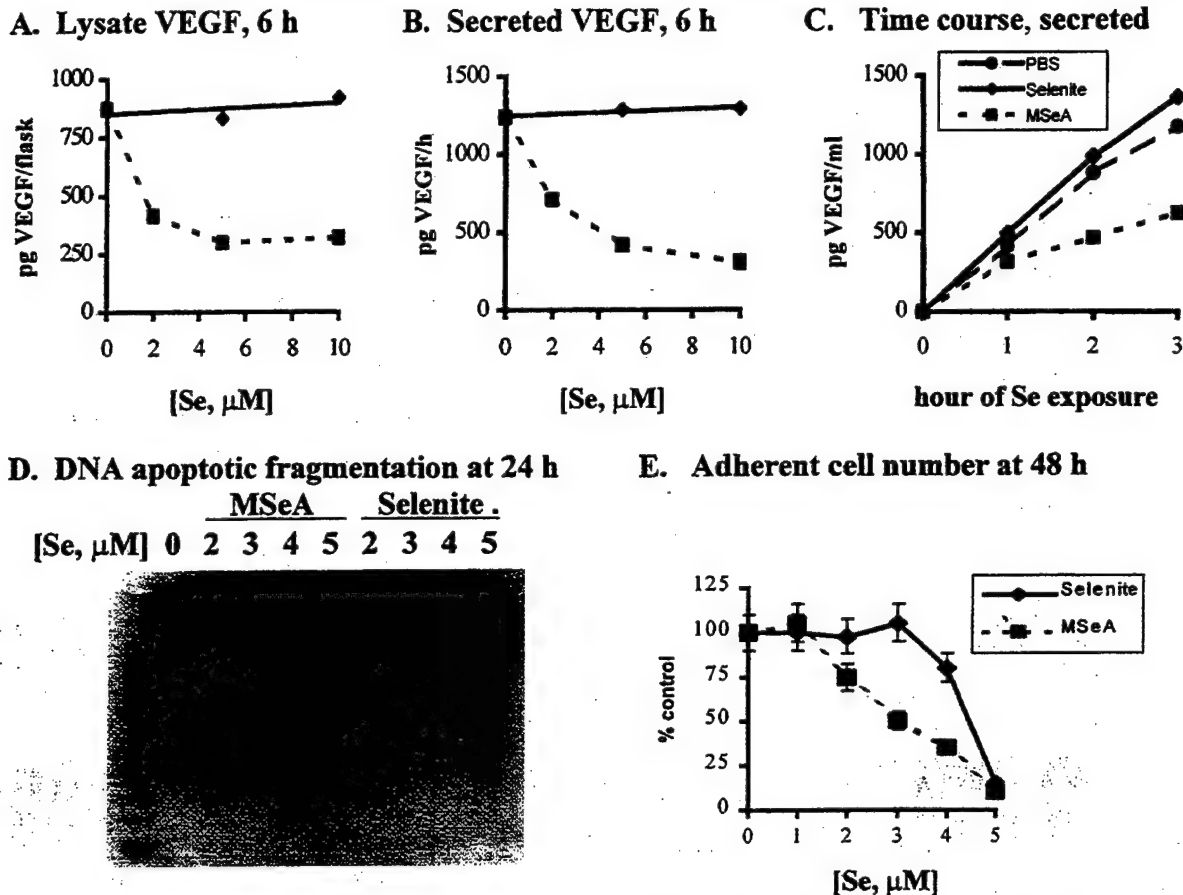


Figure 5. Concentration-dependent effects of selenite (diamonds) and MSeA (squares) on VEGF protein levels in DU145 cell lysate (A) and conditioned medium (B) after exposure for 6 h in serum rich medium. (C) Acute time course of effects of exposure to Se as sodium selenite (10 µM, diamonds) or MSeA (5 µM, squares) in 10% FBS medium on VEGF secretion by DU145 prostate cancer cells. In these short-term exposure experiments, near-confluent DU145 cells were treated with Se in 10% FBS medium or serum-free medium (identical patterns of responses were observed, data not shown). VEGF was assayed in triplicates by ELISA (R&D Systems, Minneapolis, MN). (D) DNA nucleosomal fragmentation assay after 24 h of exposure to MSeA or selenite (adherent and detached cells were combined for DNA extraction). (E) Effect of exposure to increasing concentrations of selenite or MSeA in 10% FBS medium for 48 h on the number of adherent DU145 cells in six-well plates. Error bars indicate SEM of six random fields counted.

### MseA inhibition of VEGF expression was also observed in breast cancer cells and independent of phospho-MAPK1/2

In support of the generality of this inhibitory effect of methyl Se on VEGF expression, two human breast cancer cell lines (MCF-7 and MDA-MB-468) tested thus far showed the same Se metabolite specificity of inhibition irrespective of the serum levels in the treatment medium (Figure 7A and B). It appeared that a greater concentration of MSeA was required to induce a similar extent of inhibition on VEGF expression in the breast cancer cell lines than in the DU145 prostate cancer cell line.

In contrast to vascular endothelial cells in which MSeA exposure led to a decreased level of phospho-MAPK1/2, treatment of DU145 prostate or MDA-MB-468 breast cancer cells with MSeA did not decrease the levels of phospho-MAPK1/2 within the time frame of suppression of VEGF expression (Figure 7C), suggesting a mechanism of inhibition of VEGF expression independent of MAPK1/2 activity.

## DISCUSSION

Although mechanisms underlying the cancer chemopreventive activity of Se are not fully understood, animal and cell culture models have yielded much insight. Of particular significance, the work of Ip and colleagues [4,11,12] has implicated methylselenol as the active in vivo Se metabolite pool for anticancer activity. These studies indicated that the mammary cancer–preventive efficacy of a given Se compound appears to depend on the rate of its metabolic conversion to the methylselenol pool. Subsequent studies by us and others had shown that the methyl Se pool induces numerous cellular, biochemical, and gene expression responses that are distinct from those induced by Se forms that entered the hydrogen selenide pool [38–42]. For example, MSeCN and Se-methylselenocysteine,
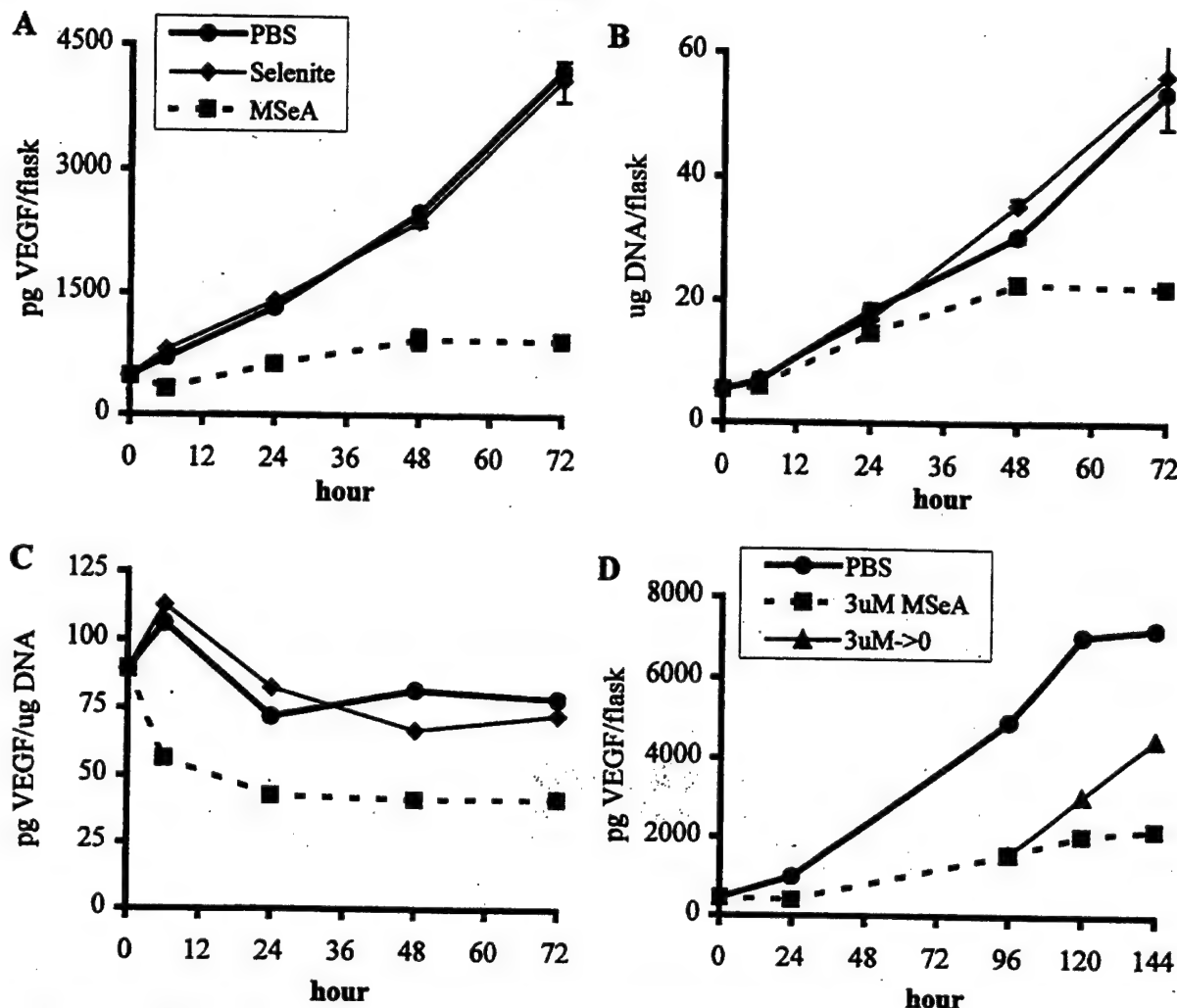
Figure 6. (A–C) Effects of daily exposure to low-dose MSeA (3 μM, squares) or selenite (3 μM, diamonds) on cellular VEGF content (A, total; C, normalized to DNA) and DNA content (B) of DU145 cells (two T25 flasks per datum point, each flask assayed in duplicate). Selenium exposure was initiated when cells were 40–50% confluent (log phase). Every 24 h, spent medium was removed and fresh complete medium (10% FBS) with sodium selenite or MSeA was fed. (D) Reversibility of effects of low-dose exposure to MSeA on VEGF expression in DU145 cells. After 96 h of exposure to 3 μM MSeA, one group of flasks remained on MSeA treatment, and the other group was washed with fresh medium once and then fed fresh complete medium for 24 and 48 h.

another methylselenol proximal precursor present in Se-enriched garlic and other seleniferous plants, induce exclusively apoptosis of cancerous mammary epithelial cells without induction of DNA single-strand breaks [40–42]. In contrast, sodium selenite and sodium selenide rapidly (within hours of Se exposure) induce DNA single-strand breaks (i.e., genotoxic) and lead to subsequent cell death by a composite of acute lysis and apoptosis [38–40]. These inorganic Se compounds and the methylselenol precursors also exert a differential antiproliferative effect, as assessed by [$^3$H]thymidine incorporation into DNA, and arrest the cells at different stages of the cell cycle [40–42]. More recently, specific inhibitory effects on cyclin-dependent kinases [43] and protein kinase C [44] have been attributed to the methylselenol pool. Together these findings indicate the presence of at least two

different pools of Se metabolites that induce distinct types of biochemical and cellular responses. Key features of these differences are schematically illustrated in Figure 8. It is noteworthy that only a single methylation reaction separates the two pools of Se metabolites.

We recently reported data supporting an antiangiogenic activity of Se at chemopreventive intake levels as a novel mechanism for cancer chemoprevention [6]. The present study extended that work and provided in vitro evidence of methyl Se–specific inhibition of the expression of two proteins critical for angiogenesis: MMP-2 by vascular endothelial cells and VEGF by cancer epithelial cells. The data support a rapid, primary, and sustained inhibitory action of the methyl Se pool on these proteins. Specifically, first with respect to MMP-2 expression in HUVECs, exposure to either MSeA or MSeCN led

## A. MCF-7, Secreted VEGF (6 h)



## B. MDA-MB468, Secreted VEGF (3 h)



## C.
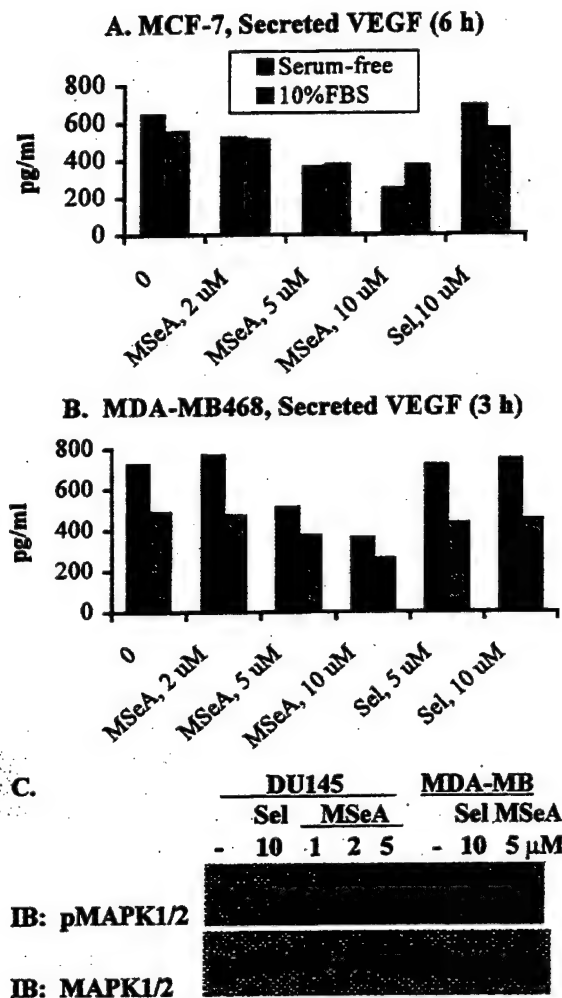


Figure 7. Effects of MSeA or sodium selenite on VEGF protein secreted by MCF-7 (A, 6-h treatment) and MDA-MB-468 breast cancer cells (B, 3-h treatment). Serum levels in the treatment medium were as indicated in panel A. (C) Lack of inhibitory effect by MSeA and selenite exposure (3 h) on phospho-MAPK1/2 levels in DU145 and MDA-MB-468 cancer cell lines.



Figure 8. Schematic relation of selenium precursors (dotted rectangles) that enter two metabolite pools that induce distinct biochemical and cellular effects. The genotoxicity (or lack of) and apoptogenic effects were based on studies with mammary cancer epithelial cells and leukemia cells [38–42]. The present study provides data supporting methylselenol-specific inhibitory effects on MMP-2 expression by vascular endothelial cells and VEGF expression by cancer epithelial cells.

to an Se concentration–dependent reduction of MMP-2 gelatinolytic activity (Figure 1A). Quantitation of the MMP-2 protein using western blot and ELISA analyses showed that a reduction of the protein level largely accounted for the loss of gelatinolytic activity (Figures 1C and 3C). The methyl Se–specific inhibition occurred rapidly (~0.5 h; Figures 2A and 3C) and appeared to persist well after the Se source was withdrawn (Figure 2B). The onset of inhibitory action on HUVEC MMP-2 level far preceded that of growth arrest and apoptosis responses, which required 25 h or longer exposure to MSeA (Figure 2C). Because neither MSeA nor MSeCN reacted directly in the test tube with MMP-2 protein to lead to its inactivation (Figure 1B), the observed inhibitory effect on MMP-2 expression must be a cell-dependent process or processes. In contrast to these methylselenol

immediate precursors, Se forms that enter the hydrogen selenide pool, at least during the time frame of the experiments performed, did not significantly decrease MMP-2 expression. The data, therefore, were consistent with the methylselenol precursors or their common product methylselenol triggering a cellular process or mechanism leading to the reduction of MMP-2 protein level (Figure 8). Technologic advances in quantitating the cellular hydrogen selenide and methylselenol levels should provide more direct support for this hypothesis.

As far as mechanisms are concerned, it will be important to determine whether an inhibition of MMP-2 gene transcription or an increase of MMP-2 protein turnover account for the methyl Se–specific reduction of MMP-2 protein level. Although an inhibition of gene transcription and mRNA translation is possible, the very fast inhibitory action of methyl Se on MMP-2 (~30 min) suggests that a mechanism involving the rapid degradation of cellular MMP-2 protein may also be triggered. It will also be important to determine whether MMP-2 expression in capillary microvascular endothelial cells, the likely targets of angiogenic stimulation, is inhibited by methyl Se with the same specificity and efficacy as in the vein endothelial cells (HUVECs) employed in the current study.

It is noteworthy that exposure to methyl Se induced phospho-MAPK1/2 inactivation (dephosphorylation) in the vascular endothelial cells, an effect that was lacking by either selenite or selenide exposure (Figure 3A and B). To our knowledge, this is the first time an Se metabolite-specific inhibitory effect on MAPK1/2 signaling has been described. However, the onset of the reduction of phospho-

MAPK1/2 level was preceded by the reduction of MMP-2 expression (Figure 3C). Such a temporal relation precluded the methyl Se inhibition of phospho-MAPK1/2 signaling as a mediating event in its acute inhibition of MMP-2 expression.

In addition to the methyl Se–specific inhibitory effects observed in monolayer culture on HUVEC MMP-2 expression and phospho-MAPK1/2, we observed profound inhibitory effects of MSeA and MSeCN on HUVEC retraction and viability in the three-dimensional context of capillary tubes formed on Matrigel (Figure 4). Such effects were methyl Se specific as they were not observed with selenite (Figure 4) or selenide (data not shown) at higher doses. These results suggest that methyl Se was likely more efficacious than selenite or selenide at inhibiting vascular endothelial cell viability and cell motility (for retraction) in a capillary histogenic environment relevant for angiogenic switch regulation. Future work will determine whether methyl Se inhibition of the MAPK signaling cascade and MMP-2 expression contributes to the observed effects on endothelial cell viability and motility in such a three-dimensional context.

With regard to VEGF expression in cancer epithelial cells, we observed a methyl Se–specific inhibition on VEGF protein level in the prostate cancer DU145 cell line and two breast cancer cell lines tested thus far. The inhibitory action on VEGF expression by MSeA was rapid (within 1–2 h; Figure 5C) irrespective of the serum level in which the cells were treated and independent of phosphorylation status of MAPK1/2 in the cancer cells (Figure 7). In addition, the inhibitory effect was elicited by exposure concentrations that did not negatively affect cell viability (Figures 5 and 6). In an attempt to simulate chemopreventive application of Se in a chronic, low-dose exposure context, we observed that daily exposure to MSeA exerted a sustained suppression of VEGF expression without evidence of developing resistance (Figure 6C). Further, withdrawal of MSeA exposure led to the de-repression of VEGF expression (Figure 6D), indicating a reversible mechanism of inhibition of VEGF expression by MSeA under the low-dose exposure context. This observation suggests that continued presence of methyl Se is necessary to inhibit VEGF expression.

VEGF plays a crucial role in vasculogenesis and angiogenesis in normal physiologic and pathologic states as indicated by germline knockout experiments in which a loss of even one VEGF allele leads to embryonic lethality in heterozygotes, and homozygous mutant embryonic stem cells are incapable of forming tumor [45,46]. Whereas overexpression of VEGF is linked to increased angiogenesis and more aggressive tumor behavior [47,48], antiangiogenic interventions, especially those based on VEGF antibodies or interference of signal transduction through its receptors [49–53], have been shown to

result in the inhibition of tumor growth and induction of endothelial apoptosis. The methyl Se-specific inhibitory effect on VEGF expression observed in the present work may therefore represent an important mechanism for the regulation of the angiogenic switch in early lesions by chemopreventive intake of Se.

The rapid inhibitory action of methyl Se on the expression of MMP-2 and VEGF suggests a commonality of mechanisms to bring about a reduction of the cellular level of the respective proteins. Further investigation of the biochemical and cellular processes involved in the reduction of their protein levels will shed light on how methyl Se activates such mechanisms. A salient feature of the two molecules is that both are secretory proteins containing intramolecular or intermolecular disulfide bridges critical for their activity or function [13,54]. One attractive hypothesis is that methylselenol generated intracellularly may disrupt such disulfide bridges, leading to destabilization of these proteins and selective proteolysis.

In summary, the present results support the hypothesis that the methyl Se metabolite pool, probably methylselenol, exerts potent and primary inhibitory effects on two proteins, with significant implications for angiogenesis switch regulation (as schematically summarized in Figure 8). Particularly noteworthy is the remarkable inhibitory efficacy, with $IC_{50}$ of ~2 μM after just a few hours of exposure. As reference values, the mean plasma Se concentration of subjects without Se supplementation in a recent human trial was ~1.5 μM, and Se supplementation (200 μg/d as selenized yeast) brought the mean Se level to ~2.5 μM [1]. Therefore, the methyl Se–specific inhibitory activities on these proteins may be physiologically pertinent for angiogenic switch regulation in early transformed lesions in vivo in the context of cancer chemoprevention, which aims at retarding and blocking the growth and progression of early lesions. The antiangiogenic attributes reported in this study and the growth arrest and apoptogenic activities without genotoxicity (Figure 8) make the methylselenol precursors attractive chemopreventive agents for considerations in humans.

## REFERENCES

1. Clark LC, Combs GF Jr, Turnbull BW, et al. Effects of selenium supplementation for cancer prevention in patients with carcinoma of the skin. A randomized controlled trial. Nutritional Prevention of Cancer Study Group. JAMA 1996; 276:1957–1963.
2. Yu SY, Zhu YJ, Li WG. Protective role of selenium against hepatitis B virus and primary liver cancer in Qidong. Biol Trace Elem Res 1997;56:117–124.
3. Blot WJ, Li JY, Taylor PR, Guo W, Dawsey SM, Li B. The Linxian trials: Mortality rates by vitamin-mineral intervention group. Am J Clin Nutr 1995;62(suppl):1424S–1426S.
4. Ip C. Lessons from basic research in selenium and cancer prevention. J Nutr 1998;128:1845–1854.
5. Combs GF Jr, Gray WP. Chemopreventive agents: Selenium. Pharmacol Ther 1998;79:179–192.
6. Jiang C, Jiang W, Ip C, Ganther H, Lu JX. Selenium-induced inhibition of angiogenesis in mammary cancer at chemo-preventive levels of intake. Mol Carcinog 1999;26:213–225.
7. Folkman J. Tumor angiogenesis: Therapeutic implications. N Engl J Med 1971;285:1182–1186.
8. Hanahan D, Folkman J. Patterns and emerging mechanisms of the angiogenic switch during tumorigenesis. Cell 1996; 86:353–364.
9. Bouck N, Stellmach V, Hsu SC. How tumors become angiogenic. Adv Cancer Res 1996;69:135–174.
10. Zetter BR. Angiogenesis and tumor metastasis. Annu Rev Med 1998;49:407–424.
11. Ip C, Ganther HE. Activity of methylated forms of selenium in cancer prevention. Cancer Res 1990;50:1206–1211.
12. Ip C, Hayes C, Budnick RM, Ganther HE. Chemical form of selenium, critical metabolites, and cancer prevention. Cancer Res 1991;51:595–600.
13. Coussens LM, Werb Z. Matrix metalloproteinases and the development of cancer. Chem Biol 1996;3:895–904.
14. Itoh T, Tanioka M, Yoshida H, Yoshioka T, Nishimoto H, Itohara S. Reduced angiogenesis and tumor progression in gelatinase A–deficient mice. Cancer Res 1998;58:1048–1051.
15. Deryugina EI, Bourdon MA, Reisfeld RA, Strongin A. Re-modeling of collagen matrix by human tumor cells requires activation and cell surface association of matrix metallo-proteinase-2. Cancer Res 1998;58:3743–3750.
16. Hiraoka N, Allen E, Apel IJ, Gyetko MR, Weiss SJ. Matrix metalloproteinases regulate neovascularization by acting as pericellular fibrinolysins. Cell 1998;95:365–377.
17. Leung DW, Cachianes G, Kuang WJ, Goeddel DV, Ferrara N. Vascular endothelial growth factor is a secreted angiogenic mitogen. Science 1989;246:1306–1309.
18. Keck PJ, Hauser SD, Krivi G, et al. Vascular permeability factor, an endothelial cell mitogen related to PDGF. Science 1989;246:1309–1312.
19. Brown LF, Guidi AJ, Tognazzi K, Dvorak HF. Vascular permeability factor/vascular endothelial growth factor and vascular stroma formation in neoplasia. Insights from in situ hybridization studies. J Histochem Cytochem 1998;46:569–575.
20. Guidi AJ, Abu-Jawdeh G, Tognazzi K, Dvorak HF, Brown LF. Expression of vascular permeability factor (vascular end-othelial growth factor) and its receptors in endometrial carcinoma. Cancer 1996;78:454–460.
21. Guidi AJ, Schnitt SJ, Fischer L, et al. Vascular permeability factor (vascular endothelial growth factor) expression and angiogenesis in patients with ductal carcinoma in situ of the breast. Cancer 1997;80:1945–1953.
22. Abu-Jawdeh GM, Faix JD, Niloff J, et al. Strong expression of vascular permeability factor (vascular endothelial growth factor) and its receptors in ovarian borderline and malignant neoplasms. Lab Invest 1996;74:1105–1115.
23. Brown LF, Berse B, Jackman RW, et al. Expression of vascular permeability factor (vascular endothelial growth factor) and its receptors in breast cancer. Hum Pathol 1995;26:86–91.
24. Fukumura D, Xavier R, Sugiura T, et al. Tumor induction of VEGF promoter activity in stromal cells. Cell 1998;94: 715–725.
25. Yoshizawa K, Willett WC, Morris SJ, et al. Study of pre-diagnostic selenium level in toenails and the risk of advanced prostate cancer. J Natl Cancer Inst 1998;90:1219–1224.
26. Davis RJ. The mitogen-activated protein kinase signal trans-duction pathway. J Biol Chem 1993;268:14553–14556.
27. Davis RJ. MAPKs: New JNK expands the group. Trends Biochem Sci 1994;19:470–473.
28. Reddy KB, Krueger JS, Kondapaka SB, Diglio CA. Mitogen-activated protein kinase (MAPK) regulates the expression of progelatinase B (MMP-9) in breast epithelial cells. Int J Cancer 1999;82:268–273.
29. Johansson N, Ala-Aho R, Uitto V, et al. Expression of collagenase-3 (MMP-13) and collagenase-1 (MMP-1) by transformed keratinocytes is dependent on the activity of p38 mitogen-activated protein kinase. J Cell Sci 2000;113: 227–235.
30. Lamoreaux WJ, Fitzgerald ME, Reiner A, Hasty KA, Charles ST. Vascular endothelial growth factor increases release of gelatinase A and decreases release of tissue inhibitor of metalloproteinases by microvascular endothelial cells in vitro. Microvasc Res 1998;55:29–42.
31. Doanes AM, Hegland DD, Sethi R, Kovesdi I, Bruder JT, Finkel T. VEGF stimulates MAPK through a pathway that is unique for receptor tyrosine kinases. Biochem Biophys Res Commun 1999;255:545–548.
32. Yu Y, Sato JD. MAP kinases, phosphatidylinositol 3-kinase, and p70 S6 kinase mediate the mitogenic response of human endothelial cells to vascular endothelial growth factor. J Cell Physiol 1999;178:235–246.
33. Gupta K, Kshirsagar S, Li W, et al. VEGF prevents apoptosis of human microvascular endothelial cells via opposing effects on MAPK/ERK and SAPK/JNK signaling. Exp Cell Res 1999;247:495–504.
34. Hata Y, Rook SL, Aiello LP. Basic fibroblast growth factor induces expression of VEGF receptor KDR through a protein kinase C and p44/p42 mitogen-activated protein kinase-dependent pathway. Diabetes 1999;48:1145–1155.
35. Ip C, el-Bayoumy K, Upadhyaya P, Ganther H, Vadhanavikit S, Thompson H. Comparative effect of inorganic and organic selenocyanate derivatives in mammary cancer chemoprevention. Carcinogenesis 1994;15:187–192.
36. Kubota Y, Kleinman HK, Martin GR, Lawley TJ. Role of laminin and basement membrane in the morphological differentiation of human endothelial cells into capillary-like structures. J Cell Biol 1988;107:1589–1598.
37. Hansen MB, Nielsen SE, Berg K. Re-examination and further development of a precise and rapid dye method for measuring cell growth/cell kill. J Immunol Methods 1989; 119:203–210.
38. Lu JX, Kaeck M, Jiang C, Wilson AC, Thompson HJ. Selenite induction of DNA strand breaks and apoptosis in mouse leukemic L1210 cells. Biochem Pharmacol 1994;47:1531–1535.
39. Wilson AC, Thompson HJ, Schedin PJ, Gibson NW, Ganther HE. Effect of methylated forms of selenium on cell viability and the induction of DNA strand breakage. Biochem Pharmacol 1992;43:1137–1141.
40. Lu JX, Jiang C, Kaeck M, et al. Dissociation of the genotoxic and growth inhibitory effects of selenium. Biochem Pharmacol 1995;50:213–219.
41. Lu JX, Pei H, Ip C, Lisk D, Ganther H, Thompson HJ. Effect of an aqueous extract of selenium enriched garlic on in vitro markers and in vivo efficacy in cancer prevention. Carcinogenesis 1996;17:1903–1907.

42. Kaeck M, Lu JX, Strange R, Ip C, Ganther HE, Thompson HJ. Differential induction of growth arrest inducible genes by selenium compounds. Biochem Pharmacol 1997;53: 921–926.

43. Sinha R, Medina D. Inhibition of cdk2 kinase activity by methylselenocysteine in synchronized mouse mammary epithelial tumor cells. Carcinogenesis 1997;18:1541–1547.

44. Sinha R, Kiley SC, Lu JX, et al. Effects of methylselenocysteine on PKC activity, cdk2 phosphorylation and gadd gene expression in synchronized mouse mammary epithelial tumor cells. Cancer Lett 1999;146:135–145.

45. Ferrara N, Carver-Moore K, Chen H, et al. Heterozygous embryonic lethality induced by targeted inactivation of the VEGF gene. Nature 1996;380:439–442.

46. Carmeliet P, Ferreira V, Breier G, et al. Abnormal blood vessel development and lethality in embryos lacking a single VEGF allele. Nature 1996;380:435–439.

47. Zhang HT, Craft P, Scott PA, et al. Enhancement of tumor growth and vascular density by transfection of vascular endothelial cell growth factor into MCF-7 human breast carcinoma cells. J Natl Cancer Inst 1995;87: 213–219.

48. McLeskey SW, Tobias CA, Vezza PR, Filie AC, Kern FG, Hanfelt J. Tumor growth of FGF or VEGF transfected MCF-7 breast carcinoma cells correlates with density of specific microvessels independent of the transfected angiogenic factor. Am J Pathol 1998;153:1993–2006.

49. Borgstrom P, Hillan KJ, Sriramarao P, Ferrara N. Complete inhibition of angiogenesis and growth of microtumors by anti-vascular endothelial growth factor neutralizing antibody: Novel concepts of angiostatic therapy from intravital videomicroscopy. Cancer Res 1996;56:4032–4039.

50. Borgstrom P, Bourdon MA, Hillan KJ, Sriramarao P, Ferrara N. Neutralizing anti-vascular endothelial growth factor antibody completely inhibits angiogenesis and growth of human prostate carcinoma micro tumors in vivo. Prostate 1998;35:1–10.

51. Meeson AP, Argilla M, Ko K, Witte L, Lang RA. VEGF deprivation-induced apoptosis is a component of programmed capillary regression. Development 1999;126: 1407–1415.

52. Benjamin LE, Golijanin D, Itin A, Pode D, Keshet E. Selective ablation of immature blood vessels in established human tumors follows vascular endothelial growth factor withdrawal. J Clin Invest 1999;103:159–165.

53. Benjamin LE, Keshet E. Conditional switching of vascular endothelial growth factor (VEGF) expression in tumors: induction of endothelial cell shedding and regression of hemangioblastoma-like vessels by VEGF withdrawal. Proc Natl Acad Sci USA 1997;94:8761–8766.

54. Claffey KP, Senger DR, Spiegelman BM. Structural requirements for dimerization, glycosylation, secretion, and biological function of VPF/VEGF. Biochim Biophys Acta 1995; 1246:1–9.

Lu3

# Caspases as Key Executors of Methyl Selenium-induced Apoptosis (Anoikis) of DU-145 Prostate Cancer Cells[1]

## Cheng Jiang, Zaisen Wang, Howard Ganther, and Junxuan Lu[2]

*AMC Cancer Research Center, Denver, Colorado 80214 [C. J., Z. W., J. L.], and University of Wisconsin-Madison, Madison, Wisconsin 53706 [H. G.]*

## ABSTRACT

Apoptosis induction may be a mechanism mediating the anticancer activity of selenium. Our earlier work indicated that distinct cell death pathways are likely involved in apoptosis induced by the $CH_3SeH$ and the hydrogen selenide pools of selenium metabolites. To explore the role of caspases in cancer cell apoptosis induced by selenium, we examined the involvement of these molecules in the death of the DU-145 human prostate carcinoma cells induced by methylseleninic acid (MSeA), a novel penultimate precursor of the putative critical anticancer metabolite $CH_3SeH$. Sodium selenite, a representative of the genotoxic selenium pool, was used as a reference for comparison. The results show that MSeA-induced apoptosis was accompanied by the activation of multiple caspases (caspase-3, -7, -8, and -9), mitochondrial release of cytochrome $c$ (CC), poly(ADP-ribose) polymerase (PARP) cleavage, and DNA fragmentation. In contrast, selenite-induced apoptotic DNA fragmentation was observed in the absence of these changes, but was associated with the phosphorylation of c-Jun-$NH_2$-terminal kinase 1/2 and p38 mitogen-activated protein kinase/stress-activated protein kinase 2. A general caspase inhibitor, benzyloxycarbonyl-Val-Ala-Asp-(OMe) fluoromethyl ketone, blocked MSeA-induced cleavage of procaspases and PARP, CC release, and DNA nucleosomal fragmentation, but did not prevent cell detachment. Furthermore, PARP cleavage and caspase activation were confined exclusively to detached cells, indicating that MSeA induction of cell detachment was a prerequisite for caspase activation and apoptosis execution. This process therefore resembled "anoikis," a special mode of apoptosis induction in which adherent cells lose contact with the extracellular matrix. Additional experiments with irreversible caspase inhibitors show that MSeA-induced anoikis involved caspase-3- and -7-mediated PARP cleavage that was initiated by caspase-8 and probably amplified through CC-caspase-9 activation and a feedback activation loop from caspase-3. Taken together, the data support a methyl selenium-specific induction of DU-145 cell apoptosis that involves cell detachment as a prerequisite (anoikis) and is executed principally through caspase-8 activation and its cross-talk with multiple caspases.

## INTRODUCTION

The trace element selenium is an essential micronutrient for humans and animals. The current recommended daily allowance is 55 $\mu$g for a healthy adult (1). Two human cancer prevention trials have indicated that a supranutritional selenium supplement (*i.e.*, 200 $\mu$g daily) might be an effective preventive agent for several major cancers, including those of the prostate, lung, colon (2), and liver (3). The results corroborate findings in various animal models that selenium possesses a potent cancer chemopreventive activity when its intake exceeds the nutritional requirement by ~10-fold (4). The studies in these model systems have provided significant insights on the potential mechanisms of action. It has been shown that a mono-methyl selenium species, possibly methylselenol ($CH_3SeH$), may be a critical *in vivo* selenium metabolite against chemically induced mammary

carcinogenesis; the cancer preventive efficacy of a given selenium compound may depend on the rate of its metabolic conversion to that active form (4–6). Selenium-enriched garlic, of which selenium-methylselenocysteine constitutes a major selenium component, exerted a lasting protective effect even when provided for as little as 1 month in the early promotion stage of mammary carcinogenesis (7, 8). These findings suggest that a chemopreventive intake of selenium may exert protection against cancer development by inducing the loss of transformed epithelial cells *in vivo*. Because lesion size is governed by the balance between rates of cell proliferation and cell death, the significance of a cell deletion action is further implicated by the lack of a detectable antiproliferative effect of a selenium dose that conferred effective chemoprevention *in vivo* in a chemically induced mammary carcinogenesis model (9).

Regarding the cell deletion action of selenium, our previous work documented distinct proapoptotic effects of different chemical forms (pools) of selenium on mammary tumor epithelial cells *in vitro* (8, 10, 11). Immediate precursors of $CH_3SeH$, such as selenium-methylselenocyanate and selenium-methylselenocysteine, were shown to induce exclusively apoptosis of mammary tumor epithelial cells without induction of DNA single strand breaks (8, 10). On the other hand, sodium selenite and sodium selenide, which feed into the hydrogen selenide ($H_2Se$) pool (12), induced DNA single strand breaks (*i.e.*, genotoxic) within a few hours of selenium exposure and subsequent cell death by a composite of acute lysis and apoptosis (10). However, little is known of the execution pathway(s) of methyl selenium-induced cancer cell apoptosis.

Programmed cell death induced by physiological/pathological cues often is characterized by marked changes in cellular morphology, including chromatin condensation, membrane blebbing, nuclear breakdown, and the appearance of membrane-enclosed apoptotic bodies (13). Biochemically, internucleosomal DNA fragmentation and caspase-mediated cleavage of PARP[3] and key cytoskeletal proteins principally underlie these cellular and nuclear changes (14, 15). PARP cleavage essentially inactivates the enzyme by destroying its ability to respond to DNA strand breaks for repair, and it also blocks necrosis resulting from PARP-mediated $NAD^+$/ATP depletion to ensure an irreversible apoptotic death (16). PARP cleavage has now been recognized as a sensitive marker of caspase-mediated apoptosis.

Caspases are aspartate-specific cysteine proteases, existing as latent intracellular zymogens (14, 15). Once activated by apoptotic signals, they can systematically dismantle the cell by cleaving key cellular and nuclear proteins with defined substrate specificities (14, 15). According to their sequence of action in apoptosis signaling, the more than 14 caspases are organized into apoptotic initiator caspases (caspase-2, -8, -9, and -10), apoptotic executioner caspases (caspase-3, -6, and -7), and cytokine processor caspases (caspase-1, -4, -5, -11, -12, -13, and -14). The initiator caspases appear to have some specificity for dif-

[3] The abbreviations used are: PARP, poly(ADP-ribose) polymerase; FADD, Fas-associated death domain (Mort-1); CC, cytochrome $c$; APAF-1, apoptosis protease activation factor-1; MSeA, methylseleninic acid; zVADfmk, benzyloxycarbonyl-Val-Ala-Asp-(OMe) fluoromethyl ketone; zDEVDfmk, benzyloxycarbonyl-Asp-Glu-Val-Asp-(OMe) fluoromethyl ketone; zIETDfmk, benzyloxycarbonyl-Ile-Glu-Thr-Asp-(OMe) fluoromethyl ketone; zLEHDfmk, benzyloxycarbonyl-Leu-Glu-His-Asp-(OMe) fluoromethyl ketone; PKB, protein kinase B; JNK, c-Jun-$NH_2$-terminal kinase; SAPK, stress-activated protein kinase; MAPK, mitogen-activated protein kinase; p-NA, p-nitroaniline.

ferent types of upstream apoptosis signals as well as preferred downstream substrate procaspases. In fact, two general activation cascades have been described (14–17). The first involves cell death receptor-mediated signaling through caspase-8. Once the receptor is activated, the adapter molecule FADD becomes recruited to the receptor, allowing binding and autocleavage activation of procaspase-8. The active caspase-8 in turn cleaves executioner procaspases (caspase-3, -6, and -7), leading to their activation. The second, termed the "apoptosome" cascade, involves activation of procaspase-9 by CC released from mitochondria. Once in the cytosol, CC binds to APAF-1, which then permits recruitment of procaspase-9, resulting in the oligomerization and autoactivation of procaspase-9. Active caspase-9 then cleaves and activates executioner procaspases. The mitochondrial pathway has been shown to be triggered by diverse chemotherapeutic agents (16, 17). Furthermore, there have been ample examples of cross-talk between these two cascades in many apoptosis models. For example, caspase-8-cleaved BID, a Bcl-2 interacting protein, had been shown to amplify CC release from mitochondria (18, 19). Recent reports have shown a feedback amplification of CC release by downstream effector caspases (20–22). Therefore, depending on the apoptosis signal, the death-receptor/caspase-8 cascade or the CC/APAF-1/caspase-9 cascade can play either a direct initiating or an indirect amplifying role in caspase activation and apoptosis execution.

To explore the role of caspases in cancer cell apoptosis induced by selenium, particularly by $CH_3SeH$, we examined the involvement of these molecules in the death of the DU-145 human prostate carcinoma cells induced by methylseleninic acid ($CH_3SeO_2H$; MSeA) in contrast to selenite, used as a reference. MSeA is a novel, penultimate $CH_3SeH$ precursor that is water soluble, nonvolatile, and ideal for cell culture delivery for mechanistic investigations. We chose to use a human prostate carcinoma cell line for this study because the prostate appears to be a sensitive organ site for cancer chemoprevention by selenium in a recent prevention trial (2). Our data show that MSeA-induced nucleosomal DNA fragmentation was accompanied by the activation of multiple caspases (caspase-3, -7, -8, and -9), PARP cleavage, and mitochondrial release of CC, whereas apoptotic DNA fragmentation induced by selenite was observed in the absence of these changes. Furthermore, the data support MSeA induction of cell detachment as a prerequisite for the activation of caspases in an apoptosis execution process resembling "anoikis," a special mode of apoptosis induction in which adherent cells lose contact with the extracellular matrix (23).

## MATERIALS AND METHODS

**Chemicals and Reagents.** Sodium selenite pentahydrate was purchased from J.T. Baker, Inc (Phillipsburg, NJ). MSeA synthesis has been described elsewhere (24), and concentrated stocks were stored in small aliquots at −80°C. Intracellularly, MSeA probably reacts with reduced glutathione to generate $CH_3SeH$. The caspase inhibitors zVADfmk (general), zDEVDfmk (caspase-3 and -7; see Ref. 25 for specificity), zIETDfmk (caspase-8), and zLEHDfmk (caspase-9) were from Enzyme Systems Inc. (Dublin, CA). Reagent kits for CC ELISA and caspase colorimetric activity assays were purchased from R&D Systems (Minneapolis, MN) and used per the manufacturer's instructions. Antibodies for PARP and caspases were purchased from Cell Signaling Technology (apoptosis sampler kit, cat. no. 9915; Beverly, MA) and BD PharMingen (San Diego, CA). Phospho-specific antibodies for AKT/PKB, JNK and p38 MAPK were purchased from New England Biolabs (Beverly, MA).

**Cell Culture and Selenium Treatments.** DU-145 prostate cancer cells were kindly provided by R. Agarwal (AMC Cancer Research Center), who originally obtained these cells from the American Type Culture Collection. The cells had been passaged ~50 times when we took possession. DU-145 cells were cultured in RPMI 1640 supplemented with 10% fetal bovine serum and 2 mM L-glutamine (no antibiotics). For the DNA fragmentation assay, caspase activity and immunoblot analyses, cells were treated in T75 or T25

flasks. When cells reached 50–70% confluence, the medium was changed, and the cells were treated with selenium or other agents. To standardize selenium exposure, cells were given fresh medium at a volume-to-surface area ratio of 0.2 ml/cm² (15 ml for a T75 flask and 5 ml for a T25 flask). Concentrated selenium stock (aqueous solution stored at −80°C) was diluted in PBS to 1 mM immediately before use. In experiments in which caspase inhibitors were used, the inhibitors (dissolved in DMSO) and MSeA were mixed into treatment medium first and then fed to cells. DMSO was added to groups that did not receive inhibitors to control for solvent effects. The final concentration of DMSO was ≤2 μl/ml and did not by itself induce adverse cellular responses. Representative morphological responses to selenium exposure were documented with a Polaroid camera at ×200 magnification under a phase-contrast microscope. All experiments were replicated two or more times.

**DNA Isolation and Gel Electrophoresis.** DNA isolation and gel electrophoresis were as described previously (26). Briefly, after selenium exposure, conditioned medium was collected, and detached cells were recovered by centrifugation at 200 × g for 5 min at room temperature. Adherent cells were lysed and scraped in 1 ml of a buffer containing 10 mM Tris-HCl (pH 8.0), 100 mM EDTA, 0.5% SDS, and 0.5 mg/ml proteinase K and pooled with the detached cells. After digestion at 50°C for 3 h, the lysate was extracted twice with phenol-chloroform. Nucleic acids were precipitated with 0.6 volume of isopropanol in the presence of 0.2 M NaCl. The pellet was resuspended in 30 μl of 10 mM Tris-HCl, 1 mM EDTA (pH 7.5); treated with RNase to digest RNA; loaded onto an 1.5% agarose gel containing 0.1 μg/ml ethidium bromide; and electrophoresed. Gels were photographed with Polaroid films using UV illumination and digitized with a scanner.

**Immunoblot Analyses.** After selenium exposure for a defined length of time, detached cells were collected as above by centrifugation. The cell pellet was washed once in ice-cold PBS. Adherent cells were washed twice in PBS, lysed in radioimmunoprecipitation assay buffer [50 mM Tris-HCl (pH 7.4), 150 mM NaCl, 2 mM EDTA, 50 mM NaF, 1% Triton X-100, 1% sodium deoxycholate, 0.1% SDS, 1 mM DTT, 5 mM sodium orthovanadate, 1 mM phenylmethylsulfonyl fluoride, and 38 μg/ml aprotinin (added fresh)], and pooled with the detached cell pellet. After sonication, the lysate was centrifuged (14,000 × g for 20 min at 4°C), and supernatant was recovered. The protein content was quantified by the Bradford dye-binding assay (Bio-Rad Laboratories, Richmond, CA). Forty (for PARP, AKT, JNK, and p38 MAPK) or 100 μg (for caspases) of total protein were size-separated by electrophoresis on 10, 12, or 15% SDS-polyacrylamide gels, depending on the sizes of target proteins. The proteins were electroblotted onto nitrocellulose membranes and probed using primary antibodies commercially obtained from Cell Signaling Technology, New England Biolabs, or other vendors and detected by enhanced chemiluminescence. In many cases, antibodies from multiple sources for a protein of interest were used to verify specificity of detection. Positive-control samples obtained from the antibody suppliers were used whenever available. The X-ray films were digitized using a transmission scanner, and the signal intensity was quantified using the UN-SCAN-IT gel scanner software (Silk Scientific, Inc., Orem, UT).

**Caspase Activity Assays.** After selenium treatment of a defined length, the detached cells were harvested by centrifugation at 200 × g for 5 min at room temperature as above, washed once with PBS, and the cell pellets were held on ice. The adherent cells were washed twice with PBS, scraped off in 500 μl of ice-cold lysis buffer provided with R&D Systems caspase assay kits, and pooled with the detached cells. After sonication, the lysate was centrifuged for 20 min at 14,000 × g at 4°C. The resulting supernatants were analyzed for protein concentration by the Bradford dye-binding assay and stored at −20°C until used for caspase colorimetric enzymatic activity assays per the manufacturer's instruction using 96-well plate. Equal amounts of protein from different treatments were used, and the assays were set up on ice. Absorbance was recorded on a plate reader at 405 nm immediately after the start of the assay and after 10–16 h of incubation at 37°C. The net increase of absorbance was indicative of enzyme activity.

**CC Assay.** Mitochondria-free cytosol was prepared according to a method described for prostate cancer cells (27). Briefly, after selenium treatment of a defined length, the detached floaters were harvested by centrifugation at 200 × g for 5 min at room temperature as above, washed once with PBS, and the cell pellets were held on ice. The adherent cells were washed twice with PBS, scraped off in 500–700 μl of ice-cold hypotonic buffer [20 mM HEPES-KOH (pH 7.4), 10 mM KCl, 1.5 mM MgCl₂, 1 mM sodium EDTA, 1 mM

## A. Phase contrast morphology
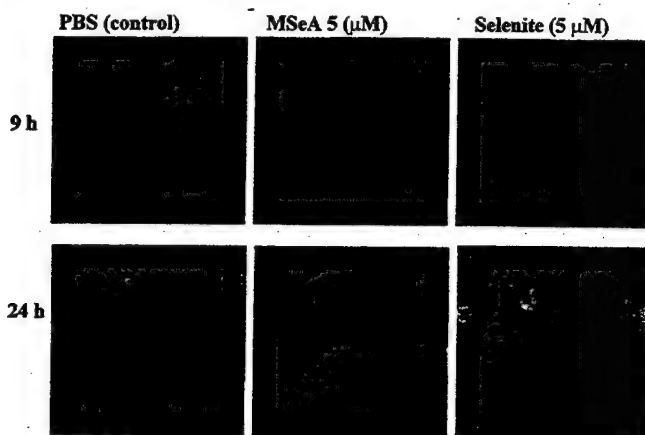


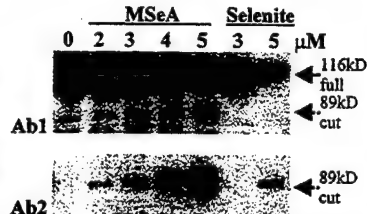## B. DNA fragmentation at 24 h    C. PARP Cleavage at 24 h



Fig. 1. *A*, phase contrast photomicrographs depicting representative morphological responses of DU-145 prostate cancer cells at 9 and 24 h of exposure to 5 μM MSeA or selenite. Note profound cell retraction and rounding at 9 h and detached or loosely adhered rounded cells at 24 h for MSeA-treated cells. For selenite-exposed cells, note prominent cytosolic vacuoles in adherent cells at 9 h and vacuolated adherent cells and floaters (out of focus) at 24 h. Magnification, ×200. *B*, agarose gel (1.5%) electrophoretic detection of nucleosomal DNA fragmentation at 24 h of exposure to increasing concentrations of MSeA or selenite. The *leftmost lane* was loaded with 100-bp DNA size markers. Inverted image was used to better show fragmented DNA. *C*, immunoblot detection of PARP cleavage at 24 h of exposure to increasing concentrations of MSeA or selenite. Antibody 1 (*Ab1*) detected both the full-length (116 kDa) and cleavage product (89 kDa) of PARP. The increased sensitivity of detection by Ab2 in the *bottom panel* was attributable to the use of an antibody that specifically recognized only the cleaved PARP (cat. no. 9915; Cell Signaling Technology). Adherent cells and detached floaters were combined for cell lysate preparations for these analyses.

sodium EGTA, 1 mM DTT, 250 mM sucrose, and protease inhibitors], and pooled with floaters. After incubation on ice for 20 min, cells were further disrupted by Dounce homogenization for 50 strokes. Nuclei and cellular debris were removed by centrifugation at 1000 × g for 10 min at 4°C. Supernatants were further centrifuged for 20 min at 14,000 × g at 4°C to pellet mitochondria. The resulting supernatants were analyzed for protein concentration by Bradford dye binding and stored at −80°C until analyzed for CC content using an ELISA kit from R&D Systems. Equal amounts of protein from different treatments were used for these assays.

## RESULTS

**Morphological Responses and DNA Nucleosomal Fragmentation.** Exposure of DU-145 cells in log-phase monolayer culture to 5 μM MSeA led to cell retraction (elongated rod shapes) and rounding by 9 h and subsequent detachment of individual cells from the culture vessels (Fig. 1A). Some, but not all, detached cells (floaters) displayed the grape-like fragmented morphology typical of apoptotic bodies under a phase-contrast microscope. In contrast, exposure to sodium selenite led to the appearance of prominent cytoplasmic vacuoles by 9 h and detached floaters later (Fig. 1A). Despite the different morphological responses elicited by the two forms of selenium, both MSeA- and selenite-treated cells displayed DNA nucleosomal fragmentation typical of apoptotic cell death at 24 h of exposure (Fig. 1B).

**PARP Cleavage Was Detected Mainly in MSeA-exposed Cells.** In dose-response experiments, PARP cleavage was detected in MSeA-treated cells after 24-h exposure at as low as 3 μM and increased in a dose-dependent manner (Fig. 1C). On the other hand, PARP cleavage was minimal in cells exposed to 5 μM selenite (Fig. 1C) that had undergone a comparable extent of DNA nucleosomal fragmentation (Fig. 1B). Instead, the level of full-length PARP expression decreased in selenite-exposed apoptotic cells. These results indicate that PARP cleavage was involved in apoptosis execution induced by MSeA, but was minimally, if at all, involved in apoptosis induced by selenite within the time frame of the study.

**Multiple Caspase Activities and Mitochondrial Release of CC Were Detected in MSeA-exposed, but not Selenite-exposed, Cells.** To define which caspases were involved in PARP cleavage during apoptosis induced by MSeA, we analyzed the enzymatic activities of DU-145 cell lysates against tetrapeptide substrates DEVDp-NA (for caspases-3 and caspase-7), IETDp-NA (for caspase-8) and LE-HDp-NA (for caspase-9) after 24-h exposure to 5 μM selenium as either MSeA or selenite (Fig. 2, A–C). The relative hydrolytic activities toward the respective substrates were 5.3-, 1.7-, and 2.1-fold in MSeA-treated cells compared with untreated control cells, whereas no changes in the activities of these enzymes were detected in the
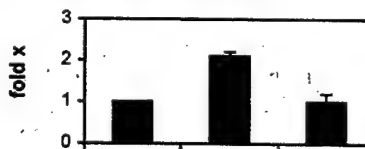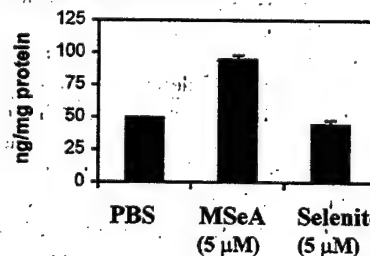


Fig. 2. *A–C*, enzymatic activities of cell lysates toward tetrapeptide caspase substrates in DU-145 prostate cancer cells at 24 h of exposure to 5 μM MSeA or selenite. The chromogenic substrates were DEVD-pNA (caspase-3-like and caspase-7; *A*), IETD-pNA (caspase-8; *B*), and LEHD-pNA (caspase-9; *C*). The caspase activity was expressed as fold relative to untreated controls and represented mean and SD (*bars*) of three independent experiments done on different occasions. *D*, CC content in postmitochondrial cytosol preparations of DU-145 prostate cancer cells at 24 h of exposure to 5 μM MSeA or selenite measured using a CC ELISA. Adherent cells and floaters were combined for the analyses of caspases and CC. Protein contents of the cell lysates were measured to equalize input of protein from different groups for each assay.
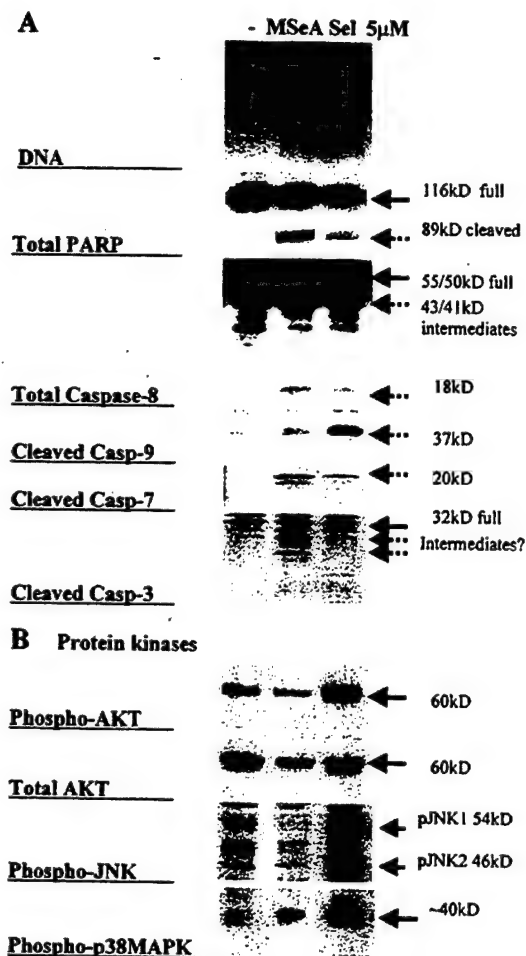
## A



## B Protein kinases

Fig. 3. *A,* immunoblot analyses of the cleavage patterns of selected caspases in DU-145 prostate cancer cells at 26 h of exposure to 5 μM selenium as MSeA or selenite (*Sel*). *Solid arrows* indicate full-length proteins. *Dashed arrows* indicate cleavage intermediates and final products. *?* indicates that intermediates have not been identified. *B,* phosphorylation status of selected protein kinases involved in cell survival and cellular stress and apoptosis signaling in DU-145 prostate cancer cells at 24 h of exposure to 5 μM selenium as MSeA or selenite. Adherent cells and floaters were combined for cell lysate preparations for immunoblot analyses.

selenite-treated cells. The cytosolic CC level was increased 2-fold in the MSeA-treated cells, but not in selenite-treated cells (Fig. 2*D*). These results indicate that CC release might be involved in some aspect of caspase activation in MSeA-induced apoptosis.

By immunoblot detection, cleavage of procaspase-8, -9, -3, and -7 was detected in MSeA-treated cells at 26 h of exposure, corresponding to significant PARP cleavage and DNA fragmentation (Fig. 3*A*). On the other hand, selenite-exposed cells did not cleave procaspase-3, slightly increased procaspase-7 cleavage, and minimally cleaved PARP despite pronounced DNA nucleosomal fragmentation (Fig. 3*A*). Paradoxically, the extent of procaspase-9 cleavage in the selenite-treated cells was much greater than in MSeA-treated cells (Fig. 3*A*), although caspase-9 activity was not detected in the selenite-treated cells (Fig. 2*C*). Similarly, selenite-exposed cells underwent increased cleavage of procaspase-8 compared with untreated control cells, but failed to hydrolyze the IETDp-NA substrate in the caspase-8 enzyme assay.

The discrepancy between procaspase-9 cleavage (suggesting activation; Fig. 3*A*) and the lack of measurable hydrolysis of LEHDp-NA (Fig. 2*C*) in selenite-exposed cells might be in part attributable to increased phosphorylation (suggesting activation) of AKT/PKB (Fig. 3*B*), a survival enzyme (28) that has been shown to inhibit apoptosis

at least in part through an inactivation of caspase-9 (29) and the proapoptotic BAD protein (30, 31) by phosphorylation. The selenite-exposed cells, but not those treated with MSeA, also had a significant induction of the phosphorylation of JNK1 (p54), JNK2 (p46), and p38 MAPK/SAPK2 (Fig. 3*B*), two protein kinase pathways that have been linked to stress responses and apoptosis (32). These results suggest potential alternative pathways that might contribute to selenite-induced apoptosis signaling and execution independent of caspases and PARP cleavage.

**Temporal Relationship of Caspase Activation and PARP Cleavage in MSeA-exposed Cells.** To further define the involvement of caspase in MSeA-induced apoptosis, we analyzed the kinetic patterns of procaspase cleavage in time course experiments (Fig. 4). In an acute exposure setting (experiment 1), the appearance of procaspase-8 cleavage intermediates of 43 or 41 kDa was observed at 6 h, whereas the final cleavage products of procaspase-8, -9, and -7 were detectable by 10 h of exposure when PARP cleavage became apparent. The activation of these three enzymes preceded induction of the expression of what appeared to be cleavage intermediate(s) of procaspase-3 by at least 2 h. In experiment 2, the levels of cleaved caspase-8 and -9 peaked at 16 h, whereas those for caspase-3 and -7 peaked at 20 h. These cleavage patterns suggest that the initial PARP cleavage before caspase-3 activation was likely attributable to cleaved caspase-7 or -9 and that, once activated, caspase-3 might further amplify PARP cleavage.

Measurement of enzyme activity indicated that hydrolysis of IETDp-NA (caspase-8 activity) increased significantly at 12 h of MSeA exposure and peaked at 16 h, whereas hydrolysis of DEVDp-NA (caspase-3 and -7 activity) increased with the same time frame, but peaked at 20 h (Fig. 5). The hydrolysis of LEHDp-NA (caspase-9 activity) also peaked at 20 h (Fig. 5). Together, the cleavage patterns and activity measurements suggest that the activation of caspase-8 was mostly an upstream event for caspase-mediated PARP cleavage during MSeA-induced apoptosis.

**A General Caspase Inhibitor Abolished MSeA-induced PARP Cleavage, CC Release, and DNA Fragmentation.** Cotreatment of DU-145 cells with zVADfmk (80 μM) blocked, as expected, MSeA-induced cleavage of procaspase-8, -9, -3, and -7 completely at 20 h of exposure (Fig. 6*A*). This general caspase inhibitor also completely blocked PARP cleavage and DNA fragmentation (Fig. 6*A*) and mitochondrial CC release (Fig. 6*B*). These results indicate that these three events are caspase dependent and that the CC/caspase-9 activation cascade might be a secondary amplification, rather than an initiating, pathway in MSeA-induced apoptosis execution.

Contrary to its inhibitory efficacy on these apoptosis-execution events, zVADfmk did not block cell retraction and rounding, nor did it decrease the number of cells that subsequently detached to become floaters by 20 h (Fig. 6*C*). Cleavage of PARP and procaspase-3 and -7 was detected exclusively in the MSeA-induced floaters, and was not detectable in the adherent cells (Fig. 6*C*). The inhibitor blocked the cleavage of procaspase-3 and -7 and PARP in the MSeA-induced floaters (Fig. 6*C*). These observations indicate that MSeA-induced cell detachment is a prerequisite for caspase activation and PARP cleavage. This mode of apoptosis induction closely resembled anoikis, in which adherent cells undergo apoptosis after becoming detached from the extracellular matrix (23).

**Effects of Specific Caspase Inhibitors on MSeA-induced PARP Cleavage and DNA Fragmentation.** To delineate the relative contributions of the various caspases, especially with reference to the two activation cascades described in the "Introduction" (14, 15) for MSeA-induced PARP cleavage, we next examined the impacts of irreversible caspase inhibitors zIETDfmk (for caspase-8), zLEHDfmk (for caspase-9), zDEVDfmk (for caspase-3 and, at higher level, for
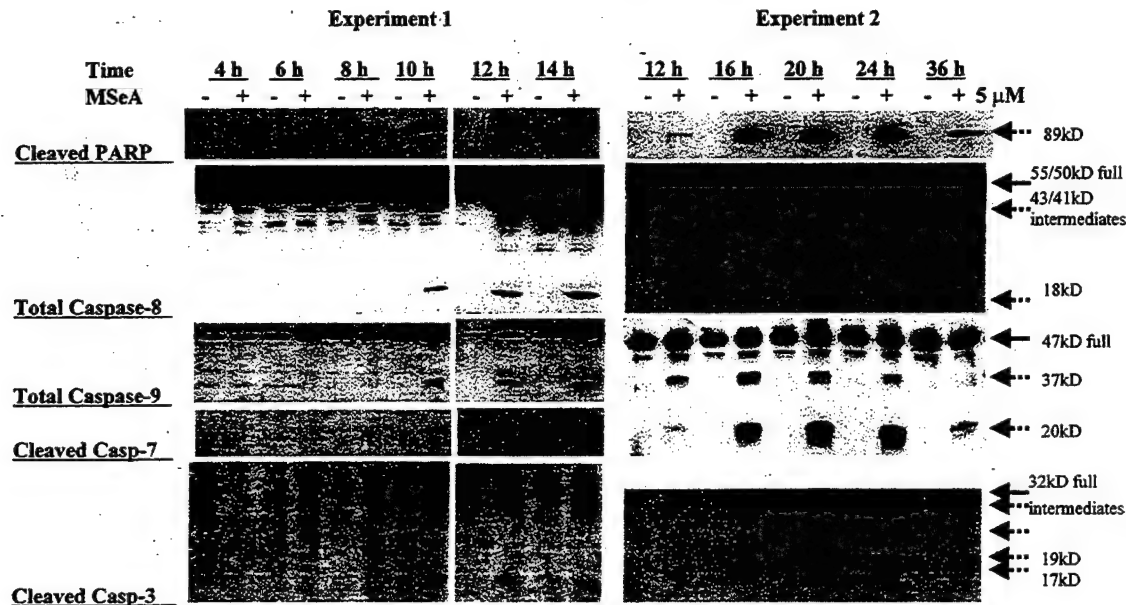
Fig. 4. Immunoblot analyses of the time course of MSeA-induced cleavage of PARP and selected caspases in DU-145 prostate cancer cells exposed to 5 μM MSeA. Adherent cells and floaters were combined for cell lysate preparations for these immunoblot analyses. The experiments were conducted several weeks apart, which might account for the slight difference in the time of onset of caspase activation and PARP cleavage between them. *Solid arrows* indicate full-length proteins; *dashed arrows* indicate possible cleavage intermediates and final products.

caspase-7; Ref. (25) and zVADfmk (for all caspases) at a concentration of 40 μM for each inhibitor. As shown in Fig. 7A, at 40 μM the general caspase inhibitor zVADfmk completely blocked MSeA-induced PARP cleavage, which is in excellent agreement with the data presented in Fig. 6 for 80 μM inhibitor. The caspase-8 inhibitor zIETDfmk decreased PARP cleavage by 90%, and the caspase-9 inhibitor zLEHDfmk decreased PARP cleavage by 40%. When the two inhibitors were used together, the effect was the same as for the caspase-8 inhibitor alone, indicating that caspase-9 might be a downstream component of the caspase-8 activation cascade rather than as an independent pathway.

The effects of these inhibitors on the caspase cleavage patterns and PARP cleavage provided further support for this scenario. As shown in Fig. 7B, the caspase-8 inhibitor zIETDfmk decreased the cleavage of procaspase-9 by 90% and completely blocked the generation of the cleaved caspase-7 (20 kDa) and caspase-3 (17 kDa). The caspase-9 inhibitor zLEHDfmk decreased the extent of active caspase-3 (17 kDa product) by 60% and active caspase-7 by 70%, whereas it had little effect on the accumulation of the cleaved caspase-9 itself. Blockage of the caspase-8 activity decreased the extent of MSeA-induced PARP cleavage by 90%, and the caspase-9 inhibitor decreased PARP cleavage by 60% in this experiment, in good agreement with the previous experiment.

The caspase-3-like inhibitor zDEVDfmk blocked MSeA-induced PARP cleavage by ~97%, establishing caspase-3 as a major player in PARP cleavage (Fig. 7B) with minor contribution from caspase-7 to this activity. Surprisingly, this inhibitor produced nearly complete inhibition not only of caspase-3 cleavage, but also of caspase-9 cleavage. These results, coupled with the delayed activation of caspase-3 in the time course experiments (Fig. 4), suggest a possible feedback loop from caspase-3 to caspase-9. zDEVDfmk significantly reduced (~80%) but did not completely block procaspase-7 cleavage, which might be attributable to the initial caspase-8 and -9 activities leading to procaspase-7 cleavage before the feedback loop from caspase-3 was established. On the basis of these cleavage patterns and the fact that zVADfmk blocked CC release from mitochondria (Fig.
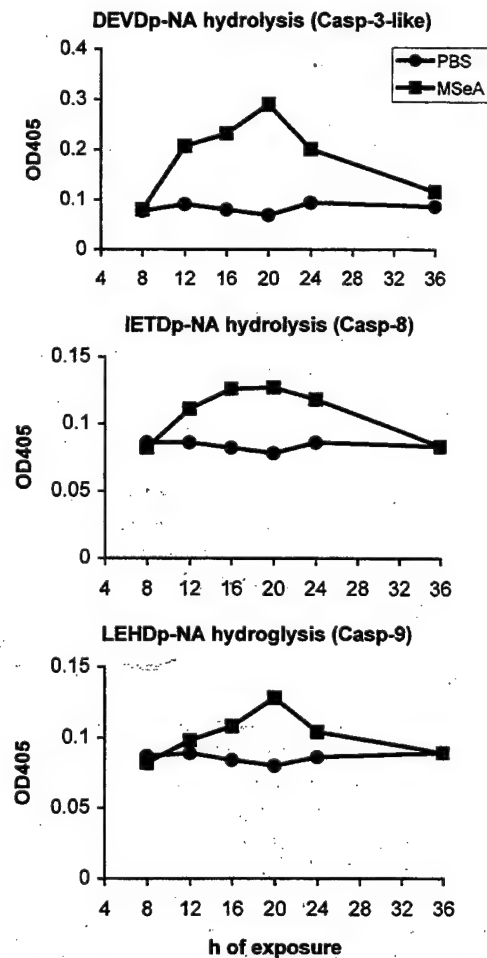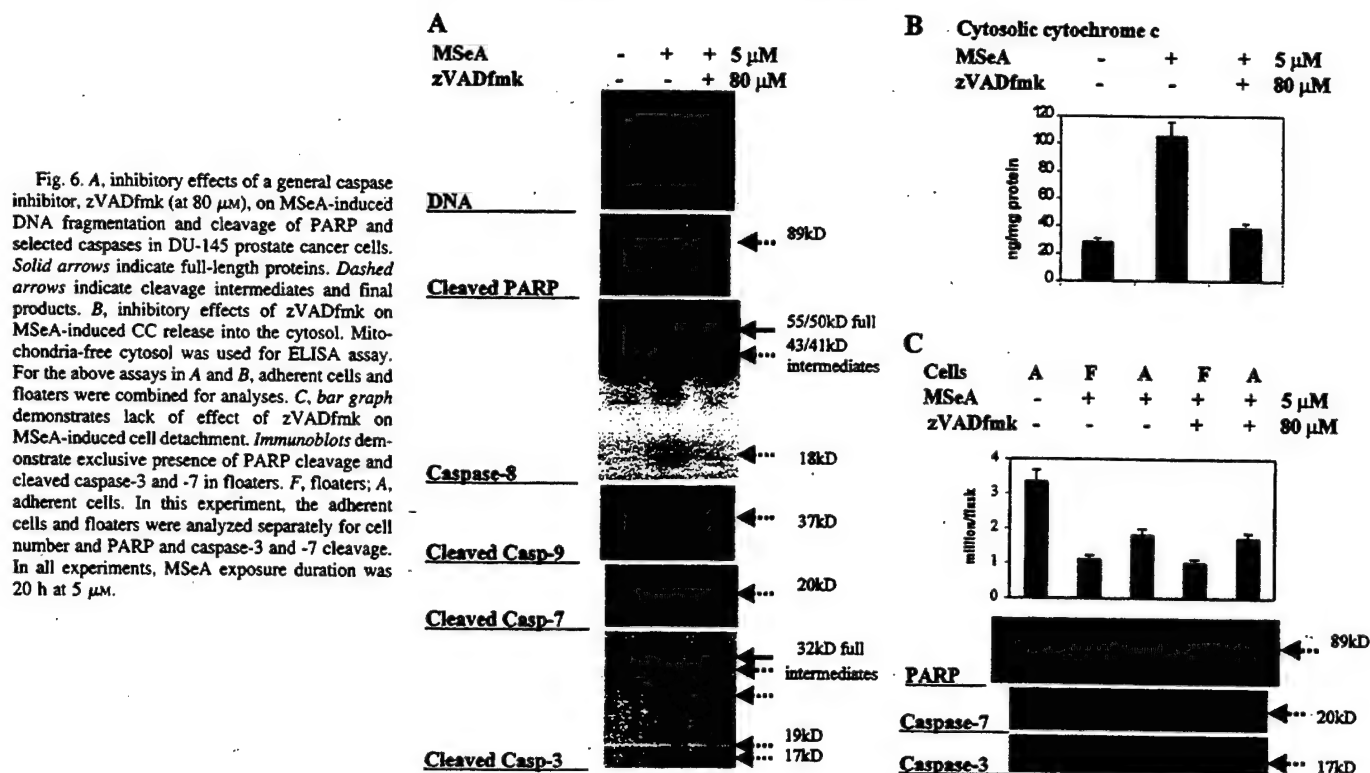


Fig. 5. Time course of caspase substrate hydrolysis activities in DU-145 prostate cancer cells exposed to 5 μM MSeA. Adherent and detached cells were pooled for lysate preparation for the enzyme assays. The chromogenic substrates used were DEVDp-NA (for caspase-3 and 7), IETDp-NA (for caspase-8), and LEHDp-NA (for caspase-9), respectively. High background absorbance (OD) in controls was attributable to protein precipitation over the course of a ≥10-h incubation. Each *point* represents the mean of duplicate flasks, each with triplicate measurements.

Fig. 6. *A*, inhibitory effects of a general caspase inhibitor, zVADfmk (at 80 μM), on MSeA-induced DNA fragmentation and cleavage of PARP and selected caspases in DU-145 prostate cancer cells. *Solid arrows* indicate full-length proteins. *Dashed arrows* indicate cleavage intermediates and final products. *B*, inhibitory effects of zVADfmk on MSeA-induced CC release into the cytosol. Mitochondria-free cytosol was used for ELISA assay. For the above assays in *A* and *B*, adherent cells and floaters were combined for analyses. *C, bar graph* demonstrates lack of effect of zVADfmk on MSeA-induced cell detachment. *Immunoblots* demonstrate exclusive presence of PARP cleavage and cleaved caspase-3 and -7 in floaters. *F*, floaters; *A*, adherent cells. In this experiment, the adherent cells and floaters were analyzed separately for cell number and PARP and caspase-3 and -7 cleavage. In all experiments, MSeA exposure duration was 20 h at 5 μM.

6*B*), we propose a putative scheme of caspase-3 feedback activation of caspase-9 through a mitochondria/CC release mechanism (see Fig. 8).

In addition, the various inhibitors did not block the conversion of procaspase-8 to the 43/41 kDa intermediate forms, but appeared to inhibit the generation or maturation of the 18-kDa active caspase-8 form as indicated by the retarded migration of the expected band (Fig. 7*B*). These observations suggest a possible feedback loop from the downstream caspases, most likely caspase-3, to caspase-8 for the full activation/processing of caspase-8 in MSeA-exposed DU-145 cells (see Fig. 8).

Despite the effective blockage of PARP cleavage by zDEVDfmk or zIETDfmk, DNA fragmentation was detected, albeit at a reduced extent compared with MSeA exposure alone (Fig. 7*B*). These results, together with the complete blockage of DNA fragmentation (Fig. 6*A*) and PARP cleavage (Figs. 6*A* and 7*A*) by the general caspase inhibitor zVADfmk, indicate the likelihood that additional caspases contribute to DNA fragmentation activity and PARP cleavage induced by MSeA exposure (see Fig. 8).

## DISCUSSION

**Two Selenium Metabolite Pools Induce Prostate Cancer Cell Apoptosis Execution by Distinct Mechanisms.** The data presented above document for the first time, to our knowledge, the involvement of PARP cleavage (Fig. 1) and the activation of multiple caspases (Figs. 2 and 3) during apoptosis execution induced by a mono-methyl selenium compound, MSeA. The data also ruled out caspase activation during the same time frame for apoptosis execution induced by selenite, which has been shown by us and others to be genotoxic (8, 10, 11, 26). Instead, apoptotic DNA fragmentation in selenite-exposed cells was associated with the phosphorylation of JNK1/2 and p38 MAPK/SAPK2, whereas these two stress- and apoptosis-signaling kinases (32) were not phosphorylated in the MSeA-treated cells (Fig. 3*B*). Furthermore, selenite exposure increased the phosphorylation of AKT/PKB (Fig. 3*B*), a protein kinase known to mediate cell survival

in many cell types (28). The activation of AKT provides one potential explanation for the inactivation of caspase-9 in selenite-treated cells (Fig. 2 *versus* Fig. 3) through AKT-mediated caspase-9 phosphorylation (29). A recent report has shown that nanomolar concentrations of selenite inhibited caspase-3 activity by a redox mechanism both in the test tube and in cell culture (33). It is therefore possible that selenite might have also inhibited the activities of caspase-8 and -9 as well as caspase-3 in our study (Fig. 2, *A–C*) through a redox modification of the critical cysteine residual in the active center of each caspase. Taken together, these data with the two selenium compounds clearly demonstrate that distinct modes of apoptosis signaling and execution were induced in DU-145 cells by the two metabolite pools, as diagramed schematically in Fig. 8. These results agree with and extend our earlier findings of the differential biochemical and cellular actions of these two selenium pools with mammary cancer cells (10, 11).

**Caspases as Essential Executors of MSeA-induced Apoptosis (Anoikis).** Pertaining to the role of caspases in MSeA-induced PARP cleavage and apoptosis execution, the general caspase inhibitor zVADfmk completely blocked MSeA-induced CC release, PARP cleavage, and DNA fragmentation, establishing caspase activation as an essential and necessary upstream mediating event of these apoptotic processes (Fig. 6, *A* and *B*). However, it did not prevent MSeA-induced cell detachment (Fig. 6*C*), and caspase-3 and -7 activation and PARP cleavage were detected exclusively in the MSeA-induced floaters, but not in the MSeA-exposed adherent cells (Fig. 6*C*). These results support MSeA-induced cell detachment as a prerequisite for caspase activation. This mode of cell death induction closely resembles detachment-induced anoikis (23).

As mentioned in the "Introduction," two caspase-activation cascades, *i.e.*, the death receptor/caspase-8 pathway and the CC/APAF-1/caspase-9 apoptosome pathway, have been demonstrated for activation of downstream executioner caspases in numerous apoptosis models (14–17). As far as caspase cascades involved in anoikis are
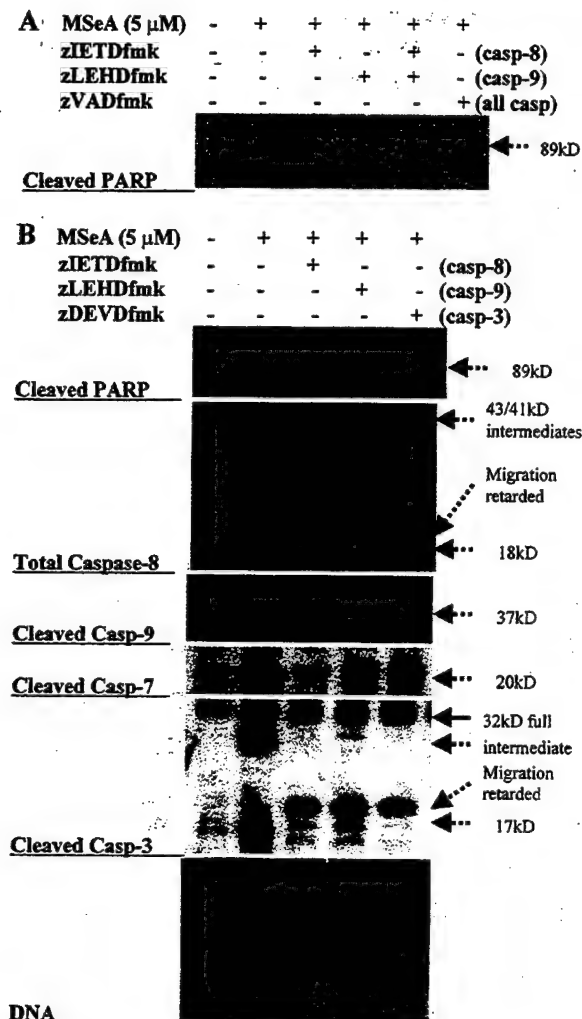
Fig. 7. *A*, effects of a general caspase inhibitor (*zVADfmk*) and an inhibitor of caspase-8 (*zIETDfmk*) or caspase-9 (*zLEHDfmk*), individually or combined, on MSeA-induced PARP cleavage in DU-145 cells at 20 h of exposure. *B*, effects of an inhibitor of caspase-8, caspase-9 or caspase-3 (*zDEVDfmk*) on MSeA-induced cleavage of PARP and selected caspases and DNA fragmentation in DU-145 cells at 20 h of exposure. In both experiments, each inhibitor was used at a final concentration of 40 μM. Both adherent cells and floaters were combined for these analyses. *Solid arrows* indicate expected full-length proteins. *Dashed arrows* indicate cleavage intermediates and final products. *Diagonal arrows* indicate unidentified cleavage intermediates with altered migration patterns.

concerned, it has been shown that detachment-induced apoptosis requires death receptor-related and death domain-containing proteins (34) and that apoptosis is blocked by a dominant-negative form of FADD (35). In these studies, detachment induced strong activation of caspase-8 and -3 (34, 35). In addition, recent reports have shown a caspase-dependent CC release from mitochondria during anoikis (36). These findings support the primary role of the death receptor/caspase-8 pathway for anoikis execution with the CC/caspase-9 cascade as a secondary amplification pathway. This generalization appears to fit the patterns of caspase activation induced by MSeA in DU-145 cells as discussed next.

**Caspase-8 Is Functionally Upstream of Other Caspases with Potential Feedback Loop(s) in MSeA-induced Anoikis.** The temporal sequence of MSeA-induced caspase cleavage patterns (Fig. 4) indicated that the activation of caspase-8 (*e.g.*, occurrence of p43/p41 cleavage intermediates) preceded caspase-9 and -7, all of which occurred prior to activation of caspase-3. The activity measurements were consistent with the temporal kinetic patterns of activation observed above (Fig. 5). Because caspase-3 has much higher specific

activity for PARP cleavage than either caspase-7 or -9 (25), the delayed cleavage of caspase-3 subsequent to the activation of caspase-8, -9, and -7 might account for the accelerated PARP cleavage once apoptosis execution has initiated.

Using irreversible inhibitors for selected caspases, we attempted to further delineate the paths of caspase activation and their relationship to PARP cleavage and DNA fragmentation induced by MSeA (Fig. 7). Several lines of evidence support the scenario that the CC/caspase-9 cascade may be an integral component, rather than an independent pathway, of the death receptor/caspase-8 activation cascade(s). First, as shown in Fig. 7*A*, the caspase-8 inhibitor blocked PARP cleavage to the same extent as both caspase-8 and caspase-9 inhibitors used together. As shown in Fig. 7*B*, the caspase-8 inhibitor almost completely blocked procaspase-9 cleavage as well as cleavage of procaspase-7 and -3. The caspase-9 inhibitor, on the other hand, decreased but did not completely block the extent of cleavage of procaspase-3 (to the 17-kDa active product) or procaspase-7, although it had little effect on the accumulation of the cleaved caspase-9 itself. The latter outcome would be predicted from a serial upstream-downstream, rather than a parallel, relationship between caspase-8 and -9. How caspase-8 mediates activation of caspase-9, whether via a direct cleavage effect or BID-induced CC release/caspase-9 activation (17, 18), remains to be determined.

zDEVDfmk (a more potent inhibitor for caspase-3 than for caspase-7; Ref. 25) almost completely blocked PARP cleavage (Fig. 7*B*), which is consistent with the primary effector role of caspase-3 in executing PARP cleavage as documented in many other model sys-
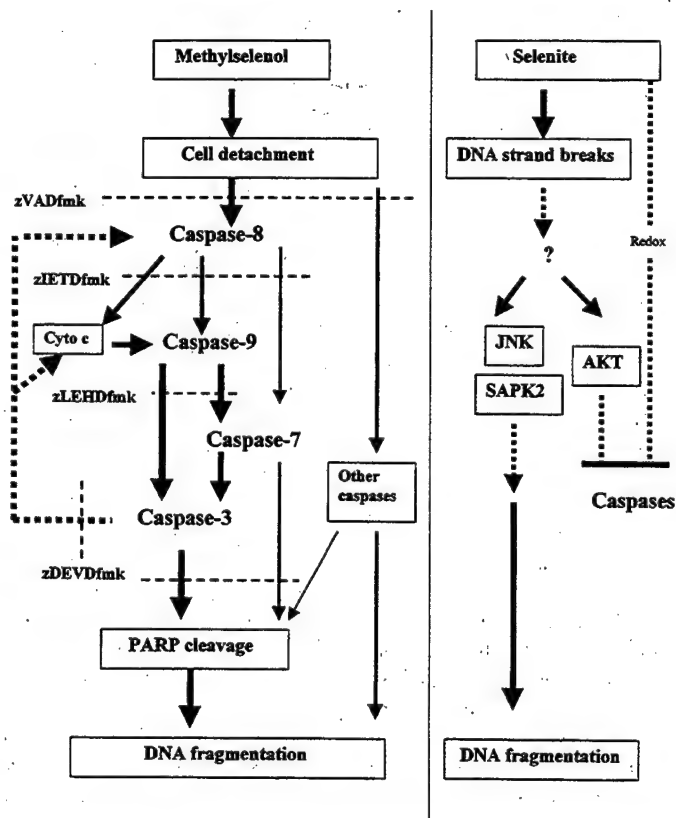


Fig. 8. Proposed pathways of MSeA-induced caspase activation and relationships to mitochondria release of CC (*cyto c*), PARP cleavage, and DNA nucleosomal fragmentation during apoptosis execution in DU-145 prostate cancer cells. *Solid arrows* indicate probable events. *Dashed arrows* indicate likely feedback loops from caspase-3 to upstream initiator caspases. *Thin dashed lines* indicate steps where caspase inhibitors used in this study exert their effects. Selenite-induced changes are outlined on the *right* for comparison. The gentotoxic activity of selenite (DNA single strand breaks) was based on our earlier results in leukemia and mammary cancer cell lines (8, 10, 26).

tems (14–17). zDEVDfmk not only blocked the activation of caspase-3, but also significantly decreased cleavage of procaspase-9, indicating that a feedback loop might be involved in the full activation of the caspase-9 cascade (Fig. 7B). Recently, caspase-3 activation has been shown to amplify CC release from the mitochondria, via cleavage of either BID or Bcl-2 (20–22). The fact that CC release from mitochondria in MSeA-exposed cells was caspase dependent (Figs. 2 and 6) suggests that the CC/APAF-1/caspase-9 cascade may also be a part of the feedback amplification loop for overall MSeA-induced PARP cleavage (Fig. 8). In addition to the feedback loop from caspase-3 to caspase-9, our data appear to also indicate a feedback loop from caspase-3 to caspase-8 (Fig. 8). The various inhibitors, including zDEVDfmk for caspase-3, did not block the conversion of pro-caspase-8 to the 43/41 kDa intermediate forms, but appeared to inhibit the generation or maturation of the 18-kDa active form of caspase-8 as indicated by the retardation of migration (Fig. 7B). Studies are in progress to test these hypotheses.

**Additional Caspases Might Contribute to MSeA-induced DNA Fragmentation Activity.** Although the inhibition data support the prominent role of caspase-8 → caspase-9, -7 → caspase-3 for PARP cleavage, these caspases do not fully account for DNA fragmentation as a result of exposure to MSeA (Fig. 7B). These results, when considered together with the complete blockage of DNA fragmentation by zVADfmk (Fig. 6), suggest that additional caspases may contribute to the DNA fragmentation activity in MSeA-exposed DU-145 cells (Fig. 8).

**Relevance of Anoikis Induction by Methyl Selenium in Cancer Chemoprevention.** The remarkable efficacy of MSeA in inducing DU-145 cancer cell apoptosis as judged by PARP cleavage (~3 $\mu$M; Fig. 1C) is noteworthy. As reference values, the mean plasma selenium concentration of subjects without selenium supplementation in the recent human trial was ~1.5 $\mu$M (2). Selenium supplementation (200 $\mu$g/day as selenized yeast) that was associated with a >50% reduction in the risk for prostate, colon, and lung cancers brought the mean selenium level to ~2.5 $\mu$M (2). DU-145 prostate cancer cells, originally derived from an aggressive metastatic carcinoma, are independent of androgen for growth, capable of anchorage-independent growth (i.e., resistant to anoikis), and have extended survivability upon trophic factor withdrawal (37). Therefore, the apoptosis (anoikis) sensitivity of such malignant cells to MSeA would be expected to be much lower than that of transformed prostate epithelial cells in early lesions, which represent the likely targets of chemoprevention by selenium. Although the work reported here focused on induction of anoikis of this aggressive metastatic prostate cancer cell line by MSeA treatment, we speculate that the anoikis mechanism may apply to prostate epithelial cells in early lesions in a pharmacological as well as a chemoprevention context. In other words, achievable serum levels of MSeA might be enough to induce anoikis of transformed prostate epithelial cells in early lesions. Further work is needed to establish the relevance of induction of anoikis by methyl selenium for the chemoprevention of prostate carcinogenesis.

In summary, the data show that MSeA-induced DU-145 cell detachment is a prerequisite for caspase activation and PARP cleavage in an apoptosis execution pathway that is principally initiated by caspase-8 → caspase-9, -7 → caspase-3 and is likely amplified by feedback loop(s) from caspase-3. Many mechanistic questions remain. For example, is integrin-signaling inhibition involved in MSeA induction of cell detachment and caspase activation? Are death receptor molecules and their adapters, such as FADD, involved in the initial stage of caspase-8 activation? Does the AKT/PKB survival pathway, whose phosphorylation was decreased at 24 h of exposure to MSeA, play a role in MSeA-anoikis signaling and execution? Are the Bcl-2 family of anti- and pro-apoptosis proteins, such as Bid and BAD,

involved in MSeA-induced anoikis? Answers to these questions will help to elucidate how methyl selenium triggers the signaling and execution of cancer cell anoikis.

## REFERENCES

1. Institute of Medicine, Food, and Nutrition Board. Dietary Reference Intakes. Vitamin C, Vitamin E, Selenium, and Carotenoids. Washington, DC: National Academy Press, 2000.
2. Clark, L. C., Combs, G. F., Jr., Turnbull, B. W., Slate, E. H., Chalker, D. K., Chow, J., Davis, L. S., Glover, R. A., Graham, G. F., Gross, E. G., et al. Effects of selenium supplementation for cancer prevention in patients with carcinoma of the skin. A randomized controlled trial. Nutritional Prevention of Cancer Study Group. JAMA, 276: 1957–1963, 1996.
3. Yu, S. Y., Zhu, Y. J., and Li, W. G. Protective role of selenium against hepatitis B virus and primary liver cancer in Qidong. Biol. Trace Elem. Res., 56: 117–124, 1997.
4. Ip, C. Lessons from basic research in selenium and cancer prevention. J. Nutr., 128: 1845–1854, 1998.
5. Ip, C., and Ganther, H. E. Activity of methylated forms of selenium in cancer prevention. Cancer Res., 50: 1206–1211, 1990.
6. Ip, C., Hayes, C., Budnick, R. M., and Ganther, H. E. Chemical form of selenium, critical metabolites, and cancer prevention. Cancer Res., 51: 595–600, 1991.
7. Ip, C., Lisk, D. J., and Thompson, H. J. Selenium-enriched garlic inhibits the early stage but not the late stage of mammary carcinogenesis. Carcinogenesis (Lond.), 17: 1979–1982, 1996.
8. Lu, J., Pei, H., Ip, C., Lisk, D., Ganther, H., and Thompson, H. J. Effect of an aqueous extract of selenium enriched garlic on in vitro markers and in vivo efficacy in cancer prevention. Carcinogenesis (Lond.), 17: 1903–1907, 1996.
9. Ip, C., Thompson, H. J., and Ganther, H. E. Selenium modulation of cell proliferation and cell cycle biomarkers in normal and premalignant cells of the rat mammary gland. Cancer Epidemiol. Biomark. Prev., 9: 49–54, 2000.
10. Lu, J., Jiang, C., Kaeck, M., Ganther, H., Vadhanavikit, S., Ip, C., and Thompson, H. Dissociation of the genotoxic and growth inhibitory effects of selenium. Biochem. Pharmacol., 252: 7392–7394, 1995.
11. Kaeck, M., Lu, J., Strange, R., Ip, C., Ganther, H., and Thompson, H. J. Differential induction of growth arrest inducible genes by selenium compounds. Biochem. Pharmacol., 53: 921–926, 1997.
12. Ganther, H. E. Pathways of selenium metabolism including respiratory excretory products. J. Am. Coll. Toxicol., 5: 1–5, 1986.
13. Kerr, J. F., Wyllie, A. H., and Currie, A. R. Apoptosis: a basic biological phenomenon with wide-ranging implications in tissue kinetics. Br. J. Cancer., 26: 239–257, 1972.
14. Earnshaw, W. C., Martins, L. M., and Kaufmann, S. H. Mammalian caspases: structure, activation, substrates, and functions during apoptosis. Annu. Rev. Biochem., 68: 383–424, 1999.
15. Wolf, B. B., and Green, D. R. Suicidal tendencies: apoptotic cell death by caspase family proteinases. J. Biol. Chem., 274: 20049–20052, 1999.
16. Martin, D. S., Bertino, J. R., and Koutcher, J. A. ATP depletion plus pyrimidine depletion can markedly enhance cancer therapy: fresh insight for a new approach. Cancer Res., 60: 6776–6783, 2000.
17. Budihardjo, I., Oliver, H., Lutter, M., Luo, X., and Wang, X. Biochemical pathways of caspase activation during apoptosis. Annu. Rev. Cell Dev. Biol., 15: 269–290, 1999.
18. Li, H., Zhu, H., Xu, C. J., and Yuan, J. Cleavage of BID by caspase 8 mediates the mitochondrial damage in the Fas pathway of apoptosis. Cell, 94: 491–501, 1998.
19. Luo, X., Budihardjo, I., Zou, H., Slaughter, C., and Wang, X. Bid, a Bcl2 interacting protein, mediates cytochrome c release from mitochondria in response to activation of cell surface death receptors. Cell, 94: 481–490, 1998.
20. Slee, E. A., Keogh, S. A., and Martin, S. J. Cleavage of BID during cytotoxic drug and UV radiation-induced apoptosis occurs downstream of the point of Bcl-2 action and is catalysed by caspase-3: a potential feedback loop for amplification of apoptosis-associated mitochondrial cytochrome c release. Cell Death Differ., 7: 556–565, 2000.
21. Chen, Q., Gong, B., and Almasan, A. Distinct stages of cytochrome c release from mitochondria: evidence for a feedback amplification loop linking caspase activation to mitochondrial dysfunction in genotoxic stress induced apoptosis. Cell Death Differ., 7: 227–233, 2000.
22. Kirsch, D. G., Doseff, A., Chau, B. N., Lim, D. S., de Souza-Pinto, N. C., Hansford, R., Kastan, M. B., Lazebnik, Y. A., and Hardwick, J. M. Caspase-3-dependent cleavage of Bcl-2 promotes release of cytochrome c. J. Biol. Chem., 274: 21155–21161, 1999.
23. Frisch, S. M., and Francis, H. Disruption of epithelial cell-matrix interactions induces apoptosis. J. Cell Biol., 124: 619–626, 1994.
24. Jiang, C., Jiang, W., Ip, C., Ganther, H., and Lu, J. Selenium-induced inhibition of angiogenesis in mammary cancer at chemopreventive levels of intake. Mol. Carcinog., 26: 213–225, 1999.
25. Margolin, N., Raybuck, S. A., Wilson, K. P., Chen, W., Fox, T., Gu, Y., and Livingston, D. J. Substrate and inhibitor specificity of interleukin-1 $\beta$-converting enzyme and related caspases. J. Biol. Chem., 272: 7223–7228, 1997.
26. Lu, J., Kaeck, M., Jiang, C., Wilson, A. C., and Thompson, H. J. Selenite induction of DNA strand breaks and apoptosis in mouse leukemic L1210 cells. Biochem. Pharmacol., 47: 1531–1535, 1994.
27. Carson, J. P., Kulik, G., and Weber, M. J. Antiapoptotic signaling in LNCaP prostate cancer cells: a survival signaling pathway independent of phosphatidylinositol 3'-kinase and Akt/protein kinase B. Cancer Res., 59: 1449–1453, 1999.

28. Marte, B. M., and Downward, J. PKB/Akt: connecting phosphoinositide 3-kinase to cell survival and beyond. Trends Biochem. Sci., *22*: 355–358, 1997.

29. Cardone, M. H., Roy, N., Stennicke, H. R., Salvesen, G. S., Franke, T. F., Stanbridge. E., Frisch, S., and Reed, J. C. Regulation of cell death protease caspase-9 by phosphorylation. Science (Washington DC), *282*: 1318–1321, 1998.

30. Datta, S. R., Dudek, H., Tao, X., Masters, S., Fu, H., Gotoh, Y., and Greenberg, M. E. Akt phosphorylation of BAD couples survival signals to the cell-intrinsic death machinery. Cell, *91*: 231–241, 1997.

31. del Peso, L., Gonzalez-Garcia, M., Page, C., Herrera, R., and Nunez, G. Interleukin-3-induced phosphorylation of BAD through the protein kinase Akt. Science (Washington DC), *278*: 687–689, 1997.

32. Ichijo, H. From receptors to stress-activated MAP kinases. Oncogene, *18*: 6087–6093, 1999.

33. Park, H. S., Huh, S. H., Kim, Y., Shim, J., Lee, S. H., Park, I. S., Jung, Y. K., Kim, I. Y., and Choi, E. J. Selenite negatively regulates caspase-3 through a redox mechanism. J. Biol. Chem., *275*: 8487–8491, 2000.

34. Frisch, S. M. Evidence for a function of death-receptor-related, death-domain-containing proteins in anoikis. Curr. Biol., *9*: 1047–1049, 1999.

35. Rytomaa, M., Martins, L. M., and Downward, J. Involvement of FADD and caspase-8 signaling in detachment-induced apoptosis. Curr. Biol., *9*: 1043–1046, 1999.

36. Rytomaa, M., Lehmann, K., and Downward, J. Matrix detachment induces caspase-dependent cytochrome *c* release from mitochondria: inhibition by PKB/Akt but not raf signaling. Oncogene, *19*: 4461–4468, 2000.

37. Tang, D. G., Li, L., Chopra, D. P., and Porter, A. T. Extended survivability of prostate cancer cells in the absence of trophic factors: increased proliferation, evasion of apoptosis, and the role of apoptosis proteins. Cancer Res., *58*: 3466–3479, 1998.

Lu 4

# Antimitogenic and Proapoptotic Activities of Methylseleninic Acid in Vascular Endothelial Cells and Associated Effects on PI3K-AKT, ERK, JNK and p38 MAPK Signaling[1]

Zaisen Wang, Cheng Jiang, Howard Ganther, and Junxuan Lü[2]

*AMC Cancer Research Center, Denver, Colorado 80214 [Z. W., C. J., J. L.], and University of Wisconsin, Madison, Wisconsin 53706 [H. G.]*

## ABSTRACT

Inhibiting the mitogenic response of vascular endothelial cells may in part mediate the antiangiogenic and anticancer activity of supranutritional selenium supplements. Our previous work had shown that methylseleninic acid (MSeA), a precursor of the critical anticancer methylselenol metabolite pool, was a potent inhibitor of the growth and survival of human umbilical vein endothelial cells (HUVECs). Here we investigated the effects of MSeA on selected protein kinase signaling transduction pathways to characterize their role in methylselenium induction of HUVEC cell cycle arrest and apoptosis. Exposure of asynchronous HUVECs for 30 h to 3–5 $\mu$M MSeA led to a profound $G_1$ arrest, and exposure to higher levels of MSeA not only led to $G_1$ arrest but also to DNA fragmentation and caspase-mediated cleavage of poly(ADP-ribose)polymerase, both biochemical hallmarks of apoptosis. Immunoblot analyses indicated that $G_1$ arrest induced by the sublethal doses of MSeA was associated with dose-dependent reductions of the levels of phospho-protein kinase B (also known as AKT or PKB), phospho-extracellular signal regulated kinase (ERK) 1/2, and phospho-Jun NH$_2$-terminal kinases 1/2 in the absence of any change in p38 mitogen-activated protein kinase (MAPK) phosphorylation. Apoptosis induced by MSeA was associated with an increased phosphorylation of p38 MAPK in addition to the dephosphorylation of the above kinases. In HUVECs deprived of endothelial cell growth supplement (ECGS) for 48 h, resumption of ECGS stimulation resulted in an ~10-fold increase in mitogenic response, as indicated by [$^3$H]thymidine incorporation into DNA. The ECGS-stimulated mitogenic response was inhibited in a dose-dependent manner by MSeA exposure with a IC$_{50}$ ~1 $\mu$M and a complete blockage at 3 $\mu$M. Wortmannin, an inhibitor of phosphatidylinositol 3-kinase (PI3K) upstream of AKT, potently inhibited the ECGS-stimulated DNA synthesis (IC$_{50}$, ~40 nM). Combining MSeA with Wortmannin showed an additive antimitogenic effect. An inhibitor of MAPK/ERK kinase 1, PD98059, also inhibited ECGS-stimulated DNA synthesis (IC$_{50}$, ~55 $\mu$M), but combining PD98059 with MSeA had an effect similar to that when PD98059 was used alone. A time-course experiment indicated that PI3K (AKT and ribosomal protein S6 kinase) activation occurred between 6 and 12 h of ECGS stimulation, and 3 $\mu$M MSeA exposure decreased AKT phosphorylation after 12 h of exposure, whereas no inhibitory effect was observed for ERK1/2 phosphorylation throughout the 30-h exposure duration. Additional experiments indicated that MSeA, Wortmannin, or a more specific PI3K inhibitor, LY294002, seemed to target, in the mid- to late-$G_1$ phase, a common mechanism(s) controlling $G_1$ progression to S while having no inhibitory effect on DNA synthesis once S-phase had initiated. Taken together, the results support a potent inhibitory activity at achievable serum levels of MSeA on ECGS-stimulated mitogenesis in the mid- to late-$G_1$ phase, and the target(s) of this inhibitory activity seems to be PI3K or components of this signal pathway. At pharmacological levels of exposure, modulation of ERK1/2 and other protein kinases may be relevant for the proapoptotic action of MSeA.

## INTRODUCTION

Sustained angiogenesis is obligatory for the genesis and progression of solid tumors (1–3). One of the key angiogenic responses upon stimulation of vascular endothelial cells with polypeptide angiogenic factors is signaling through receptor protein kinase pathways leading to cell cycle entry and progression of the normally quiescent vascular endothelial cells to provide sufficient number of cells for the growing capillaries (1–3). Agents that interfere with endothelial cell mitogenesis and survival can therefore be of significant cancer chemopreventive potential and utility. In this regard, we have previously reported (4, 5) that MSeA,[3] a novel penultimate precursor of the putative active chemopreventive selenium metabolite methylselenol pool (6–8), exerted a potent inhibitory action on the growth and survival (through apoptosis) of HUVECs. Such an inhibitory activity provides a potential mechanism to account for the observed antiangiogenic and cancer chemopreventive activity of selenium (4). However, how the antimitogenic and proapoptotic effects of the methylselenol pool are mediated in the vascular endothelial cells and, more specifically, whether protein kinase signaling pathways are involved in mediating these activities have yet to be investigated.

The primary function of vascular endothelial cells as lining of blood vessels requires that their mitogenic signaling and responses be different from most other cell types with reference to typical polypeptide growth factors such as platelet-derived growth factor and epidermal growth factor. Such specificity ensures the essential quiescent state of vascular endothelial cells in mature individuals or organs until angiogenesis is called for, such as in wound healing or carcinogenesis. The unique mitogenic signaling behavior of vascular endothelial cells is in part attributable to their possession of special receptors for endothelial-specific mitogens such as VEGF (9). Much work has focused on VEGF signaling through its receptors, which belong to the platelet-derived growth factor receptor-family of receptor tyrosine kinases. Upon activation, these receptors dimerize and/or oligomerize, after which autophosphorylation and transphosphorylation of their tyrosine residues in the intracellular domain occur. These phospho-tyrosine molecules act as docking sites for adaptor signaling molecules and nonreceptor tyrosine kinases, generating signal cascades that culminate into vascular endothelial cellular responses such as mitogenesis, hyperpermeability, increased motility, and matrix degradation through matrix metalloproteinases (10).

Several protein kinase cascades (11–14) have been investigated for their involvement in the vascular endothelial mitogenic, apoptotic, and other responses (15–24). The PI3K is a heterodimer of a $M_r$ 85,000 (p85) adaptor subunit and a $M_r$ 110,000 (p110) catalytic subunit (11). Activated p110 catalyzes the phosphorylation of mem-

---

[3] The abbreviations used are: MSeA, methylseleninic acid; HUVEC, human umbilical vein endothelial cell; VEGF, vascular endothelial growth factor; PI3K, phosphatidylinositol 3-kinase; PDK, phosphatidylinositol-dependent kinase; PKB, protein kinase B (also known as AKT); S6K, ribosomal protein S6 kinase; MAPK, mitogen-activated protein kinase; ERK, extracellular signal regulated kinase; MEK, MAPK/ERK kinase; P38 MAPK, also known as stress-activated protein kinase 2; SAPK, stress-activated protein kinase; ECGS, endothelial cell growth supplement; JNK, Jun NH$_2$-terminal kinase; PARP, poly(ADP-ribose)polymerase; TCA, trichloroacetic acid.

brane phosphatidylinositol 4,5-bisphosphate in the D3 position to generate phosphatidylinositol 3,4,5-trisphosphate. Phosphatidylinositol 3,4,5-trisphosphate and its phospholipid phosphatase product, phosphatidylinositol 3,4-bisphosphate, accumulate in the membrane, creating docking sites for two lipid-binding protein kinases, namely PDK1 and AKT, which bind to these lipids via their pleckstrin homology domains. AKT becomes activated as a result of this plasma membrane localization and by its phosphorylation on both Thr308 and Ser473 catalyzed by PDK1 and an unidentified but provisionally named PDK2, respectively. Once activated, AKT can inhibit apoptosis by a number of actions, including phosphorylation and inactivation of the proapoptotic Bcl-2 homologue Bad (20, 21), the apoptosis-initiating enzyme caspase-9 (22), and the forkhead family transcription factor that mediates transcription of proapoptotic gene products (23). The PI3K and its other downstream substrate, S6K, have been shown to mediate the stimulatory effects of VEGF or serum on DNA synthesis in HUVECs and other endothelial cells (15–17, 24).

The classic MAPK/ERK pathway is a key component in the transduction of signals leading to growth and transformation in many cell types (12, 13). It consists of a linear cascade of protein kinases: Raf, MEK, and MAPK/ERK. ERK1/2 are acutely activated upon growth factor stimulation. The ERK pathway has been shown to contribute to the mitogenic responses of HUVECs to VEGF or serum (15–17). In addition to the PI3K and ERK pathways, the p38 MAPK/SAPK2 pathway seemed to mediate the motility-stimulating effects of VEGF with a concomitant antimitogenic action in HUVECs (16, 18). In numerous cell lines, the JNK/SAPK1 pathway as well as the p38 MAPK pathway are involved in apoptosis signaling and regulation (14). The interplay of the signals from the various pathways in turn command cell cycle entry and progression by modulating the balance of cyclins and cyclin-dependent kinase inhibitors within cyclin-dependent kinase-cyclin complexes, which in turn inactivate *retinoblastoma* protein by phosphorylation and $G_1$ transition, leading to DNA replication and mitosis (25).

The objective of this study was to define the effects of MSeA on mitogenesis and protein kinase signaling in the HUVEC model to identify potential target pathways/molecules for the methyl selenium action. We have chosen as endothelial mitogen for the present work, ECGS, a bovine pituitary extract probably made up of a mixture of multiple angiogenic factors (26, 27). This was based on the rationale that tumor angiogenesis would likely be driven by multiple angiogenic factors in addition to VEGF.

## MATERIALS AND METHODS

**Chemicals and Reagents.** MSeA was synthesized as described elsewhere (4). MSeA most likely reacts with reduced glutathione intracellularly to form intermediates that can undergo additional reduction to methylselenol ($CH_3SeH$; 28). Bovine ECGS, heparin, PD98059, Wortmannin, and an antibody for $\beta$-actin were purchased from Sigma Chemical Co., St. Louis, MO. LY294002 was purchased from CalBiochem-Novabiochem Corp., La Jolla, CA. [Methyl-[$^3$H]]thymidine (20 Ci/mmol) was purchased from DuPont-New England Nuclear, Wilmington, DE. Recombinant human VEGF165 was obtained from Becton Dickinson, Bedford, MA. HUVECs were obtained from American Type Culture Collection, Manassas, VA, and used within 15 passages upon receipt. Antibodies specific for cleaved PARP (p89), cleaved caspase-3, and cleaved caspase-7 and those for protein kinases and their phosphorylated forms (AKT Ser473, S6K Thr421/Ser424, ERK1/2 Thr202/Tyr204, MEK1 Ser217/221, JNK Thr183/tyr185, and P38 MAPK Thr180/Tyr182) were purchased from Cell Signaling Technology, Beverly, MA.

**Cell Cycle Distribution and Apoptosis Evaluation.** HUVECs were propagated in F12K medium containing 10% fetal bovine serum, 2 mM L-glutamine, 100 $\mu$g/ml of heparin, and 30 $\mu$g/ml of bovine ECGS, as described previously (4, 5). HUVECs were seeded in $T_{25}$ or $T_{75}$ flasks at 60–70%

confluence and were treated in fresh complete medium with increasing concentrations of MSeA for 30 h or as otherwise specified. Detached floaters and adherent cells were pooled together and analyzed for cell cycle distribution by flow cytometry and for DNA nucleosomal fragmentation. DNA was extracted and analyzed as previously described (29). Cleavage of PARP (30), caspase-3, and caspase-7 as evidence of caspase-mediated apoptosis was analyzed by immunoblotting with antibodies specific for the cleaved products as we have previously described (31). To standardize Se exposure among different cell culture vessels, 0.2 ml of medium was used per $cm^2$ of vessel surface (*e.g.*, 15 ml for a $T_{75}$ flask, 5 ml for a $T_{25}$ flask).

**HUVEC Synchronization and [$^3$H]thymidine Incorporation into DNA.** HUVECs were seeded in $T_{25}$ flasks in complete growth medium until 70–80% confluent and then were fed the above medium without ECGS for 48 h. To determine the effect of MSeA on ECGS-stimulated cell proliferation, [$^3$H]thymidine (0.4 $\mu$Ci/ml) and ECGS were added to the synchronized cells simultaneously. The DNA synthetic activity was measured as [$^3$H]thymidine cumulative incorporation into the TCA-precipitable fraction during 30 h of ECGS stimulation, unless otherwise specified as in selected time course experiments.

**Immunoblot Analyses.** Cell lysates were prepared in lysis buffer [50 mM Tris-HCl (pH 7.4), 150 mM NaCl, 2 mM EDTA, 50 mM sodium fluoride, 1% Triton X-100, 1% sodium deoxycholate, 0.1% SDS, 1 mM dithiothreitol, 5 mM sodium orthovanadate, and 1 mM phenylmethylsulfonyl fluoride and 38 $\mu$g aprotinin/ml were added fresh]. Supernatants after centrifugation (14,000 g × 20 min; 4°C) were recovered and the protein content was quantified by the Bradford dye-binding assay (Bio-Rad Laboratories, Richmond, CA). Six or 20 $\mu$g of total protein was size-separated by electrophoresis on 10 or 12% SDS-polyacrylamide gels, depending on the size of the target protein being investigated. The proteins were electroblotted onto nitrocellulose membranes and probed with antibodies for the phosphorylated AKT, ERK1/2, S6K, P38 MAPK, or JNK and those for cleaved caspase-3, caspase-7, or cleaved PARP. Membranes were stripped by incubation in Re-Blot 1× antibody stripping solution (Chemicon International, Inc., Temecula, Ca) for 20 min at 28°C and reprobed for the respective total protein kinase content or $\beta$-actin for verifying loading evenness.

## RESULTS

### Part I: Effects of MSeA in Asynchronous Cells

**MSeA Induced $G_1$ Arrest at Low Exposure Level and Caspase-Associated Apoptosis at High Level.** Exposure of asynchronous HUVECs in complete growth medium (10% serum, 30 $\mu$g/ml ECGS and other endothelial additives) for 30 h to 3–7 $\mu$M MSeA led to an enrichment of cells in $G_0$-$G_1$ phase of the cell cycle and a significant reduction of cells in S and $G_2$-M phases (Fig. 1). The decrease of the fraction of the proliferating cells (*i.e.*, S plus $G_2$-M) was 44, 60, and 52% for the MSeA exposure concentration of 3, 5, and 7 $\mu$M, respectively. Exposure of HUVECs to higher levels (*e.g.*, 10 $\mu$M or greater) of MSeA led not only to $G_1$ arrest but also to cell death by apoptosis as indicated by an increase in the sub-$G_0$-$G_1$ fraction of apoptotic bodies (Fig. 1). Biochemically, apoptosis was characterized as DNA nucleosomal fragmentation (Fig. 2A) and cleavage of PARP (Fig. 2B), a key substrate of apoptosis executioner caspases (30, 31). The executioner caspases (*e.g.*, caspase-3 and caspase-7) were cleaved (indicative of activation) in a dose-dependent manner to MSeA exposure (Fig. 2B). These results indicated that exposure to a level of MSeA >5 $\mu$M induced caspase activation and apoptosis in asynchronous HUVECs.

**MSeA Modulated Phosphorylation Status of Multiple Protein Kinases.** To determine the potential involvement of protein kinase pathways in MSeA-induction of $G_1$ arrest and caspase-mediated apoptosis, we surveyed the phosphorylation status (indicative of activation states) of the four major protein kinases after asynchronous HUVECs were exposed to increasing concentrations of MSeA for 30 h (Fig. 3). Exposure to subapoptotic doses of MSeA (3–5 $\mu$M) led to a dose-dependent reduction of the levels of phospho-AKT (Ser473),

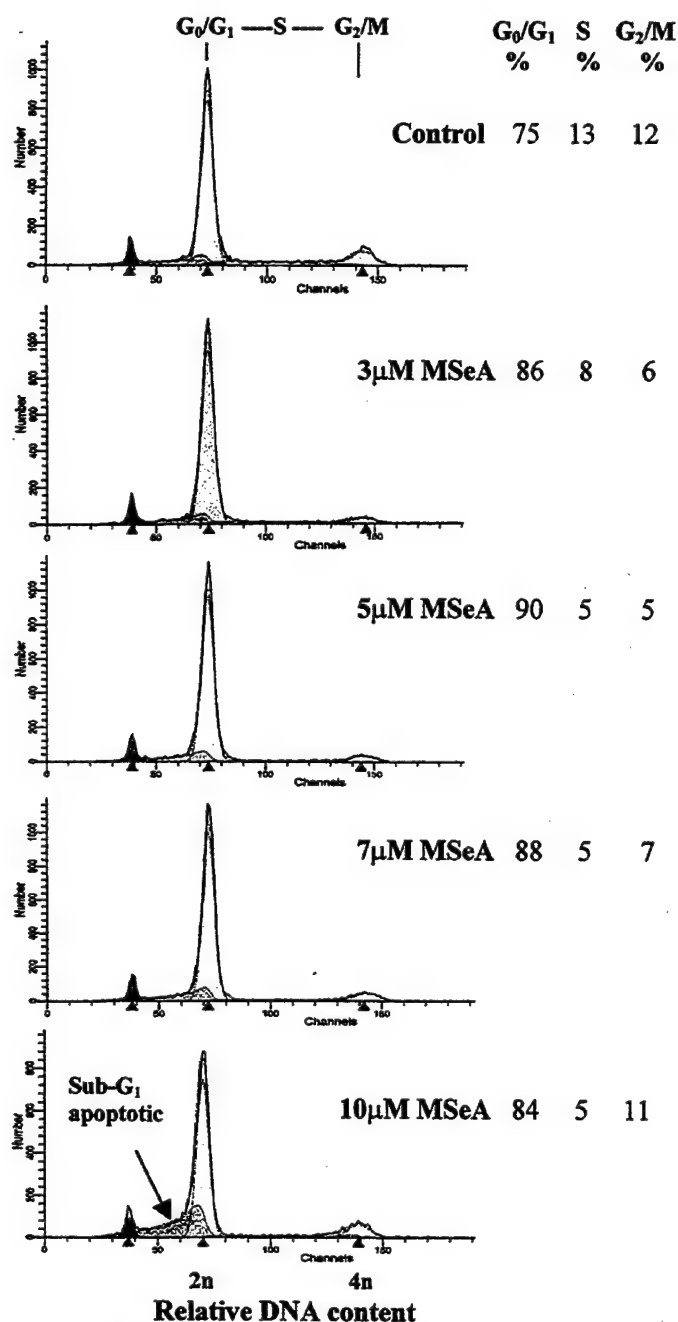| | $G_0/G_1$ % | S % | $G_2/M$ % |
|---|---|---|---|
| Control | 75 | 13 | 12 |
| 3μM MSeA | 86 | 8 | 6 |
| 5μM MSeA | 90 | 5 | 5 |
| 7μM MSeA | 88 | 5 | 7 |
| 10μM MSeA | 84 | 5 | 11 |

Fig. 1. Flow cytometric analyses of effects of MSeA exposure of asynchronous HUVECs on their cell cycle distribution after 30 h of treatment. The percentage of distribution data for each treatment group was the average of two flasks. The data were representative of three independent experiments. The enrichment of $G_0$-$G_1$ population and the depletion of cells in S and $G_2$-M phases in groups exposed to <7 μM MSeA indicated $G_1$ arrest. The increase in sub-$G_0$-$G_1$ fraction in cells treated with 10 μM MSeA indicated the presence of apoptotic bodies.

phospho-ERK1/2 (Thr202/Tyr204), and phospho-JNK1/2 (Thr183/Tyr185) and did not change p38 MAPK phosphorylation (Thr180/Tyr182) status. The observed reduction of phosphorylation status in response to MSeA exposure was not caused by a decrease of the total protein content of the respective protein kinases (Fig. 3).

In cells exposed to an apoptogenic level of MSeA (*e.g.*, 10 μM), an increased level of phosphorylation of p38 MAPK was observed in addition to AKT, ERK1/2, and JNK dephosphorylation. These results indicated that MSeA-induced modulation of AKT, ERK1/2, and JNK kinase pathways were associated with $G_1$ arrest, whereas such alter-

ations in concert with an enhanced p38 MAPK phosphorylation were likely involved in the proapoptotic action of MSeA in HUVECs.

## Part II. Antimitogenic Effects of MSeA in ECGS-Stimulated Cells

**ECGS-stimulated Cell Cycle Progression Model.** To more sensitively define the $G_1$ arrest activity of MSeA on HUVECs and the signal transduction mechanisms involved, next we examined effects of MSeA in an ECGS-depletion and stimulation model. To verify the mitogenic response of this model, ECGS was omitted from the complete growth medium for ~48 h to partially synchronize HUVECs and its stimulatory effect was compared with that of recombinant VEGF at 20 ng/ml, a level that has been shown to produce maximal mitogenic stimulation on HUVECs (15–17), during a 24-h stimulation period (Fig. 4A). ECGS treatment stimulated DNA synthesis, assessed as [³H]thymidine incorporation into TCA-precipitable DNA, by ~10-fold (Fig. 4A). In comparison, VEGF stimulation increased DNA synthesis by only ~90% (Fig. 4A). These results indicated that ECGS was a much stronger mitogen than VEGF for the HUVECs *in vitro*.

Flow cytometry analyses of cell cycle distribution after ECGS depletion in the presence of 10% serum and other endothelial supplements showed that 73% cells were in $G_0$-$G_1$, 3% in S, and 24% in $G_2$-M phases, respectively (n = 3 flasks). Upon ECGS stimulation, the distribution pattern remained unchanged for 12 h and subsequently cells entered S-phase between 12 h and 18 h and the percentage of S-phase cells peaked at 24 h (Fig. 5A). The time course of [³H]thymidine incorporation mirrored the cell cycle distribution pattern, showing a sudden rise in DNA synthetic activity between 12 h and 18 h of ECGS stimulation (Fig. 5B). On the basis of these results, we standardized the ECGS-deprivation protocol for 48 h for assessing the MSeA effects in the rest of the work.

**MSeA Potently Inhibited ECGS-stimulated $G_1$ to S Progression.** MSeA treatment that was initiated either 3 h before (experiment 1) or simultaneously with ECGS stimulation (experiment 2) decreased
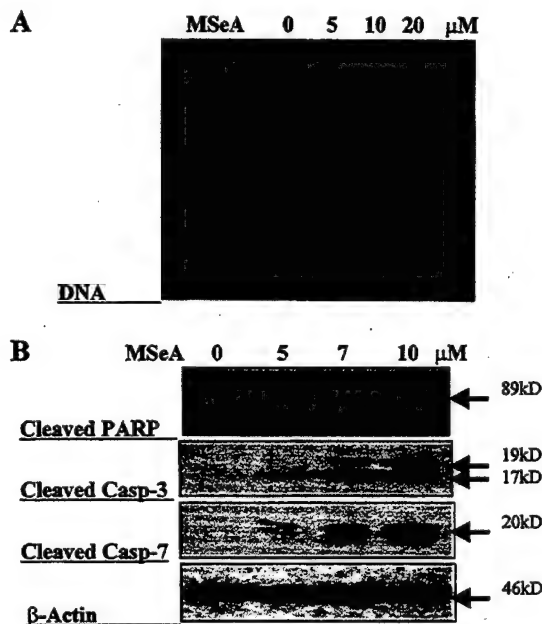


Fig. 2. Biochemical markers of apoptosis execution induced by MSeA exposure of asynchronous HUVECs for 30 h. *A*, agarose gel electrophoretic analysis of DNA extracted from HUVECs after MSeA exposure. Detached cells and remaining adherent cells were pooled together for DNA extraction. DNA size marker was multiples of 100 bp. *B*, detection of cleaved PARP, cleaved casaspe-3, and cleaved caspase-7 in MSeA-exposed cells by Western blot. β-Actin was reprobed to indicate evenness of loading of protein extract from each treatment. *Arrows*, proteins of expected sizes of the cleaved PARP, cleaved caspase-3, cleaved caspase-7, or full length β-actin.
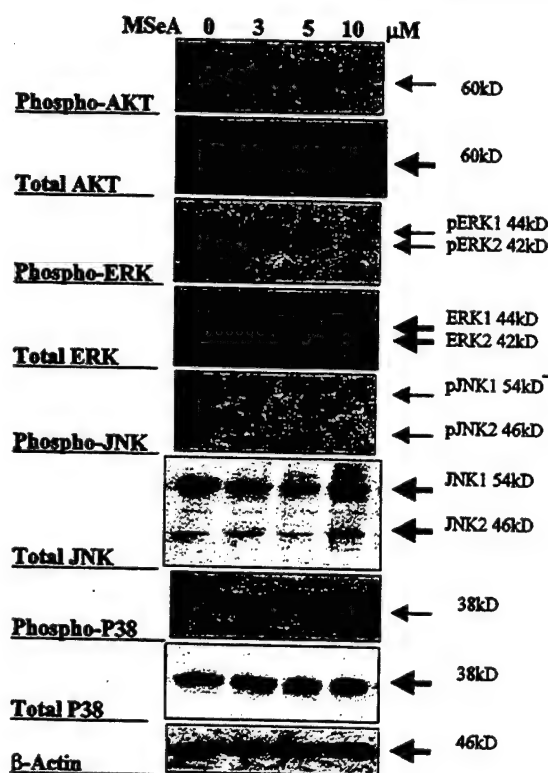
Fig. 3. Effects of MSeA exposure of asynchronous HUVECs for 30 h on the phosphorylation status and expression level of selected protein kinases as detected by immunoblot analyses. β-Actin expression was reprobed to indicate evenness of loading of protein extract from each treatment. *Bold arrows*, total proteins of expected sizes; *thin arrows*, respective phosphorylated kinases.

[³H]thymidine incorporation into DNA dose-dependently during 30 h of ECGS exposure (Fig. 4B). The inhibitory potency was remarkable with an $IC_{50}$ of ~1 μM MSeA and a complete blockage to the unstimulated basal level at 3 μM (Fig. 4B). Flow cytometry data (Fig. 5A) corroborated the DNA synthesis results (Figs. 4B and 5B) in that exposure to 3 μM MSeA completely blocked the progression of $G_1$ cells into S-phase.

Exposure to 7 μM or higher level of MSeA led to detectable caspase-mediated PARP cleavage in the synchronized HUVECs (Fig. 4C). Taken together, the [³H]thymidine incorporation and cell cycle distribution results demonstrated an excellent inhibitory potency of MSeA on ECGS-stimulated cell cycle progression from $G_1$ to S-phase. Furthermore, the data indicated that the primary antimitogenic activity of serum achievable levels of MSeA ($IC_{50}$, ~1 μM) was independent of the proapoptotic action of MSeA exposure at pharmacological levels (e.g., >5 μM).

**Effects of MSeA on ECGS-stimulated PI3K and ERK Signaling Events.** In a time-course experiment designed to delineate the likely sequence of events involving PI3K and ERK1/2 pathways in ECGS-stimulated HUVEC cell cycle progression and in MSeA-induced $G_1$ arrest, ECGS stimulation did not significantly increase the phosphorylation of the PI3K targets AKT and S6K within the first 6 h of exposure, but increased AKT phosphorylation (~5×) and S6K phosphorylation (~8×) at 12 h (Fig. 6A). ECGS stimulated ERK1/2 phosphorylation by ~4×, ~10× and ~8× after 6, 12, and 30 h, respectively (Fig. 6A). The above phosphorylation changes of AKT, S6K, and ERK1/2 occurred with little change in the total protein content of the respective protein kinases. In an experiment examining the phosphorylating status of MEK1 and ERK1/2 during acute exposure to ECGS, it was observed that MEK1 phosphorylation already peaked at 5 min of ECGS stimulation and declined gradually after 5

min (Fig. 6B). ERK1/2 phosphorylation plateaued within 5 min and was sustained throughout 30 min. ERK1 showed a slight decrease of phosphorylation afterward. Taken together, these data suggest that upon ECGS-stimulation, PI3K activation (indicated by AKT-, S6K-phosphorylation) was likely activated between 6 h and 12 h during mid- to late-$G_1$ progression; whereas MEK1-ERK1/2 activation was likely involved in signaling for $G_1$ entry within a few minutes of ECGS stimulation in this model.

The effects of MSeA exposure on these kinases were dependent on the dosage. At 3 μM, which completely blocked ECGS-stimulated $G_1$-S progression (e.g., [³H]thymidine incorporation and flow cytometry data as shown in Figs. 4B and 5), MSeA did not decrease the levels of ERK1/2- or S6K-phosphorylation throughout the 30-h duration (Fig. 6A). This level of MSeA exposure decreased AKT phos-
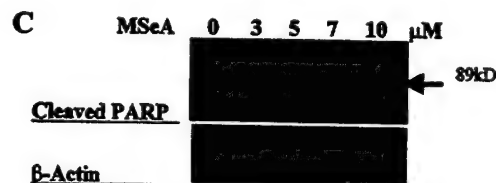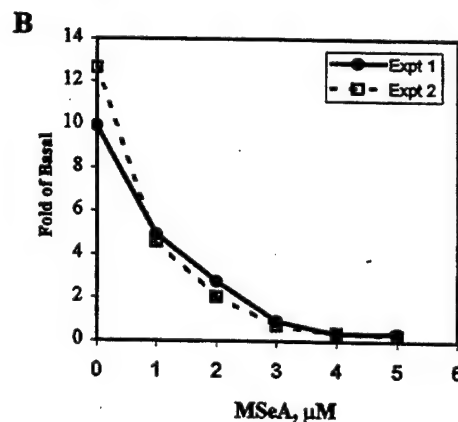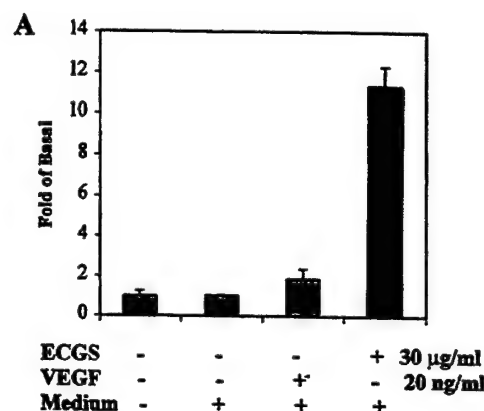






Fig. 4. A, a comparison of the mitogenic effect of endothelial cell growth supplement (ECGS, 30 μg/ml) *versus* VEGF (20 ng/ml) on HUVECs previously deprived of ECGS for 52 h. [³H]thymidine was added at the time of treatment with ECGS or VEGF for 24 h. [³H]thymidine incorporation into DNA was measured by TCA precipitation and extensive washing and followed by liquid scintillation. Unstimulated basal activity was set as unity. Results represented mean and SD of triplicate flasks. Fresh serum-containing medium (*medium*) without either of the above angiogenic factors did not have stimulatory activity. B, dose-dependent inhibitory effect of MSeA on ECGS-stimulated [³H]thymidine incorporation into TCA-precipitable DNA. [³H]thymidine was added at the time of treatment with ECGS for 30 h. In experiment 1, MSeA was added 3 h before ECGS stimulation. In experiment 2, MSeA was added simultaneously with ECGS stimulation. Each experiment was done in duplicate flasks; results reflect mean values, with SD <10% of respective means. C, immunoblot detection of cleaved PARP in synchronized HUVECs exposed to ECGS and MSeA for 30 h. *Arrow*, cleaved PARP. β-Actin was reprobed to indicate evenness of loading of protein extract from each treatment.
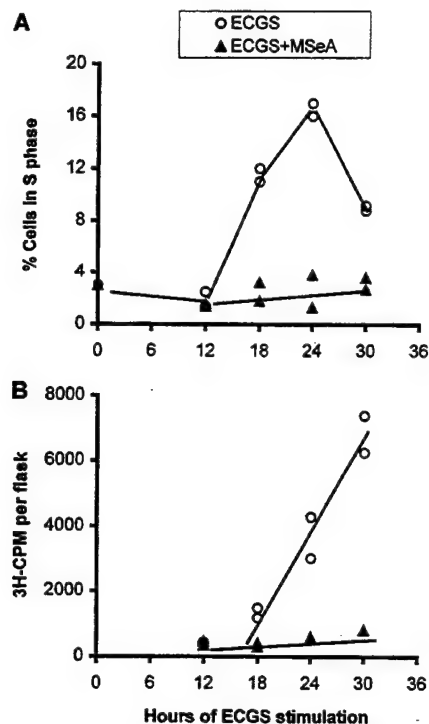
A



B



**Hours of ECGS stimulation**

Fig. 5. A, flow cytometry analyses of S-phase fraction as a function of time after ECGS stimulation of ECGS-deprived HUVECs and the effect of 3 $\mu$M MSeA added simultaneously with ECGS stimulation. Each point represents the result of an individual flask ($n = 2$ flasks/group). B, DNA synthesis activity ([³H]thymidine incorporation, TCA-precipitated cpm/T25 flask) as a function of time after ECGS stimulation and the effect of 3 $\mu$M MSeA added simultaneously with ECGS stimulation. [³H]thymidine was added simultaneously with ECGS stimulation at 0 h. Each point represents the result of an individual flask ($n = 2$ flasks/group).

phorylation at 30 h. MSeA exposure at 5 $\mu$M decreased ECGS-stimulated phosphorylation of ERK1/2 at 6 h, AKT and S6K (p70) phosphorylation at 12 h (Fig. 6A). During acute exposure (Fig. 6B), 10 $\mu$M MSeA treatment simultaneous with ECGS stimulation did not decrease MEK1 phosphorylation until 30 min of exposure and decreased phosphorylation of ERK1/2 at 3 h. These data therefore implicated an involvement of the inactivation of PI3K and/or ERK1/2 pathway activities for the antimitogenic action of MSeA, probably through a mechanism(s) well after the initial MEK-ERK mediated signaling had taken place.

**Effects of PI3K and MEK1 Inhibitors with MSeA on ECGS-stimulated DNA Synthesis.** To test the role of the PI3K and MEK-ERK1/2 pathways in ECGS-stimulated mitogenesis and MSeA-induced $G_1$ arrest, we next examined the impact of a PI3K inhibitor, Wortmannin (Ref. 32) and a MEK1 inhibitor, PD98059. With Wortmannin preloaded for 1.5 h before ECGS stimulation, a potent inhibition of [³H]thymidine incorporation was observed with IC$_{50}$ ~35 nM (Fig. 7A). PD98059 (preloaded for 1.5 h) also inhibited ECGS-stimulated DNA synthesis, but at relatively high concentrations (IC$_{50}$, ~55 $\mu$M; Fig. 7A).

In a separate experiment (Fig. 7B), Wortmannin (40 nM) alone inhibited [³H]thymidine incorporation by ~60%, and PD98059 (60 $\mu$M) alone inhibited by ~72%. The two inhibitors combined completely blocked ECGS-stimulated DNA synthesis. These results indicated that the PI3K and MEK1-ERK pathways could independently contribute to ECGS-stimulated cell cycle entry and/or progression to S phase, during which [³H]thymidine was incorporated into the DNA. Exposure to 1 $\mu$M MSeA alone inhibited [³H]thymidine incorporation by ~38% (Fig. 7B). Combining MSeA with Wortmannin had a near additive inhibitory effect on ECGS-stimulated DNA synthesis (81%;

Fig. 7B). However, MSeA combined with PD98059 had an effect similar (78%) as that when PD98059 was used alone (72%). These results suggested that the antimitogenic activity of a low level MSeA exposure, e.g., 1 $\mu$M, might share a common target(s) with the PI3K inhibitor, and not with the mechanism that was regulated by the MEK1 inhibitor.

**Cell Cycle Stage-specific Effects of MSeA versus PI3K or MEK1 Inhibitors on $G_1$/S Progression.** To define further when during ECGS-stimulated cell cycle entry and progression MSeA exerted the inhibitory activity, we exposed HUVECs to 3 $\mu$M MSeA either simultaneously with ECGS stimulation (agent exposure lag time = 0), or at 6 h (early mid-$G_1$), 12 h (late $G_1$), or 24 h (peak S phase) after ECGS stimulation had commenced (agent exposure lag time = 6, 12, or 24 h). As shown in Fig. 8A, MSeA exposure after cells had been stimulated for 6 h had the same inhibitory effect on [³H]thymidine incorporation as simultaneous exposure. MSeA exposure that was commenced after cells had been stimulated by ECGS for 12 h (i.e., a few hours before onset of S-phase as shown in Fig. 5) was still profoundly inhibitory, although was slightly less effective than when the MSeA exposure was simultaneous with ECGS. After 24 h of cell cycle progression, which coincided with peak DNA synthesis activity as shown in Fig. 5, MSeA exposure was totally ineffective at decreasing [³H]thymidine incorporation, indicating that MSeA did not have an acute inhibitory effect on additional DNA synthesis once cells had started S phase. Taken together, the data indicate that the anti-
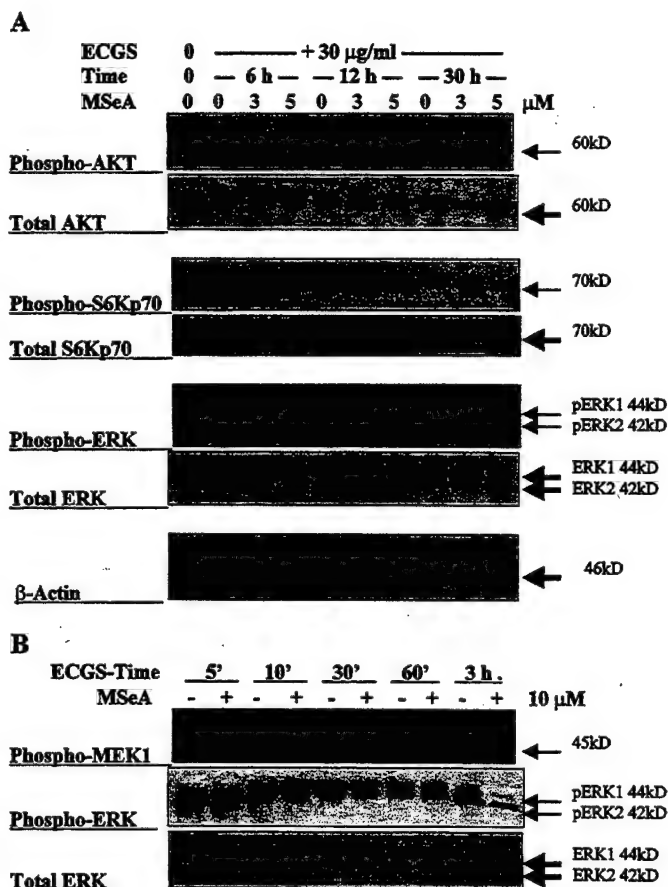
A



B



Fig. 6. A, time course of effects of MSeA on AKT, S6K, and ERK1/2 phosphorylation status and expression profile in ECGS-stimulated HUVEC detected by immunoblot analyses. $\beta$-Actin expression was reprobed to indicate evenness of loading of protein extract from each treatment. Bold arrows, total proteins; thin arrows, respective phosphorylated kinases. Treatments with MSeA and ECGS were started simultaneously. B, acute effects of MSeA exposure on ECGS-stimulated MEK-ERK phosphorylation changes in HUVEC. ECGS was added at 100 $\mu$g/ml in this experiment.
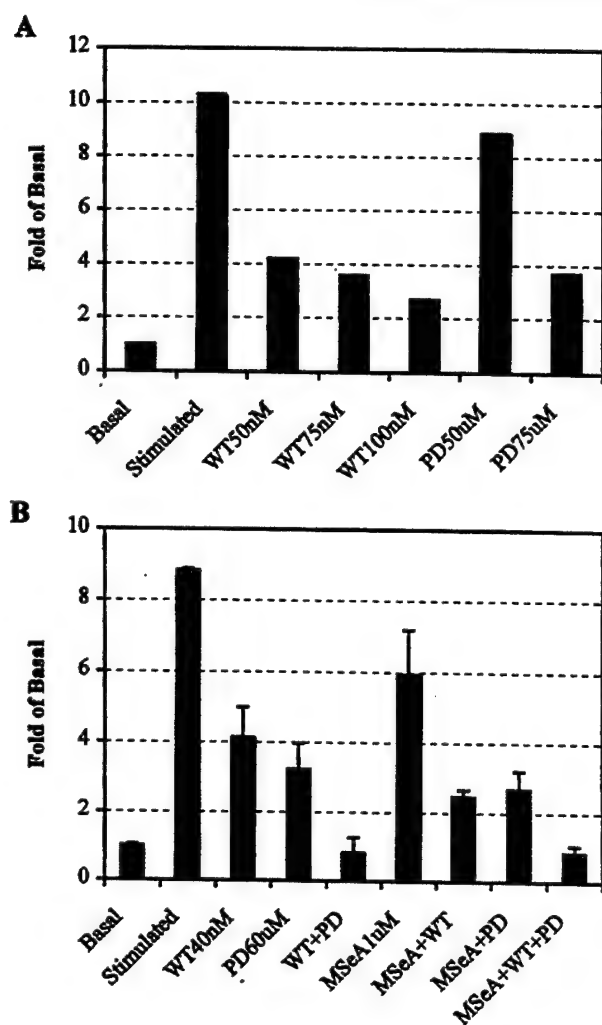
Fig. 7. A, effects of a PI3K inhibitor Wortmannin (WT) or a MEK1 inhibitor PD98059 (PD) on ECGS-stimulated [³H]thymidine incorporation into HUVEC DNA at 30 h. Inhibitors were preloaded for 1.5 h before ECGS stimulation. DMSO was used as solvent vehicle and was added to the basal as well as stimulated controls. B, effects of combining 1 μM MSeA with these inhibitors on ECGS-stimulated [³H]thymidine incorporation into DNA at 30 h. Inhibitors were preloaded for 1.5 h before ECGS stimulation. Unstimulated basal activity was set as unity. Results were the average of duplicate flasks with SD shown.

mitogenic action of MSeA was exerted specifically during mid- to late-$G_1$ phase.

Interestingly, Wortmannin became progressively more inhibitory on ECGS-stimulated DNA synthesis as the lag time between Wortmannin treatment and ECGS stimulation was increased from 0 to 12 h (Fig. 8B). Wortmannin treatment after 24 h of ECGS-stimulation was ineffective on DNA synthesis (Fig. 8B). Because of the known instability of Wortmannin in neutral pH (33), the data suggested that the onset time of PI3K pathway participation in ECGS-stimulated cell cycle progression was at mid- to late-$G_1$ phase. This is because the longer the lag time between Wortmannin addition and ECGS stimulation, the greater the effective concentration of the inhibitor to block the PI3K activity that was required for mediating HUVEC progression from $G_1$ to S phase. This conclusion was supported further by the pattern of inhibitory effect of a more stable and specific PI3K inhibitor, LY294002 (34), which showed a pattern that was identical to that of MSeA (Fig. 8C).

In contrast to the similarities of mid- to late-$G_1$ arresting action shared among MSeA and the PI3K inhibitors, the MEK1 inhibitor PD98059 moderately inhibited DNA synthesis only when given simultaneously (i.e., with preloading for 1.5 h) with ECGS stimulation

(Fig. 8D), and lost the inhibitory activity when provided at 6 h or later. The PI3K and MEK1 inhibitor data were consistent with the notion that MEK1-ERK1/2 signaling was an early event during ECGS-stimulated HUVEC cell cycle entry, rather than for mediating $G_1$ progression; whereas PI3K activation was required during mid- to late-$G_1$ to mediate signaling for $G_1$ progression toward S phase.

## DISCUSSION

Vascular endothelial cell proliferation is an essential component of the angiogenic responses. Inhibiting angiogenic factor-driven mitogenesis will therefore be an important means of achieving selective antiangiogenic action, because vascular endothelial cells in normal adult tissues are essentially quiescent. In this context, we have shown that serum-achievable levels of MSeA potently inhibited ECGS-stimulated HUVEC mitogenesis in vitro. The data established that when cycling HUVECs were exposed to subapoptotic levels of MSeA, they became arrested in the $G_1$ phase (Fig. 1). Furthermore, in an ECGS-depletion/stimulation model, MSeA inhibited, in a dose-

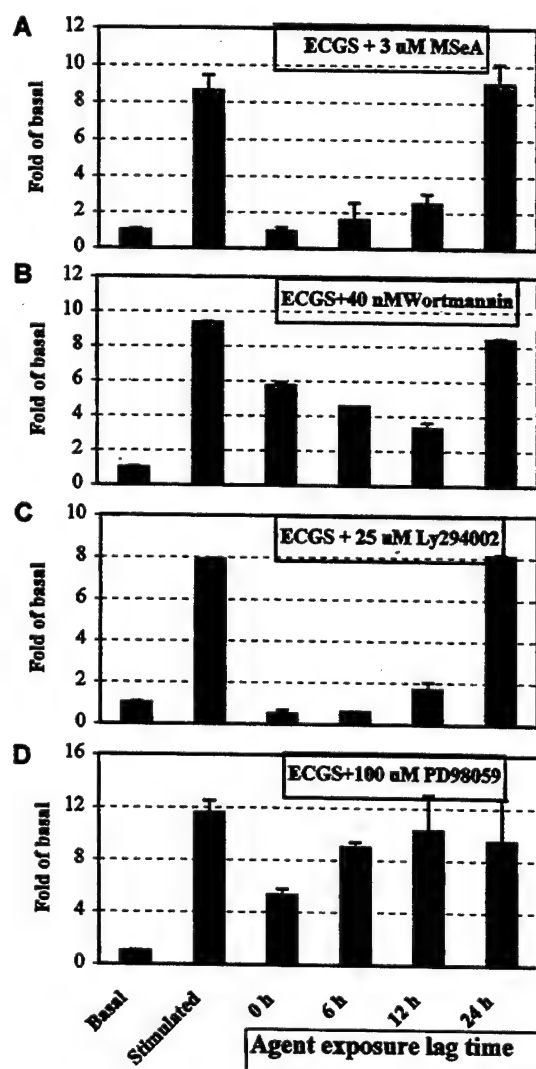

Fig. 8. Cell cycle stage-specific effects of (A) MSeA, (B) Wortmannin, (C) LY294002, or (D) PD98059 on ECGS-stimulated [³H]thymidine incorporation into HUVEC DNA during 30 h of ECGS stimulation. MSeA (3 μM) or inhibitor treatment was either simultaneous with ECGS (agent exposure lag time = 0) or after ECGS stimulation had commenced for 6, 12, or 24 h, respectively (agent exposure lag time = 6, 12, or 24 h). Unstimulated basal activity was set as unity. Results for MSeA (A) were average of three independent experiments, each with duplicate flasks, with SD shown. Results for the kinase inhibitors were the average of two flasks.

dependent manner, ECGS-stimulated HUVEC cell cycle progression into S phase (measured as [³H]thymidine incorporation into DNA and by flow cytometry) with an $IC_{50}$ of 1 $\mu$M and a complete blockage at 3 $\mu$M (Figs. 4B and 5). Such an excellent inhibitory potency was remarkable, considering that, in a recent cancer prevention trial (35), the average plasma selenium level of United States adults was ~1.5 $\mu$M, and selenium supplementation that was associated with a >50% reduction of prostate, lung, and colon cancer risks brought that level to ~2.4 $\mu$M.

Furthermore, the data show that when the exposure level exceeded the selenium level normally present in human serum, MSeA decreased HUVEC survival by the induction of apoptosis that involved caspase activation, PARP cleavage, and DNA fragmentation (Figs. 2 and 4C). The proapoptotic activity of MSeA reported here and elsewhere in a capillary histogenic context when cultured on Matrigel (5) may be pharmacologically achievable and relevant for potential therapeutic applications of methylselenium for cancer treatment. The $G_1$-specific antimitogenic activity and the caspase-mediated proapoptotic activity of methylselenium, along with its potent inhibitory action on endothelial matrix metalloproteinase-2 expression (4, 5) and cancer cell expression of VEGF (5), provide plausible and relevant metabolite-specific mechanisms to account for the antiangiogenic action of selenium that we have described recently (4).

An objective of the present work was to explore the role of the protein kinase signaling pathways in the antimitogenic and proapoptotic actions of methylselenium in vascular endothelial cells using HUVECs as a model. To this end, we have shown that MSeA exposure for 30 h dose-dependently modulated all four major mitogenic and survival pathways examined: i.e., AKT, ERK1/2, p38 MAPK, and JNK1/2 (Fig. 3). Specifically, $G_1$ arrest induced by the exposure to subapoptotic doses of MSeA (less or equal to 5 $\mu$M) for 30 h was associated with dose-dependent reductions of the levels of phospho-AKT, phospho-ERK1/2, and phospho-JNK1/2 in the absence of a change in p38 MAPK phosphorylation. It is noteworthy that JNK1/2 phosphorylation (i.e., activation) was not increased, but rather was decreased, in MSeA-induced HUVEC apoptosis. This finding is in contrast with other well-established apoptosis models in which JNK activation has been shown to be crucial for apoptosis signaling (14). In this regard, we have shown that MSeA-induced apoptosis of DU-145 prostate carcinoma cells did not involve JNK activation (31), whereas selenite-induced apoptosis was associated with an increased phosphorylation of both JNK and P38 MAPK (31). Furthermore, HUVEC apoptosis induced by higher levels of MSeA exposure (e.g., 10 $\mu$M or greater) was accompanied by an increased phosphorylation of p38 MAPK. These results suggest that the inhibition of PI3K, MEK-ERK1/2, and/or JNK pathways might be involved in the HUVEC $G_1$ arrest activity of MSeA, whereas p38 MAPK induction in addition to the above kinase modulations might either be responsible for or a consequence of HUVEC apoptosis induced by MSeA.

Prompted by these observations, we analyzed the effects of MSeA in an ECGS-depletion/stimulation model of HUVEC cell cycle progression to more precisely delineate possible cause-effect relationships among inhibition of PI3K and/or MEK1-ERK pathways and $G_1$ arrest activity. After establishing the approximate cell cycle parameters of this model (Fig. 5) and the phosphorylation (activation) and expression profiles of PI3K targets AKT and S6K as well as those for MEK1 and ERK1/2 (Fig. 6), we showed with pharmacological inhibitors of PI3K and MEK1 that these two pathways could independently contribute to ECGS-stimulated HUVEC mitogenesis (Fig. 7A). Furthermore, we showed that two PI3K inhibitors, despite their structural differences and distinct mechanisms of action (32, 34), recapitulated the mid- to late-$G_1$ stage-specific arresting action of MSeA on ECGS-stimulated HUVEC cell cycle progression to S phase (Fig. 8).

To our knowledge, the current work provided several lines of evidence describing for the first time an antimitogenic action of a methylselenol precursor through a common mechanism(s) or target(s) shared with inhibitors of PI3K. First, MSeA exposure that was commenced after the cell cycle had progressed for 12 h was nearly as inhibitory as MSeA exposure that was initiated at the time of ECGS stimulation (Fig. 8A). The 12-h time point corresponded to late-$G_1$ phase before S entry (Fig. 5). However, after 24 h of ECGS-stimulation, when the S phase was at peak occurrence (Fig. 5), MSeA exposure was totally ineffective at decreasing [³H]thymidine incorporation, indicating that MSeA did not inhibit DNA synthesis per se once cells had entered S phase (Fig. 8A). Second, the mid- to late-$G_1$-specific action of MSeA was shared by PI3K inhibitors, Wortmannin (Fig. 8B) and LY294002 (Fig. 8C), but not by an MEK1 inhibitor, PD98059 (Fig. 8D). Specifically, the closer to $G_1$-S boundary when Wortmannin was introduced, the greater its effectiveness at blocking S entry was observed (Fig. 8B). This increasing potency was consistent with the known instability of Wortmannin in neutral aqueous medium (33) and thereby a greater effective concentration of this inhibitor to inhibit PI3K for mediating $G_1$-S transition when introduced at 12 h. The stable PI3K inhibitor LY294002, which is a competitive inhibitor of the ATP binding site (34), showed an identical pattern of inhibitory effect as MSeA (Fig. 8C). Despite a different mechanism of inhibition on PI3K from Wortmannin, which irreversibly binds to the $M_r$ 110,000 catalytic subunit (32), the data based on LY294002 provided additional support for the above assertion based on Wortmannin data. This commonality of target pathway(s) of action during mid- to late $G_1$ provided a plausible explanation of the additive inhibitory action of MSeA and Wortmannin when used together at low concentrations (Fig. 7B). Finally, the delayed onset of AKT and S6K phosphorylation (PI3K targets) after ECGS stimulation had proceeded for longer than 6 h but within 12 h suggested the participation of this pathway(s) during mid- to late $G_1$ to mediate $G_1$ progression to S phase (Fig. 6A). The observation that MSeA exposure at 3 $\mu$M for >12 h decreased AKT phosphorylation (Fig. 6A) was consistent with an inhibition of PI3K itself or its upstream or downstream components by MSeA. The precise nature of the interactions between the monomethylated selenium pool and PI3K itself or other components in its pathways (i.e., methyl selenium targets) merits additional investigation.

The inhibitory activity of MSeA on $G_1$ progression in HUVECs observed in our study seemed to be in good agreement with the finding of Sinha et al. in a synchronized mammary epithelial cell model (28). They have shown that MSeA exposure for a brief period (as short as 15 min) in the mid-$G_1$ phase (6 h after release of $G_1$ block in that model) inhibited subsequent [³H]thymidine incorporation in the mammary epithelial cells. When the exposure was started at 12 h, a time frame in that model corresponding to the start of S phase, MSeA failed to inhibit ongoing DNA synthesis. It was not yet established whether the PI3K pathway or other protein kinase pathways were involved in the mid-$G_1$-specific action of MSeA in the mammary model.

Our results did not support ERK1/2 dephosphorylation as a mediating event for the antimitogenic action of serum-achievable levels of MSeA. Specifically, the time course experiment (Fig. 6A) indicated that the potent antimitogenic effect of 3 $\mu$M MSeA was observed in the absence of ERK1/2 phosphorylation change throughout the duration of 30 h. The antimitogenic activity of a low level (e.g., 1 $\mu$M) MSeA exposure was not additive with that of an MEK1 inhibitor (Fig. 7B). However, at higher levels of exposure that might be relevant pharmacologically (e.g., 5 $\mu$M or greater), MSeA could effectively inhibit the MEK1-ERK1/2 pathway (Fig. 6A), likely with a delayed kinetics of action after MEK1-ERK1/2 signaling had been accom-

plished (Fig. 6*B*). These observations indicated either an antimitogenic action of a low level of MSeA exposure that was totally independent of ERK1/2 or, if this pathway were involved, that the point of action by MSeA would have to be downstream of ERK1/2 phosphorylation mechanisms. Although nonspecific inhibitory action of kinase inhibitors on enzyme activities other than the purported target enzymes has been reported in other cell types (*e.g.*, Ref. 36), the collective body of evidence, including that generated with these inhibitors in the present study, strongly supports a PI3K pathway-related inhibitory mechanism for the mid- to late-$G_1$-specific arresting action of MSeA observed here.

In summary, the data support a potent antimitogenic action of achievable serum levels of MSeA on human vascular endothelial cells targeting a mechanism controlling $G_1$ progression in the mid- to late-$G_1$ phase of the HUVEC cell cycle. The target(s) seemed to be PI3K itself or other components of this pathway. In addition, the data suggest that the inhibitory effects of MSeA on additional protein kinase pathways such as ERK1/2 and JNK1/2 or activation effects on p38 MAPK could also be involved in vascular endothelial apoptotic responses in a pharmacological or therapeutic context of MSeA exposure.

## ACKNOWLEDGMENTS

## REFERENCES

1. Folkman, J. The role of angiogenesis in tumor growth. Semin. Cancer Biol., *3:* 65–71, 1992.
2. Hanahan, D., and Folkman, J. Patterns and emerging mechanisms of the angiogenic switch during tumorigenesis. Cell, *86:* 353–364, 1996.
3. Bouck, N., Stellmach, V., and Hsu, S. C. How tumors become angiogenic. Adv. Cancer Res., *69:* 135–174, 1996.
4. Jiang, C., Jiang, W., Ip, C., Ganther, H., and Lu, J. X. Selenium-induced inhibition of angiogenesis in mammary cancer at chemopreventive levels of intake. Mol. Carcinog., *26:* 213–225, 1999.
5. Jiang, C., Ganther, H., and Lu, J. X. Monomethyl selenium-specific inhibition of MMP-2 and VEGF expression: implications for angiogenic switch regulation. Mol Carcinog., *29:* 236–250, 2000.
6. Ip, C., and Ganther, H. E. Activity of methylated forms of selenium in cancer prevention. Cancer Res., *50:* 1206–1211, 1990.
7. Ip, C., Hayes, C., Budnick, R. M., and Ganther, H. E. Chemical form of selenium, critical metabolites, and cancer prevention. Cancer Res., *51:* 595–600, 1991.
8. Ip, C. Lessons from basic research in selenium and cancer prevention. J. Nutr., *128:* 1845–1854, 1998.
9. Ferrara, N. Vascular endothelial growth factor and the regulation of angiogenesis. Recent Prog. Horm. Res., *55:* 15–35, 2000.
10. Dvorak, H. F. VPF/VEGF and the angiogenic response. Semin. Perinatol., *24:* 75–78, 2000.
11. Vanhaesebroeck, B., and Alessi, D. R. The PI3K-PDK1 connection: more than just a road to PKB. Biochem. J., *346:* 561–576, 2000.
12. Dhanasekaran, N., and Premkumar Reddy, E. Signaling by dual specificity kinases. Oncogene, *17:* 1447–1455, 1998.
13. Roovers, K., and Assoian, R. K. Integrating the, MAP kinase signal into the $G_1$ phase cell cycle machinery. Bioessays, *22:* 818–826, 2000.
14. Leppa, S., and Bohmann, D. Diverse functions of JNK signaling and c-Jun in stress response and apoptosis. Oncogene, *18:* 6158–6162, 1999.
15. Thakker, G. D., Hajjar, D. P., Muller, W. A., and Rosengart, T. K. The role of phosphatidylinositol 3-kinase in vascular endothelial growth factor signaling. J. Biol. Chem., *274:* 10002–10007, 1999.
16. Yu, Y., and Sato, J. D. MAP kinases, phosphatidylinositol 3-kinase, and p70 S6 kinase mediate the mitogenic response of human endothelial cells to vascular endothelial growth factor. J. Cell. Physiol., *178:* 235–246, 1999.
17. Wu, L. W., Mayo, L. D., Dunbar, J. D., Kessler, K. M., Baerwald, M. R., Jaffe, E. A., Wang, D., Warren, R. S., and Donner, D. B. Utilization of distinct signaling pathways by receptors for vascular endothelial cell growth factor and other mitogens in the induction of endothelial cell proliferation. J. Biol. Chem., *275:* 5096–5103, 2000.
18. Rousseau, S., Houle, F., Landry, J., and Huot, J. p38 MAP kinase activation by vascular endothelial growth factor mediates actin reorganization and cell migration in human endothelial cells. Oncogene, *15:* 2169–2177, 1997.
19. Ilan, N., Mahooti, S., and Madri, J. A. Distinct signal transduction pathways are utilized during the tube formation and survival phases of *in vitro* angiogenesis. J. Cell Sci., *111:* 3621–3631, 1998.
20. Datta, S. R., Dudek, H., Tao, X., Masters, S., Fu, H., Gotoh, Y., and Greenberg, M. E. Akt phosphorylation of BAD couples survival signals to the cell-intrinsic death machinery. Cell, *91:* 231–241, 1997.
21. del Peso, L., Gonzalez-Garcia, M., Page, C., Herrera, R., and Nunez, G. Interleukin-3-induced phosphorylation of BAD through the protein kinase Akt. Science (Wash. DC), *278:* 687–689, 1997.
22. Cardone, M. H., Roy, N., Stennicke, H. R., Salvesen, G. S., Franke, T. F., Stanbridge, E., Frisch, S., and Reed, J. C. Regulation of cell death protease caspase-9 by phosphorylation. Science (Wash. DC), *282:* 1318–1321, 1998.
23. Brunet, A., Bonni, A., Zigmond, M. J., Lin, M. Z., Juo, P., Hu, L. S., Anderson, M. J., Arden, K. C., Blenis, J., and Greenberg, M. E. Akt promotes cell survival by phosphorylating and inhibiting a Forkhead transcription factor. Cell, *96:* 857–868, 1999.
24. Vinals, F., Chambard, J. C., and Pouyssegur, J. p70 S6 kinase-mediated protein synthesis is a critical step for vascular endothelial cell proliferation. J. Biol. Chem., *274:* 26776–26782, 1999.
25. Sherr, C. J. The Pezcoller lecture: cancer cell cycles revisited. Cancer Res., *60:* 3689–3695, 2000.
26. Evans, C. H., and DiPaolo, J. A. Equivalency of endothelial cell growth supplement to irradiated feeder cells in carcinogen-induced morphologic transformation of Syrian hamster embryo cells. J. Natl. Cancer Inst., *68:* 127–131, 1982.
27. Maciag, T., Hoover, G. A., and Weinstein, R. High and low molecular weight forms of endothelial cell growth factor. J. Biol. Chem., *257:* 5333–5336, 1982.
28. Sinha, R., Unni, E., Ganther, H. E., and Medina, D. Methylseleninic acid, a potent growth inhibitor of synchronized mouse mammary epithelial tumor cells *in vitro.* Biochem. Pharmacol., *61:* 311–317, 2001.
29. Lu, J. X., Kaeck, M., Jiang, C., Wilson, A. C., and Thompson, H. J. Selenite induction of DNA strand breaks and apoptosis in mouse leukemic L1210 cells. Biochem. Pharmacol., *47:* 1531–1535, 1994.
30. Duriez, P. J., and Shah, G. M. Cleavage of poly(ADP-ribose) polymerase: a sensitive parameter to study cell death. Biochem. Cell Biol., *75:* 337–349, 1997.
31. Jiang, C., Wang, Z., Ganther, H., and Lu, J. X. Caspases as key executors of methyl selenium-induced apoptosis (anoikis) of DU-145 prostate cancer cells. Cancer Res., *61:* 3062–3070, 2001.
32. Yano, H., Nakanishi, S., Kimura, K., Hanai, N., Saitoh, Y., Fukui, Y., Nonomura, Y., and Matsuda, Y. Inhibition of histamine secretion by Wortmannin through the blockade of phosphatidylinositol 3-kinase in RBL-2H3 cells. J. Biol. Chem., *268:* 25846–25856, 1993.
33. Merck index, 11th edition, #9964.
34. Vlahos, C. J., Matter, W. F., Hui, K. Y., and Brown, R. F. A specific inhibitor of phosphatidylinositol 3-kinase, 2-(4-morpholinyl)-8-phenyl-4H-1-benzopyran-4-one (LY294002). J. Biol. Chem., *269:* 5241–5248, 1994.
35. Clark, L. C., Combs, G. F., Jr., Turnbull, B. W., *et. al.* Effects of selenium supplementation for cancer prevention in patients with carcinoma of the skin. A randomized controlled trial. Nutritional Prevention of Cancer Study Group. JAMA, *276:* 1957–1963, 1996.
36. Yart, A., Laffargue, M., Mayeux, P., Chretien, S., Peres, C., Tonks, N., Roche, S., Payrastre, B., Chap, H., and Raynal, P. A critical role for phosphoinositide 3-kinase upstream of Gab1 and SHP2 in the activation of ras and mitogen-activated protein kinases by epidermal growth factor. J. Biol. Chem., *276:* 8856–8864, 2001.

# ▮ BRIEF COMMUNICATION▮

# Induction of Caspase-Mediated Apoptosis and Cell-Cycle G$_1$ Arrest by Selenium Metabolite Methylselenol

**Zaisen Wang, Cheng Jiang, and Junxuan Lü\***

*Center for Cancer Causation and Prevention, AMC Cancer Research Center, Denver, Colorado*

Previous work based on mono-methyl selenium compounds that are putative precursors of methylselenol has strongly implicated this metabolite in the induction of caspase-mediated apoptosis of human prostate carcinoma and leukemia cells and G$_1$ arrest in human vascular endothelial and cancer epithelial cells. To test the hypothesis that methylselenol itself is responsible for exerting these cellular effects, we examined the apoptotic action on DU145 human prostate cancer cells and the G$_1$ arrest effect on the human umbilical vein endothelial cells (HUVECs) of methylselenol generated with seleno-L-methionine as a substrate for L-methionine-α-deamino-γ-mercaptomethane lyase (EC4.4.1.11, also known as methioninase). Exposure of DU145 cells to methylselenol so generated in the sub-micromolar range led to caspase-mediated cleavage of poly(ADP-ribose) polymerase, nucleosomal DNA fragmentation, and morphologic apoptosis and resulted in a profile of biochemical effects similar to that of methylseleninic acid (MSeA) exposure, as exemplified by the inhibition of phosphorylation of protein kinase AKT and extracellularly regulated kinases 1/2. In HUVEC, methylselenol exposure recapitulated the G$_1$ arrest action of MSeA in mitogen-stimulated G$_1$progression during mid-G$_1$ to late G$_1$. This stage specificity was mimicked by inhibitors of phosphatidylinositol 3-kinase. The results support methylselenol as an active selenium metabolite for inducing caspase-mediated apoptosis and cell-cycle G$_1$ arrest. This cell-free methylselenol-generation system is expected to have significant usefulness for studying the biochemical and molecular targeting mechanisms of this critical metabolite and may constitute the basis of a novel therapeutic approach for cancer, using seleno-L-methionine as a prodrug.
© 2002 Wiley-Liss, Inc.

Key words: selenium; methylselenol; L-methionine-α, γ-lyase; seleno-L-methionine; apoptosis; G$_1$ arrest

## INTRODUCTION

Recent human cancer prevention trials have indicated that selenium may be an effective chemopreventive agent for cancer that arises at many organ sites [1,2]. Methylselenol has been implicated for more than a decade as a critical in vivo selenium metabolite pool for anticancer activity [3–5]. Using mono-methyl selenium compounds that are putative precursors of methylselenol, we have identified several cellular, biochemical, and gene-expression responses that are distinct from those induced by selenium forms that enter the hydrogen selenide pool [6–9]. For example, methylselenocyanate and Se-methylselenocysteine induce apoptosis of mammary tumor epithelial cells without induction of DNA single-strand breaks [6–9]. On the other hand, the hydrogen selenide precursors sodium selenite and sodium selenide, for example, within an hour of exposure induce DNA single-strand breaks (i.e., genotoxic) and subsequent cell death by a combination of acute lysis and apoptosis [6–9].

We have reported that methylseleninic acid (MSeA), a novel methylselenol precursor, induces

DU145 human prostate carcinoma cell apoptosis through caspase-dependent execution [10]. Specifically, apoptosis induced by MSeA involves cell detachment, the activation of multiple caspases, mitochondrial release of cytochrome c, cleavage of poly(ADP-ribose) polymerase (PARP), and DNA nucleosomal fragmentation [10]. The last three actions require active caspases, as demonstrated with pharmacological inhibitors of these death proteases [10]. Independent of and complementing

our work with MSeA, Se-methylselenocysteine has been shown to cause caspase-dependent apoptosis of HL-60 human leukemia cells [11], which grow in suspension culture and do not require cell attachment for survival and mitogenesis. In contrast to methyl selenium compounds, selenite exposure induces apoptotic DNA fragmentation with minimal involvement of caspase-mediated execution in both prostate cancer and leukemia cell lines [10,11].

Furthermore, methyl selenium compounds have been shown to cause $G_1$ arrest in cancer epithelial cells [7–9] and in vascular endothelial cells [12], whereas selenite exposure induces S-phase arrest [7–9]. We have shown that MSeA exposure inhibits mitogen-stimulated human umbilical vein endothelial cell (HUVEC) $G_1$ progression to S phase, and the inhibitory activity appears to target a mechanism in mid-$G_1$ to late $G_1$ phase [12]. This stage-specific action can be mimicked by inhibitors of phosphatidylinositol 3-kinase (PI3K), suggesting a potential target pathway [12]. In a synchronized mouse mammary tumor cell culture model, exposure to MSeA or other methylselenol precursors during the mid-$G_1$ to late $G_1$ stage of cell-cycle progression was found to inhibit potently the progression to S phase [13]. These results suggest the possibility that methylselenol targets a critical mechanism of cell-cycle $G_1$-to-S progression despite the diverse nature of the mitogenic stimuli and signaling pathways in the different cell types [12,13].

Although the results obtained with various methyl selenium compounds have implicated methylselenol strongly as a common metabolite for the activities of $G_1$ arrest and apoptosis in diverse cell types, these studies have not been able to establish directly that methylselenol is responsible for inducing these cellular effects. In this communication, we provide experimental evidence that methylselenol generated in cell-culture medium by L-methionine-α-deamino-γ-mercaptomethane lyase (EC4.4.1.11, also known as methioninase or METase) using seleno-L-methionine (SeMet) as a substrate (by the following well-characterized reaction [14]) can recapitulate these cellular and biochemical effects:

$$CH_3SeCH_2CH_2CH[NH_2]COOH + H_2O$$
$$\rightarrow CH_3SeH + 2\text{-ketobutyrate} + NH_3$$

## MATERIALS AND METHODS

### Chemicals and Reagents

MSeA ($CH_3SeO_2H$) was synthesized as described elsewhere [13,15] and was generously provided by Dr. Howard Ganther (University of Wisconsin-Madison). Intracellularly, MSeA most likely reacts with reduced glutathione to generate methylselenol ($CH_3SeH$) [13]. Bovine endothelial cell growth supplement (ECGS), heparin, SeMet, and L-methio-

nine were purchased from Sigma Chemical Co. (St. Louis, MO). Antibodies for total or cleaved PARP, total and phospho protein kinase AKT (AKT) and extracellularly regulated protein kinase (ERK1/2) were purchased from Cell Signaling Technology (Beverly, MA). [*Methyl*-$^3$H]thymidine (20 Ci/mmol) was purchased from Du Pont-New England Nuclear (Wilmington, DE).

### Methylselenol Generation

Purified METase of *Pseudomonas putida* (catalog no. 133-11933) and recombinant METase based on the gene from *Trichomonas vaginalis* produced in *Escherichia coli* (catalog no. 529-51731) were purchased from Wako Pure Chemical Industries, Ltd. (Richmond, VA). The enzyme preparations were reconstituted in phosphate-buffered saline shortly before use. For cell treatments, substrates for the enzyme (methionine or SeMet) were added first into the culture medium. Then the enzyme preparation was added directly into the cell-culture medium. Dose-response experiments were carried out with respect to METase activity and SeMet concentration, to establish conditions for comparing the morphologic and biochemical responses of cells to methylselenol versus MSeA.

### Cell Lines and Culture Conditions

Cells were grown in humidified chambers at 37°C with 5% $CO_2$. DU145 human prostate cancer cells were cultured in RPM 1640 medium supplemented with 10% fetal bovine serum and 2 mM L-glutamine, as described previously [10]. HUVECs were obtained from American Type Culture Collection (Manassas, VA) and were propagated in F12K medium containing 10% fetal bovine serum, 2 mM L-glutamine, 100 µg/mL heparin, and 30 µg/mL bovine ECGS, as described previously [12,15]. All cell-culture work was performed without antibiotics.

### DU145 Apoptosis

Representative gross morphologic responses to selenium agents or other treatments were documented with a Polaroid camera at 200× magnification under a phase-contrast microscope [10]. DNA nucleosomal fragmentation as a marker of apoptosis was analyzed by gel electrophoresis as described earlier [10]. As an indicator of caspase-mediated apoptosis execution and for comparing biochemical action profiles elicited by methylselenol versus MSeA, we analyzed the cleavage status of PARP and the phosphorylation status of AKT and ERK1/2 by immunoblot analyses, as described elsewhere [10].

### HUVEC $G_1$-S Progression Model

The ECGS-stimulated HUVEC cell-cycle progression model was used as we have described elsewhere [12]. In this model, it takes approximately 16 h from

the time of ECGS initial stimulation for cells to reach S phase, which peaks at 24 h [12]. Briefly, HUVECs were seeded in $T_{25}$ flasks in complete growth medium to 70–80% confluence and then were fed the described medium without ECGS for 48 h, to arrest cells in $G_0$. To compare the effects of methylselenol versus MSeA on ECGS-stimulated cell-cycle progression to S phase, [³H]thymidine (0.2 µCi/mL) and ECGS were added simultaneously with the selenium agents for 30 h. DNA synthetic activity was measured as cumulative [³H]thymidine incorporation into the trichloroacetic acid–precipitable fraction during 30 h of ECGS stimulation.

### $G_1$-Stage–Specific Effect of Methylselenol

In earlier work we have shown that MSeA exerts its $G_1$ arresting activity after between 6 and 12 h of ECGS stimulation (mid-$G_1$ to late $G_1$), an effect that can be recapitulated by P13K inhibitors [12]. To determine whether methylselenol exerted a similar mid-$G_1$ to late $G_1$ action, 3 µM SeMet plus METase (~0.02 U/mL) was introduced either simultaneously with ECGS stimulation (lag time = 0) or 6 h (early-$G_1$ to mid-$G_1$), 12 h (late $G_1$), or 24 h (peak S phase) after ECGS stimulation had commenced (lag time = 6, 12, or 24 h). Ly294002 was dissolved in dimethylsulfoxide and used at a concentration of 25 µM following the same dosing schedule as for the selenium agents. The final dimethylsulfoxide concentration was below 0.1% by volume. The DNA synthetic activity was measured as [³H]thymidine cumulative incorporation into the trichloroacetic acid–precipitable fraction during 30 h of ECGS stimulation.

### RESULTS

### Gross Morphologic Responses Induced by Methylselenol Versus MSeA Exposure

In experiment 1, exposure of DU145 cells to 5 µM MSeA for 20 h induced cellular retraction into angular shapes (Figure 1A, panel f). A small proportion of the cells detached, displaying typical grapelike apoptotic bodies under phase-contrast microscopy. In the absence of METase, exposure to SeMet at up to 100 µM (which is approximately two orders of magnitude higher than the human plasma selenium level) did not cause cellular retraction and detachment, nor did this treatment induce visible morphologic features of apoptosis (Figure 1A, panel b). Similarly, METase plus its regular substrate L-methionine (Met) at 100 µM had no effect on these parameters (Figure 1A, panel e).

When METase (0.08 U/mL) was added into the medium with SeMet, as little as 1 µM SeMet induced morphologic responses similar to those of 5 µM MSeA exposure (Figure 1A, panel c vs. panel f), and a significant increase in morphologic features of apoptosis were apparent between 1 and 10 µM SeMet (Figure 1A panels c and d). METase plus 100 µM SeMet led to rapid cell retraction and detachment within a few hours of exposure, and by 20 h only remnants of dead cells remained (not shown). These results indicated that methylselenol, not SeMet or the regular products of METase (i.e., methylthiol, 2-ketobutyrate, and $NH_3$) [14], accounted for induction of morphologic features of apoptosis under the conditions tested here.

### Caspase-Mediated Apoptosis Induced by Methylselenol Versus MSeA Exposure

Earlier we showed that in DU145 cells PARP cleavage is a sensitive marker of caspase-mediated apoptosis induced by MSeA exposure [10]. In experiment 1, we analyzed PARP cleavage status to compare the efficacy of methylselenol with that of MSeA for inducing caspase-mediated apoptosis (Figure 1A, immunoblot). In accord with the lack of morphologic apoptosis responses, neither exposure to SeMet at up to 100 µM (lane b) nor exposure to METase with its regular substrate methionine at 100 µM (lane e) induced PARP cleavage. On the other hand, in the presence of METase (0.08 U/mL), methylselenol generated from 1 µM SeMet induced an extent of PARP cleavage similar to that of 5 µM MSeA exposure (lane c vs. lane f). The extensive PARP cleavage induced by methylselenol released from 10 µM SeMet (lane d) corroborated the massive morphologic apoptosis response (panel d). Compared with lane d, the decline in the extent of cleaved PARP in cells exposed to 100 µM SeMet plus METase suggested that other acute death execution mechanisms, in addition to caspase-mediated cleavage of PARP, probably were responsible for the rapid and massive death responses.

In subsequent experiments, we examined the dose responses of DU145 cells to SeMet initial concentrations and METase activity levels, to establish conditions that permitted a fair comparison of biochemical responses elicited by methylselenol versus MSeA. The $K_m$ values of METase for Met (1.33 mM) and SeMet (0.51 mM) [14] are much higher than the concentrations of substrates in our experiments (i.e., 100 µM Met present in the cell-culture medium and up to 100 µM added SeMet). The velocity of methylselenol generation thereby is predicted to be an approximate linear function of the SeMet substrate concentration or the absolute amount of enzyme added, according to the Michaelis-Menten equation: $v = V_{max}*[\text{substrate}]/(K_m + [\text{substrate}]) \cong V_{max}*[\text{substrate}]/K_m$, when $K_m \gg [\text{substrate}]$.

As shown in Figure 1B, with 0.02 U/mL METase (experiment 2), methylselenol generated from 5 µM SeMet produced an extent of PARP cleavage similar to that of exposure to 5 µM MSeA, whereas with 0.1 U/mL METase (experiment 3), methylselenol produced from 1 µM SeMet was as effective as 5 µM

## A. Morphology (Experiment 1)
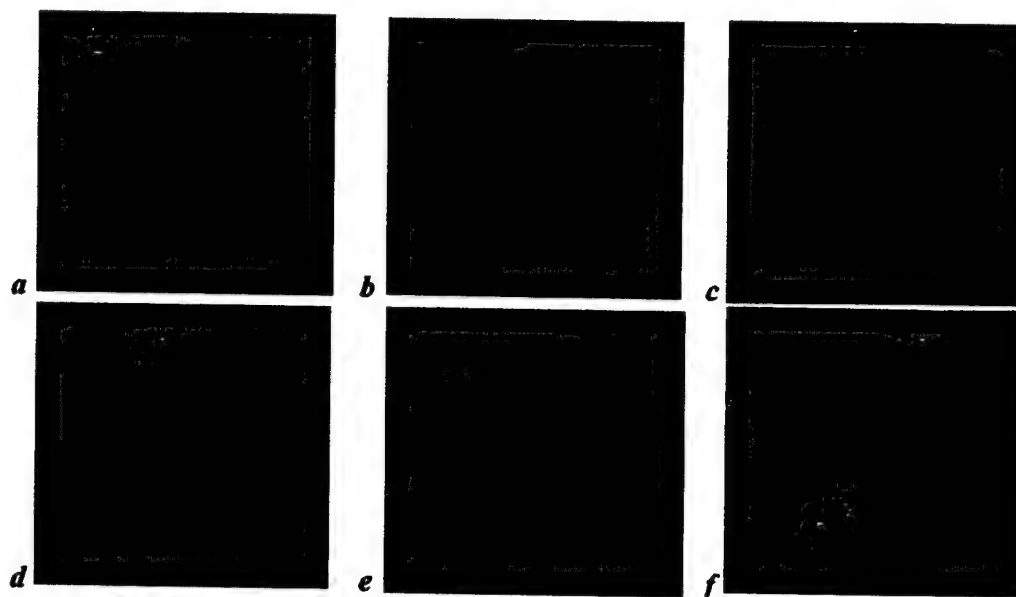


**PARP status**

| Treatment | a | | b | c | d | | e | f | |
|---|---|---|---|---|---|---|---|---|---|
| | - | | | SeMet | | | Met | MSeA | |
| | - | 1 | 10 | 100 | 1 | 10 | 100 | 100 | 5 | (μM) |
| METase | - | - | - | - | + | + | + | + | - | (0.08u/ml) |

← 115kD

PARP ◄···· 89kD

## B. Dose response to SeMet

(Experiment 2)

| | - | SeM | Met | SeMet | | | | MSeA | |
|---|---|---|---|---|---|---|---|---|---|
| | - | 10 | 10 | 1 | 2 | 5 | 10 | 5 | 10 |
| METase | - | - | 0.02 | + | + | + | + | - | - |

PARP

(Experiment 3)

| | - | SeM | Met | SeMet | | | | MSeA | | |
|---|---|---|---|---|---|---|---|---|---|---|
| | - | 5 | 5 | 0.5 | 1 | 2 | 5 | 5 | 10 | (μM) |
| | - | - | 0.1 | + | + | + | + | - | - | (u/ml) |

←115kD
◄···89kD

## C. Dose response to METase

(Experiment 4)

| | - | SeM | Met | SeMet | | | | MSeA | |
|---|---|---|---|---|---|---|---|---|---|
| | - | 10 | 10 | 10 | 10 | 10 | 10 | 5 | 10 |
| METase | - | - | 0.2 | .02 | .05 | 0.1 | 0.2 | - | - |

(Experiment 5)

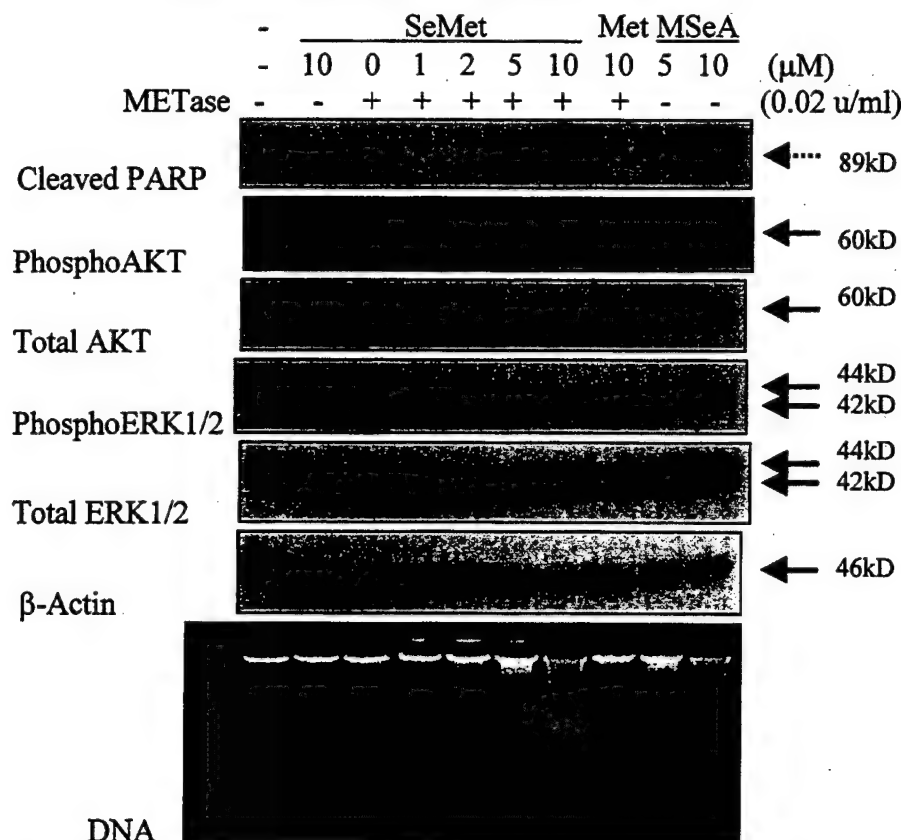| | - | SeM | Met | SeMet | | | | MSeA | | |
|---|---|---|---|---|---|---|---|---|---|---|
| | - | 10 | 10 | 10 | 10 | 10 | 5 | 10 | (μM) |
| | - | - | .01 | .001 | .005 | .01 | - | - | (u/ml) |

Figure 2. Immunoblot analyses of the effects of methylselenol versus MSeA on AKT and ERK1/2 phosphorylation status in DU145 cells after 20 h exposure and their relationship to apoptosis parameters. Apoptosis was assessed by detection of cleaved PARP (89 kd) and by DNA nucleosomal fragmentation. The level of total AKT or ERK1/2 remained unaffected by methyl selenium exposure. β-Actin was immunoblotted for gel-loading correction.

MSeA for inducing apoptosis. Because the enzyme preparations are expensive, it would be more economical to use a moderate yet physiologically relevant SeMet concentration with low METase levels to produce the desirable methylselenol generation velocity. In accord with this rationale, we determined that at an initial SeMet concentration of 10 μM, ≥ 0.01 U/mL METase produced a robust apoptosis response, as detected by DNA nucleosomal fragmentation, whereas 0.001 U/mL was not sufficient and 0.005 U/mL was marginal (Figure 1C, experiments 4 and 5).

### Effects of Methylselenol Versus MSeA Exposure on AKT and ERK1/2 Phosphorylation

Next we compared the phosphorylation status of these protein kinases to determine whether direct methylselenol exposure produced biochemical action profiles similar to those of MSeA (Figure 2). We previously showed that MSeA-induced apoptosis in DU145 cells is associated with a decreased level of phosphorylation of AKT [10], an important survival kinase in many cell types [16]. As with MSeA exposure, methylselenol exposure decreased the phosphorylation level of AKT in a dose-dependent manner for the SeMet substrate and, to a lesser extent, that of ERK1/2, which have been known to mediate mitogenesis and/or survival in many cell types [17]. These inhibitory effects of methylselenol and MSeA appeared to be inversely proportional to the extent of PARP cleavage and DNA nucleosomal fragmentation that they induced (Figure 2). Neither methylselenol exposure nor MSeA exposure affected the total protein level of AKT or ERK1/2,

Figure 1. (A) Representative phase-contrast photomicrographs (200×) of DU145 human prostate cancer cells after 20 h of exposure to (a) phosphate-buffered saline as vehicle control, (b) 100 μM SeMet alone, (c and d) 0.08 U/mL METase plus increasing levels of SeMet (c, 1 μM; d, 10 μM), (e and f) METase plus its regulate substrate Met at (e) 100 μM or (f) 5 μM MSeA. As a marker of caspase-mediated apoptosis, the PARP cleavage status of treated cells at 20 h of exposure was assessed by immunoblotting, using a primary antibody that recognized both the full-length and cleavage products. The solid arrow points to intact PARP (115 kDa), and the dashed arrow points to cleavage product (89 kDa). Lanes corresponding to the picture panels are marked. (B) Apoptosis response (PARP cleavage) as a function of SeMet substrate concentration. Five times more METase was used in experiment 3 (0.1 U/mL) compared with experiment 2 (0.02 U/mL). (C) Apoptosis response (DNA fragmentation) as a function of METase activity level (experiment 4, range 0.02–0.2 U/mL; experiment 5, range 0.001–0.01 U/mL) while the initial SeMet concentration was held at 10 μM.

indicating that the inhibitory effect of methylselenol on these protein kinases probably takes place through mechanisms that regulate phosphorylation (kinases, phosphatases) and their enzyme activities without changing the total number of molecules of the respective enzyme. These results show that methylselenol gnerated in the cell-culture medium induced caspase-mediated apoptosis markers and biochemical end points similar those of MSeA exposure.

### Effects of Methylselenol Versus MSeA on ECGS-Stimulated HUVEC $G_1$-to-S Progression

In an ECGS-stimulated $G_0/G_1$ entry and $G_1/S$ progression model, our earlier work has shown that MSeA potently inhibits mitogen-driven progression from $G_1$ to S phase [12]. In this model, exposure for 30 h to methylselenol inhibited ECGS-stimulated [$^3$H]thymidine incorporation into DNA, with an $IC_{50}$ of $\sim 1$ μM for the SeMet substrate (Figure 3A).
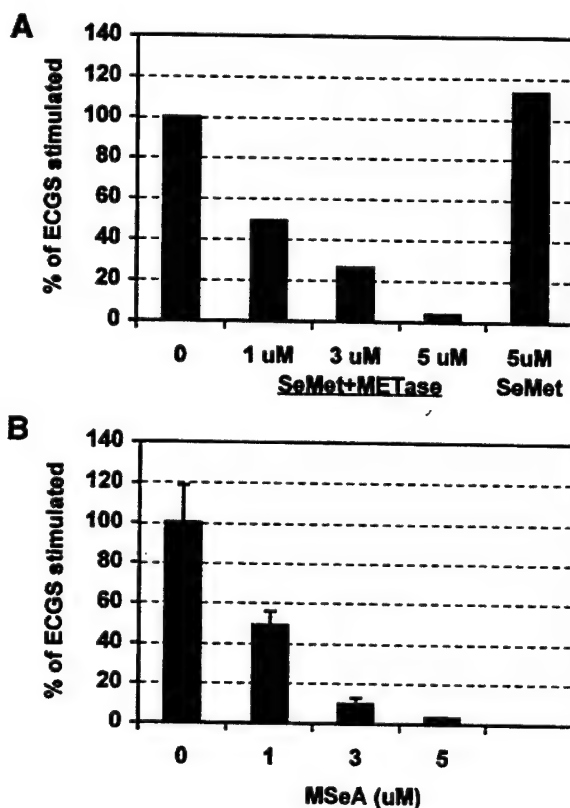
Figure 3. Dose-dependent inhibitory effects of enzymatically generated methylselenol (A) and MSeA (B) on ECGS-stimulated [$^3$H]thymidine incorporation into HUVEC DNA. METase was ~0.02 U/mL. [$^3$H]thymidine was added at time of ECGS stimulation for 30 h. The selenium treatments were commenced at the time of ECGS stimulation. ECGS-stimulated activity was set as 100%. The unstimulated basal incorporation value averaged ~10% of ECGS stimulation. (A) Each column represents the average of duplicate flasks with variation less than 10% of respective mean value. (B) Each column represents the mean of three independent experiments with duplicate flasks. The error bars indicate standard deviations of the respective mean values.

The dose-response pattern was identical to that of MSeA exposure (Figure 3B). As a negative control, SeMet without METase did not inhibit ECGS-stimulated DNA synthesis during 30 h of exposure (Figure 3A).

### $G_1$-Stage–Specific Action of Methylselenol Versus MSeA Exposure

We tested whether methylselenol also exerted the mid-$G_1$ to late $G_1$ stage-specific inhibitory action of MSeA, an effect that is mimicked by P13K inhibitors [12]. Methylselenol generated by METase plus 3 μM SeMet inhibited ECGS-stimulated progression to S phase by ~94% when the exposure was simultaneous with ECGS stimulation (lag time = 0) and inhibited by ~93% when the exposure was delayed for 6 h (early -$G_1$ to mid-$G_1$) (Figure 4, open bars). Even when exposure was started at 12 h of ECGS stimulation (late $G_1$), methylselenol inhibited S-phase entry by ~60%. When the cells had entered peak S phase at 24 h, however, direct methylselenol exposure produced a minimal (~20%) inhibitory effect. The overall inhibitory pattern was nearly identical to that of MSeA exposure (Figure 4, filled bars) or a P13K inhibitor, LY294002 (Figure 4, striped bars). These results and data presented elsewhere [12] suggest that the antimitogenic action of methylselenol is exerted specifically at mid-$G_1$ to late $G_1$ phase (between 6 and 12 h), probably through a target pathway shared with P13K inhibitors.

### DISCUSSION

The data presented here showed that direct exposure to enzymatically generated methylselenol recapitulated the apoptotic action of a methylselenol precursor compound, MSeA, in DU145 cells and its $G_1$-arresting action in HUVECs. Specifically, direct methylselenol exposure of DU145 cells not only induced the same morphologic changes, PARP cleavage, and DNA nucleosomal fragmentation (Figure 1) but also exerted the same biochemical action profiles as did MSeA exposure, in terms of the phosphorylation status of AKT and ERK1/2 (Figure 2). Regarding the cell-cycle effect, methylselenol exposure, like MSeA exposure, appeared to target a control mechanism(s) in mid-$G_1$ to late $G_1$ (Figure 4). Because a P13K inhibitor, LY294002, could mimic the stage-specific effect of both methyl selenium agents, PI3K itself, or its downstream effector molecules, could be targeted specifically by methylselenol. Future efforts will be directed at identifying the molecular targets of methylselenol for regulating $G_1$-to-S progression. The direct methylselenol generation system reported here is expected to have significant utility for studying such biochemical and molecular targeting mechanisms in cell-free assays and in cell-culture models.

The excellent efficacy of methylselenol for inducing DU145 cancer cell apoptosis and inhibiting
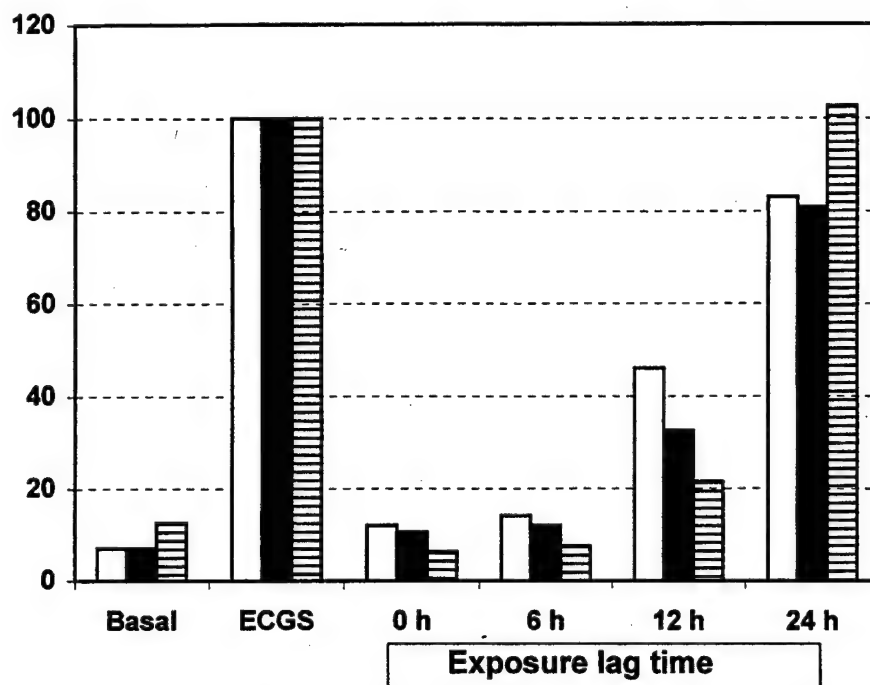
Figure 4. Cell cycle–stage effects of methylselenol generated by METase (~0.02 U/mL) with 3 µM SeMet as substrate (open bars), 3 µM MSeA (filled bars), 25 µM PI3K inhibitor LY294002 (striped bars) on ECGS-stimulated [³H]thymidine incorporation into HUVEC DNA during 30 h of ECGS stimulation. Methyl selenium or LY294002 treatment was either simultaneous with ECGS (lag time = 0 h) or after ECGS stimulation had commenced for 6, 12, or 24 h, respectively (exposure lag time = 6, 12, or 24 h). ECGS-stimulated activity was set as 100%. Each column represents the average of duplicate flasks with variation less than 10% of the respective mean value.

ECGS-stimulated $G_1$-S progression is noteworthy in terms of its relevance to cancer chemoprevention and therapy. Whereas SeMet exposure as high as 100 µM did not affect DU145 cell survival during the time frame of our experiments, methylselenol released from as little as 1 µM SeMet in the presence of sufficient METase significantly induced caspase-mediated apoptosis of prostate cancer cells (Figure 1) and inhibited mitogen-stimulated HUVEC cell-cycle progression to S phase (Figure 3). These results suggest that a submicromolar amount of methyl-selenol should be sufficient to exert these actions. Although people who do not take selenium supplements usually have very little protein-free selenium in their serum [18], the level of nonprotein selenium metabolites is expected to increase sharply with chemopreventive or therapeutic use [19]. Under such conditions, the extra selenium that is not needed for selenoproteins is expected to enrich the methylselenol pool by the methylation pathway [20]. As a reference value, the mean plasma selenium concentration of subjects without selenium supplementation in recent human trials is ~1.5 µM [1]. Supplementation (200 µg/day as selenized yeast) that is associated with a greater than 50% reduction in the risk of prostate, colon, and lung cancers brings the mean selenium level to ~2.4 µM [1]. It remains to be determined whether in vivo methylselenol can reach the submicromolar levels, especially in the tumor local environment, that have the adverse impact on vascular endothelial cell proliferation and angiogenesis and cancer cell survival reported here.

Pertinent to the apoptotic action of methylselenol on cancer cells, it has been reported that in METase gene–transduced tumor cells, the cytocidal activity of SeMet is increased 1000-fold compared with nontransduced cells in vitro [21]. Furthermore, SeMet treatment of nude mice bearing tumor cells expressing the METase transgene significantly inhibits ascites tumor growth and prolongs host survival [21], demonstrating a potential for METase gene therapy using SeMet as a prodrug substrate. The clinical utility of the methylselenol generation system described in this communication as a novel therapy, through intratumoral or tumor-targeted delivery of METase and either systemic or localized delivery of SeMet substrate, merits investigation.

## ACKNOWLEDGMENTS

## REFERENCES

1. Clark LC, Combs GF Jr, Turnbull BW, et al. Effects of selenium supplementation for cancer prevention in patients with carcinoma of the skin: A randomized controlled trial.

Nutritional Prevention of Cancer Study Group. JAMA 1996; 276:1957–1963.

2. Yu SY, Zhu YJ, Li WG. Protective role of selenium against hepatitis B virus and primary liver cancer in Qidong. Biol Trace Elem Res 1997;56:117–124.

3. Ip C, Ganther HE. Activity of methylated forms of selenium in cancer prevention. Cancer Res 1990;50:1206–1211.

4. Ip C, Hayes C, Budnick RM, Ganther HE. Chemical form of selenium, critical metabolites, and cancer prevention. Cancer Res 1991;51:595–600.

5. Ip C. Lessons from basic research in selenium and cancer prevention. J Nutr 1998;128:1845–1854.

6. Lü J, Jiang C, Kaeck M, et al. Dissociation of the genotoxic and growth inhibitory effects of selenium. Biochem Pharmacol 1995;252:7392–7394.

7. Lü J, Pei H, Ip C, Lisk D, Ganther H, Thompson HJ. Effect of an aqueous extract of selenium enriched garlic on in vitro markers and in vivo efficacy in cancer prevention. Carcinogenesis 1996;17:1903–1907.

8. Kaeck M, Lü JX, Strange R, Ip C, Ganther H, Thompson HJ. Differential induction of growth arrest inducible genes by selenium compounds. Biochem Pharmacol 1997;53:921–926.

9. Lü JX. Apoptosis and angiogenesis in cancer prevention by selenium. In: Nutrition and cancer prevention. New York: Kluwer/Plenum Publishers, 2000. p 131–145.

10. Jiang C, Wang Z, Ganther H, Lü JX. Caspases as key executors of methyl selenium induced apoptosis (anoikis) of DU145 human prostate cancer cells. Cancer Res 2001;61:3062–3070.

11. Kim T, Jung U, Cho DY, Chung AS. Se-methylselenocysteine induces apoptosis through caspase activation in HL-60 cells. Carcinogenesis 2001;22:559–565.

12. Wang Z, Jiang C, Ganther H, Lü JX. Anti-mitogenic and pro-apoptotic activities of methylseleninic acid in vascular endothelial cells and associated effects on PI3K-AKT, ERK, JNK and p38MAPK signaling. Cancer Res 2001;61:7171–7178.

13. Sinha R, Unni E, Ganther HE, Medina D. Methylseleninic acid, a potent growth inhibitor of synchronized mouse mammary epithelial tumor cells in vitro. Biochem Pharmacol 2001;61:311–317.

14. Esaki N, Tanaka H, Uemura S, Suzuki T, Soda K. Catalytic action of L-methionine gamma-lyase on selenomethionine and selenols. Biochemistry 1979;18:407–410.

15. Jiang C, Jiang W, Ip C, Ganther H, Lü JX. Selenium-induced inhibition of angiogenesis in mammary cancer at chemopreventive levels of intake. Mol Carcinog 1999;26:213–225.

16. Datta SR, Brunet A, Greenberg ME. Cellular survival: A play in three Akts. Genes Dev 1999;13:2905–2927.

17. Kolch W. Meaningful relationships: The regulation of the Ras/Raf/MEK/ERK pathway by protein interactions. Biochem J 2000;351(Pt 2):289–305.

18. Marchante-Gayon JM, Sanchez-Uria JE, Sanz-Medel A. Serum and tissue selenium contents related to renal disease and colon cancer as determined by electrothermal atomic absorption spectrometry. J Trace Elem Med Biol 1996;10:229–236.

19. Combs GF Jr, Gray WP. Chemopreventive agents: Selenium. Pharmacol Ther 1998;79:179–192.

20. Ganther HE. Pathways of selenium metabolism including respiratory excretory products. J Amer Coll Toxicol 1986;5:1–5.

21. Miki K, Xu M, Gupta A, et al. Methioninase cancer gene therapy with selenomethionine as suicide prodrug substrate. Cancer Res 2001;61:6805–6810.

# Anti-Angiogenic Potential of a Cancer Chemopreventive Flavonoid Antioxidant, Silymarin: Inhibition of Key Attributes of Vascular Endothelial Cells and Angiogenic Cytokine Secretion by Cancer Epithelial Cells

Cheng Jiang, Rajesh Agarwal, and Junxuan Lü[1]

*Center for Cancer Causation and Prevention, AMC Cancer Research Center, Denver, Colorado 80214*

In recent studies, we have shown that silymarin, a naturally occurring flavonoid antioxidant, exhibits anti-cancer effects against several epithelial cancers. Here, we assessed its potential as an anti-angiogenic agent employing human umbilical vein endothelial cells (HUVEC) and human prostate and breast cancer epithelial cells. When sub-confluent HUVEC were treated for 48 h, adherent cell number decreased by 50 and 90% at 50 and 100 $\mu$g/ml doses, respectively. Apoptotic cell death principally accounted for cell loss at >50 $\mu$g/ml doses. In biochemical analysis, silymarin treatment of HUVEC for 6 h resulted in a concentration-dependent decrease in the secretion and cellular content of matrix metalloproteinase (MMP)-2/gelatinase A. Silymarin also inhibited HUVEC tube formation (*in vitro* capillary differentiation) on a reconstituted extracellular matrix, Matrigel. In other studies, 5 to 6 h exposure of DU145 prostate, and MCF-7 and MDA-MB-468 breast cancer cells to silymarin resulted in a dose-dependent decrease in the secreted vascular endothelial growth factor (VEGF) level in conditioned media without any visible change in cell morphology. The inhibitory effect of silymarin on VEGF secretion occurred as early as 1 h. These observations indicate a rapid inhibitory action of silymarin on the secretion of this primary angiogenic cytokine by cancer epithelial cells. Taken together, the results of this study support the hypothesis that silymarin possesses an anti-angiogenic potential that may critically contribute to its cancer chemopreventive efficacy. © 2000 Academic Press

*Key Words:* silymarin; HUVEC; MMP-2/gelatinase A; *in vitro* capillary differentiation; vascular endothelial growth factor; angiogenesis switch.

[1] To whom correspondence should be addressed at AMC Cancer Research Center, 1600 Pierce Street, Denver, CO 80214. Fax: 303-239-3560. E-mail: luj@amc.org.

It is now well established that angiogenesis, that is, the growth of capillary vessels from existing blood vessels, is obligatory for the growth and progression of solid cancers (1–3). During solid cancer genesis, initiated cells undergo clonal expansion in an avascular state when the expanding lesions are small enough to take in nutrients and to expel metabolic wastes by diffusion. However diffusion is not sufficient to support continued growth of the lesion beyond a certain physical size (estimated ~2 mm diameter) because the expanding lesions consume nutrients at a rate proportional to their volume whereas the supply of nutrients is delivered at a rate proportional to their surface area (4, 5). In order for avascular lesions to progress beyond the size limit imposed by simple diffusion, they must turn on their angiogenic switch to form a neo-vasculature. Angiogenesis critically depends on several conditions such as the endothelial cells must proliferate to provide the necessary number of cells for the growing vessels, the activated endothelial cells must secrete matrix metalloproteinases (MMP) required to break down surrounding tissue matrix and the endothelial cells must be capable of movement/migration. In addition, the angiogenic stimuli (for example, hypoxia and production of angiogenic cytokines such as vascular endothelial growth factor [VEGF]) must be sustained. Because of the critical dependence of tumor growth and metastasis on angiogenesis, therapeutic strategies have been developed targeting various aspects of the angiogenic processes, many with promising results. Cancer chemoprevention aims to block or reduce the occurrence or progression of human malignancies by the chronic administration of naturally occurring or synthetic chemical agents. Chemoprevention can be most effective on early lesions, the fate and growth of which are likely to be more critically dependent on angiogenesis. Since the vascular endothelial cells constitute the first line of exposure to blood-borne agents, it is plausible that cancer chemopreventive

activity of many agents may be attributable, at least in part, to anti-angiogenic properties through an inhibition of one or more of the angiogenic responses of the endothelial cells.

Fruits, vegetables, tea as well as many medicinal herbs and plants have been shown to be rich sources of phytochemicals with chemoprevention potential for some kinds of human cancer (6–9). Naturally occurring polyphenolic antioxidants are among these phytochemicals that have received increasing attention in recent years (6–9). Silymarin is a polyphenolic flavonoid antioxidant isolated from milk thistle (*Silybum marianum (L.) Gaertn*) and is used clinically as a liver detoxicant for almost three decades (10, 11). Several studies in recent past have shown anti-carcinogenic effects of silymarin in short-term bioassays (12–14). More recently, we have shown the cancer preventive efficacy of silymarin in several mouse skin tumorigenesis models (15–19), and its anti-cancer potential for human breast, prostate and cervical cancers (20–24).

Whereas all the mechanistic studies done with silymarin in recent years have focused on the cancer epithelial cells as the targets, the present study was conducted to explore potential inhibitory effects of silymarin on key parameters critical for tumor angiogenesis. In this paper, we report that silymarin treatment of human umbilical vein endothelial cells (HUVEC) inhibits their growth and survival, the secretion and expression of matrix metalloproteinases (MMPs) and capillary tube formation (*in vitro* angiogenesis). In addition, we report a rapid inhibitory action of silymarin on the secretion of a primary angiogenic cytokine VEGF by human prostate and breast cancer epithelial cells. Together, these results support an anti-angiogenic activity of silymarin that may contribute critically to its cancer chemopreventive potential.

## MATERIALS AND METHODS

*Chemicals and reagents.* Silymarin, bovine endothelial cell growth supplement (ECGS) and heparin were purchased from Sigma Chemical Co. (St. Louis, MO). Matrigel was purchased from Becton-Dickinson Labware (Bedford, MA). VEGF ELISA kit was purchased from R&D Systems (Minneapolis, MN).

*Cell lines and cell culture.* HUVEC cells, DU145 prostate cancer cells, and MCF-7 and MDA-MB-468 breast cancer cells were obtained from American Type Culture Collection (Manassas, VA). HUVEC were propagated in F12K medium containing 10% fetal bovine serum (FBS), 2 mM L-glutamine, 100 $\mu$g/ml of heparin (Sigma Chemical Co., St. Louis, MO) and 30 $\mu$g/ml of bovine endothelial cell growth supplement (ECGS) (Sigma Chemical Co.) as described previously (25). DU145 cells were cultured in RPMI1640 medium supplemented with 10% FBS. MCF-7 and MDA-MB-468 breast cancer cells were cultured in DMEM medium supplemented with 10% FBS and 2 mM L-glutamine.

*HUVEC growth/survival.* Cells were seeded into 6-well plates for 24–48 h to reach ~50% confluence. Fresh medium was replaced and silymarin was added from 100× stock solutions prepared in DMSO/

ethanol (20:80). In all the studies, the selection of silymarin doses was based on our earlier studies showing anti-proliferative and differentiation-inducing effects in several human epithelial carcinoma cells (20–24). Morphological responses were monitored over time under a phase contrast microscope. Adherent cells after 48 h of treatment were fixed in 1% glutaraldehyde and stained. The cell number was counted under 100× magnification for 5 random fields for each condition. The experiment was repeated at least once.

*Zymogram analysis for MMP-2.* HUVEC were grown in 6-well plates in complete medium for 24–48 h to near confluence. The cells were washed two times with PBS to remove spent medium and fed serum-free medium supplemented with 100 $\mu$g ECGS/ml and treated with silymarin for 6 h (a time frame that did not result in any visible morphological changes). Conditioned medium and cell lysate (prepared in 1% Triton X-100, 0.5 M Tris-HCl, pH 7.6, 200 mM NaCl) were analyzed for gelatinolytic activities on substrate gels as we previously described (25). The gels were digitized with a transmission scanner and band intensity (on inverted images) was quantified using the UN-SCAN-IT gel scanner software (Silk Scientific, Inc. Orem, UT). As a comparison for the efficacy of silymarin to inhibit HUVEC MMP-2, curcumin, a polyphenolic component of the food flavor turmeric, was included in some experiments. Curcumin has been reported to potently inhibit MMP-2 expression and tube formation in this model (26).

*Capillary tube formation on Matrigel (in vitro angiogenesis).* The method of Kubota *et al.* was used (27). When seeded on Matrigel, a reconstituted extracellular matrix preparation of EHS mouse sarcoma, vascular endothelial cells undergo rapid *in vitro* differentiation into capillary like structures (27), providing a simple assay for assessing impact of agents on endothelial differentiation process which requires cell-matrix interaction, intercellular communication as well as cell motility. To examine the effect of silymarin on this process, HUVEC were treated in two ways in relationship to the time frame of cell seeding onto the Matrigel. (A) Silymarin simultaneous with cell seeding: Twenty-four-well cell culture plates were coated with 0.3 ml of Matrigel and allowed to solidify at 37°C for 1 h. Then 0.5 ml medium was added to each well and silymarin was added at 2 times of the desired concentrations. HUVEC were trypsinized and 20,000 or 40,000 cells were added per well in 0.5 ml medium. Tube formation was observed periodically over time under a phase contrast microscope. Representative Polaroid pictures were taken at 6 or 17 h. (B) Treatment of preformed tubes: HUVEC were seeded onto Matrigel for 6 h to form rudimentary tubes, then the medium was replaced and silymarin was added. Tube morphology was observed over time and representative Polaroid pictures were taken at 20 h after the initiation of silymarin treatment. Curcumin was included in some experiments as a comparison for the efficacy of silymarin to inhibit tube formation. The experiments were repeated twice.

*VEGF secretion and expression in cancer epithelial cells.* In dose-response experiments, DU145 prostate cancer cells and MCF-7 (estrogen dependent) and MDA-MB-468 (estrogen independent) breast cancer cells were grown in T25 flasks in complete medium until confluence (~48 h). The spent medium was removed, and cells were washed 3× with PBS. Cells were treated in serum-free medium with increasing concentrations of silymarin. Conditioned media and cell lysates were analyzed for VEGF protein content by an ELISA kit as per manufacturer's instructions (R&D Systems, Minneapolis, MN). In time course experiments, confluent DU145 or MDA-MB-468 cells were treated in serum-free media with solvent vehicle (DMSO/ ethanol), 50 or 100 $\mu$g/ml silymarin. Serial 1-ml aliquots were taken of the culture media for VEGF ELISA. Each sample was measured in triplicate. Experiments were repeated at least once.

## RESULTS

*HUVEC growth and survival.* As shown in Fig. 1 (A–D), treatment with silymarin for 48 h led to a

**A** Solvent vehicle　　　**B** Silymarin 50 μg/ml

**C** Silymarin 75 μg/ml　　**D** Silymarin 100 μg/ml
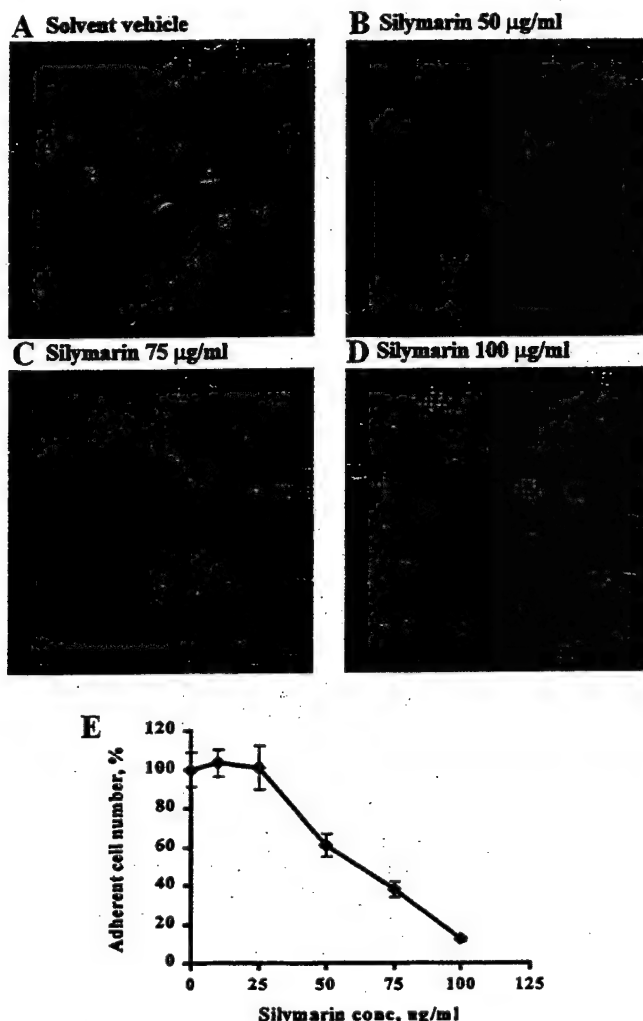
**E**

FIG. 1. Effect of silymarin treatment on HUVEC growth and survival. (A–D) Representative phase-contrast photomicrographs of HUVEC at 48 h after treatment was initiated with DMSO/ethanol vehicle (A), 50 (B), 75 (C), and 100 (D) μg/ml of silymarin. Most floaters showed typical apoptotic morphology such as cell retraction, condensation, and fragmentation into apoptotic bodies. (E) Adherent cell number as a function of initial silymarin treatment concentration. Each data point represented the mean ± SEM of the adherent cells in 5 randomly chosen fields.

concentration-dependent decrease of cells remaining adherent to the culture vessel and an increase of detached floaters. The adherent cell number was inhibited by 50 and 90% at 50 and 100 μg/ml doses of silymarin, respectively (Fig. 1E). The floaters displayed typical apoptotic morphology as indicated by cell condensation and fragmentation into apoptotic bodies. Such floaters did not re-attach or grow upon reseeding into silymarin-free fresh medium (data not shown).

*HUVEC MMP-2 expression.* Treatment with silymarin for 6 h, an exposure time that did not result in any visible morphological changes, led to a

concentration-dependent decrease of MMP-2 (72 kD gelatinase A) in the conditioned media (i.e., secreted MMP) as detected by gelatin zymogram analyses (Fig. 2A). The extent of inhibition of the secreted MMP-2 by 100 μg/ml of silymarin was comparable to that induced by 25 μM curcumin, which has been shown to inhibit HUVEC MMP-2 and *in vitro* angiogenesis (26). In the cell lysate (Fig. 2B), 100 μg/ml silymarin inhibited MMP-2 by 67% and this effect was greater than that exerted by 25 μM curcumin, even though the secreted MMP-2 was decreased to the same extent by both compounds at the respective concentrations. At 50 μg/ml dose, silymarin did not decrease MMP-2 in the cell lysate even though it decreased the secreted MMP-2 by as much as 63%, indicating that at this level, silymarin might only inhibit the secretion of MMP-2 from the cells but not the cellular level. Incubation of the control medium (MMP-2 containing) with silymarin directly in the test tube did not inhibit its zymographic activity (data not shown), indicating a cellular dependent process for the inhibitory action on MMP-2 secretion and expression by silymarin.

*In vitro angiogenesis on Matrigel by HUVEC.* In experiments assessing the inhibitory effects on capillary tube formation, silymarin exposure, commenced at the time of seeding HUVEC onto Matrigel,



**A** Conditioned medium　　　**B** Cell lysate

| | Silymarin | Curc | | Silymarin | Curc |
|---|---|---|---|---|---|
| 0 | 50　100 | | 0 | 50　100 | |

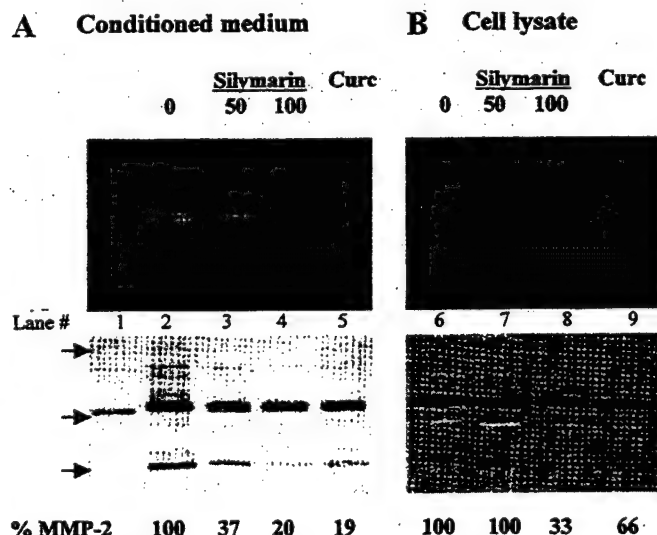Lane #　1　2　3　4　5　　6　7　8　9

% MMP-2　100　37　20　19　　100　100　33　66

FIG. 2. Effect of silymarin or curcumin on secreted (A) and cell-associated (B) matrix metalloproteinase-2 detected by gelatin substrate gel zymography. HUVEC were treated in serum-free medium supplemented with 100 μg/ml of ECGS with silymarin or curcumin for 6 h. The conditioned media (A, lanes 2–5) and cell lysates (B) were analyzed on gelatin I impregnated substrate gels. Silymarin concentrations were 50 and 100 μg/ml. Curcumin treatment concentration was 25 μM. Inverted images of the zymograms (lower panels) were used for densitometric quantitation. The relative pixel density for the 72 kD gelatinase A/MMP-2 was shown below each lane. Arrowheads on the left mark position of molecular weight standards corresponding to (from top) 97, 66, and 47 kD. Lane 1 was serum-free medium as a blank control.
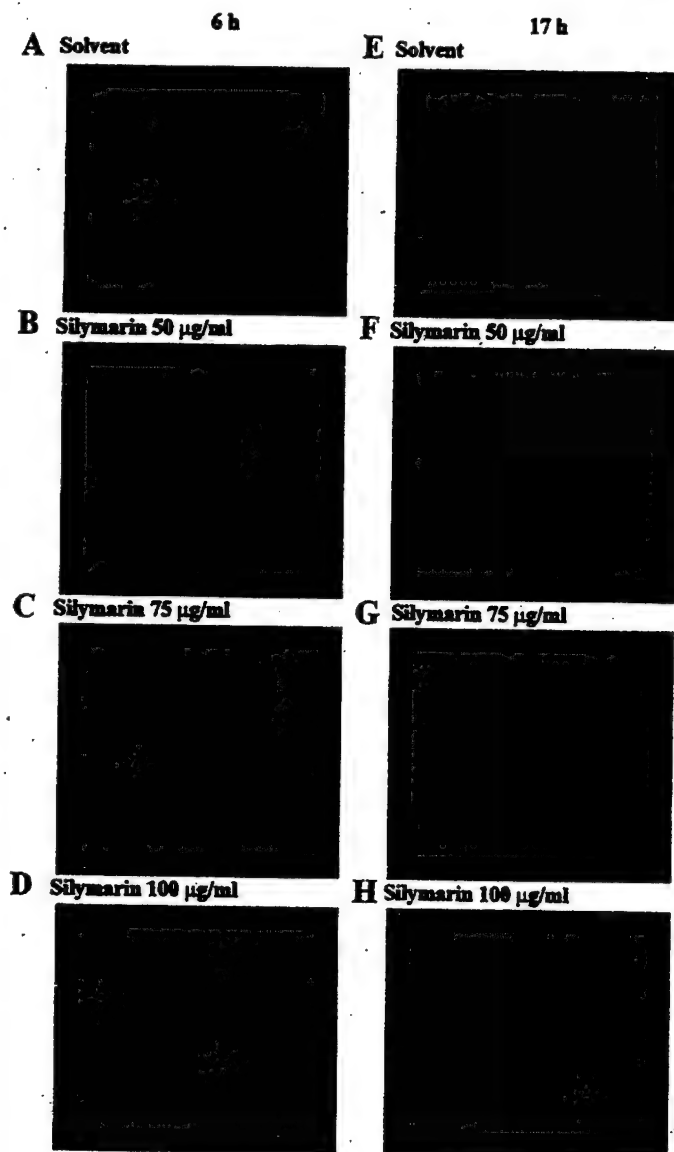
cells for 6 h decreased the secreted (in conditioned medium) VEGF content in a concentration dependent manner, resulting in a complete block by the 100 µg/ml dose (Table 1). Such inhibitory effect was observed in the absence of a reduction of the cell lysate VEGF content (Table 1). In human breast cancer cells, silymarin exposure reduced VEGF level in conditioned media in both MDA-MB 468 and MCF-7 cell lines (Table 1). The impact of silymarin on the cellular VEGF content was similar to that on DU145 cells, i.e., in MCF-7 cells as well as MDA-MB 468 cells at low to intermediate exposure levels, a reduction of secreted VEGF level was not associated with decreased cellular
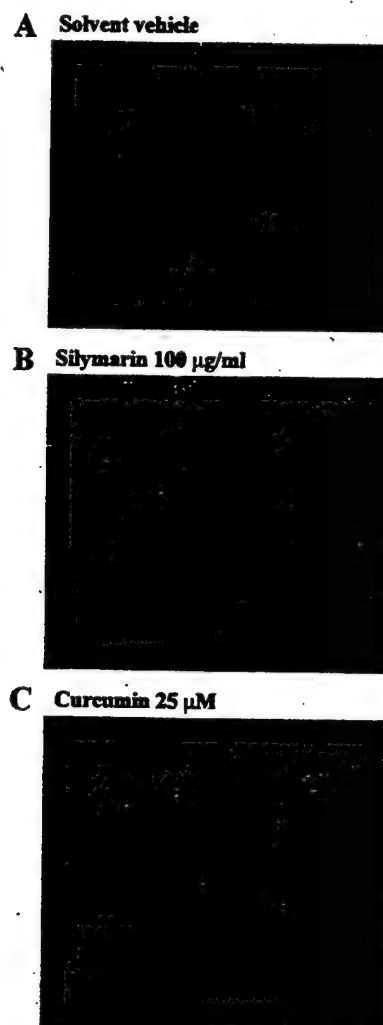


**FIG. 3.** Effect of silymarin on HUVEC capillary tube formation (*in vitro* differentiation) on Matrigel. HUVEC (20,000 cells/per well) in medium containing 10% serum was seeded into Matrigel precoated 24-well plate and treated with DMSO/ethanol solvent vehicle (A, E) or increasing concentrations of silymarin (B–D, F–H). Representative phase contrast photomicrographs (100× magnification) were taken at 6 h (A–D) and 17 h (E–H) after seeding. Each experiment condition was performed in duplicate wells and the experiments were repeated twice.



**FIG. 4.** Effect of silymarin or curcumin treatment on preformed HUVEC tubes. HUVEC (40,000 per well) were seeded into Matrigel pre-coated 24-well plate for 6 h for tube formation. The unattached cells and conditioned medium were removed and the tubes washed in fresh medium. The preformed tubes were treated with DMSO/ethanol vehicle (A), silymarin (B, 100 µg/ml) or curcumin (C, 25 µM). The cells were fixed in 1% glutaldehyde at 20 h after seeding and representative phase-contrast photomicrographs (100× magnification). Each experiment condition was performed in duplicate wells and the experiment was repeated twice.

concentration-dependently inhibited tube formation at both 6 (Figs. 3A–D) and 17 h (Figs. 3E–H), achieving almost a complete block at the 100 µg/ml dose. Silymarin exposure of pre-formed tubes led to the retraction of cells and capillary disintegration (Fig. 4B versus 4A). The efficacy of silymarin at 100 µg/ml was comparable to that of 25 µM curcumin (Fig. 4C).

*VEGF secretion by cancer epithelial cells.* Silymarin treatment of DU145 human prostate carcinoma

**TABLE 1**

Effects of Silymarin Treatment on Vascular Endothelial Growth Factor (VEGF) Content in Conditioned Media (Secreted) and in Prostate and Breast Cancer Cell Lysates

| Cell line | Silymarin µg/ml | Exposure time, h | VEGF in medium pg/flask | VEGF in lysate pg/flask |
|---|---|---|---|---|
| DU145 | 0 | 6 | $4272 \pm 516^{a1,2}$ | $640 \pm 54^c$ |
| | 25 | 6 | $4128 \pm 480^a$ | $760 \pm 16^b$ |
| | 50 | 6 | $2658 \pm 264^b$ | $894 \pm 10^a$ |
| | 100 | 6 | $72 \pm 1^c$ | $758 \pm 22^b$ |
| MDA-MB-468 | 0 | 5 | $7815 \pm 480^a$ | $1112 \pm 24^a$ |
| | 25 | 5 | $6150 \pm 165^b$ | $1222 \pm 42^a$ |
| | 50 | 5 | $5300 \pm 105^c$ | $1140 \pm 26^a$ |
| | 100 | 5 | $2590 \pm 65^d$ | $742 \pm 14^b$ |
| MCF-7 | 0 | 6 | $3420 \pm 120^c$ | $455 \pm 24$ |
| | 50 | 6 | $3156 \pm 246^a$ | $447 \pm 9$ |
| | 100 | 6 | $2178 \pm 102^b$ | $501 \pm 22$ |

[1] Mean $\pm$ sd; $n = 3$ replicates.

[2] Data were analyzed by one-way ANOVA. Dissimilar superscripts indicate significant difference between means ($P < 0.05$).

VEGF content (Table 1). The exception was MDA-MB cells treated with 100 µg/ml silymarin where cellular VEGF content was decreased. In time course experiments, the secretion of VEGF was significantly decreased at 1 h of exposure to silymarin in both DU145 and MDA-MB 468 cells (Fig. 5). The inhibitory effects in all three cell lines were observed in the absence of morphological changes such as cell retraction, rounding, detachment or cytoplasmic vaccuolation.

## DISCUSSION

A number of recent studies by Agarwal and associates (15–24) have shown that silymarin possesses significant chemopreventive and anti-cancer activity. Although cell culture studies have revealed many insights concerning the potential direct effects of silymarin exposure on cancer epithelial cells with respect to growth and survival signaling and cell cycle regulation, there has been no published work to address the potential impacts of silymarin on vascular endothelial cells and angiogenesis. The results of the present study support a potential anti-angiogenic activity of silymarin. Because tumor epithelial cells *in vivo* depend on angiogenesis to provide nutrients for their growth and survival, it is plausible that an anti-angiogenic effect may play a primary role in mediating the cancer chemopreventive activity of silymarin.

In the present study, first, silymarin inhibited endothelial cell growth and survival through induction of apoptosis in a concentration dependent manner (Fig. 1). Because angiogenic factor-stimulated proliferation of endothelial cells is crucial for capillary sprouting, growth inhibition and apoptosis induction can be one

mechanism for silymarin to inhibit angiogenic response. Second, silymarin inhibited endothelial MMP-2 secretion and expression (Fig. 2) and such an effect occurred rapidly prior to the onset of any morphological changes. Because matrilytic activity of angiogenically-stimulated endothelial cells via MMP-2 is another important requirement for capillary sprouting (28–31), the inhibition of MMP-2 secretion and expression by silymarin may provide an inhibitory mechanism on angiogenesis independent of and/or in addition to endothelial growth arrest and apoptosis. Furthermore, silymarin inhibited *in vitro* capillary formation on Matrigel, a process requiring cell-matrix interaction, inter-cellular communications as well as cell motility, to name a few. It was noteworthy that the inhibitory effect on tube formation manifested whether the treatment was initiated simultaneous with seeding cells on the Matrigel (Fig. 3) or when the tubes had preformed (Fig. 4). These results support an anti-
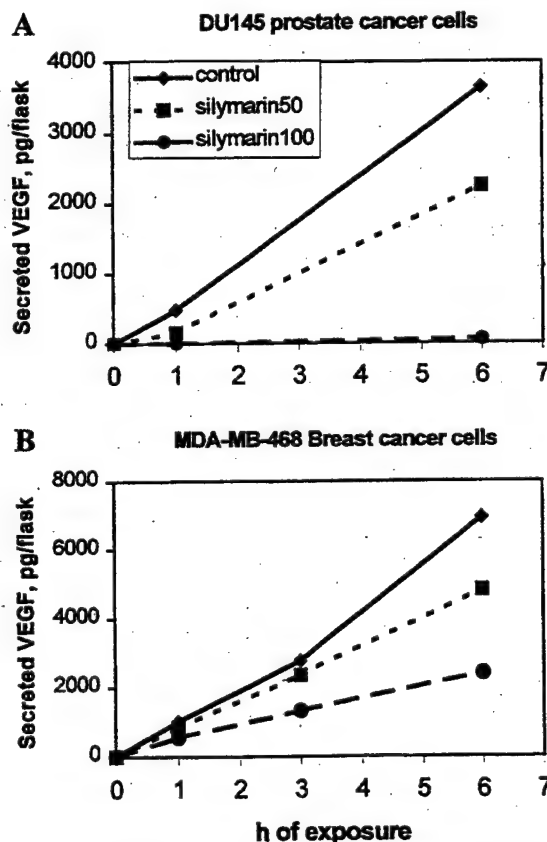


**FIG. 5.** Representative time course of silymarin effects on VEGF secretion by DU145 prostate cancer cells (A) and MDA-MB-468 breast cancer cells (B) in serum-free media. Confluent cells in T25 flasks were treated with solvent vehicle (DMSO/ethanol) or silymarin in 6 ml serum-free medium. At designated time points, 1-ml aliquots of conditioned media were taken for VEGF assay by ELISA. Each data point represents the mean of triplicate measurements. SD < 5% of respective means.

angiogenic potential for silymarin through multifaceted effects on endothelial proliferation and survival and matrix degradation activity and the capillary differentiation process. Work is in progress to further substantiate an anti-angiogenic effect of silymarin in other human endothelial cells in culture and in *in vivo* models.

In addition to these inhibitory effects on endothelial responses and *in vitro* angiogenesis, silymarin also exerted a rapid inhibitory action on the secretion of VEGF by cancer epithelial cells (Table 1 and Fig. 5). VEGF, also known as vascular permeability factor (VPF) (32, 33), plays several critical roles in vasculogenesis as well as angiogenesis. Its expression is so crucial that germ-line knockout of even one VEGF allele leads to embryonic lethality and homozygous knockout embryonic stem cells are incapable of forming tumors (34, 35). Whereas overexpression of VEGF is linked to increased angiogenesis and more aggressive tumor behavior (36, 37), anti-angiogenic interventions based on VEGF antibodies or interference of signal transduction through its receptors (38–42) have been shown to result in the inhibition of tumor growth and induction of endothelial apoptosis. Transformed epithelial cells have been shown to be the major source of VEGF expression in many types of solid cancers (43–46), however, recent data suggest that stromal cells and even vascular endothelial cells may also express VEGF in the hypoxic angiogenic microenvironment of tumors (47). These findings are supported by the observations that certain oncogenic mutations constitutively upregulate VEGF expression (48–51), and that cancer epithelial hypoxia, as a result of dysregulated cellular proliferation (5), is a potent *in vivo* inducer of VEGF expression (52, 53). The inhibitory effect of silymarin on secretion of VEGF in cancer epithelial cells, therefore, may be an important mechanism to negatively regulate the angiogenic switch of avascular lesions, further contributing to the overall control of lesion growth and progression.

The manners by which epithelial VEGF and endothelial MMP-2 were inhibited by silymarin are noteworthy and suggestive of a commonality with regard to the mechanisms of action by silymarin on these secretory proteins. In DU145 and MCF-7 cancer cell lines, silymarin exposure decreased secreted VEGF in the conditioned media without a reduction of cellular VEGF protein level (Table 1). In the MDA-MB468 cell line, exposure at low to intermediate levels of silymarin (25 or 50 µg/ml) decreased secreted VEGF level without lowering the cellular VEGF content, and only at the higher exposure level (100 µg/ml) a reduction of cellular VEGF level was observed (Table 1). This pattern was similarly to that observed for HUVEC MMP-2 expression in that an intermediate level of silymarin exposure (50 µg/ml) significantly decreased secreted MMP-2 level without a change in cellular MMP-2 (Fig.

2). These results from both epithelial and endothelial cells suggest that a primary action of silymarin may involve preferential targeting of the secretion and/or export (exocytosis) of these proteins critical for angiogenic switch regulation. We are currently investigating such mechanisms.

When the results of the present study showing cell death effect of silymarin on HUVEC were compared to those published by us showing anti-proliferative, but not cytotoxic and apoptotic effects, in several different human carcinoma and normal epithelial cells (20–24), it is important to emphasize here that apoptotic effect of silymarin is possibly specific to vascular endothelial cells. Based on these results, there is a possibility that on one hand silymarin is an anti-proliferative and a differentiation-inducing agent for cancer epithelial cells and on the other hand is both an anti-proliferative and an apoptogenic agent for vascular endothelial cells that are involved in neo-vascularization. These dual effects of silymarin possibly make it a useful agent for the prevention and therapy of epithelial cancers in humans.

In summary, this study, for the first time, documents the inhibitory actions of silymarin on several angiogenic responses, including growth and survival, MMP-2 expression and *in vitro* angiogenesis, of vascular endothelial cells as well as an inhibitory effect on the secretion of a primary angiogenic cytokine VEGF by cancer epithelial cells. The anti-angiogenic activity reported in this paper combined with the previously published multi-faceted broad spectrum anti-cancer effects of silymarin support the merit of further investigations to assess and define its cancer chemopreventive and/or therapeutic potential for humans.

## ACKNOWLEDGMENTS

## REFERENCES

1. Folkman, J. (1971) Tumor angiogenesis: Therapeutic implications. *N. Engl. J. Med.* **285,** 1182–1186.

2. Hanahan, D., and Folkman, J. (1996) Patterns and emerging mechanisms of the angiogenic switch during tumorigenesis. *Cell* **86,** 353–364.

3. Zetter, B. R. (1998) Angiogenesis and tumor metastasis. *Annu. Rev. Med.* **49,** 407–424.

4. Sutherland, R. M. (1988) Cell and environment interactions in tumor microregions: The multicell spheroid model. *Science* **240,** 177–184.

5. Brown, J. M., and Giaccia, A. J. (1998) The unique physiology of solid tumors: Opportunities (and problems) for cancer therapy. *Cancer Res.* **58,** 1408–1416.

6. Morse, M. A., and Stoner, G. D. (1993) Cancer chemoprevention: principles and prospects. *Carcinogenesis* **14,** 1737–1746.

7. Perchellet, J.-P., and Perchellet, E. M. (1989) Antioxidants and

multistage carcinogenesis in mouse skin. *Free Radical Biol. Med.* **7**, 377–408.

8. Dragsted, L. O. (1998) Natural antioxidants in chemoprevention. *Arch. Toxicol. Suppl.* **20**, 209–226.

9. Mukhtar, H., and Agarwal, R. (1996) Skin cancer chemoprevention. *J. Invest. Dermatol. Sym. Proc.* **1**, 209–214.

10. Vogel, G., Trost, W., and Braatz, R. (1975) Studies on the pharmacodynamics, including site and mode of action, of silymarin: The antihepatotoxic principle from Silybum mar. (L) Gaertn. *Arzneimittelforsch* **25**, 82–89.

11. Ferenci, P., Dragosics, B., Dittrich, H., *et al.* (1989) Randomized controlled trial of silymarin treatment in patients with cirrhosis of the liver. *J. Hepatol.* **9**, 105–113.

12. Steele, V. E., Kelloff, G. J., Wilkinson, B. P., and Arnold, J. T. (1990) Inhibition of transformation in cultured rat tracheal epithelial cells by potential chemopreventive agents. *Cancer Res.* **50**, 2068–2074.

13. Rudd, C. J., Suing, K. D., Pardo, K., and Kelloff, G. (1990) Evaluation of potential chemopreventive agents using a mouse epidermal cell line, JB6. *Proc. Am. Assoc. Cancer Res.* **31**, 127. [Abstract]

14. Mehta, R. G., and Moon, R. C. (1991) Characterization of effective chemopreventive agents in mammary gland *in vitro* using an initiation-promotion protocol. *Anticancer Res.* **11**, 593–596.

15. Katiyar, S. K., Korman, N. J., Mukhtar, H., and Agarwal, R. (1997) Protective effects of silymarin against photocarcinogenesis in mouse skin model. *J. Natl. Cancer Inst.* **89**, 556–566.

16. Lahiri-Chatterjee, M., Katiyar, S. K., Mohan, R. R., and Agarwal, R. (1999) A flavonoid antioxidant, silymarin, affords exceptionally high protection against tumor promotion in SENCAR mouse skin tumorigenesis model. *Cancer Res.* **59**, 622–632.

17. Zhao, J., Lahiri-Chatterjee, M., Sharma, Y., and Agarwal, R. (1999) Inhibitory effect of a flavonoid antioxidant silymarin on benzoyl peroxide-induced tumor promotion, oxidative stress and inflammatory responses in SENCAR mouse skin. *Carcinogenesis* **21**, 811–816.

18. Agarwal, R., Katiyar, S. K., Lundgren, D. W., and Mukhtar, H. (1994) Inhibitory effect of silymarin, an anti-hepatotoxic flavonoid, on 12-O-tetradecanoylphorbol-13-acetate-induced epidermal ornithine decarboxylase activity and mRNA in SENCAR mice. *Carcinogenesis* **15**, 1099–1103.

19. Zi, X., Mukhtar, H., and Agarwal, R. (1997) Novel cancer chemopreventive effects of a flavonoid antioxidant silymarin: Inhibition of mRNA expression of an endogenous tumor promoter TNFa. *Biochem. Biophys. Res. Commun.* **239**, 334–339.

20. Zi, X., Feyes, D. K., and Agarwal, R. (1998) Anti-carcinogenic effect of a flavonoid antioxidant silymarin in human breast cancer cells MDA-MB 468: Induction of G1 arrest through an increase in Cip1/p21 concomitant with a decrease in kinase activity of CDKs and associated cyclins. *Clin. Cancer Res.* **4**, 1055–1064.

21. Zi, X., Grasso, A. W., Kung, H.-J., and Agarwal, R. (1998) A flavonoid antioxidant silymarin inhibits activation of erbB1 signaling, and induces cyclin-dependent kinase inhibitors, G1 arrest and anti-carcinogenic effects in human prostate carcinoma DU145 cells. *Cancer Res.* **58**, 1920–1929.

22. Ahmad, N., Gali, H., Javed, S., and Agarwal, R. (1998) Skin cancer chemopreventive effects of a flavonoid antioxidant silymarin are mediated via impairment of receptor tyrosine kinase signaling and perturbation in cell cycle progression. *Biochem. Biophys. Res. Commun.* **247**, 294–301.

23. Zi, X., and Agarwal, R. (1999) Silibinin decreases prostate-specific antigen with cell growth inhibition via G1 arrest, leading to differentiation of prostate carcinoma cells: Implications for prostate cancer intervention. *Proc. Natl. Acad. Sci. USA* **96**, 7490–7495.

24. Zi, X., and Agarwal, R. (1999) Modulation of mitogen-activated protein kinase activation and cell cycle regulators by the potent skin cancer preventive agent silymarin. *Biochem. Biophys. Res. Commun.* **263**, 528–536.

25. Jiang, C., Jiang, W., Ip, C., Ganther, H., and Lu, J. (1999) Selenium-induced inhibition of angiogenesis in mammary cancer at chemopreventive levels of intake. *Mol. Carcinogenesis* **26**, 213–225.

26. Thaloor, D., Singh, A. K., Sidhu, G. S., Prasad, P. V., Kleinman, H. K., and Maheshwarim, R. K. (1998) Inhibition of angiogenic differentiation of human umbilical vein endothelial cells by curcumin. *Cell Growth Differ.* **9**, 305–312.

27. Kubota, Y., Kleinman, H. K., Martin, G. R., and Lawley, T. J. (1988) Role of laminin and basement membrane in the morphological differentiation of human endothelial cells into capillary-like structures. *J. Cell Biol.* **107**, 1589–1598.

28. Coussens, L. M., and Werb, Z. (1996) Matrix metalloproteinases and the development of cancer. *Chem. Biol.* **3**, 895–904.

29. Itoh, T., Tanioka, M., Yoshida, H., Yoshioka, T., Nishimoto, H., and Itohara, S. (1998) Reduced angiogenesis and tumor progression in gelatinase A-deficient mice. *Cancer Res.* **58**, 1048–1051.

30. Deryugina, E. I., Bourdon, M. A., Reisfeld, R. A., and Strongin, A. (1998) Remodeling of collagen matrix by human tumor cells requires activation and cell surface association of matrix metalloproteinase-2. *Cancer Res.* **58**, 3743–3750.

31. Hiraoka, N., Allen, E., Apel, I. J., Gyetko, M. R., and Weiss, S. J. (1998) Matrix metalloproteinases regulate neovascularization by acting as pericellular fibrinolysins. *Cell* **95**, 365–377.

32. Leung, D. W., Cachianes, G., Kuang, W. J., Goeddel, D. V., and Ferrara, N. (1989) Vascular endothelial growth factor is a secreted angiogenic mitogen. *Science* **246**, 1306–1309.

33. Keck, P. J., Hauser, S. D., Krivi, G., *et al.* (1989) Vascular permeability factor, an endothelial cell mitogen related to PDGF. *Science* **246**, 1309–1312.

34. Ferrara, N., Carver-Moore, K., Chen, H., *et al.* (1996) Heterozygous embryonic lethality induced by targeted inactivation of the VEGF gene. *Nature* **380**, 439–442.

35. Carmeliet, P., Ferreira, V., Breier, G., *et al.* (1996) Abnormal blood vessel development and lethality in embryos lacking a single VEGF allele. *Nature* **380**, 435–439.

36. Zhang, H. T., Craft, P., Scott, P. A., *et al.* (1995) Enhancement of tumor growth and vascular density by transfection of vascular endothelial cell growth factor into MCF-7 human breast carcinoma cells. *J. Natl. Cancer Inst.* **87**, 213–219.

37. McLeskey, S. W., Tobias, C. A., Vezza, P. R., Filie, A. C., Kern, F. G., and Hanfelt, J. (1998) Tumor growth of FGF or VEGF transfected MCF-7 breast carcinoma cells correlates with density of specific microvessels independent of the transfected angiogenic factor. *Am. J. Pathol.* **153**, 1993–2006.

38. Borgstrom, P., Hillan, K. J., Sriramarao, P., and Ferrara, N. (1996) Complete inhibition of angiogenesis and growth of microtumors by anti-vascular endothelial growth factor neutralizing antibody: Novel concepts of angiostatic therapy from intravital videomicroscopy. *Cancer Res.* **56**, 4032–4039.

39. Borgstrom, P., Bourdon, M. A., Hillan, K. J., Sriramarao, P., and Ferrara, N. (1998) Neutralizing anti-vascular endothelial growth factor antibody completely inhibits angiogenesis and growth of human prostate carcinoma micro tumors in vivo. *Prostate* **35**, 1–10.

40. Meeson, A. P., Argilla, M., Ko, K., Witte, L., and Lang, R. A. (1999) VEGF deprivation-induced apoptosis is a component of programmed capillary regression. *Development* **126**, 1407–1415.

41. Benjamin, L. E., Golijanin, D., Itin, A., Pode, D., and Keshet, E.

(1999) Selective ablation of immature blood vessels in established human tumors follows vascular endothelial growth factor withdrawal. *J. Clin. Invest.* **103,** 159–165.

42. Benjamin, L. E., and Keshet, E. (1997) Conditional switching of vascular endothelial growth factor (VEGF) expression in tumors: Induction of endothelial cell shedding and regression of hemangioblastoma-like vessels by VEGF withdrawal. *Proc. Natl. Acad. Sci. USA* **94,** 8761–8766.

43. Guidi, A. J., Abu-Jawdeh, G., Tognazzi, K., Dvorak, H. F., and Brown, L. F. (1996) Expression of vascular permeability factor (vascular endothelial growth factor) and its receptors in endometrial carcinoma. *Cancer* **78,** 454–460.

44. Guidi, A. J., Schnitt, S. J., Fischer, L., *et al.* (1997) Vascular permeability factor (vascular endothelial growth factor) expression and angiogenesis in patients with ductal carcinoma in situ of the breast. *Cancer* **80,** 1945–1953.

45. Abu-Jawdeh, G. M., Faix, J. D., Niloff, J., *et al.* (1996) Strong expression of vascular permeability factor (vascular endothelial growth factor) and its receptors in ovarian borderline and malignant neoplasms. *Lab Invest.* **74,** 1105–1115.

46. Brown, L. F., Berse, B., Jackman, R. W., *et al.* (1995) Expression of vascular permeability factor (vascular endothelial growth factor) and its receptors in breast cancer. *Hum. Pathol.* **26,** 86–91.

47. Fukumura, D., Xavier, R., Sugiura, T., *et al.* (1998) Tumor induction of VEGF promoter activity in stromal cells. *Cell* **94,** 715–725.

48. Rak, J., Mitsuhashi, Y., Bayko, L., *et al.* (1995) Mutant ras oncogenes upregulate VEGF/VPF expression: Implications for induction and inhibition of tumor angiogenesis. *Cancer Res.* **55,** 4575–4580.

49. Grugel, S., Finkenzeller, G., Weindel, K., Barleon, B., and Marme, D. (1995) Both v-Ha-Ras and v-Raf stimulate expression of the vascular endothelial growth factor in NIH 3T3 cells. *J. Biol. Chem.* **270,** 25915–25919.

50. Mazure, N. M., Chen, E. Y., Yeh, P., Laderoute, K. R., and Giaccia, A. J. (1996) Oncogenic transformation and hypoxia synergistically act to modulate vascular endothelial growth factor expression. *Cancer Res.* **56,** 3436–3440.

51. Arbiser, J. L., Moses, M. A., Fernandez, C. A., *et al.* (1997) Oncogenic H-ras stimulates tumor angiogenesis by two distinct pathways. *Proc. Natl. Acad. Sci. USA* **94,** 861–866.

52. Forsythe, J. A., Jiang, B. H., Iyer, N. V., *et al.* (1996) Activation of vascular endothelial growth factor gene transcription by hypoxia-inducible factor 1. *Mol. Cell. Biol.* **16,** 4604–4613.

53. Damert, A., Ikeda, E., and Risau, W. (1997) Activator-protein-1 binding potentiates the hypoxia-inducible factor-1-mediated hypoxia-induced transcriptional activation of vascular-endothelial growth factor expression in C6 glioma cells. *Biochem. J.* **327**(Pt 2), 419–423.

*Lu7*

# Antiangiogenic Activity of Selenium in Cancer Chemoprevention: Metabolite-Specific Effects

## Junxuan Lu and Cheng Jiang

*Abstract: We review recent data that support a potential antiangiogenic effect of selenium (Se) in the chemoprevention of cancer and data that contrast two pools of Se metabolites, namely, methylselenol vs. hydrogen selenide, that differentially affect proteins and cellular processes crucial to tumor angiogenesis regulation. With regard to tumor angiogenesis, the chemopreventive effect of increased Se intake on chemically induced mammary carcinogenesis has been associated with reduced intratumoral microvessel density and an inhibition of the expression of vascular endothelial growth factor. The in vitro data show that monomethyl Se potently inhibits cell cycle progression of vascular endothelial cells to the S phase, endothelial expression of matrix metalloproteinase-2, and cancer epithelial expression of vascular endothelial growth factor with concentrations giving half-maximal inhibition that are within the plasma range of Se in US adults. The methyl Se-specific activities may therefore be physiologically pertinent for angiogenic switch regulation in early lesions in vivo in the context of cancer chemoprevention, which aims at retarding and blocking the growth and progression of early lesions. We argue for the antiangiogenic action of Se, especially the methyl Se pool of metabolites, as a primary mechanism for preventing avascular lesion growth. Contrary to the currently held paradigm, we speculate that there is a potential role for selenoproteins in regulating the growth and fate of transformed epithelial cells.*

## Introduction

The micronutrient selenium (Se) has long been implicated to have an anticancer potential by epidemiological and laboratory studies. The landmark cancer prevention trial by Larry Clark, Gerald Combs, Jr., and co-workers demonstrated for the first time that an Se supplement (200 µg/day) provided as selenized yeast (Se-yeast) to a skin cancer patient population otherwise adequate in Se nutrition might be a safe and effective preventive agent for several major human epithelial cancers, including those of the prostate, lung, and colon, while lacking protective activity against second primary skin cancer (Ref. 1 and updates in this issue). A community-scale intervention study and a small-scale clini-

cal trial in China also indicated preventive efficacy of Se against liver cancer (2). Encouraged by these results, two new clinical trials sponsored by the National Cancer Institute have begun recruiting patients to verify the preventive efficacy of Se-yeast or its major constituent selenomethionine for prostate cancer (Southwest Oncology Group, SWOG Protocol S0000) and lung cancer (Eastern Cooperative Oncology Group, ECOG Protocol E5597). A better understanding of the mechanisms through which Se exerts anticancer activity will be important for helping to interpret the outcomes of these new "definitive" trials and to develop safer and more effective Se agents for cancer prevention, especially in organ site-specific manners. At this crucial juncture of Se translation research, this special issue as a fitting tribute to Larry Clark for his pioneering work provides a timely review and synthesis of the status of the field and a forum to discuss and define future directions.

On a personal note, one of us ("Johnny" Lu) became acquainted with Larry Clark in 1984 at Cornell University as a fresh graduate student of Jerry Combs. Johnny even helped translate some materials from Chinese scientific literature when data were being gathered to support the landmark Se trial (1) as we know it today. While working on zinc toxicity for his Ph.D. degree, Johnny witnessed a lot of human plasma samples being analyzed for Se in Jerry's laboratory for that trial although, at the time, without much appreciation of the significance of the undertaking. That changed significantly after he embarked on a cancer research career. He holds great respect and admiration for the leadership and perseverance of Larry and his collaborators for bringing that trial to fruition and for the determination and courage displayed by Larry for continuing to push for additional Se trials even when he was dying of prostate cancer. In honor of Larry's memory, we review our recent work on Se and angiogenesis regulation as a potential novel mechanism of cancer prevention by Se.

## Known "Mechanisms" of Se Anticancer Activity

Even though, for convenience reasons, the anticancer potential of Se is often described in terms of the element, a vast

literature base indicates that it is expressed as a function of the dose and chemical form in which the element resides, not elemental Se per se (3,4). With respect to "mechanisms," a number of them have been investigated: antioxidant protection (via SeCys-glutathione peroxidases), altered carcinogen metabolism, enhanced immune surveillance, cell cycle effects, enhanced apoptosis (3,4), and, more recently, inhibition of neoangiogenesis (5,6). The mechanisms that are actually involved in cancer prevention by Se will likely depend on the dose and form of Se compounds, the Se status of the individual, perhaps the type and etiology of malignancy, and even the organ sites. It is probable that Se supplementation of individuals with relatively low or frankly deficient Se intakes can be expected to support enhanced antioxidant protection as a result of increased expression of the SeCys enzymes or enhanced immune surveillance (4).

On the other hand, in the trial of Clark et al. (1) and in animal models (3,4), cancer-preventive effects have been observed at Se intakes that are more than sufficient to correct nutritional deficiency. That is, Se appears to be antitumorigenic at intake levels that are substantially higher than those associated with maximal expression of the known SeCys-containing glutathione peroxidase enzymes (3,4). In this context of cancer chemoprevention, methylselenol or related monomethyl Se species have been implicated as a candidate in vivo active metabolite pool (3,7,8). We and others have used cell culture models to seek a better understanding of how the different pools of Se inhibit survival of tumor cells through apoptosis induction (9–12). This aspect of the work has been reviewed recently (13). [For additional information related to apoptosis induction, see pertinent articles in this issue and our recent work documenting caspase-dependent apoptosis execution pathways induced by the methyl Se pool (14).]

We focus on the regulation of angiogenesis by Se, especially by specific Se metabolite pools in cancer prevention. We limit the scope of discussion to those forms of Se that feed into the genotoxic hydrogen selenide pool or the nongenotoxic methylselenol pool of Se metabolites (Fig. 1) (6,13). There is no literature documentation on the antiangiogenic attributes of other Se forms, such as synthetic aromatic organo-Se compounds. We review pertinent data that support methylselenol-specific inhibitory activities on angiogenic switch mechanisms in vascular endothelial cells [endothelial mitogenesis and matrix metalloproteinase (MMP) expression] and in the tumor epithelial cells (angiogenic cytokine expression) (Fig. 1). We discuss a model of cancer prevention by Se based on the interaction of epithelial lesions and the vasculature that supports such lesions.

## Angiogenesis Is Obligatory for Carcinogenesis

Carcinogenesis is a multistep process of tumor initiation, promotion, progression, and metastasis. Human cancers likely involve a gradual accumulation of genetic and epigenetic changes over a period of decades. Because cancer
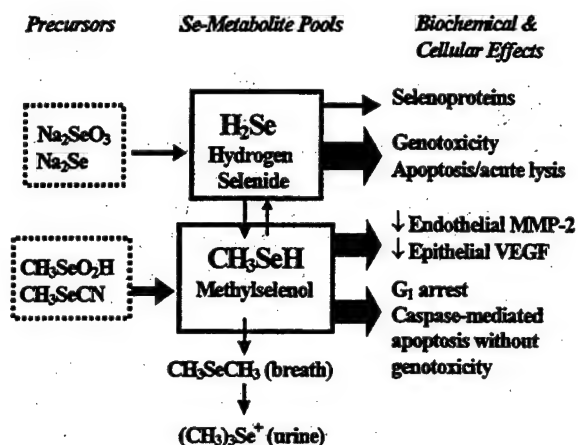


Figure 1. Schematic relationship of Se precursors feeding into genotoxic hydrogen selenide pool or nongenotoxic methylselenol pool of metabolites that exert distinct biochemical and cellular effects. Inhibitory activities by methylselenol pool on protein molecules and cellular processes relevant to angiogenesis support Se metabolite-specific mechanisms for angiogenic switch control (6). Genotoxicity (or lack of) effect of the 2 Se pools was based on studies with mammary cancer epithelial cells and leukemia cells (13). $CH_3SeO_2H$, methylseleninic acid; $CH_3SeCN$, methylselenocyanate; MMP-2, matrix metalloproteinase-2; VEGF, vascular endothelial growth factor. (Modified from Refs. 6 and 13.)

initiation is arguably inevitable, the major thrust of prevention research in animal tumor models and in clinical cancer trials has been on targeting promotion and progression stages. Angiogenesis, i.e., the process of formation of new microvessels from existing vessels, is a critical and obligatory component of promotion, progression, and metastasis of solid cancers, most of which are of epithelial origin (15–18). At the onset of solid tumor genesis, initiated cells undergo clonal expansion in an avascular state, because the expanding lesions are small enough to take in nutrients and to expel metabolic wastes by diffusion. However, diffusion is not sufficient to support any continued growth of the lesion beyond a certain physical size (estimated to be a few $mm^3$), because the expanding lesions consume nutrients at a rate proportional to their volume, whereas the supply of nutrients is delivered at a rate proportional to their surface area. It has been estimated that such "dormant" avascular lesions exist in high prevalence in organs of asymptomic adults. In order for lesions to grow beyond this size limit imposed by simple diffusion, they must turn on their angiogenic switch (15–17) to form neovasculature to provide the necessary nutrients and factors and remove metabolite wastes. Therefore, tumor angiogenic switch control can provide a logical and attractive target for the chemoprevention of cancer.

## Angiogenesis Is Regulated Through Epithelial and Endothelial Compartments

Angiogenesis in solid epithelial tumors is controlled through at least two principal cell compartments: the transformed epithelial cells, which serve as a main source of angiogenic factors, and the vascular endothelial cells, which

constitute the targets for the angiogenic signals (15–18). On the tumor cell side, the production of angiogenic stimulatory cytokines by cancer epithelial cells is a major means of controlling the angiogenic switch. Most prominent among the positive factors is vascular endothelial growth factor (VEGF)/vascular permeability factor (19,20). Cancer epithelial cells are the main source of VEGF expression (21–25), although recent data indicate that other cell types can also express it in a tumorigenic environment (26). VEGF plays a crucial role in vasculogenesis and angiogenesis, since in germ-line knockout experiments, a loss of even one VEGF allele leads to the abnormal formation of intra- and extraembryonic vessels and embryonic lethality, indicating a tight dose-dependent regulation of embryonic vessel development by VEGF (27,28). Furthermore, VEGF-null embryonic stem cells exhibit a dramatically reduced ability to form tumors in nude mice (28). Whereas overexpression of VEGF is linked to increased angiogenesis and more aggressive tumor behavior (29,30), antiangiogenic interventions, especially those based on VEGF antibodies or interference of signal transduction through its receptors (31–35), have been shown to result in the inhibition of tumor growth and induction of endothelial apoptosis. Because hypoxia is common in avascular lesions (36) and because hypoxia (37) and certain oncogenic mutations (38–41) and autocrine or paracrine growth factors in the tumor (42–44) are potent inducers of its expression, VEGF is a probable primary stimulator for the angiogenic switch in early lesions, which are the likely responsive targets of chemoprevention.

On the vascular side, the endothelial cells respond to angiogenic stimulation through three key processes (15–17): 1) increased expression and secretion of MMPs (45) to break down the outer sheath and extracellular matrix of existing vessels for the endothelial cells to sprout through, 2) increased cell motility for remodeling and invasion during the sprouting process, and 3) mitogenic signaling leading to cell cycle entry and cell division to provide the number of cells necessary for elongating the new sprout. The crucial role of specific MMPs, such as MMP-2, in tumor angiogenesis has been documented using knockout as well as other model approaches (46,47). Inhibiting one or more of these processes can negatively impact the endothelial response(s) to a given angiogenic signal. As discussed below, methylselenol precursors inhibit with significant potency the endothelial expression of MMP-2, its mitogenesis stimulated by angiogenic factors, and its survival via caspase-mediated apoptosis.

## In Vivo Findings

### Antiangiogenic Activity Was Associated With Mammary Cancer Prevention by Se

We recently initiated work to explore the hypothesis that Se may exert cancer-chemopreventive activity, at least in part, through an antiangiogenic mechanism (5). In a chemoprevention setting, Se (3 ppm) as Se-garlic (*experiment 1*) or selenite (*experiment 2*) was fed for ~2 mo to Sprague-Dawley rats that were given a single intraperitoneal injection of methylnitrosourea to initiate mammary carcinogenesis 1 wk earlier. The microvessels in the mammary tumors were visualized with immunohistochemical staining for factor VIII, and the microvessel number (counts/0.5 mm², 10 fields) in "hot-spot" stromal areas was counted. Mammary carcinomas in the Se-fed rats was 34% (*experiment 1*) and 24% (*experiment 2*) lower than in rats fed the control diet (Table 1). When categorized by the size of the microvessels, the reduction of microvessel density in the Se-fed groups was almost exclusively confined to the small microvessels (1–4 cells in diameter). The microvessel density of the uninvolved mammary glands was not decreased by Se-garlic treatment (Table 1). Similar results were obtained when established

**Table 1.** Effects of a Chemopreventive Level of Dietary Se as Se-Garlic or Selenite on Microvessel Density of NMU-Induced Rat Mammary Carcinomas and Noninvolved Mammary Glands[a,b]

| | n | Density, counts/0.5 mm² | | | |
| --- | --- | --- | --- | --- | --- |
| | | Large vessels | Medium vessels | Small vessels | Total vessels |
| *Experiment 1* | | | | | |
| Carcinomas | | | | | |
| Control | 9 | 5 ± 1 | 10 ± 1 | 55 ± 6 | 69 ± 6 |
| Se-garlic | 6 | 3 ± 1 | 8 ± 2 | 35 ± 6* | 46 ± 6* |
| Mammary glands | | | | | |
| Control | 6 | 1.8 ± 0.5 | 2.7 ± 0.4 | 4.2 ± 0.8 | 8.7 ± 0.7 |
| Se-garlic | 6 | 1.3 ± 0.4 | 2.0 ± 0.7 | 3.8 ± 0.6 | 7.2 ± 0.9 |
| *Experiment 2* | | | | | |
| Carcinomas | | | | | |
| Control | 8 | 0.9 ± 0.4 | 4 ± 2 | 75 ± 5 | 80 ± 4 |
| Selenite | 4 | 0.3 ± 0.3 | 4 ± 3 | 57 ± 2* | 61 ± 3* |

*a:* Values are means ± SE. Vessels are classified as follows: >9 cells in diameter (large), 5–9 cells in diameter (medium), and 1–4 cells in diameter (small). NMU, 1-methyl-1-nitrosourea. Data are from Ref. 5.
*b:* Statistical significance is as follows: *, significantly different from control, P < 0.05.

mammary carcinomas were treated acutely through bolus doses of Se (5). These results indicated a potential anti-angiogenic effect of chemopreventive intake of Se and that the effect was neoplasia specific. Because growing and newly sprouted microvessels are likely to be smaller, the observed reduction of small vessels by Se treatments indicated that a mechanism(s) governing the genesis of new vessels might be inhibited.

### Se Decreased Expression of VEGF in Some Carcinomas

The expression level of VEGF in mammary carcinomas was measured by Western blot analyses (5). On the basis of the limited number of samples analyzed, two of five carcinomas in the Se-garlic group and two of four carcinomas in the selenite group showed a marked reduction in VEGF expression to almost nondetectable levels. These results indicated that VEGF downregulation might be involved in some, but not all, tumors. Similar to the chemoprevention setting, acute Se treatment of established mammary carcinomas showed a marked reduction of VEGF expression in some, but not all, treated carcinomas (5).

### In Vitro Metabolite-Specific Antiangiogenic Attributes

To define the mechanisms underlying the antiangiogenic activity of chemopreventive levels of Se intake, we have examined the effects of direct Se exposure in cell culture on the expression of VEGF by cancer epithelial cells, the expression of MMP-2 in human umbilical vein endothelial cells (HUVECs) (6), and the mitogenesis and survival of HUVECs (48). A number of methylselenol precursors, including methylseleninic acid (MSeA) and methylselenocyanate (MSeCN), were used to enrich the methylselenium (methyl Se) pool in vitro. The results suggest a methyl-selenol-specific inhibition of the angiogenic switch mechanisms through multiple processes.

### Methyl Se-Specific Inhibitory Effect on VEGF Expression

We recently showed that brief exposure of human DU 145 prostate cancer cells to increasing concentrations of MSeA decreased both cellular (Fig. 2A) and secreted VEGF levels in an Se concentration-dependent manner (6), with the concentration resulting in half-maximal inhibition ($IC_{50}$) of ~2 µM, which is within range of plasma Se concentration in most US residents (mean ~1.5 µM) (1). The inhibitory effect of MSeA on VEGF expression was independent of serum level in the medium and the confluence status of the cells and was detectable within 2 h of exposure (Fig. 2B). In contrast, exposure to selenite in the same dose range or higher did not decrease VEGF expression.

Longer exposure of DU 145 cells to MSeA or sodium selenite above some threshold levels led to apoptosis as indicated by DNA nucleosomal fragmentation (Fig. 2C). The inhibitory effect of MSeA on VEGF expression was ob-



**A. DU-145 cellular VEGF, 6 h**
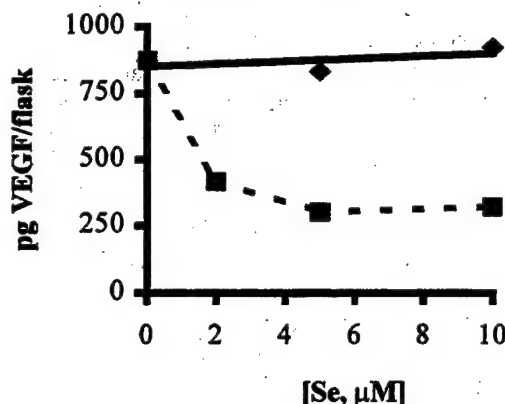
**B. Time course, secreted**
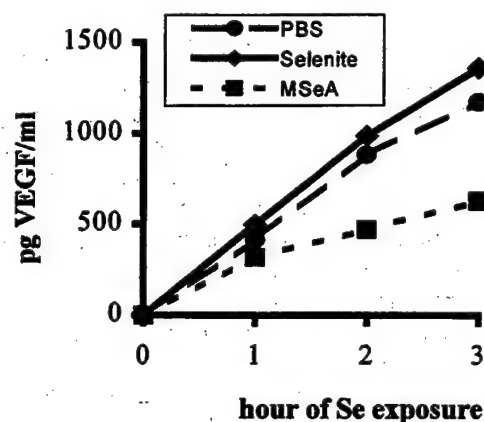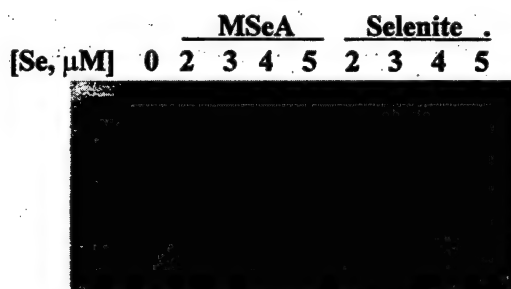
**C. DNA fragmentation at 24 h**

Figure 2. A: concentration-dependent effects of methylseleninic acid (MSeA, squares) and selenite (diamonds) on VEGF protein levels in DU 145 prostate carcinoma cell lysate after 6 h of exposure in serum-rich medium. Secreted VEGF in conditioned medium had similar response curves. B: acute time course of effects of exposure to Se as MSeA (5 µM, squares) or as sodium selenite (10 µM, diamonds) on VEGF expression in DU 145 cells. In these short-term exposure experiments, near-confluent DU 145 cells were treated with Se in 10% fetal bovine serum medium. Treatment in serum-free medium showed identical patterns of responses. VEGF was assayed with an enzyme-linked immunosorbent assay kit (R & D Systems, Minneapolis, MN). C: DNA nucleosomal fragmentation assay as an apoptosis marker after 24 h of exposure to MSeA or selenite (adherent and detached cells were combined for DNA extraction). (Modified from Ref. 6.)

served at a concentration (2 µM) that was twofold lower than that needed to induce significant apoptosis (≥ 4 µM). Chronic exposure of DU 145 cells to low-level MSeA mimicking a daily supplement regimen indicated a sustained inhibition of VEGF expression (6). Although selenite and MSeA were almost equipotent for inducing DNA apoptotic fragmentation (Fig. 2C), selenite did not inhibit VEGF expression by acute or chronic exposure. In support of the generality of this methyl Se-inhibitory effect on VEGF expression, two human breast cancer cell lines (MCF-7 and MDA-MB-468) showed the same Se metabolite specificity of inhibition irrespective of the serum level in the treatment medium (6). Taken together, these data support a primary and sustained methyl Se-specific inhibitory activity of serum-achievable Se on the expression of VEGF in cancer epithelial cells independently of cell death induction.

## Methyl Se-Specific Inhibition of Endothelial MMP-2 Expression

As documented recently (6), treatment of HUVECs for 6 h with MSeA led to a concentration-dependent reduction of the secreted 72-kDa MMP-2 gelatinolytic activity in the conditioned medium (Fig. 3A). The inhibitory efficacy was remarkable, with an $IC_{50}$ of ~2 µM. Similarly, treatment with MSeCN resulted in a concentration-dependent decrease of MMP-2, and the inhibitory efficacy was comparable to that of MSeA (Fig. 3A). In contrast, treatment with hydrogen selenide precursors (up to 20 µM sodium selenite or 50 µM sodium selenide) did not significantly decrease MMP-2 in the conditioned medium (Fig. 3A).

Incubation of HUVEC-conditioned medium (containing secreted MMP-2) with all four Se forms in the test tube for 6 h at 37°C did not decrease the gelatinolytic activity (Fig. 3B), indicating that MSeA or MSeCN per se did not react directly with MMP-2 protein to inactivate its activity. The inhibitory action of these methylselenol precursor compounds was, therefore, dependent on cellular metabolism. Western blot analyses for the MMP-2 protein level in conditioned medium of HUVECs treated with MSeA indicated that a reduction in the MMP-2 protein level closely paralleled the observed loss of MMP-2 gelatinolytic activity (Fig. 3C), whereas selenite treatment had a minimal effect on the gelatinolytic activity and the MMP-2 protein level (Fig. 3C). The inhibitory effect of MSeA on MMP-2 was rather rapid, in that ~50% reduction was detected within 30 min of exposure (Fig. 3D). Together, these results indicate that methylselenol or its related monomethyl metabolites in the serum-achievable range ($IC_{50}$ ~2 µM) exert a rapid inhibitory effect on MMP-2 expression in vascular endothelial cells.

## Methyl Se Potently Inhibited Angiogenic Factor-Driven Mitogenesis of Endothelial Cells Independently of Apoptosis Induction

We recently used a synchronized HUVEC model to more sensitively define the effect of methyl Se on angiogenic factor-stimulated mitogenesis (48). The bovine pituitary extract

endothelial cell growth supplement (ECGS) was omitted from the complete medium for >48 h to arrest cells in the $G_0/G_1$ phase. Resumption of ECGS stimulation resulted in a >10-fold incorporation of [³H]thymidine within 24 h (Fig. 4A). MSeA treatment that was initiated 3 h before or simultaneously with ECGS stimulation decreased the ECGS-stimulated DNA synthesis dose dependently with an $IC_{50}$ of ~1 µM and completely blocked this parameter at 3 µM (Fig. 4A). The potent antimitogenic activity was independent of apoptosis induction, which required >5 µM MSeA after 30 h of exposure, as indicated by caspase-mediated cleavage of poly(ADP-ribose) polymerase and DNA fragmentation, both being biochemical hallmarks of apoptosis (Fig. 4B).

## Summary and Discussion

The data reviewed above support a potential antiangiogenic activity of Se in vivo (5) and, furthermore, clearly contrast the differential effects of methylselenol vs. hydrogen selenide pools on multiple aspects of angiogenesis regulation (6). The in vitro data show that methyl Se potently inhibits ECGS-induced cell cycle progression of vascular endothelial cells to the S phase ($IC_{50}$ ~1 µM). In addition, methyl Se exerts an inhibitory activity on endothelial expression of MMP-2 ($IC_{50}$ ~2 µM) and on epithelial expression of VEGF ($IC_{50}$ ~2 µM). As reference values, the mean plasma Se concentration of subjects without Se supplementation in the trial of Clark et al. (1) was ~1.5 µM, and Se supplementation (200 µg/day as selenized yeast) brought the mean Se level to ~2.4 µM. Therefore, the methyl Se-specific antimitogenic activity and inhibitory activities on VEGF and MMP-2 proteins may be physiologically very pertinent for angiogenic switch regulation in early transformed lesions in vivo in the context of cancer chemoprevention, which aims at retarding and blocking the growth and progression of early lesions. Our data also show that methyl Se can induce apoptosis of vascular endothelial cells through caspase-mediated execution, but such a proapoptotic effect may be relevant only in a pharmacological context of Se exposure.

## Integrating Endothelial and Epithelial Mechanisms for Cancer Prevention by Se

Before our work that was reviewed here, much mechanistic research had focused on how Se affected the cancer epithelial cells through antiproliferative and proapoptotic pathways (3,13). Because epithelial lesions do not exist in isolation in vivo but, instead, intimately interact with the stroma and vasculature, cancer prevention function is likely achieved through integrating the actions of Se on epithelial as well as nonepithelial targets. The physiochemistry of Se delivery to transformed epithelial cells in in vivo lesions may be a major determinant of the actual mechanism(s) as well as the processes that are invoked to regulate the growth and fate of the solid lesion. To this end, we speculated earlier (13) that Se delivery to epithelial cells in the avascular le-
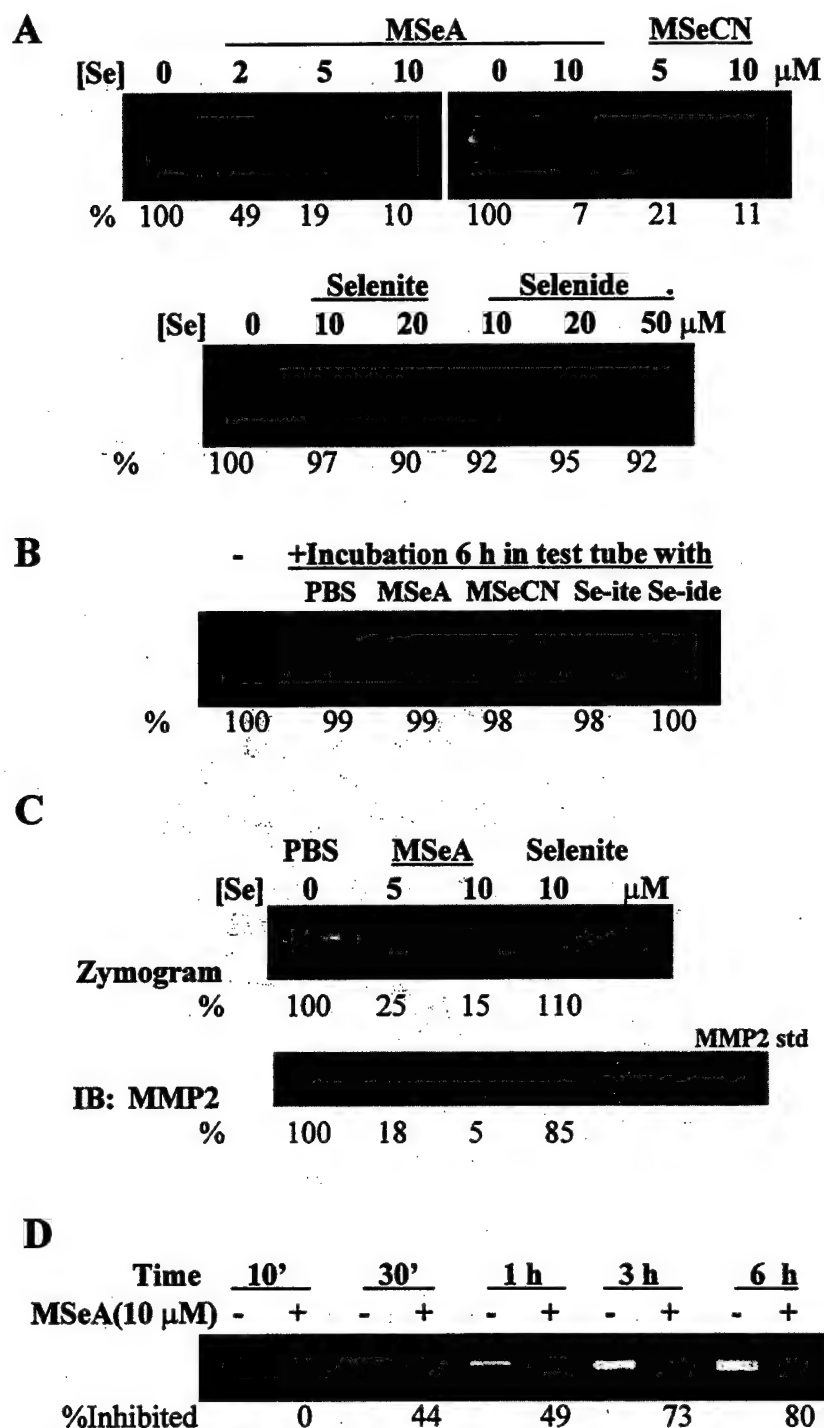
**Figure 3.** A: inhibitory specificity of selenium forms on human umbilical vein endothelial cell (HUVEC) MMP-2. Representative gelatin substrate gel zymographic analyses of MMP-2 were carried out in conditioned media of HUVECs treated for 6 h (in separate experiments) with MSeA, methylselenocyanate (MSeCN), sodium selenite, or sodium selenide in serum-free medium supplemented with endothelial cell growth supplement (ECGS, 100 µg/ml). Relative pixel density as percentage of control cells is shown below each lane. B: lack of MMP-2 inactivation by direct incubation of HUVEC-conditioned medium with Se compounds in test tubes at 37°C for 6 h. Each Se was added to 10 µM. C: immunoblot (IB) analyses of MMP-2 protein in conditioned media. HUVECs were treated with MSeA or selenite for 3 h. Aliquots of conditioned media were analyzed by zymography for gelatinolytic activity. Bulk of conditioned media was concentrated ~50-fold using Centricon spin filters and analyzed by Western blot. Pro-MMP-2 protein (10 ng) was used as standard. D: time course of MSeA (10 µM)-induced inhibition of MMP-2 expression in HUVECs. Aliquots of media taken at various time points were analyzed by zymography. Percent inhibition relative to phosphate-buffered saline (PBS)-treated control at each time point is shown below treated lanes. (Modified from Ref. 6.)
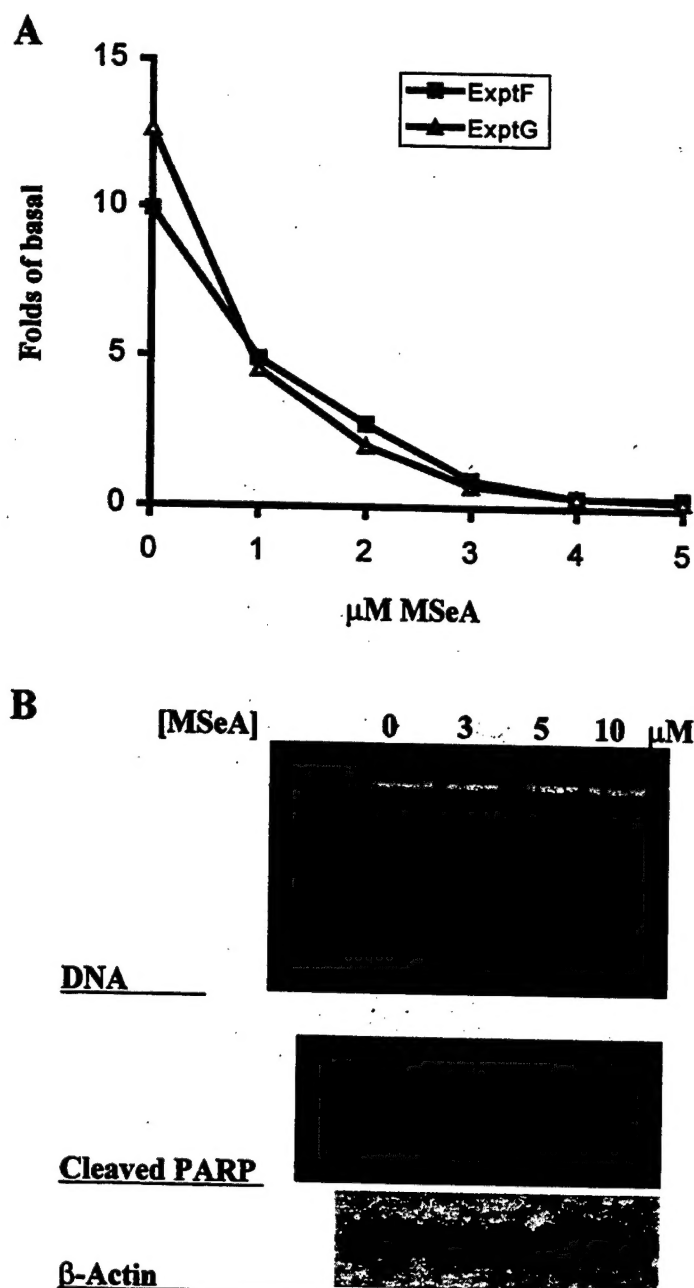
**Figure 4.** A: inhibitory effect of MSeA on ECGS-stimulated [³H]thymidine incorporation into DNA of synchronized HUVECs. [³H]thymidine was added at time of treatments with ECGS for 30 h. In *experiment F*, MSeA was added simultaneously with ECGS. In *experiment G*, MSeA was added 3 h before ECGS. B: biochemical markers of apoptosis. Detached and adherent cells were used for DNA extraction and for detection of cleaved poly(ADP-ribose) polymerase (PARP) in MSeA-exposed HUVECs by Western blot. β-Actin was reprobed to indicate evenness of loading of protein extract from each treatment.

sions may follow a concentration gradient similar to oxygen tension, which has been known to decline precipitously as the distance to the nearby microvessel increases, resulting in a hypoxic state in the interior of such lesions (36) (Fig. 5A). Should such a declining gradient exist for Se, a "conditional Se deficiency" state may be created inside, expanding microscopic avascular epithelial lesions even when the Se supply is sufficient to saturate selenoprotein activities in the serum or normal tissues.

This model predicts that more Se is required to enrich Se metabolite pools within the avascular lesions in order to elicit antimitogenic and proapoptotic pathways in the transformed epithelial cells. Furthermore, more Se is required to support the activity of key selenoproteins such as thioredoxin reductases and Se-glutathione peroxidases in cells within the epithelial lesions so as to reregulate their transformation status/physiology. This model may warrant a reevaluation of the current paradigm that discounts the likelihood of involvement of Se-glutathione peroxidases and other selenoproteins for the chemopreventive activity of Se (3,4). Consistent with this speculation, the prostate cancer-preventive effect of 200 µg of Se as Se-yeast in the trial of Clark
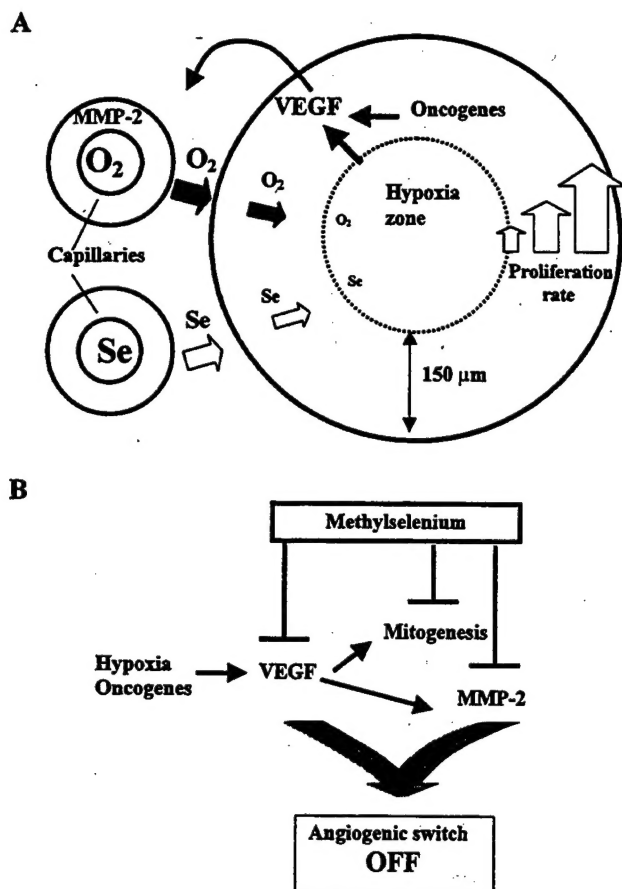
**A**

**B**

**Figure 5.** A: a hypothetical model of Se delivery to epithelial cells within an avascular lesion analogous to oxygen diffusion. A conditional Se deficiency is speculated in cells that are also hypoxic. Increased VEGF expression due to hypoxia and oncogenic mutations may be a primary stimulatory signal for angiogenesis switch in early lesions. B: methylselenol-specific inhibitory effects on angiogenic switch. In vitro data support an inhibition of cancer epithelial expression of VEGF, endothelial mitogenesis, and MMP-2 expression, turning off the switch.

et al. appeared to be most prominent in patients with entry plasma Se in the lowest tertile (49).

This model also highlights the need for investigations that incorporate hypoxia as a feature of the solid lesions in evaluation of the efficacy of Se to induce growth arrest and cell death responses as well as angiogenesis regulation. Hypoxia is known to affect cellular energy metabolism and cellular redox states (36). It would be important to address whether a hypoxic state alters the proapoptotic efficacy of the different pools of Se metabolites. Hypoxia is a potent stimulus for the angiogenic switch by stimulating VEGF expression (37). An inhibitory activity by methyl Se on the ability of the epithelial lesions to produce this angiogenic factor represents a metabolite-specific avenue through which Se can regulate angiogenesis and carcinogenesis (Fig. 5B).

In addition to the Se delivery considerations in epithelial lesions, strong arguments can be made in support of anti-endothelial and antiangiogenesis actions as primary effectors of cancer prevention by Se metabolites. The angiogenic microenvironment is likely conducive for selective targeting of stimulated vascular endothelial cells by blood-borne Se metabolites. Several physical and biological features of endothelial cells and the newly formed vessels stand out in contrast to tumor cells: 1) as lining of blood vessels, endothelial cells are the first line of exposure to blood Se; 2) vascular endothelial cells in nonangiogenic environment are essentially quiescent and protected by pericytes and smooth muscle cells; and 3) angiogenic factor-stimulated endothelial cells undergo mitogenic and other responses to form new sprouts, which are leaky and not as protected as are existing vessels (50). Sustained angiogenic stimulation provided by the transformed cells in the expanding lesions is essential for continued angiogenesis within a tumor, in contrast to normal angiogenesis during menstrual cycle or wound healing, for example, where expression of angiogenic regulators (positive and negative factors) is tightly controlled (51). This fact is clearly articulated by the saying that "cancer is a wound that never heals." Such a difference may provide a plausible biological basis for selectivity against malignancy through suppressing tumor angiogenesis. Our data suggest that, in a chemoprevention context, the increased circulating and tissue levels of Se metabolites, especially the monomethyl Se pool, can exert a direct antimitogenic activity on the vascular endothelial cells (Fig. 5B) and perhaps even induce apoptosis. Because endothelial cells are much less susceptible to mutagenesis than are epithelial cells, the wild-type p53 tumor suppressor status of the endothelial cells can ensure p53-dependent growth arrest and apoptosis. The methylselenol specific inhibitory activity on endothelial MMP-2 expression (Fig. 5B) will further dampen the endothelial responsiveness to angiogenic stimulation. These direct anti-endothelial effects combined with inhibitory action on epithelial expression of VEGF can serve as a powerful control for the angiogenic switch and, hence, carcinogenesis (Fig. 5B).

The new paradigm advocated here emphasizes the nonepithelial and epithelial targets for Se action. The angiogenic switch regulatory activities described for the methyl Se pool may provide a mechanism for novel biochemical and molecular markers of cancer prevention by Se. The specific nature of the angiogenic switch control mechanisms (52) and a difference in the ability to generate methylselenol may underscore organ site specificity of cancer-preventive activity of Se, as has been documented in the trial of Clark et al. (prostate, colon, and lung vs. skin). These issues merit further investigation.

### Acknowledgments and Notes

Pierce St., Denver, CO 80214. Phone: 303-239-3348. FAX: 303-239-3560. E-mail: luj@amc.org.

## References

1. Clark LC, Combs GF Jr, Turnbull BW, Slate EH, Chalker DK, et al.: Effects of selenium supplementation for cancer prevention in patients with carcinoma of the skin: a randomized controlled trial. Nutritional Prevention of Cancer Study Group. *JAMA* 276, 1957–1963, 1996.

2. Yu SY, Zhu YJ, and Li WG: Protective role of selenium against hepatitis B virus and primary liver cancer in Qidong. *Biol Trace Elem Res* 56, 117–124, 1997.

3. Ip C: Lessons from basic research in selenium and cancer prevention. *J Nutr* 128, 1845–1854, 1998.

4. Combs GF Jr and Gray WP: Chemopreventive agents: selenium. *Pharmacol Ther* 79, 179–192, 1998.

5. Jiang C, Jiang W, Ip C, Ganther H, and Lu JX: Selenium-induced inhibition of angiogenesis in mammary cancer at chemopreventive levels of intake. *Mol Carcinog* 26, 213–225, 1999.

6. Jiang C, Ganther H, and Lu JX: Monomethyl selenium-specific inhibition of MMP-2 and VEGF expression: implications for angiogenic switch regulation. *Mol Carcinog* 29, 236–250, 2000.

7. Ip C and Ganther HE: Activity of methylated forms of selenium in cancer prevention. *Cancer Res* 50, 1206–1211, 1990.

8. Ip C, Hayes C, Budnick RM, and Ganther HE: Chemical form of selenium, critical metabolites, and cancer prevention. *Cancer Res* 51, 595–600, 1991.

9. Lu JX, Jiang C, Kaeck M, Ganther H, Vadhanavikit S, et al.: Dissociation of the genotoxic and growth inhibitory effects of selenium. *Biochem Pharmacol* 50, 213–219, 1995.

10. Lu JX, Pei H, Ip C, Lisk D, Ganther H, et al.: Effect of an aqueous extract of selenium-enriched garlic on in vitro markers and in vivo efficacy in cancer prevention. *Carcinogenesis* 17, 1903–1907, 1996.

11. Kaeck M, Lu JX, Strange R, Ip C, Ganther HE, et al.: Differential induction of growth arrest inducible genes by selenium compounds. *Biochem Pharmacol* 53, 921–926, 1997.

12. Sinha R and Medina D: Inhibition of cdk2 kinase activity by methylselenocysteine in synchronized mouse mammary epithelial tumor cells. *Carcinogenesis* 18, 1541–1547, 1997.

13. Lu JX: Apoptosis and angiogenesis in cancer prevention by selenium. In *Nutrition and Cancer Prevention: New Insights Into the Role of Phytochemicals.* New York: Kluwer Academic/Plenum, 2000, pp 131–145.

14. Jiang C, Wang Z, Ganther H, and Lu JX: Caspases as key executors of methyl selenium-induced apoptosis (anoikis) of DU-145 human prostate cancer cells. *Cancer Res* 61, 3062–3070, 2001.

15. Folkman J: The role of angiogenesis in tumor growth. *Semin Cancer Biol* 3, 65–71, 1992.

16. Hanahan D and Folkman J: Patterns and emerging mechanisms of the angiogenic switch during tumorigenesis. *Cell* 86, 353–364, 1996.

17. Bouck N, Stellmach V, and Hsu SC: How tumors become angiogenic. *Adv Cancer Res* 69, 135–174, 1996.

18. Zetter BR: Angiogenesis and tumor metastasis. *Annu Rev Med* 49, 407–424, 1998.

19. Leung DW, Cachianes G, Kuang WJ, Goeddel DV, and Ferrara N: Vascular endothelial growth factor is a secreted angiogenic mitogen. *Science* 246, 1306–1309, 1989.

20. Keck PJ, Hauser SD, Krivi G, Sanzo K, Warren T, et al.: Vascular permeability factor, an endothelial cell mitogen related to PDGF. *Science* 246, 1309–1312, 1989.

21. Grunstein J, Roberts WG, Mathieu-Costello O, Hanahan D, and Johnson RS: Tumor-derived expression of vascular endothelial growth factor is a critical factor in tumor expansion and vascular function. *Cancer Res* 59, 1592–1598, 1999.

22. Brown LF, Guidi AJ, Tognazzi K, and Dvorak HF: Vascular permeability factor/vascular endothelial growth factor and vascular stroma formation in neoplasia. Insights from in situ hybridization studies. *J Histochem Cytochem* 46, 569–575, 1998.

23. Guidi AJ, Abu-Jawdeh G, Tognazzi K, Dvorak HF, and Brown LF: Expression of vascular permeability factor (vascular endothelial growth factor) and its receptors in endometrial carcinoma. *Cancer* 78, 454–460, 1996.

24. Guidi AJ, Schnitt SJ, Fischer L, Tognazzi K, Harris JR, et al.: Vascular permeability factor (vascular endothelial growth factor) expression and angiogenesis in patients with ductal carcinoma in situ of the breast. *Cancer* 80, 1945–1953, 1997.

25. Abu-Jawdeh GM, Faix JD, Niloff J, Tognazzi K, Manseau E, et al.: Strong expression of vascular permeability factor (vascular endothelial growth factor) and its receptors in ovarian borderline and malignant neoplasms. *Lab Invest* 74, 1105–1115, 1996.

26. Fukumura D, Xavier R, Sugiura T, Chen Y, Park EC, et al.: Tumor induction of VEGF promoter activity in stromal cells. *Cell* 94, 715–725, 1998.

27. Carmeliet P, Ferreira V, Breier G, Pollefeyt S, Kieckens L, et al.: Abnormal blood vessel development and lethality in embryos lacking a single VEGF allele. *Nature* 380, 435–439, 1996.

28. Ferrara N, Carver-Moore K, Chen H, Dowd M, Lu L, et al.: Heterozygous embryonic lethality induced by targeted inactivation of the VEGF gene. *Nature* 380, 439–442, 1996.

29. Zhang HT, Craft P, Scott PA, Ziche M, Weich HA, et al.: Enhancement of tumor growth and vascular density by transfection of vascular endothelial cell growth factor into MCF-7 human breast carcinoma cells. *JNCI* 87, 213–219, 1995.

30. Aonuma M, Saeki Y, Akimoto T, Nakayama Y, Hattori C, et al.: Vascular endothelial growth factor overproduced by tumour cells acts predominantly as a potent angiogenic factor contributing to malignant progression. *Int J Exp Pathol* 80, 271–281, 1999.

31. Borgstrom P, Hillan KJ, Sriramarao P, and Ferrara N: Complete inhibition of angiogenesis and growth of microtumors by anti-vascular endothelial growth factor neutralizing antibody: novel concepts of angiostatic therapy from intravital videomicroscopy. *Cancer Res* 56, 4032–4039, 1996.

32. Benjamin LE and Keshet E: Conditional switching of vascular endothelial growth factor (VEGF) expression in tumors: induction of endothelial cell shedding and regression of hemangioblastoma-like vessels by VEGF withdrawal. *Proc Natl Acad Sci USA* 94, 8761–8766, 1997.

33. Borgstrom P, Bourdon MA, Hillan KJ, Sriramarao P, and Ferrara N: Neutralizing anti-vascular endothelial growth factor antibody completely inhibits angiogenesis and growth of human prostate carcinoma micro tumors in vivo. *Prostate* 35, 1–10, 1998.

34. Meeson AP, Argilla M, Ko K, Witte L, and Lang RA: VEGF deprivation-induced apoptosis is a component of programmed capillary regression. *Development* 126, 1407–1415, 1999.

35. Benjamin LE, Golijanin D, Itin A, Pode D, and Keshet E: Selective ablation of immature blood vessels in established human tumors follows vascular endothelial growth factor withdrawal. *J Clin Invest* 103, 159–165, 1999.

36. Brown JM and Giaccia AJ: The unique physiology of solid tumors: opportunities (and problems) for cancer therapy. *Cancer Res* 58, 1408–1416, 1998.

37. Levy AP, Levy NS, Wegner S, and Goldberg MA: Transcriptional regulation of the rat vascular endothelial growth factor gene by hypoxia. *J Biol Chem* 270, 13333–13340, 1995.

38. Rak J, Mitsuhashi Y, BayKo L, Filmus J, Shirasawa S, et al.: Mutant *ras* oncogenes upregulate VEGF/VPF expression: implications for induction and inhibition of tumor angiogenesis. *Cancer Res* 55, 4575–4580, 1995.

39. Grugel S, Finkenzeller G, Weindel K, Barleon B, and Marme D: Both v-Ha-Ras and v-Raf stimulate expression of the vascular endothelial growth factor in NIH 3T3 cells. *J Biol Chem* 270, 25915–25919, 1995.

40. Mazure NM, Chen EY, Yeh P, Laderoute KR, and Giaccia AJ: Oncogenic transformation and hypoxia synergistically act to modulate vascular endothelial growth factor expression. *Cancer Res* 56, 3436–3440, 1996.

41. Arbiser JL, Moses MA, Fernandez CA, Ghiso N, Cao Y, et al.: Oncogenic H-*ras* stimulates tumor angiogenesis by two distinct pathways. *Proc Natl Acad Sci USA* **94**, 861–866, 1997.

42. Akagi Y, Liu W, Zebrowski B, Xie K, and Ellis LM: Regulation of vascular endothelial growth factor expression in human colon cancer by insulin-like growth factor-I. *Cancer Res* **58**, 4008–4014, 1998.

43. Ryuto M, Ono M, Izumi H, Yoshida S, Weich HA, et al.: Induction of vascular endothelial growth factor by tumor necrosis factor-α in human glioma cells: possible roles of SP-1. *J Biol Chem* **271**, 28220–28228, 1996.

44. Deroanne CF, Hajitou A, Calberg-Bacq CM, Nusgens BV, and Lapiere CM: Angiogenesis by fibroblast growth factor 4 is mediated through an autocrine up-regulation of vascular endothelial growth factor expression. *Cancer Res* **57**, 5590–5597, 1997.

45. Coussens LM and Werb Z: Matrix metalloproteinases and the development of cancer. *Chem Biol* **3**, 895–904, 1996.

46. Itoh T, Tanioka M, Yoshida H, Yoshioka T, Nishimoto H, et al.: Reduced angiogenesis and tumor progression in gelatinase A-deficient mice. *Cancer Res* **58**, 1048–1051, 1998.

47. Hiraoka N, Allen E, Apel IJ, Gyetko MR, and Weiss SJ: Matrix metalloproteinases regulate neovascularization by acting as pericellular fibrinolysins. *Cell* **95**, 365–377, 1998.

48. Wang Z, Jiang C, Ganther H, and Lu JX: Anti-mitogenic and pro-apoptotic activities of methylseleninic acid in vascular endothelial cells and associated effects on PI3K-AKT, ERK, JNK and p38MAPK signaling. *Cancer Res* **61**, 7171–7178, 2001.

49. Dalkin BW, Lillico AJ, Reid ME, Jacobs ET, Combs GF, et al.: Selenium and chemoprevention against prostate cancer: an update on the Clark results (abstr). *Proc Am Assoc Cancer Res 2001*, p 460.

50. Dvorak HF: VPF/VEGF and the angiogenic response. *Semin Perinatol* **24**, 75–78, 2000.

51. Torry RJ and Rongish BJ: Angiogenesis in the uterus: potential regulation and relation to tumor angiogenesis. *Am J Reprod Immunol* **27**, 171–179, 1992.

52. Eberhard A, Kahlert S, Goede V, Hemmerlein B, Plate KH, et al.: Heterogeneity of angiogenesis and blood vessel maturation in human tumors: implications for antiangiogenic tumor therapies. *Cancer Res* **60**, 1388–1393, 2000.